UNIVERSIDADE DE LISBOA

Faculdade de Farmácia

3-HYDROXY-QUINOLIN-2(1*H*)-ONES, A USEFUL SCAFFOLD: SYNTHESIS AND BIOLOGICAL EVALUATION

Roberta Paterna

Orientadores: Doutor Pedro Miguel Pimenta Góis
Professor Doutor Rui Ferreira Alves Moreira

Tese especialmente elaborada para obtenção do grau de Doutor em Farmácia, especialidade em Química Farmacêutica

2017

UNIVERSIDADE DE LISBOA

Faculdade de Farmácia

3-HYDROXY-QUINOLIN-2(1*H*)-ONES, A USEFUL SCAFFOLD: SYNTHESIS AND BIOLOGICAL EVALUATION

Roberta Paterna

Orientadores: Doutor Pedro Miguel Pimenta Góis
Professor Doutor Rui Ferreira Alves Moreira

Tese especialmente elaborada para obtenção do grau de Doutor em Farmácia, especialidade em Química Farmacêutica

Júri:

Presidente: Doutora Matilde da Luz dos Santos Duque da Fonseca e Castro, Professora Catedrática e Diretora da Faculdade de Farmácia da universidade de Lisboa

Vogais:

- Doutor Nuno Filipe Candeias, *University Lecture*
  Tampere University of Technology, Finland;
- Doutora Maria Miguéns Pereira, Professora Associada com Agregação
  Faculdade de Ciência e Tecnologia da Universidade de Coimbra;
- Doutora Maria Manuel Martinho Sequeira Barata Marques, Investigadora Auxiliar com Agregação
  Faculdade de Ciência e Tecnologia da Universidade Nova de Lisboa,
- Doutora Maria Matilde Soares Duarte Marques, Professora Catedrática
  Instituto Superior Técnico da Universidade de Lisboa;
- Doutora Ana Paula Costa dos Santos Peralta Leandro, Professora Auxiliar
  Faculdade de Farmácia da Universidade de Lisboa;
- Doutor Pedro Miguel Pimenta Góis, Professor Auxiliar
  Faculdade de Farmácia da Universidade de Lisboa, orientador.

Fundação para a Ciência e Tecnologia

2017

Statement

O presente trabalho foi desenvolvido sob orientação do Doutor Pedro Gois e co-orientaçao do Professor Doutor Rui Moreira do iMed.ULisboa (Instituto de Investigação do Medicamento), amos da Faculdade de Farmácia da Universidade de Lisboa. Este trabalho foi financiado pela Fundação para a Ciência e Tecnologia através da bolsa de doutoramento SFRH/BD/78301/2011.

This work was developed under scientific supervision of Dr. Pedro Góis and Professor Dr Rui Moreira from iMed.LULisboa (Research Institute for Medicines), faculty of pharmacy, University of Lisbon. The work was financially supported by Fundação para a Ciência e Tecnologia, through the doctoral grant SFRH/BD/78301/2011.

Ackonwledgement

First, I would like to express my gratitude to my supervisor **Dr. Pedro Gois** for the continuous support of my Ph. D studies and related research, for his patience, motivation, and immense knowledge. His guidance helped me in all the time of research and writing of this thesis.

I also acknowledge my co-supervisor **Prof. Rui Moreira** for his sage advice, insightful criticism, and patient encouragement aided my Ph.D. progress in innumerable ways.

My sincere thanks also go to **Prof. Ana Paula Leandro** from Metabolism and Genetics Group of iMed.UL who provided me the opportunity to join her team, and who gave access to the laboratory and research facilities. I have also to acknowledge the member of her group **Dr. João B. Vicente**, **Dr. João Leandro**, **Mariana P. Amaro**, **Raquel Lopes**, **Ana Carolina Costa** which helped me to understand techniques that had no previous knowledge to develop specific aspects of this project and also performed the biochemical assay.

I would like to **Dr. Raquel Frade** and **Dr. Pedro Borralho** which performed the cells assays described in this thesis.

I would also like to express my indebtedness gratitude to Fundação para a Ciência e Tecnologia for their financial support (SFRH/BD/78301/2011), and to the Faculdade de Farmácia, Universidade de Lisboa, Portugal

During this time spend in the Biorganic Chemistry Group at iMed.UL, I had the fortune to be surrounded by people that made my day-to-day routine so much happier and pleasant. Expetially **Dr. Nuno Candeias**, **Dr. Carlos Monteiro**, **Dr. Jaime Coelho**, **Dr. Alexandre Trindade**, **Drª. Filipa Siopa, Drª**. **Andreia Rosatella**, **Drª.Catarina Rodrigues, M.S. Fábio Santos**, **Dr. Pedro Cal**, **Dr Rudi Oliveira**, **Dr Svilen Simeonov, Dr Sudarshan Reddy, M.S. Joao Antonio** for all the advices

and scientific support of my project and also for being true friends that i can belive and I will be able to keep for the rest of my life. Futhermore, I can not dismiss the opportuyty of thanking all the new present members of Biorganic Chemistry Group and Medicinal Chemistry.

Special regards also to **Dr. João Rosa** that took the effort of doing an extensive review of theis thesis. Also, I would like to thanks **Dr Helio Faustino** for helped me in the last stage of my work.

I would like to thank all undergraduate students that I guided during the course of my PhD, since they helped me to grow as a scientist and person: **M.S Marcio Santos** and **M.S**. **Roberto Russo.**

I would like to thank all of my friends that helped me to be myself and to be happy during this period far from home in particular **Angela Paterna, Joao Lavrado Francesco Montalbano, Simone Tulumello**. Also, I would like to thanks my roommates and friends **Damla Uyar, Julia Plötz** who endured everyday my stress and complaints at home with a smile on their face.

Finally, I would like to thank my Mother who support was crucial all these years far from home and for all the pride that she has demostated in my little achievements that gave me the required confidence to belive in myself and capabilities. Also, I would like to thank my sister and my little nephews for their support.

Furthermore, I would like to acknowledge my deceased father and dedicate this thesis in his lovely memory.

List of Pubblications

Papers in International Scientific Periodicals with Referees

- "A Sustainable Protocol for the Aqueous Multicomponent Petasis Borono–Mannich Reaction", Candeias, N.R., Paterna R., Cal P.M.S.D., Góis, P.M.P.,. Journal of Chemical Education (**2012**), 89 (6), 799-802 (DOI: 10.1021/ed200509q)
- "Ring-Expansion Reaction of Isatins with Ethyl Diazoacetate Catalyzed by Dirhodium(II)/DBU Metal-Organic System: En Route to Viridicatin Alkaloids" Paterna, R., André, V., Duarte, M.T., Veiros, L.F., Candeias, N.R., Gois, P.M.P. European Journal of Organic Chemistry (**2013**), 28, 6280-6290. (DOI: 10.1002/ejoc.201300796)
- "Homologation Reaction of Ketones with Diazo Compounds" Candeias, N.R., Paterna R., Gois, P.M.P., (**2016**). Chemical Reviews, 116 (5), 2937–2981. (DOI:10.1021/acs.chemrev.5b00381)

Oral Communications in Scientific Conferences

- 7th iMed.ULisboa Post-graduate Students Meeting organized by iMed.ULisboa (Instituto de Investigação do Medicamento) held in Lisbon, in 2015.
- 11ºPortuguese National Meeting of Organic Chemistry and 4º Portuguese National Meeting of Medicinal Chemistry, 1-3 December **2015**, Porto, Portugal.

Poster communications in Scientific Conferences

- XII Encontro Nacional da Sociedade Portuguesa de Quimica, 2011, Braga
- Challenges in organic chemistry and chemical Biology (ISACS7) organized by RCS (Royal society of Chemistry) held in Edinburgh, 2012.
- 4th iMed.ULisboa Post-graduate Students Meeting organized by iMed.ULisboa (Instituto de Investigação do Medicamento) held in Lisbon, in 2012.
- 10º Portuguese National Meeting of Organic Chemistry and the 1st Portuguese-Brazilian Organic Chemistry Symposium, Lisbon, September 2013.
- 5th iMed.ULisboa Post-graduate Students Meeting organized by iMed.ULisboa (Instituto de Investigação do Medicamento) held in Lisbon, in 2013.
- 50th International Conference on Medicinal Chemistry RICT 2014, Rouen, July 2014.
- 6th iMed.ULisboa Post-graduate Students Meeting organized by iMed.ULisboa (Instituto de Investigação do Medicamento) held in Lisbon, in 2014.
- 6th European Conference Chemistry in the Life Sciences organized by EuCheMS (European Association for Chemical and Molecular Sciences) held in Lisbon, 2015.
- Ciência 2016 - Encontro com a Ciência e Tecnologia em Portugal, organized by Fundação para a Ciência e a Tecnologia em colaboração com a Ciência Viva held in Lisbon, 2016

Abstract

The quinolin-2(1*H*)-ones ring establish the core structure of many natural and synthetic molecules and a broad spectrum of biological properties like, antimicrobial, enzymatic and neuro protective activities, have been attributed to these molecules. Additionally, 4-hydroxyquinolin-2-ones (4HQs) and 3-hydroxyquinolin-2-ones (3HQs), derivatives of quinolin-2-one, have also been reported with promising biological properties, and have attracted much attention from the medicinal chemist community. The 3HQ core is present in the structure of naturally occurring products viridicatin, viridicatol and 3-*O*-methyl viridicatin first isolated from the mycelium of *Penicillium viridicatum*. Although, due to the reduced knowledge about 3HQs, from a synthetic and biological perspective, in the last years, the development of new methodologies for their synthesis has been stimulated and strategies based on condensations, intramolecular cyclization and ring expansions have been applied. Recently reported has nonclassical bioisosteres of α-glycine, 3HQs derivatives are potent inhibitors of the Human D-amino acid oxidase (DAAO) and due to their ability to chelates metal centres, 3HQs are counted as inhibitors of HIV-1 reserve transcriptase associated RNase H activity and as inhibitors of influenza A endonuclease.

In view of the present stat-of-the-art, 3HQs new derivatives were synthetized using a new efficient methodology centered on the emergent metal-organo-catalysed (MOC) concept. A one-pot protocol using the MOC system NHC-dirhodium(II)/DBU catalyzed Eistert ring expansion reaction of isatins with ethyl diazoacetate to afford the 3-hydroxy-4-ethylesterquinolin-2(1H)-ones core. The reaction provides the final products regioselectively and with yields ranging from good to excellent. Furthermore, DFT calculations were performed on this system and support a mechanism in which the key step is the metallocarbene formation between the 3-hydroxyindole-diazo intermediate and the dirhodium(II) complex.

After the above mentioned optimized methodology the second part of this work is dedicated to the biological activity of 3HQ and its derivatives. Various synthetic modifications have been made to introduce specific chemical group keeping the 3HQs core structure. Several compounds with different properties were synthesized and important biological studies were performed on 4-carboxamide-3HQ derivatives showed interesting biological activity as a potential anticancer lead molecule. Additionally, based on the that 3HQs can complex metallic centers and been an isoster of glycine, we hypothesized that 3HQ derivatives could be a useful platform to design new modulators of human phenylalanine hydroxylase (hPAH), the enzyme responsible by the genetic disease phenylketonuria. The new hPAH modulators were simply prepared based on ring-expansion reaction of isatins with NHS-diazoacetate catalysed by di-rhodium(II) complexes yielding 4-Carboxamide-3HQs in good-to-excellent yields. The 7-trifluoromethyl-4-carboxamide-3HQs **134**, was identified as the most efficient hPAH modulator, with an apparent binding affinity nearly identical to the natural allosteric activator L-Phenylalanine.

Therefore, as 3-hydroxyquinolies have demonstrated to be good scaffolds for the design and development of compounds with activity over phenylalanine hydroxylase and an excellent starting point for the development of novel therapeutics for a phenylketonuria.

Keywords: 3-Hydroxyquinoline-2(1*H*)-ones; Eistert Ring Expansion**;** anticancer agents; phenylalanine hydroxylase enzyme.

Resumo

O anel de quinolin-2(1*H*)-ona é a estrutura central de muitas moléculas tanto de origem natural, como sintética, e ao qual tem sido atribuído um amplo espectro de propriedades biológicas, como antimicrobianas, enzimáticas e neuro-protetoras. Para além das quinolin-2(1*H*)-onas, os seus derivados 4-hidroxiquinolin-2-onas (4HQs) e as 3-hidroxiquinolin-2-onas (3HQs) apresentam também propriedades biológicas promissoras e têm atraído muita atenção da comunidade de químicos medicinais. Recentemente relatados como bioisósteres não clásicos da α-glicina, os derivados da 3HQs são potentes inibidores da D-aminoácido oxidase humana (DAO) e devido à sua capacidade para quelar centros metálicos, as 3HQs são também apontados como inibidores da RNase H associada à transcriptase reserva do HIV-1 e como inibidores da endonuclease do vírus Influenza A. Assim, as 3HQs têm sido reconhecidas como uma estrutura química com interesse farmacológico. O núcleo 3HQ está presente na estrutura dos produtos naturais viridicatina, viridicatol e 3-O-metil viridicatina, isolados primeiramente do micélio do *Penicillium viridicatum*. No entanto, devido a reduzido numero de métodos de síntese e falta de conhecimento das propriedades biológicas, têm-se assistido nos últimos anos a um crescente interesse da comunidade científica e um estimulo no desenvolvimento de novas metodologias de síntese. Estratégias baseadas em condensações, ciclizações intramoleculares e expansões de anel, têm sido descritas com o objetivo de obter a viridicatina e seus derivados com maior eficiência.

Com base no atual estado da arte, neste trabalho foram sintetizados novos derivados da 3HQ utilizando uma nova metodologia centrada no conceito emergente metal-organo-catalise (MOC). Esta metodologia, usa o sistema NHC-diródio(II)/DBU para catalisar a reação de expansão do anel de Eistert entre a isatina e o diazoacetato de etilo para se obter o anel de 3-hidroxi-4-etilesterquinolin-2(1*H*)-ona. Assim, uma nova e eficiente metodologia de 4 passos foi desenvolvida para a síntese dos alcalóides de viridicatina através da reação de acoplamento de Suzuki-Miyaura entre os ácidos aril-borónicos e a 3-hidroxi-4-bromoquinolin-2 (1*H*)-ona,

preparada a partir da 3-hidroxi-4-etilesterquinolina-2(1*H*)-ona. A reação ocorre com boa regioseletividade e com rendimentos que variam de moderados a excelentes, e em que os alcaloides da vidicatina foram sintetizados com rendimentos superiores a 80%. Finalmente, cálculos de DFT foram realizados neste sistema, e suportam um mecanismo no qual o passo determinante é a formação de metalocarbeno entre o intermediário 3-hidroxi-indole-diazo e o complexo di-ródio (II).

Após a otimização da metodologia, a segunda fase do trabalho desenvolvido, foi dedicada à atividade biológica da 3HQ e seus derivados em linhas celulares tumorais. Assim, várias modificações sintéticas foram efetuadas para introduzir grupos químicos específicos, mantendo a estrutura base do núcleo de 3HQ. Com base na reação de expansão do anel de isatinas com diazoésteres catalisados por complexos di-ródio (II), sintetizou-se a 4-carboxilato-3HQ, com rendimentos até 92%. Utilizando o NHS-diazoacetato, as 4-carboxamida-3HQ foram preparadas de forma eficiente e esta metodologia inovadora permitiu a construção de 3HQs "semelhantes a peptídeos" com rendimentos até 88%. Entre as séries sintetizadas, a L-leucina-4-carboxamida-3HQ induziu a morte em linhas celulares tumorais MCF-7 (IC_{50} = 15,12 μM), NCI-H460 (IC_{50} = 2,69 μM) sem causar qualquer citotoxicidade apreciável em linhas celulares não tumorais (CHOK1). Assim, os estudos biológicos realizados em derivados de 4-carboxamida-3HQ mostraram atividades biológicas apreciáveis e demonstraram o seu potencial anti-tumoral.

Sendo as 3HQs agentes quelantes de centros metálicos e isosteros do amino acido glicina, neste trabalho foi colocada a hipótese das 3HQs poderem ser uma interessante plataforma para o desenvolvimento de modeladores da enzima fenilalanina hidroxilase humana (hPAH). A hPAH pertence a uma família de enzimas de hidroxilases de aminoácidos aromáticos, que inclui a hPAH, a tirosina hidroxilase (TH) e o triptofano hidroxilase (TPHs). Estas enzimas são mono-oxigenases que usam tetraidropterina (BH4) como cofator, um ião Fe(II) não-heme e o oxigénio como substrato para a catalise da hidroxilação da fenilalanina (Phe) a tirosina (Try). Durante a reação, o oxigénio molecular é clivado heteroliticamente com incorporação

sequencial de um átomo de oxigénio em BH4 e no substrato de fenilalanina. Este é o primeiro passo na degradação catabólica da Phe, e cerca de 75% da Phe obtida através da dieta, é degradada desta forma em condições fisiológicas. A fenilcetonúria, uma doença autossómica recessiva que afeta 1 em cada 10000 nados-vivos na Europa, é caracterizada por elevadas concentrações fisiológicas de Phe, devido à atividade deficiente da fenilalanina hidroxilase. Quando não tratada, a fenilcetonúria pode gerar retardo mental progressivo, dano cerebral, epilepsia e problemas neurológicos e comportamentais causados por efeitos neurotóxicos. Assim, uma vez que L-Phe é o substrato natural da PAH, foi idealizado a incorporação do aminoácido L-Phe na posição C-4 do núcleo 3HQs, o que conjuntamente com as propriedades quelantes de centros metálicos, teve como objetivo modelar a atividade da PAH. Uma pequena biblioteca de derivados L-Phe-3HQs foi sintetizada de modo a avaliar a capacidade de modulação da atividade da enzima PAH, por efeito de estabilização em seu domínio regulador e centro ativo. Dos compostos avaliados, a 3HQ **141**, demostram estabilizar o domínio regulador e, além disso, o menor efeito de inibição da atividade da PAH. Assim, a com base nos resultados obtidos, a 3HQ **141** foi escolhida como ponto de partida para o desenvolvimento de novos derivados através da introdução de diferentes aminas na posição C-4 do núcleo de 3HQ. Uma nova biblioteca de derivados de 4-carboxamida-F3CO-3HQs foi sintetizada e avaliada quanto ao seu efeito na estabilidade térmica de hPAH e na atividade enzimática. Dos compostos avaliados, o derivado **134**, contendo carboxamida com um grupo fenetilamina, foi identificado como o composto mais eficaz, capaz de aumentar diretamente a atividade de hPAH por um mecanismo de pré-ativação semelhante ao induzido pelo substrato L-Phe.

Assim, as 3-hidroxiquinolinas demonstraram assim serem bons esqueletos para o desenho e desenvolvimento de compostos com atividade sobre a fenilalanina hidroxilase e um excelente ponto de partida para o desenvolvimento de novos agentes terapêuticos para a fenilcetonúria.

Palavras-chave: 3-hidroxiquinolin-2-onas; expansão do anel de Eistert**;** atividade anti-cancerígena; fenilalanina hidroxilase.

Table of Contents

Statement i
Ackonwledgement iii
List of Pubblications v
Abstract vii
Resumo ix
Table of Contents xiii
List of Figures xvii
List of Schemes xxi
List of Tables xxv
Abbreviations and Definitions xxvii

General Introduction 1
Rational and Aims 1
Outline of the thesis 2
I. Hydroxy-quinolin-2(1*H*)-ones: A synthetic and biological overview 1
1.1 The Quinolin-2(1*H*)-one scaffold 3
Overview of 4-hydroxyquinolin-2-ones 6
1.1.1 4-Hydroxyquinolin-2-ones biology 6
1.1.2 4-Hydroxyquinolin-2-ones chemistry 8
1.2 Overview on 3-Hydroxyquinolin-2-ones 10
1.2.1 3-Hydroxyquinolin-2-ones biology 10
1.2.2 3-Hydroxyquinolin-2-ones chemistry 19
2 II. Synthesis of Viridicatin Alkaloids 31
2.1 Introduction 33

2.1.1 Combining transition metal catalysis and organocatalysis: A new emerging concept 33

2.2 Generation of metallocarbenes from diazo compounds using di-rhodium dimers 35

2.2.1 Exploring metal organo catalytic systems based on di-Rhodium complexes 37

2.2.2 Preliminary Results 42

2.2.3 Rh(II) recycling 44

2.2.4 Implementation of MOC system. 45

2.2.5 Eistert Ring expansion of isatins with EDA using a sequential DBU/$Rh_2(OAc)_4$ system 48

2.2.6 Eistert ring expansion of isatins with EDA using a one-pot relay DBU/$Rh_2(OAc)_4$ system. 50

2.2.7 Computational Study 53

2.2.8 Synthesis of Viridicatin alkaloids 59

2.2.9 Conclusion 63

3 III. Synthesis of 4-Substituted-3-Hydroxyquinolin-2(1*H*)-ones and Anticancer Activity Evaluation 65

3.1 Cancer hallmarks 67

3.2 Anti-proliferative activity and chemical modifications of the 3-hydroxyquinolin-2-ones lead core 68

3.2.1 Preliminary anti-proliferative screening 68

3.2.2Structural modifications on the 3-hydroxyquinolin-2-one lead core 87. 70

3.2.3 Conclusion 82

4 IV. Phenylalanine Hydroxylase Activation Studies 83

4.1 Phenylketonuria: an introduction. 85

4.2 Phenylalanine Hydroxylase 86

4.2.1 Regulation of phenylalanine hydroxylase 87

4.2.2 Treatment and emerging PKU therapies 89

4.3 Phenylanlanine Hydroxylase Activation 94

4.4 Conclusion 105

5 V. General Discussion and Conclusions 107

5.1 Introduction 109

5.2 Synthesis of 3HQs derivatives 110

5.3 Biological evaluation of 3-HQs 112

5.3.1 *In vitro* Anticancer Activity SAR 112

5.3.2 Biochemical studies of PAH modulators 115

5.4 Conclusions 116

6 VI. Material and Methods 119

6.1 General 121

6.1.1 Chemicals 121

6.1.2 Instrumentation 121

6.1.3 Methods 122

6.2 General method for the tandem synthesis of 3-hydroxy-2(1H)-oxoquinoline-4-ethylesters : 123

6.3 General method for the sequential synthesis of 3-hydroxy-4-ethylesterquinolin-2-(1H)-ones 123

6.4 Synthesis of 3-hydroxyquinolin-2(1H)-one 9. 129

6.5 Synthesis of 4-bromo-3-hydroxyquinolin-2(1H)-one 129

6.6 Optimization of the microwave-assisted Suzuki-Mayura reaction. 130

6.7 Preparation of α-Diazo carbonyl compounds 135

Preparation of succinimidyl diazoacetate 124 137

6.8 General synthesis of 4-carboxylate-3HQs: 138

6.9 Synthesis of 4-NHS-3HQs 125-126, 130-131 141

Synthesis of 4-carboxamide-3HQ 127-129 and 132-143: 144

7 VII. References 153

8 VIII. Appendix 171

A. Computational details 173

B. Biological Evaluation 187

B1. Cell viability assays 187

B2. Cell death assays 187

B3. Enzymatic activity assays 188

B4. Differential Scanning Fluorimetry 189

C. NMR chemical shift assignment 191

D. Structures tested in biological assays. 193

List of Figures

Figure 1.1 – Number of publications referring quinolin -2(1*H*)-ones since 1982, according to Web of Science and using "Quinolin -2(1*H*)-ones" as keyword. 3

Figure 1.2 – Putative binding mode of amide **42** in the RT RNase H catalytic site.[72] 13

Figure 1.3 – Binding of compound **43** at the endonuclease active site.[73] 14

Figure 1.4 – Characteristic pKa values of carboxylic acid, benzoic acid 48 and 3HQ **9**. 17

Figure 1.5 – Compound **9** at DAAO enzyme active side. a) Schematic representation of residues in DAAO-compound 9; b) Compound **9** (carbon atoms in magenta and oxygen in red) at h-DAAO enzyme active site. Side chains of key interacting residues are shown with carbon coloured in green and nitrogen in blue. Hydrogen bonding interactions are shown in dash. FAD is shown with carbons in cyan; b) structure of compound **9**.[9] 18

Figure 1.6 – Schematic representation of bonding interactions of compound **9** with those of carboxylic acids inhibitors (benzoic acid).[9] 18

Figure 1.7 – a) Schematic representation of 3HQ as a bioisoster of aminoacid Glycine; b) compound **9** and cofactor FAD (PDB code: 3G3E). All atoms in type code except ligand carbon atoms in orange and FAD carbons in green.[8] 19

Figure 1.8 – General strategies for the synthesis of the 3-Hydroxyquinolin-2(1*H*)-one skeleton. 20

Figure 2.1- (a) The concept of cooperative catalysis. (b) The concept of synergistic catalysis. (c) The concept of sequential or relay catalysis. 34

Figure 2.2 - General structure and reactivity of Di-rhodium(II) complexes. 36

Figure 2.3 – X-ray crystallography of **69.** 43

Figure 2.4 – X-ray crystallography of **70.** 47

Figure 2.5 – X-ray crystallography of **93.**.....50

Figure 2.6 - Energy profiles calculated for the metallocarbene formation between the 3-substituted 3-hydroxy-oxindole (**70**). The relevant bond distances (Å) are indicated, as well as the respective as well as the respective Wiberg indices (WI, italics).....54

Figure 2.7 - Energy profiles calculated for ethyl diazoacetate (eda) and dirhodium(II) tetraacetate. The relevant bond distances (Å) are indicated, as well as the respective as well as the respective Wiberg indices.....55

Figure 2.8 – Energy profiles calculated for the 1,2-aryl migration of the metallocarbene formed between the 3-substituted 3-hydroxy-oxindole and dirhodium(II) tetraacetate. The relevant bond distances (Å) are indicated, as well as the respective Wiberg indices.....56

Figure 2.9 – Mechanistic representation of the dirhodium catalyzed ring expansion reaction of 3-hydroxy oxindole.....57

Figure 2.10 - General catalytic cycle for Suzuki-Miyaura couplings.....60

Figure 3.1 - Incidence (blue) and mortality (red) of cancer worldwide. GLOBALCAN 2012 (IARC).....67

Figure 4.1 - conversion of L-Phe to L-Trr is via a pathway involving the para-hydroxylation of the benzene by PAH, the cofactor BH_4 snf molecular oxygen...86

Figure 4.2 - The domain structure of hPAH. Each hPAH subunit is classified into three structural and functional domains which are involved in regulation, catalytic activity, and oligomerization. Regulatory domain (yellow), catalytic domain (green) and tetramerization domain (blue) of the hPAH.....88

Figure 4.3 - Proposed model of PAH activation by Phenylalanine.....89

Figure 4.4 - Rational for the design of new PAH modulators.....94

Figure 4.5 – Differential scanning fluorimetry (DSF) assay.....96

Figure 4.6 – Thermal denaturation of hPAH followed by differential scanning fluorimetry (DSF). Assay Conditions: recombinat hPAH WT tetramer: 1 mg/ml

hPAH (2.5× SYPRO Orange) CFX96 Touch Real-Time system (Bio-Rad); FRET channel Melting curve: 20 to 70 ºC with increasing steps of 0.2 ºC with 1 s incubation time, using the for fluorescence acquisition 97

Figure 4.7 - DSF analysis of compounds **141** and **165-167** on the mid-point denaturation temperature of the a) regulatory domain (T_{m1}) and b) catalytic domain (T_{m2}) of hPAH. 98

Figure 4.8 - Activity of compound **20-22 and 2** in hPAH enzyme assay. 99

Figure 4.9 - a) DSF analysis of compounds **129** and **169** on the mid-point denaturation temperature of the regulatory (T_{m1}) and catalytic domain (T_{m2}) of WT-hPAH. b) Results of the activity assay for compounds **129** and **169**..... 101

Figure 4.10 – Results of 7-trifluoromethyl-4-carboxamide-3HQs in DSF assay. .. 103

Figure 4.11 – Activity assay of compounds on tetrameric wild-type *h*PAH enzyme. 104

Figure A1 - Metallocarbene conformations with and without intramolecular hydrogen bond determined at PBE1PBE/b1//PBE1PBE/b2level of theory. The energy corresponds to Gibbs Free Energy in ethanol, after thermal correction and the energy values are referred to the **70** +**$Rh_2(OAc)_4$** pair of reactants. The relevant bond distances (Å) are indicated, as well as the respective Wiberg indices (WI, italics) 175

Figure A2 - Energy profiles calculated for the dirhodium catalyzed quinolone formation. The minima and the transition states were optimized and the energy values (kcal/mol) are referred to pair of starting materials (**70**+**$Rh_2(OAc)_4$**) after thermal correction to Gibbs Free Energy in ethanol (in black) or to Gibbs free energy in vacuum at the PBE1PBE/b1 level of theory (in red). 175

Figure A3 - Energy profiles calculated for rhodium free quinolone formation, via a concerted pathway. The minima and the transition states were optimized with at the pbe1pbe/6-31G** level of theory. The energy values (kcal/mol) are referred to the Gibbs Free Energyof the 3-hydroxy-oxindole (**70**) in the **A** conformation represented. 176

Figure A4 - Energy profiles calculated for rhodium free quinolone formation, via a free carbene pathway. The minima and the transition states were optimized at the pbe1pbe/6-31G** level of theory. The energy values (kcal/mol) are referred to the Gibbs Free Energyof the 3-hydroxy-oxindole (**70**) in the **A** conformation represented. 176

Figure A5 - Energy profiles calculated for the rhodium catalyzed quinolone formation, via coordination to the carbonylic ester of the 3-hydroxy-oxindole (**5**). The minima and the transition states were optimized at the PBE1PBE/b1level of theory. The energy values (kcal/mol) are referred to the Gibbs Free Energyof the pair of starting materials represented (**J**). 177

Figure A6 - Energy profiles calculated for the dirhodium catalyzed quinolone formation, via coordination to the carbonyl of the oxindole ring. The minima and the transition states were optimized at the PBE1PBE/b1level of theory. The energy values (kcal/mol) are referred to the Gibbs Free Energyof the pair of starting materials represented (**M**). 177

Figure B3.1 - Depiction of the enzymatic reactions used in this study for evaluation of competition between substrate and compound (I - Substrate-activated condition), and activation by the compound (II - Non-activated *versus* III – Compound-activated condition). A blank reaction without the substrate was included and subtracted for each condition in order to rule out contribution of the compound to tyrosine formation. 189

Figure C1 – Assignment of ^{1}H and ^{13}C NMR spectra of **69**. 191

Figure C2 – Assigment of ^{1}H and ^{13}C NMR spectra of **31**. 191

Figure C3 – Assignment of the ^{1}H and ^{13}C NMR spectra of a) **125** and b) **126**. ... 192

Figure C4 – Assignment of the ^{1}H and ^{13}C NMR spectra of a) **130** and b) **131**. ... 192

List of Schemes

Scheme 1.1 – Tautomers of quinolin-2(1*H*)-one. 4

Scheme 1.2 – Biologically active Quinolin-2-ones and Medicinal Agents. 4

Scheme 1.3 – Structure and atom numbering of 4HQs and 3HQs. 5

Scheme 1.4 – Tautomers of 4-Hydroxyquinolin-2-ones 6

Scheme 1.5 – Representative 4-hydroxyquinolin-2-one natural products and pharmaceutical agents 6

Scheme 1.6 – Antitumor 3-carboxamide-hydroquinolin-4-ones 7

Scheme 1.7 – General Methodology for the synthesis of 4-hydroxyquinolin-2(1H)-one skeleton 9

Scheme 1.8 Synthesis of 4HQ esters from isatonic Anhydride **32** 10

Scheme 1.9 – The 3-hydroxyquinolin-2(1*H*)-one core present in the structure of naturally occurring products. 11

Scheme 1.10-Structure of 2,3-dihydroxypyridine **34** and tautomeric form of 3HQs. 11

Scheme 1.11 – Schematically representation of coordination cores. 12

Scheme 1.12 – Tautomeric form of quinoxaline. 15

Scheme 1.13 – Most active compound towards to [H-3]-glycine binding to the site associated with the NMDA receptor. in the 3HQs series. 16

Scheme 1.12 – Preparation of 2,3-dihydroxyquinoline **35** 21

Scheme 1.13 – Synthesis of 7-nitroquinolin-2-one **55** from 2-methyl-N-(2-methyl-5-nitrophenyl)formamide **51**. 21

Scheme 1.14 –Mechanism of cyclopenin conversion into viridicatin **31**. 22

Scheme 1.15 Formation of 3HQs by ring contraction of **52**. 23

Scheme 1.16 Pd-catalyzed formation of **62** using 3-bromo-4-phenylquinolinone **61**. 24

Scheme 1.17 – Eister Ring Expantion 27

Scheme 1.18 XXX 28

Scheme 2.1 - Schematic representation of the catalytic cycle of the di-Rhodium - catalyzed C-H bond activation/ C-C bond forming reaction of an α-diazoacetate with an Alkane. 37

Scheme 2.2- Rhodium catalysed three component reaction using chiral Brønsted acids. 38

Scheme 2.3 - [2+2] cycloaddition reaction between ethyl glyoxylate and trimethylsilylketene catalyzed by a di-Rhodium carboxamide 39

Scheme 2.4 - Cooperative metal-organo-catalysed reactions based on di-Rh(II) and Lewis base organo-catalysts 39

Scheme 2.5 - Potential di-Rh(II) inhibition when used in combination with Lewis base organocatalysts**.** 40

Scheme 2.6 - Molecules that can be prepared via a ring expansion strategy. 41

Scheme 2.7 - Unwanted reaction in the Metal-Organo-Catalysed ring expansion using EDA 42

Scheme 2.8 –EDA addition to isatin followed by Eistert ring expansion reaction catalysed by $Rh_2(OAc)_2$ 43

Scheme 2.9 - Recycling dirhodium(II) complex ring expansion-reaction. 45

Schema 2.10 - A metal-organo-catalytic system for the synthesis of 3HQs 46

Scheme 2.11 – One-pot reaction using *N*-methyl-isatin with EDA in the presence of DBU 15 mol% and $Rh_2(OAc)_4$ in DCM 50

Scheme 2.12 – Ligands influence on the electrophilicity of dirhodium(II) complexes 51

Scheme 2.13 – Dirhodium(II) catalysts evaluated in the one-pot Eistert ring expansion of isatins with EDA. 52

Scheme 2.14- Synthesis of 3-hydroxy-4-bromoquinolin-2(1*H*)-one **106** 60

Scheme 2.15 – Synthesis of viridicatin alkaloid derivatives based on the Suzuki-Miyaura coupling reaction of aryl-boronic acids with 3-hydroxy-4-bromoquinolin-2(1H)-ones 62

Scheme 3.1 Synthesis of 4-carboxylate substituted 3HQs **69**, **84-96** based on an Eistert ring expantion reaction of isatins with diazo acetate (EDA) catalysed by di-rhodium complexes. 69

Scheme 3.2 – Synthesis of compound **111** 71

Scheme 3.3 Synthesis of compound **112** based on an Eistert ring expansion reaction of isatins with EDA catalysed by di-rhodium complexes. 71

Scheme 3.4 – Synthesis of diazo acetates **113-115** 72

Scheme 3.5 Synthesis of 4-carboxylate substituted 3HQs **116-120** based on an Eistert ring expansion reaction of isatins with different diazo compounds, catalysed by di-rhodium complexes. 73

Scheme 3.6- Synthesis of 4-carboxamides-3HQs 75

Scheme 3.7 Alternative synthetic route for synthesis of 4-carboxamides-3HQs 75

Scheme 3.8 Preparation of succinimidyl diazoacetate **124**. 76

Scheme 3.9 Synthesis of 4-NHS -3HQs based on Eistert ring expansion reaction of protected isatins with NHS-diazo acetate, followed by an amidation step. 78

Scheme 3.10 Synthesis of 4-carboxamide-3HQs **127-129** 78

Scheme 3.11 Synthesis of 6-F_3CO-4-NHS -3HQs based on Eistert ring expansion reaction of protected isatins with NHS-diazo acetate, followed by an amidation step. 79

Scheme 3.12 Synthesis of 4-carboxamide-3HQs based on Eistert ring expansion reaction of 6-trifluoromethoxy-isatin with NHS-diazo acetate, followed by an amidation step. 80

Scheme 4.1 - Catalytic mechanism of catalytic mechanism of PAH and its intervenients: Fe, O_2 and BH_4.[155] 87

Scheme 4.2 - Chemical structure of compound with potential pharmacological chaperone ability hits from Pey *at al.* [161] 91

Scheme 4.3 - Compounds with potential pharmacological chaperone ability. Hits from Santos-Sierra *et al.* [163] 92

Scheme 4.4 - Structure of compound **161,** a Phe-like modulator with affinity to the active site of *h*PAH. 93

Scheme 4.5 - Synthesis of 4-L-Phe-3HQs **141** and **165-167.** 95

Scheme 4.6 - Synthesis of 4-L-Phe-3HQs **129** and **166.** 100

Scheme 4.7 - Compounds 7-trifluoromethyl-4-carboxamide-3HQs**.** 102

Scheme 5.1 - The 3-hydroxyquinolin-2(1H)-one (3HQ) core present in the structure of natural occurring compounds, as a carboxylic acid bioisoster and as an enzyme inhibitor. 109

Scheme 5.2 - Synthesis of 4-Ester-3HQs, 4-Carboxamide-3HQs and viridicatin derivatives 31. a) DBU, dirhodium complex (1 mol%), absolute EtOH, r.t., 3h; b) (i) NaOH, H_2O, reflux, 7h; (ii) aq HCl; (iii) NBS, DMF; c) 10 mol% $Pd(PPh_3)_4$, Na_2CO_3/H_2O, DME:H_2O 3:1, MW, 150ºC, 2h; f) TEA, $Rh_2(OAc)_4$ (1 mol%), DCM, r.t.; g)HNRR', Na_2CO_3, DMF, r.t., overnight. 111

Scheme 5.3 – Structure-activity-relationship of compound **143** towards cancer cells**.** 113

Scheme 5.4 – Structure-activity relationships (SAR) of 6-F_3OC-carboxamide-3HQ over hPAH. 116

List of Tables

Table 1.1 – 3HQs preparation through one-pot Knoevenagel condensation/epoxidation of cyanoacetanilides followed by decyanative epoxide-arene cyclization – substrate scope 25

Table 1.2 –Synthesis of 3HQs derivatives 26

Table 1.3 – Lewis Acids promoted ring expansion of α-diazo-β-hydroxy ester **70.** 29

Table 2.3- Effect of the amount of DBU in the ring expansion reaction in ethanol[a] 48

Table 2.4 – Eistert ring expansion of isatins with EDA using a sequential DBU/$Rh_2(OAc)_4$ system. 49

Table 2.4 – Eistert ring expansion of isatins with EDA using a one-pot DBU/$Rh_2(OAc)_4$ system.[a] 52

Table 2.5 - Eistert Ring expansion of isatins with EDA using a one-pot relay DBU/$Rh_2(OAc)_4$ system. 53

Table 2.5 - Catalyst screening for Suzuki-Miyaura coupling of **106** and phenylboronic acid 61

Table 3.1 – Anti-proliferative evaluation of compounds **69** and **84**-**96** against MCF-7, NCI-H460 and HT-29 cancer cell lines. 70

Table 3.2. Anti-proliferative evaluation of compounds **111-112** against MCF-7, NCI-H460 and HT-29 cancer cell lines. 72

Table 3.3 – Anti-proliferative evaluation of compounds **116-120** against MCF-7, NCI-H460 and HT-29 cancer cell lines 74

Table 3.4 – Optimization of reaction conditions of NHS-diazo addition on *N*-benzyl-isatin. 77

Table 3.3 Anti-proliferative evaluation of compounds **132**-**143** against MCF-7, NCI-H460, HT-29 AND CHOK1 cell lines. 81

Table 5.1 – Anti-proliferative activity of 7-OCF_3-3HQ series against MCF-7, NCIH460 and HT-29 cancer cell lines and CHOK1 non-cancer cell lines.....114

Abbreviations and Definitions

3HQ: 3-hydroxyquinolin-2(1H)-one

4HQ: 4-hydroxyquinolin-2(1H)-one

ACT: aspartate kinase, Chorismate mutase and TyrA

BH_4: tetrahydropterin

BMS: Bristol-Myers Squibb

CNS: Central nevous system

CHOK1: Chinese hamster ovary cells

DAOO: D-amino acid oxidase

DBU: 1,8-Diazabicyclo[5.4.0]undec-7-ene

DCM: dichloromethane

DMO: dimethyl oxalate

DIPEA: diisopropyl ethyl amine

DSF: differential scanning fluorimetry

EDA: ethyl diazoacetate

FAD: flavin adenine dinucleotide

HIV: Human Immunodeficiency Virus

hPAH: human Phenylalanine Hydroxylase

HRNase H: Ribonuclease H

HT-29: human colorectal adenocarcinoma cells

HPA: hyperphenylalaninemia

LNAA: large neutral amino acid

L-Phe: L-phenylalanine

L-Tyr: L-tyrosine

MCF-7: breast cancer cells

MS: multiple

MOC: Metal-organocatalysed system

NCI-H460: human non-small lung cancer cells

NHCs: N-heterocyclic carbenes

NMDA: N-methyl-D-aspartate

NMRAr: N-methyl-D-aspartate receptors

PAH: Phenylalanine Hydroxylas

PCs: pharmacolo

PEG-PAL Polyethylene glycol phenylalanine ammonia lyase

PKU: Phenylketonuria

RE: ring expansion

RD: regulatory domain

RT: Reverse transcriptase

SAR: structure-activity relationship

SMC: Suzuki-Miyaura reaction

SMOLs: chemically manufactured molecules

TEA: diisopropyl ethyl amine

TH: tyrosine hydroxylase

THF: Tetrahydrofuran

TNF: tumor necrosis factor

WHO: World Health Organization

WT-hPAH : wild-type human Phenylalanine Hydroxylase

General Introduction

Rational and Aims

Humankind has been enroled in the discovering new drugs for thousands of years.[1] A 90 % percent of the drugs on the market are small, chemically manufactured molecules (or SMOLs for short).[2] Furthermore, small-molecule drugs still account for approximately two-thirds of the candidates in the current robust pharmaceutical industry pipeline. [2] Computer technology coupled with emerging protein structures for identification and validation of biological target gave a great emphasis on inventive design of biologically active small molecules to generate high quality drug candidate. To keep up with the demand of new entities, development of new chemical tools for the synthesis of these molecules has been equally swift.

The 3-hydroxyquinolin-2(1*H*)-one (3HQ) core is an important motif that is present in the structure of viridicatin, viridicatol and 3-O-methyl viridicatin naturally occurring products.[3, 4] These metabolites, isolated from penicillium species, have been shown to inhibit the replication of human immunodeficiency virus and to be promising lead compounds for the development of new anti-inflammatory agents.[5, 6] Furthermore, this unique heterocycle was recognized to be a valuable bioisoster for the carboxylic acid function of α-amino acids. Although less acidic (pKa of 8.7) then a carboxylic acid,[7, 8] a series of 3HQs were prepared at Pfizer and shown to be potent inhibitors of the D-amino acid oxidase activity, eliciting similar binding interactions with the enzyme active site as the carboxylic acid containing inhibitors.[9] These discoveries were not left unnoticed, and recently this pharmacophore was found to bind to metal cofactors, by this way inhibiting the influenza A endonuclease. Prompted by these results, the main objective of this project is to synthesize novel derivatives of 3HQ scaffold and evaluated its biological activity.

The specific objectives of this PhD project are:

- to develop robust synthetic methods for the target 3HQ derivatives based on Ring Expansion with ethyl diazo acetate and cooperative Metal-Organo-Catalysed (MOC)- using di-rhodium(II) complexes in combination with Lewis base organo catalysts. These method can allow the creation of small library of 3HQs and the preparation of Viridicatin alkaloids;
- to use advanced two-dimensional NMR techniques (COSY, HMQC and HMBC) as well as elementar analisis mass and UV to confirm the chemical structure of all synthesized derivatives:
- to understand and get further insight into the reaction mechanism of the ring expansion reaction catalyzed by dirhodium complexes by Density Functional Theory (DFT)(performed by Dr Nuno Candeias).
- to evaluate 3-hydroxyquinolin-2(1H)-one derivatives as antiproliferaqtive agents and as modulators of PAH

Outline of the thesis

Chapter 1 aims to present an overview of biological activities of compounds derived from the quinolin-2(1H)-one. An overview on synthetic methodology and biological activity of the 3-Hydroxyquinolin-2(1*H*)-one scaffold and its isomer 4-Hydroxyquinolin-2(1*H*)-one are going to be discussed. Moreover this chapter aims to point out the important properties of 3HQ scaffolds as bioisoster of a-aminoacid[8] and chelator of metallic centers.[10]

Chapter 2 will discuss the design and synthetic strategy for the preparation of 3-hydroxyquinolin-2(1H)-one derivatives via ring expansion protocols based on ethyl diazo acetate and MOC system - di-Rhodium (II)/organic bases-. Characterization of obtained compounds by several methodologies, like NMR, will be discussed, as well as the synthesis and characterization of several intermediates used to achieve these derivatives. Also investigation of the mechanism of reaction by DFT calculation is

going to be discussed. Finally, the methodologies developed will be used to prepare viridicatin alkaloids and its derivatives.

Chapter 3 will present the evaluation of 3HQs library as anti-cancer agents, against a panel of cancer lines: breast cancer cells, human non-small lung cancer cells and human colorectal adenocarcinoma cells. Also the library was evaluated for toxicity using the non-cancer Chinese hamster ovary cells.

Chapter 4 aims at designing molecules based on the L-Phenylalanine and 3HQ structure to target Phenylalanine hydroxylase enzyme responsible for Phenilkenonuria disease. The objective in this progect is to stabilize the active site and the regulator domain without inhibiting severely the enzyme and restore its activity. By exploring this double stabilization mechanism we hope to develop a method that can be used to rescue the stability of a broad panel of PAH mutations.

Chapter 5 will integrate all studies described in the previous four chapters and provide a global overview of the synthesized 3HQ derivatives. Also biological activity of these compounds will be discussed

Chapter 6 will presente all the experimental procedures used to development in the present study. In particular synthetic methodologies, physical-chemical properties, biochemical studies and *in vitro* studies will be described.

Chapter I

I. Hydroxy-quinolin-2(1*H*)-ones: A synthetic and biological overview

Abstract

3HQs heterocycle is an aromatic ring system fused to a lactam ring that present an enol hydroxyl moieties as bioisoster of carboxylic acid. Although, less acidic than carboxilic acids (pka =8) series of 3HQs were shown to be potent inhibitors of the D-amino acid oxidase activity, eliciting similar binding interactions with the enzyme active site as the carboxylic acid containing inhibitors. Moreover, this acidic feature together with the lactamic nitrogen can mimic the a-aminoacid glycine, registering 3HQs as one of the limited examples of bioisoster of aminoacid.

1.1 The Quinolin-2(1*H*)-one scaffold

In the pharmaceutical industry nitrogen heterocycle compounds have paved the way for exceptional achievements in the fight against many life threatening diseases.[11] Quinolin-2(1*H*)-ones establish the basic structure of many natural and synthetic biologically active molecules and their literature has been extensively reviewed each year since 1989 in *Progress in Heterocyclic Chemistry*.[12] In figure 1.1 is displayed a chart of published papers about quinolin-2(1*H*)-ones in each year since 1982. The large number of publications depicted in the chart, suggest with no surprise, that the development of new methodologies to synthetize biologically active quinolin-2(1*H*)-ones compounds still remains as a very important goal in organic chemistry.

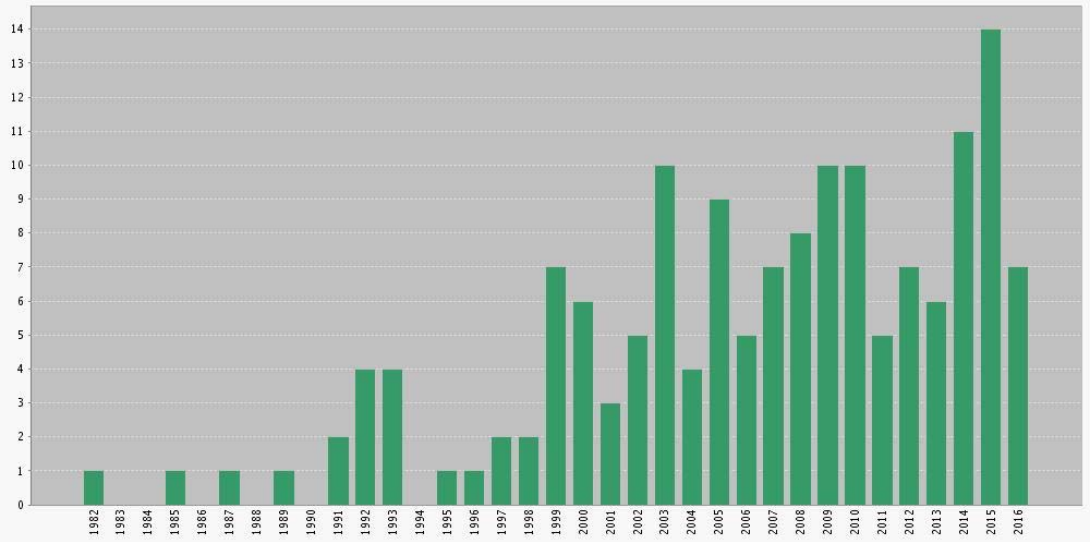

Figure 1.1 – Number of publications referring quinolin -2(1*H*)-ones since 1982, according to Web of Science and using "Quinolin -2(1*H*)-ones" as keyword.

Generally, quinolin-2(1*H*)-ones are mentioned also as carbostyrils, 2-hydroxyquinolines, 2-quinolonols, or 2-oxaquinolines. Quinolin-2(1*H*)-ones are an important class of compounds since they are a coumarin isoster. They are isomeric to quinolin-4-ones and have two tautomeric forms, the lactam form **1** and the phenolic form **2** (Scheme 1). However, in the solid state, the compound exists exclusively as the lactam form **1**.[13, 14]

As a "privileged" scaffold, the quinolin-2(1*H*)-one shows interesting biological properties and it is found in many natural products[15-18] and medicinal agents. In particular, the quinolin-2(1*H*)-one core is found in rebamipide **3**, a medicinal antiulcer agent[19], used in a number of Asian countries, or repirinast **4,** an antiallergenic compound useful in the treatment of allergic asthma (Scheme 1.2).[20]

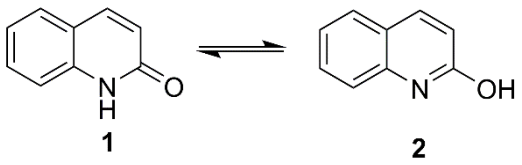

Scheme 1.1 – Tautomers of quinolin-2(1*H*)-one.

Noteworthy, a broad range of biological activities of quinolin-2-one compounds were disclosed in recent years. Members of this class of compound have been reported to show potent antimicrobial activity[21], possess neuro protective properties[22] and have also proved their potential as excellent inhibitors of acyl co-enzyme A and cholesterol acyltransferase.[23, 24]

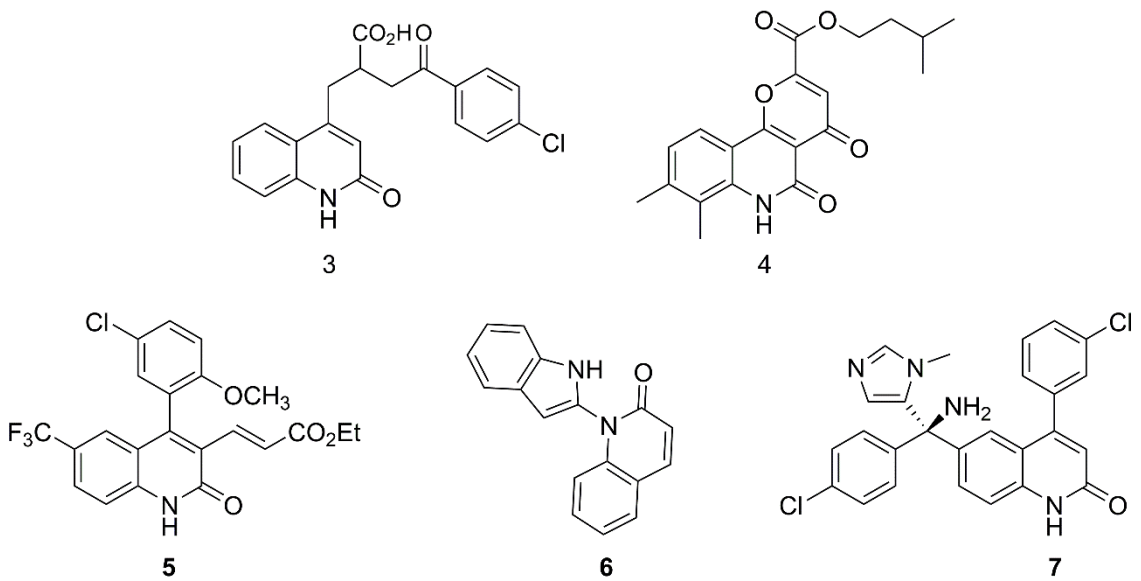

Scheme 1.2 – Biologically active Quinolin-2-ones and Medicinal Agents.

Furthermore, a group from Bristol-Myers Squibb (BMS) identified compound **5** and the related reduced allylic alcohol, as novel and potent maxi-K channel openers useful for the treatment of male erectile dysfunction.[25] A class of potent KDR (kinase insert domain-containing receptor) inhibitors, a primary mediator of tumour-induced angiogenesis containing the 1H-indole-2-yl-quinolin-2(1*H*)-one core structure **6** was reported by Merck and show great interest as potential therapeutic agents.[26] A clinically important quinolin-2(1*H*)-one was discovered by Johnson & Johnson Pharmaceutical Research & Development, with registration number R115777 (Zanestra) **7** and is currently under phase II clinical trials as a novel orally active antitumor agent. Zanestra is a 4-arylquinolin-2(1*H*)-one that emerged as a selective nonpeptide farnesyl protein antitumor inhibitor of Ras , an oncoprotein involved in the intracellular signalling pathway leading to cell proliferation.

A number of derivatives of quinolin-2-one have been reported to show different and promising biological properties and have attracted much attention from the medicinal chemist community.[18, 21, 23, 24, 26-42] In particular, 4-hydroxyquinolin-2-ones (4HQs) and 3-hydroxyquinolin-2-ones (3HQs) have demonstrated to be a very appealing class of small-size heterocycle molecules. 4HQs and 3HQs are isomeric compounds, the OH group changes in the lactam ring position from C-3 to C-4 and despite this small variation, the physicochemical properties and the biological activity of both compounds change considerably. These properties and the synthetic methods used to prepare 4HQs and 3HQs compounds will be discussed in the next section.

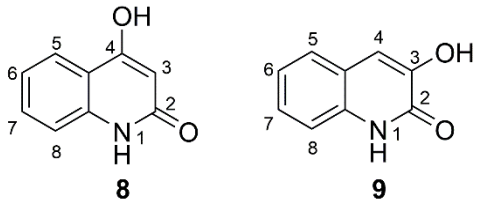

Scheme 1.3 – Structure and atom numbering of 4HQs and 3HQs.

Overview of 4-hydroxyquinolin-2-ones

1.1.1 4-Hydroxyquinolin-2-ones biology

4-Hydroxyquinolin-2-ones (**10**) derivatives are important as biologically active compounds and synthons in organic synthesis. The main feature of this hydroxyquinoline is that it can exist in three tautomeric forms, namely 2-hydroxyquinolin-4-ones (**11**) and 2, 4-dihydroxyquinolines (**12**). Normally, they exist as **10** but solvents can affect the equilibrium.

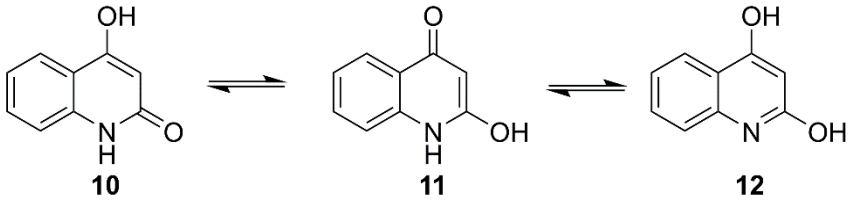

Scheme 1.4 – Tautomers of 4-Hydroxyquinolin-2-ones

This ring core is the base of a large number of alkaloids present in many medicinal plants, microbial sources and animals. Usually in nature these alkaloids are found prenilated (**13)** in the 4-hydroxy or with a methoxy groups (**14)** or substituted with anellated pyrano rings (**15)** (e.g. flinderisine, oricine, orixalone D and huajiaosimuline) that also display a wide range of biological activities.

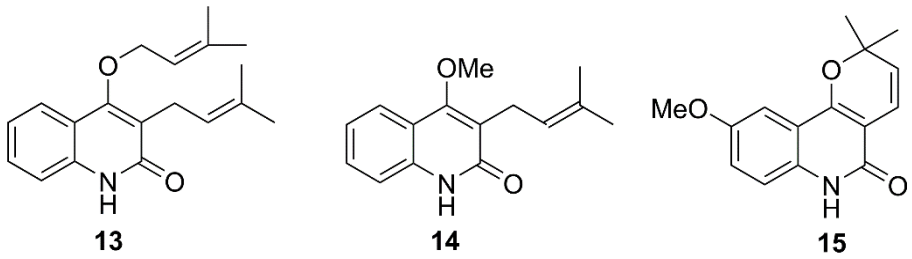

Scheme 1.5 – Representative 4-hydroxyquinolin-2-one natural products and pharmaceutical agents.

Recently a directed bioassay of the CH_2Cl_2-MeOH extract of *Euodia roxburghiana* resulted in the isolation of quinolone **13** which was shown to be active against

infectious HIV-1 in human lymphoblastoid host cells (EC_{50}=1.64 μM, IC_{50} 26.9 μM) and to inhibit the activity of the HIV-1 reverse transcriptase assay (IC_{50} = 8 mM).[43]

4-Hydroxyquinolinones have attracted considerable attention for various therapeutic areas including applications as antimicrobial agents,[44] antimalarial agents,[45] aldose reductase inhibitors,[46] anticonvulsants,[47] and RNA polymerase inhibitors for the treatment of Hepatitis C.[48]

Recently, carboxamide derivatives of 4HQs have been investigated for their important activities against auto-immune diseases such as rheumatoid arthritis, systemic lupus erythematosis and multiple sclerosis. [49-51] A remarkable representative of this derivatives is linomide **16** (Scheme 1.6), an orally active agent that consistently inhibits growth of a large series of both rodent and human prostate cancer xenografts tested in vivo. The anti-tumour ability of this compound is related to the capacity to inhibit tumour angiogenesis. It was demonstrated by a study in rats bearing linomide treated tumour, that the agent decrease the number of tumour blood vessels with a consequently reduction in the tumour bloodflowin.[52-54] A second generation of 3-carboxamide-hydroquinolin-4-ones such as ABR-215050 (tasquinimod) **17** (Scheme 1.6) inhibit the growth of a series of four additional human and rodental protate cancer model in mice.[55] The mechanism for linomide's therapeutic activities is not fully understood.

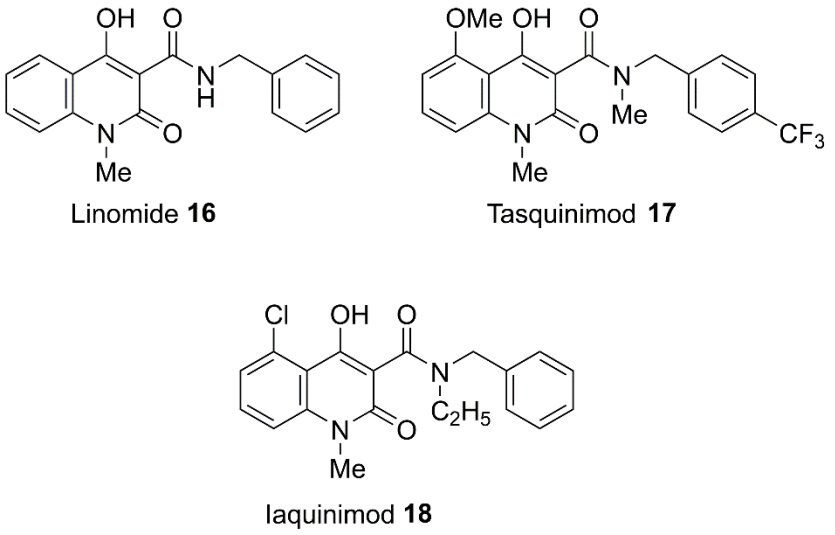

Scheme 1.6 – Antitumor 3-carboxamide-hydroquinolin-4-ones.

However considerable amount of data attribute its therapeutic activities to its ability to regulate cytokine production.[56-58] Furthermore, the production of proinflamatory cytokines involved in tumor angiogenesis by macrophages is also involved in the auto-destruction and demyelination in multiple sclerosis (MS).

Therefore, linomide was tested in a series of phase II and III trials in MS patients, although phase III trial had to be discontinued because of undesirable toxicity.[59, 60] In order to obtain more efficient compounds for the treatment of MS, an optimization of the lead compound **16** was performed. Chemical modifications and structure-activity relationship (SAR) give raise to a new series of 3-quinolinecarboxamide derivatives and compound laquinimod **18** gave a similar immune response and cytokine balance as the lead compound **16**. Currently there is an ongoing study of laquinimod in phase II to access the efficacy, safety and tolerability of the oral dose in subjects with primary progressive MS. A discontinuation of higher doses 1.2mg/day of laquinimod has been done, after the occurrence of cardiovascular events, none of which was fatal, in eight patients.[61] Nevertheless the study for lower doses 0.6mg/day is still ongoing.

1.1.2 4-Hydroxyquinolin-2-ones chemistry

One of the requirements of any synthetic strategy for drug development is that the synthetic pathway must be amenable to provide chemical diversity in order to obtain a large number of structural motifs.[62, 63] From the chemical point of view, 4HQs, possessing this enolic β-dicarbonyl moiety, have attracted chemists not only with the aim to develop simple and efficient routes to achieve highly functionalized 4-hydroxyquinolin-2-ones but also using this 4HQs as synthon for the preparation of other natural products such as dimeric quinoline alkaloids and other polycyclic heterocycles.[64] There are well documented different synthetic methods for the synthesis of 4HQs. Generally, a common route to these compounds is the intramolecular Claisen-type condensation of N-acylated anthranilate esters. The *N*-acylated anthranilate esters **19** can be acylated with malonyl chlorides **20** and cyclized

to 4HQ ester **22** under acidic conditions (Scheme 1.7 method A).[65] An alternative approach to synthetize new 4HQ derivatives has been proposed by Jonsson et *al.* Starting from aromatic 2,6-difluorobenzonitrile **23**, a double nucleophilic aromatic substitution was performed to introduce at position 5C of 4HQs core, substituents such as methoxy, dimethylamino, and thiol **27** (Scheme 1.7 method B).[61]

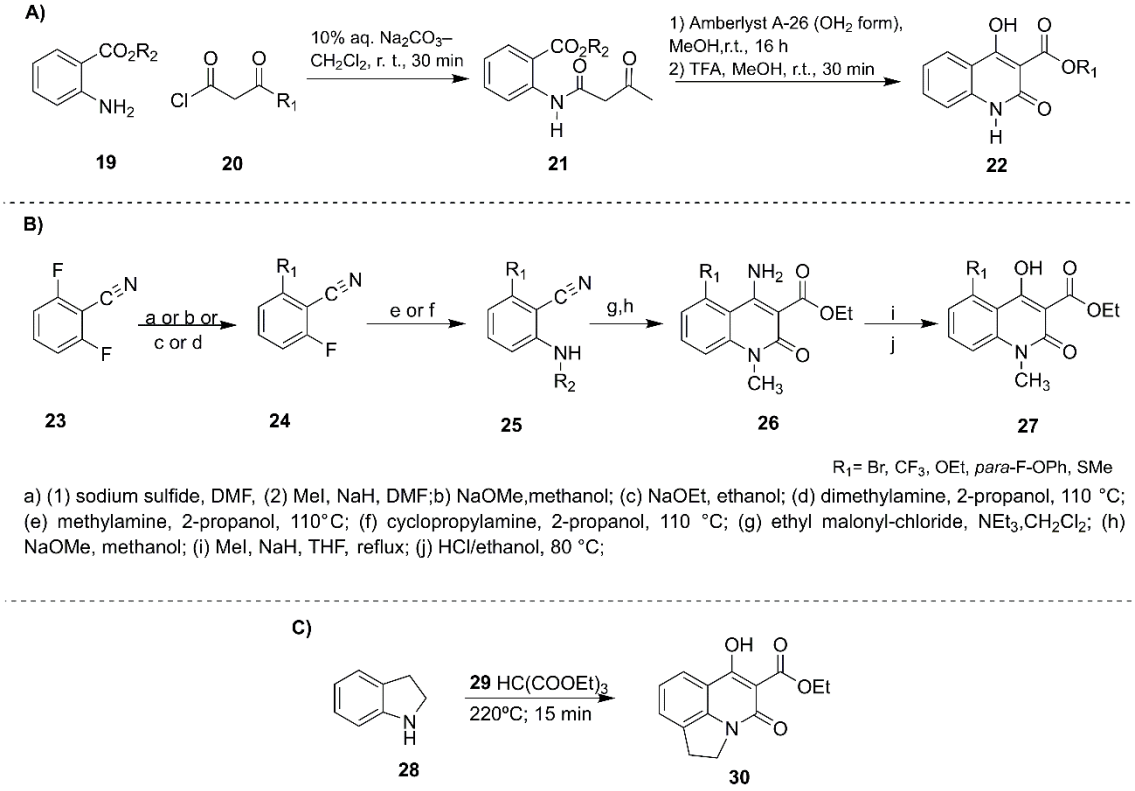

Scheme 1.7 – General Methodology for the synthesis of 4-hydroxyquinolin-2(1H)-one skeleton

Also, reaction of indoline **28** heated with an excess of methanetricarboxylates **29** yielded derivatives of 4HQs in good yield (Scheme 1.8 method C).[66]Although this transformation presents advantages for the synthesis of 4HQs, high reaction temperatures (>200 °C), limited availability of a broad range of suitably substituted starting materials, and the need to isolate the acylated intermediate prior to cyclization, limit the widespread application of the method. The most common employed method was develop by Coppola and co-workers which have synthesized 4HQs compounds using isatoic anhydrides **32** as precursors and involves an *N*-alkylation, followed by malonate addition-intramolecular cyclization sequence (Scheme 1.8). [67, 68,69]

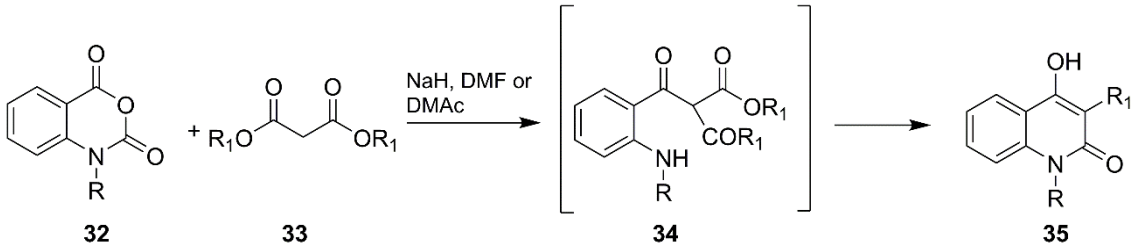

Scheme 1.8 Synthesis of 4HQ esters from isatonic Anhydride **32**

1.2 Overview on 3-Hydroxyquinolin-2-ones

1.2.1 3-Hydroxyquinolin-2-ones biology

Despite being an isomer of 4HQs, very little is known about 3-hydroxyquinolin-2(1*H*)-one (3HQs) from biological and synthetic perspectives. The 3HQ core is an important motif that is present in the structure of naturally occurring products viridicatin **31**, viridicatol **32** and 3-*O*-methyl viridicatin **33**. These metabolites, were first isolated from the mycelium of *Penicillium viridicatum* Westling and later on various strains of *Penicillium cyclopium* Westling[4] with the production of a strong, penetrating earthy odour. The earliest biological assay of **31** were done against *Escherichia coli*, *Bacillus subtilis*, and *Staphylococcus aureus* (*Micrococcus pyogenes*, var. aureus) but no antibiotic activity was found. Although some activity was observed on *in vitro* tests against *Mycobacterium tuberculosis* at a dilution of 1:15 000, while no activity against *Entamoeba histolytica* was detected.[3] The viridicatin metabolite **33** methylated in the 3-OH was isolated in 1964 by Austin and Myers from the fungus *Penicillium puberulum*.[70] It remained unexplored until 1998 when Heguy and co-worker reported its effect as inhibitor of replication of the HIV virus induced by tumor necrosis factor (TNF). Having an IC_{50} of 2.5 μM, this compound was recorded as a promising lead for the development of new anti-inflammatory agents.[5]

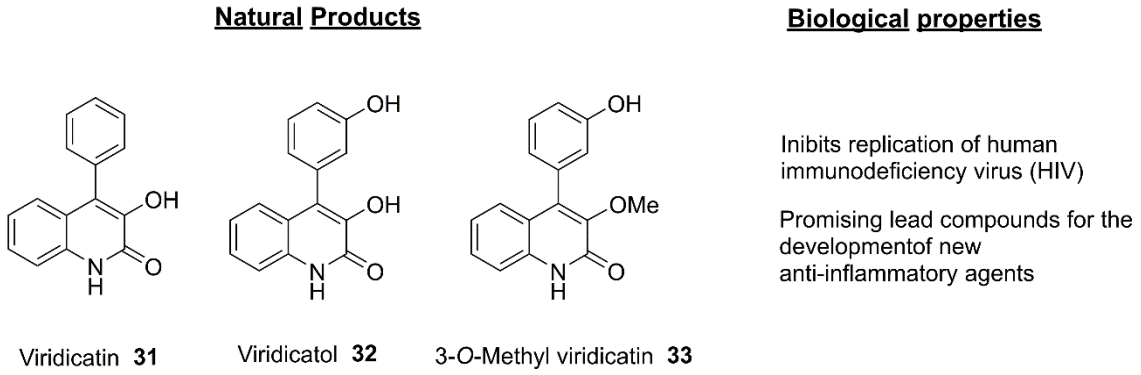

Scheme 1.9 – The 3-hydroxyquinolin-2(1*H*)-one core present in the structure of naturally occurring products.

These discoveries were not left unnoticed, and recently a group from the University of Lille, developed a series of 3HQs with potent activity against HIV-1 reserve transcriptase associated RNase H activity. Ester and amide groups were introduced at C-4 position of the 3HQs scaffold and also some modulation was performed in the benzenic moiety, which allowed the construction of a library of 19 compounds. The rational for choosing 3HQs as pharmacophore was made on the bases of its ability to complex some bivalent metals, as showed by the work of Strashnova and co-workers.[10] In their previous studies on the complexation of 2,3-dihydroxypyridine **34** with metals, they shown that this compound participates in the coordination as mono – or dicantonionic species and acts as a bridging ligand.

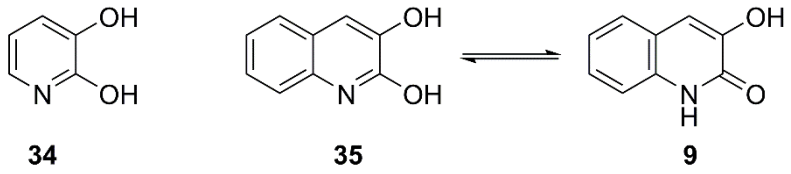

Scheme 1.10-Structure of 2,3-dihydroxypyridine **34** and tautomeric form of 3HQs.

3HQ **9** and its tautomeric form, 2,3-dihydroxyquinoline **35**, are structural analogues of 2,3-dihydropyridine **34** (Scheme 1.10). The main common characteristics of these two molecules are: a slight tautomerization, presence of several potential coordinative centres, which can yield the cationic, neutral and anionic complexes. The complex formation with 2,3- dihydroxyquinoline $(HL)_2$ show that the coordination

core structure depends mainly on the characteristics of the central metal atom and on the most stable tautomeric form of the ligand under the synthec conditions. The authors identified complexes with different metals and summarized the result as shown in the Scheme 1.11. HL_2 participates in the coordination in the monoanionic or neutral forms with the formation of chelate cycles. Two main class of coordination species are depicted (Scheme 1.11), first one represented by the formula $M(HL)_2 \cdot 2H_2O$ containing metal such Mn, Ni, Cu, where two molecules of 3HQs are coordinated with the metal and two molecules of water giving chelate cycles. The second type of coordination involved the 1:1 coordination of the 3HQ compound and the metal $Fe(HL)OH \cdot 2H_2O$ **39**, $Co(HL)OH \cdot H_2O$ **40**, while Cadmium participate as $Cd(H_2L)Cl_2$ **41**.

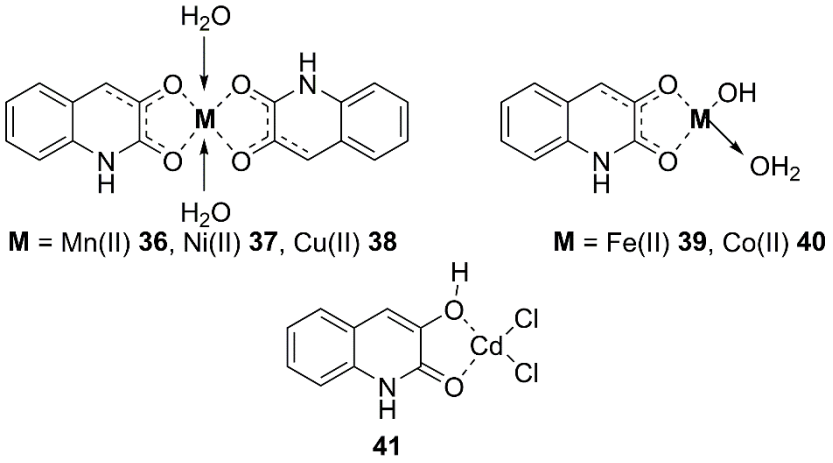

Scheme 1.11 – Schematically representation of coordination cores.

In a recent review entitled "Viral enzymes containing magnesium: Metal binding as a successful strategy in Drug design"[71] is shown that metal-activated enzymes are important targets in drug discovery and in particular for antivirals discovery. Such proteins contain one or more metal ion cofactors, prevalently located in the active site, which are essential to perform biological functions. The common features of possible efficient inhibitors of metal enzymes are resumed in: highly polar pharmacophore motives, ionisable moieties, and coplanar pre-organized structure capable of simultaneous binding two Mg^{2+} ions.[71] Based on this rational, the work of

Cotelle and co-workers[72] aimed at developing derivatives of 3HQs to target the catalytic site of the ribonuclease H (HRNase H) function, associated to the viral coded reverse transcriptase (RT). In order to complex the bivalent metals in the catalytic site of the enzyme, the author introduced a carbonyl function at position C-4 of the 3HQ scaffold. By this introduction the 3HQs comprises three oxygens, which is the ideal topology to bind two divalent cations, separated by 4–5 Å in the case of an enzyme–metals–ligand ternary complex. Such a pharmacophore can be observed in the structure of most recently discovered RNase H inhibitors.[72] The most active compounds were the 4-amido series able to inhibit the RT RNase H with an IC_{50} between 16 and 22 μM, comparable with a reference compound. The authors also performed *in silico* docking studies in order to determinate the possible binding mode. The magnesium chelation was examined in the study and the authors confirmed the ability of this three oxygen pharmacophore to chelate both metal cofactors within the active site of the enzyme. Compound **42** is an inhibitor of the enzyme with an activity of 19 μM. As shown in Figure 1.2, the quinolone scaffold is positioned in such a way that the two oxygen atoms of the carbonyl and the enol functions in positions 2 and 3 target the magnesium cations.[72]

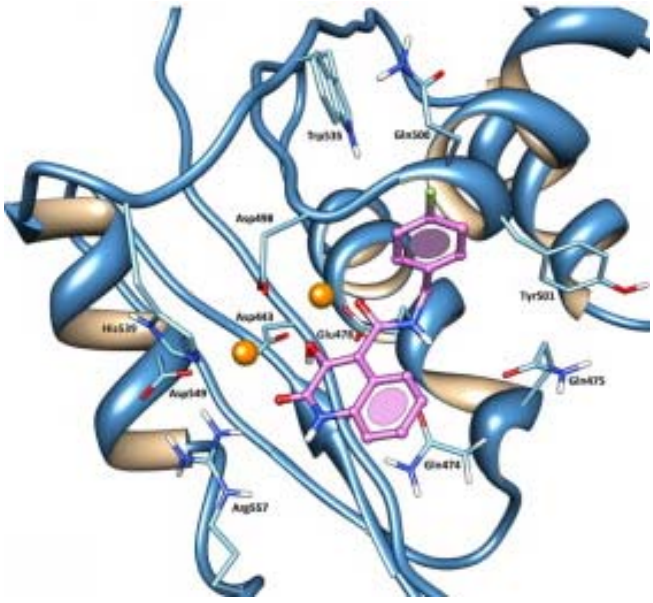

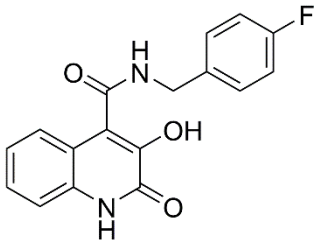

42

Inhibitor of RT RNase H (IC50 = 19 μM)

Figure 1.2 – Putative binding mode of amide **42** in the RT RNase H catalytic site.[72]

The metal-chelating properties of 3HQs inspired also the work of La Voie to develop a series of these compounds as inhibitors of Influenza A Endonuclease. The most active molecule was found to be compound 7-(*p*-fluorophenyl)-3-hydroxyquinolin-2(1*H*)-one **43** with and IC_{50} of 0.5 μM. An X-ray crystal structure of **43** complexed with influenza A endonuclease nicely disclosed that it binds through bimetal chelation at the active site as shown in Figure 1.3.[73]

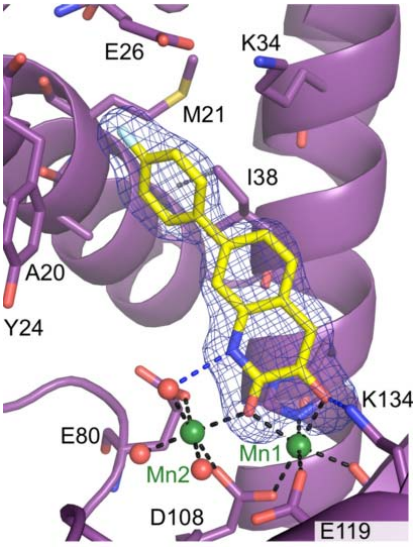

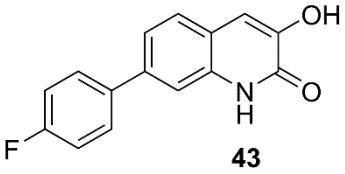

43

Metal chelator: Inhibitor of influenza A endonuclease (IC50 = 0.5 μM)

Figure 1.3 – Binding of compound **43** at the endonuclease active site.[73]

Chelation of enzyme metal cofactors is not the only property of this interesting core. Recently, with the purpose to discover ligands for N-methyl-D-aspartate (NMDA) associated glycine binding, a series of 3HQs have been synthetized. NMDA receptors (NMDARs) are glutamate-gated cation channels with high calcium permeability that play important roles in many aspects of the biology of higher organisms. They are critical for the development of the central nervous system (CNS), generation of rhythms for breathing and locomotion, and the processes underlying learning, memory, and neuroplasticity. Consequently, abnormal expression levels and altered NMDA receptor function have been implicated in numerous neurological disorders and pathological conditions (including stroke, hypoxia, ischemia, head trauma, Huntington's, Parkinson's, and Alzheimer's diseases, epilepsy, neuropathic pain, alcoholism, schizophrenia, and mood disorders).[74-76]

Based on the tautomer **45** of quinoxaline derivatives **44**, in which the amide and the enol hydroxyl moieties mimic a protonated glycine responsible for bonding with NMDA receptors, Sing-Yuen Sit and co-workers[77] synthesized twenty-four 3HQs derivatives **9**, formally isoster of quinoxoxaline tautomer **45** .

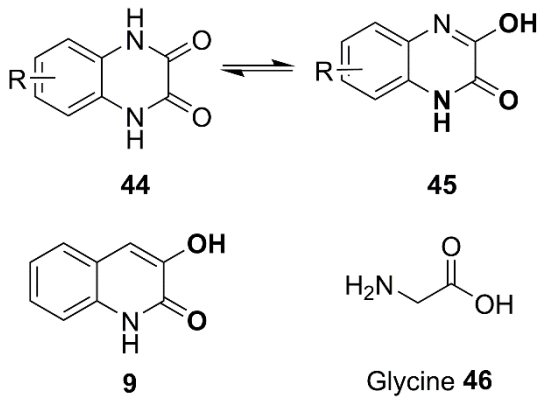

Scheme 1.12 – Tautomeric form of quinoxaline.

3HQs derivatives were studied and their ability to displace radio ligand (^{3}H)-glycine from rat cortical membranes was evaluated. All compounds demonstrated a 60% displacement of the radio ligand at 10 μM and from the results of the assay a structure-activity relationship was elucidated, supporting the 3-hydroxyquinolin-2-one heterocycles as effective structural elements for glycine ligands. Some modification on the central core was done leading to improved activity of these compounds, namely introduction of an electron withdrawing group in position C-4 and modification of the benzyl moiety resulted in more affinity for the glycine binding site on NMDA, hypothesised to be due to the increase acidity of 3-hydroxyl group. However, no activity was detected in the assay where 3-hydroxy group was methylated, identifying the free OH group as essential pharmacophore of the molecule

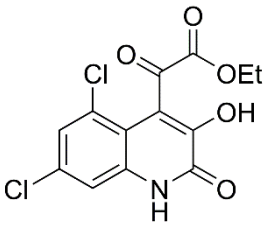

47

Scheme 1.13 – Most active compound towards to [H-3]-glycine binding to the site associated with the NMDA receptor in the 3HQs series.

Ultimately, introduction of pyruvate ester moiety at C-4 and a 5,7-dichloro pattern of substitution in the aromatic ring resulted in a substantial increase in affinity. The most active compound in this series was compound **47** with an IC_{50} of 29 nM.[77]

To better understand the biological properties of these compounds it would be important to shed light on the main essential features of this important heterocycle. This unique molecule, was recently recognized to be a valuable carboxylic acid bioisoster .[7] The carboxylic acid is an important functional group that often takes part of the pharmacophore of different therapeutic agents.[7] Furthermore, the aptitude of this group to create strong electrostatic interactions and hydrogen bonds, in association with its acidity, classify carboxylic acid as a key function in the interaction between drug and target. Despite the importance of the carboxylic acid group, it exhibit when this moiety is present in a drug, significant drawbacks namely metabolic instability, toxicity and limited diffusion across biological barriers are shown. To avoid this limitation, the replacement of carboxylic group with a surrogate or bioisoster can overcome these problems and can represent an effective strategy in drug development. Recently Ballatore and co-workers[7] provided an overview of the most commonly employed carboxylic acid (bio)isosteres and present some examples to show the use and utility of isosteres in drug design. In this review 3HQs are classified as bioisosteres of carboxylic acids, despite their lower acidity (pka = 8.7), and the authors refer to the work done by Duplantier et al. to exemplify this bioisosterism.

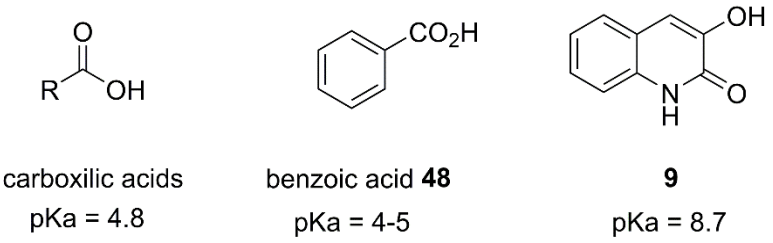

Figure 1.4 – Characteristic pKa values of carboxylic acid, benzoic acid 48 and 3HQ **9**.

The described inhibitors in literature of D-amino acid oxidase (DAAO) are small aryl carboxylic acids or acid-isosters, such as benzoic acid **48** that are ionized at the peroxisomal pH (c.a. 8). In a high-throughput screening in a functional assay to find potential inhibitors of DAAO, 3HQ **9** was identified as a potent one (IC_{50} = 4nM). Co-crystallization of **9** with the human DAAO enzyme showed that the 3-hydroxyl group of the molecule is involved in two hydrogen bonds, one with the Tyr228-OH and the other with the Arg283-NH (Figure 1.5 a). Furthermore, the 2-carbonyl group is also involved in a strong hydrogen bonding with the same Arg residue, while the lactam-NH donates a hydrogen bond to the backbone carbonyl of Gly313. Also a fundamental π-π interaction with the *re*-face of the flavin ring of flavin adenine dinucleotide (FAD) and Tyr224 is provided by the aromatic moiety of compound 8 consistent with similar structures of aryl acid bounded to DAAO.[78] Figure 1.6 shows a schematic diagram comparing the bonding interactions of compound **9** with those of carboxylic acids inhibitors (benzoic acid). The hydrogen-bonding interaction of the carboxylic moiety of benzoic acid with the enzyme active site and hydroxyquinolin-2-one behave in a very similar fashion.[9] Another important characteristic of these compounds is that 3HQs are also classified as non-classical bioisosteres of α-amino acids. Whereas classical bioisosteres include replacement of similar atoms (e.g. hydrogen with fluorine, carbon with silicon)[79] or ring-to-ring transformations (e.g. replacement of phenyl group with thiophene) nonclassic bioisosterism includes all other forms such as ring-to-chain, chain to ring transformations, functional group replacement, as well as regioisosterism.[80, 81]

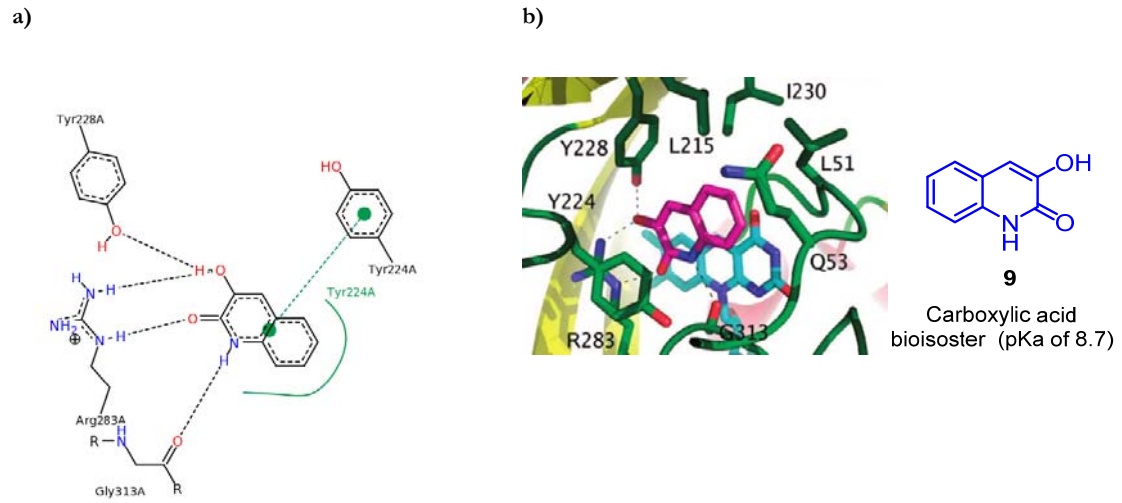

Figure 1.5 – Compound **9** at DAAO enzyme active side. a) Schematic representation of residues in DAAO-compound 9; b) Compound **9** (carbon atoms in magenta and oxygen in red) at h-DAAO enzyme active site. Side chains of key interacting residues are shown with carbon coloured in green and nitrogen in blue. Hydrogen bonding interactions are shown in dash. FAD is shown with carbons in cyan; b) structure of compound **9**.[9]

Bioisosterism of α-amino acids is mainly accomplished by replacement of the α-carboxylate with a known carboxylic acid bioisoster. In contrast, 3HQs share essential features that allow these molecules to mimic an entire α-amino acid.

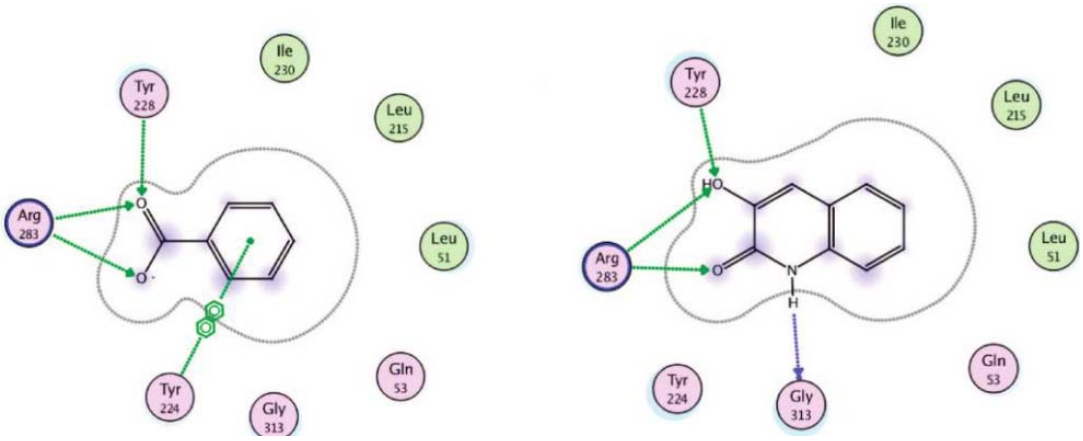

Figure 1.6 – Schematic representation of bonding interactions of compound **9** with those of carboxylic acids inhibitors (benzoic acid).[9]

As shown in the Figure 1.7 a, 3HQs present an acidic moiety that together with the lactam carbonil mimic the α-carboxylate of Glycine aminoacid, while the lactam nitrogen together with the aromatic ring system, mimic the α ammonium of the

aminoacid. The binding mode of the crystalized bioisoster **9** was compared with that of the crystalized α -amino acid Glycine that binds in the same domain of the active site of DAAO (PDB code: 3G3E) and showed a similar binding interaction as the co-crystalized amino acids in the same target.[78]

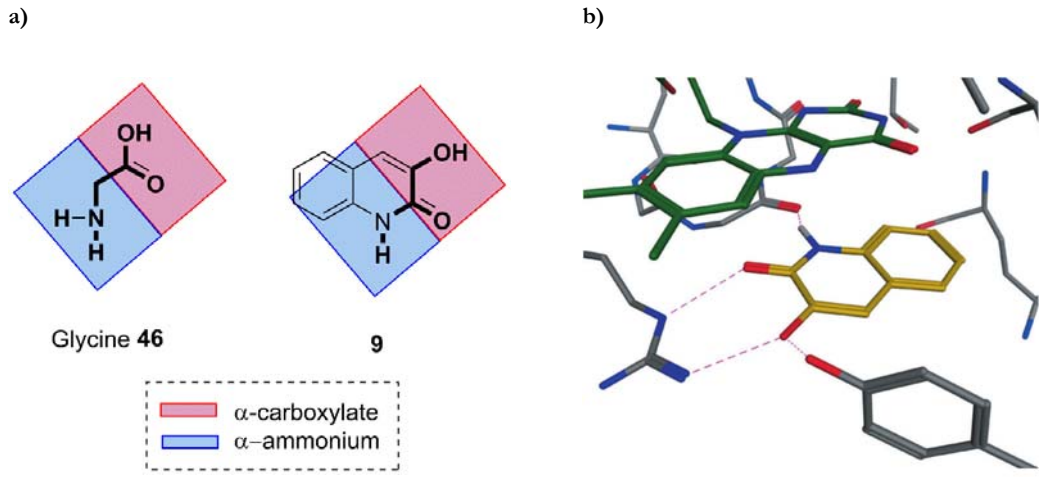

Figure 1.7 – a) Schematic representation of 3HQ as a bioisoster of aminoacid Glycine; b) compound **9** and cofactor FAD (PDB code: 3G3E). All atoms in type code except ligand carbon atoms in orange and FAD carbons in green.[8]

The 2-carbonyl together with the 3-hydroxy are involved in a strong hydrogen-bonding interaction with an Arg residue. Additionally, the 3-hydroxy group functions as a hydrogen donor to the HO of a Tyr residue, and the lactam nitrogen engages in a hydrogen-bonding interaction with the backbone carbonyl of a Gly residue (Figure 1.7 b).

1.2.2 3-Hydroxyquinolin-2-ones chemistry

Development and implementation of efficient methodologies for the preparation of relevant scaffolds, is one of the main challenges for synthetic chemists. Despite the relevant biological importance of 3-hydroxyquinolines, only a few synthetic strategies have been developed for the construction of this core and its derivatives. Several methodologies for the construction of the 3HQ core leading to the synthesis

of viridicatin **31** and viridicatiol **32** were performed in the last decades, aiming at efficiently synthetize these natural products. The important biological properties of these natural products were already discussed in the section 1.2. In this chapter will be further discussed the available synthetic methods for the preparation of 3HQs and our contribution to this efforts.

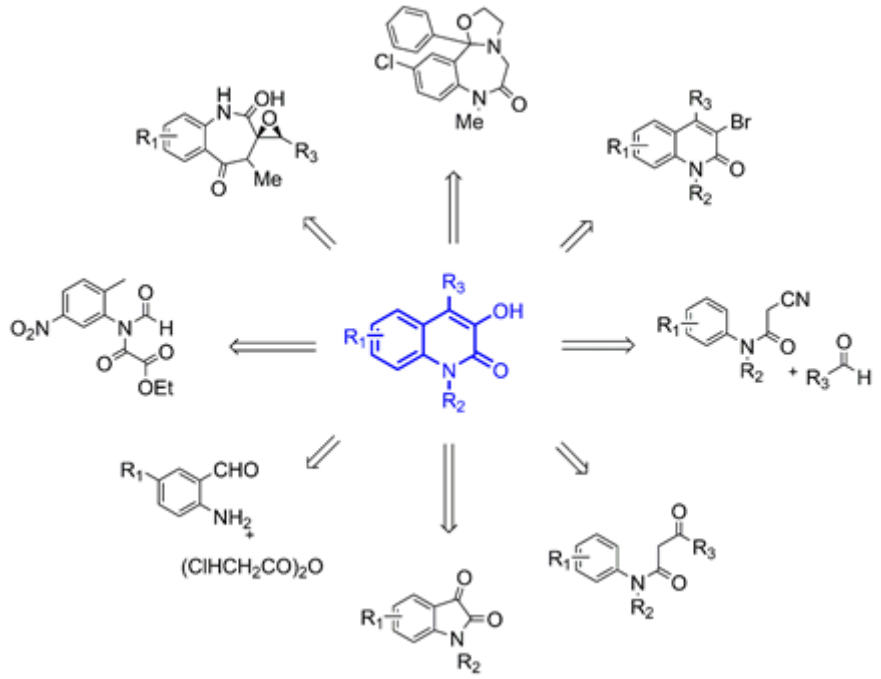

Figure 1.8 – General strategies for the synthesis of the 3-Hydroxyquinolin-2(1*H*)-one skeleton.

Extension of Diels-Reese Reaction

In 1955, inspired by the previous work of the Diels and Reese, Huntress and co-workers[182] reported for the first time the synthesis of the 2,3-dihydroxyquinoline **35**, a tautomer of 3-hydroxyquinolin-2(1*H*)-one based on the degradation of the product of Diels–Reese reaction. To confirm the structure of the hitherto, the authors prepared a parallel synthesis, in which the compound **35** was synthetized from 5-methoxy-2-aminobenzaldeyde **49** and chloroacetic anhydride, to give the corresponding 2-(*N*-chloroamino)-benzaldehyde **50** that was readily converted in to

35 by heating the intermediate **50** in the presence of methanolic aqueous potassium hydroxide (Scheme 1.12). The final product was obtained in 92% yield.

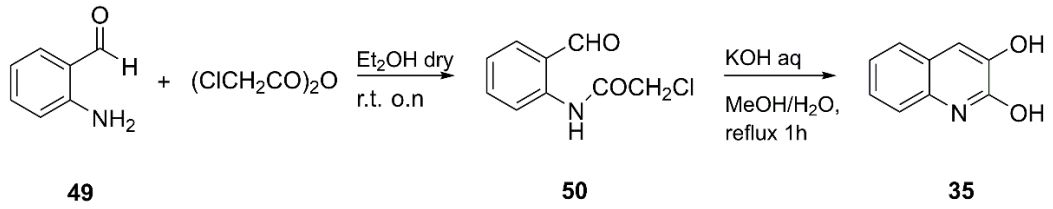

49 **50** **35**

Scheme 1.12 – Preparation of 2,3-dihydroxyquinoline **35**.

Synthesis of 5-nitro-3-hydroxyquinolin-2-ones

Another methodology developed for the construction of the 3HQ core was implemented by Brimert et *al.* In this protocol 2-Methyl-*N*-(2-methyl-5-nitrophenyl)formamide **51** was treated with potassium *tert*-butoxide and dimethyl oxalate (DMO) for 1 h at 45ºC, yielded by cyclization in 90% compound **55**.

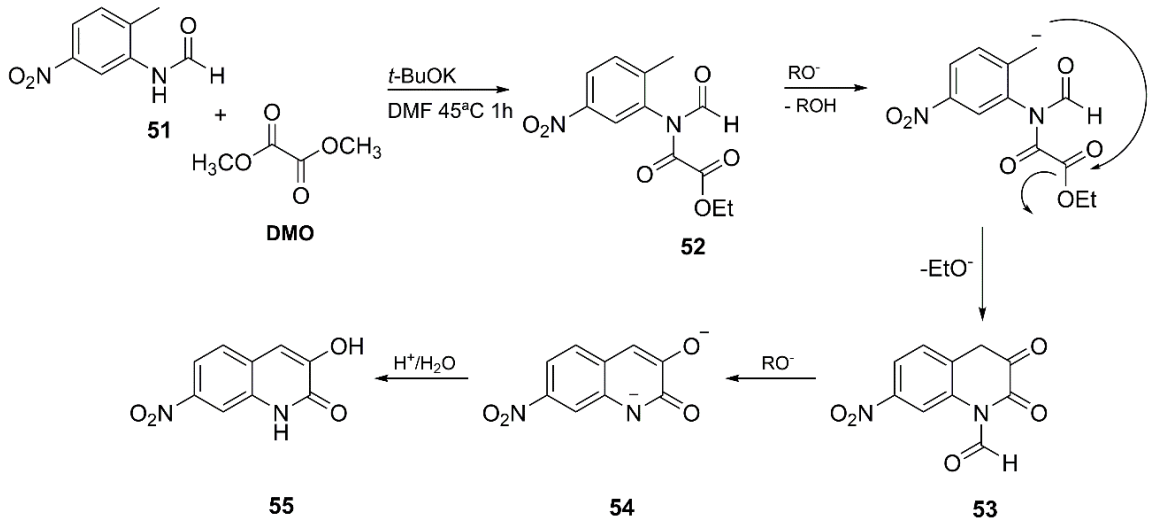

Scheme 1.13 – Synthesis of 7-nitroquinolin-2-one **55** from 2-methyl-N-(2-methyl-5-nitrophenyl) formamide **51**.

The mechanism proposed by the authors is show in the scheme below and takes into account the formation of the imide **52**, which becomes deprotonated at the

benzylic carbon due to the stabilizing effect of the electron withdrawing nitro group in *para* position An intramolecular attack of the anion at the ester carbonyl gives the *N*-formyl quinolone **53**. Deformylation and treatment with water of compound **54** gives compound **55** as crystals.[83]

Cyclopenin

Cyclopenin **56** is a metabolite of *Renicillium cyclopium* and *Penicillium viridicatum*. This metabolite is readily converted into a co-metabolite, viridicatin **31** in both acid and basic media. The same transformation, is also observed by an enzyme preparation "Cyclopenase" from *P.viridicatum*. In the work of White and co-worker the authors present the mechanism of acid- and base-catalysed rearrangement of the mould metabolite cyclopenin to its congener viridicatin.[84]

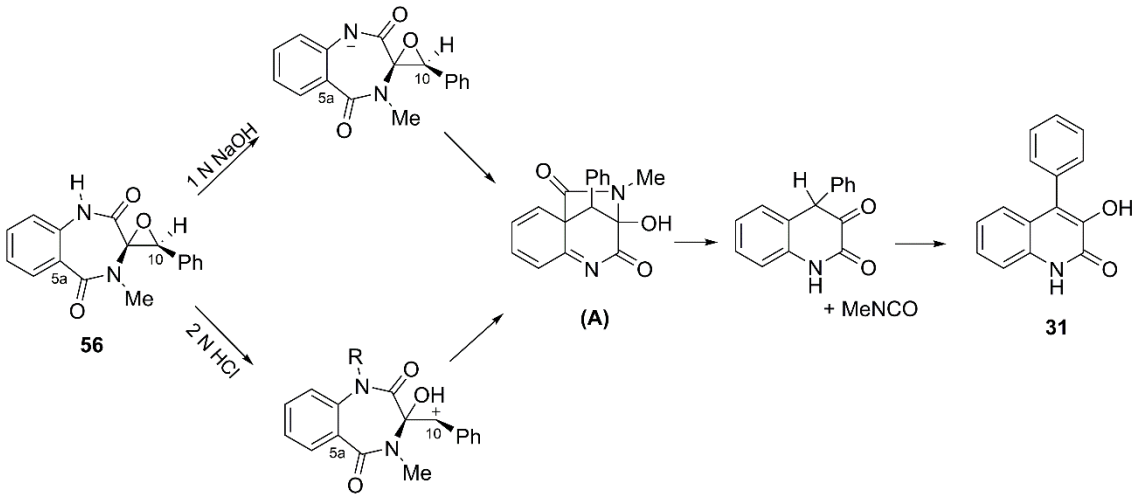

Scheme 1.14 –Mechanism of cyclopenin conversion into viridicatin **31**.

The central feature of the mechanism is the bond formation between C-10 and C-5a of **56.** This bond formation is possible due to little steric hindrance of both centres, leading to the formation of a probable tricyclic intermediate **A** that undergo in the formation of viridicatin alkaloids **31**.

Studies on benzodiazepinooxazoles

1,4–Benzodiazepines are known to rearrange to indoles, quinazolines, quinoxalines, and quinolones.[85] Interested by base-catalyzed intramolecular rearrangement of benzodiazepinooxazoles, Terada and co-workers studied the treatment of **57** with sodium hydride in dimethyl acetamide. The reaction gave two compounds, the ethanol amine derivative **58** in 10 % yield and the 3HQ **59** in 10% yield as well. The structure of the 3HQ **59** was confirmed by treatment of 5-choro-2-(N-methylbromoacetamido)benzophenone **60** with ethanolic sodium hydroxide at room temperature overnight, giving the product **59** in 33% yield[85]

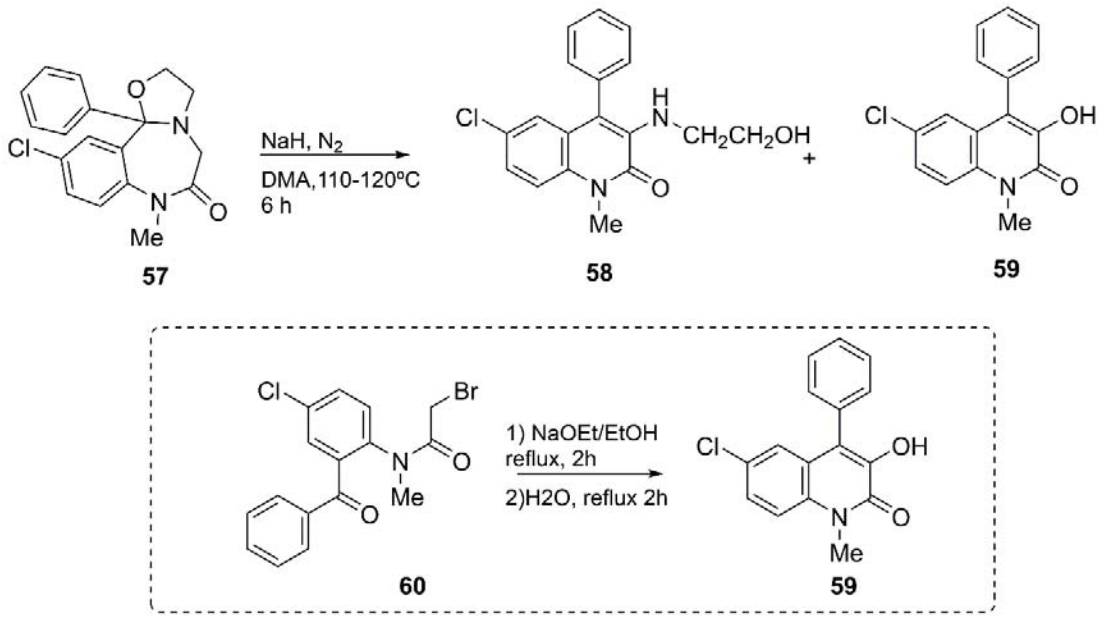

Scheme 1.15 Formation of 3HQs by ring contraction of **52**.

Synthesis of 3HQ by Pd-catalyzed coupling reaction of 3-bromo-4-phenylquinolinone mediated by tert-butyl X-Phos.

In the attempt to synthetize new bisquinolone-based mono- and diphosphine ligands of the aza-BINAP series, Kappe and co-workers prepared a 3-hydroxyquinolinone core from its bromo precursor using a recent protocol disclosed

by Buchwald and co-workers that introduced the use of *tert*-butyl X-phos as ligand in related Pd-catalyzed couplings. With this procedure, under microwave irradiation, the authors were able to synthesize 3-hydroxy-4-phenyl-1-methylquinolin-2(1*H*)-one **62** in modest yield 68% from the bromo precursor **61**.[86] (Scheme 1.16).

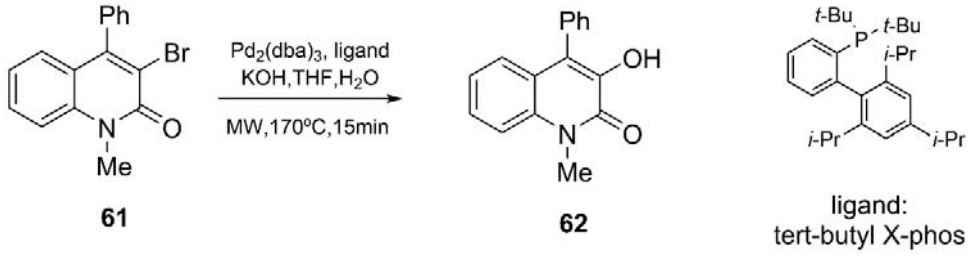

Scheme 1.16 Pd-catalyzed formation of **62** using 3-bromo-4-phenylquinolinone **61**.

Knoevenagel condensation/epoxidation

A more recent strategy to prepare this family of heterocycles was discloser in 2009 by Kobayashi and Harayama. The methodology consist in a versatile synthesis of viridicatin Alkaloids (isolated in 64-73 % yield) and its derivatives using cyanoacetanilides through an one-pot Knoevenagel condensation/ epoxidation of cyanoacetanilides followed by arene cyclization.[87] The nitrile group in molecule **63** has two main functions: as electron-withdrawing group to ease the condensation step, and also as a leaving group in the cyclization step. The noticeable feature of this methodology is the variety of cyanoacetanilides and aldehydes that can be used in the reaction yielding new viridicatin derivatives. When studying the effect of substituent R^2 on the aromatic ring in the one–pot Knoevenagel condensation/epoxidation sequence, the authors found some effect on the yields of desired epoxide. They observed that electronic effects influenced the subsequent epoxide –arene cyclization in the rate of the reaction. When the reaction is carried out bearing an electron-rich aryl group, the reaction took place smoothly and afford quinolone compound in 99% yield after 5 h (entry 1, Table 1.1), while the presence of electron withdrawing groups

such as halides (entries 2 and 3, Table 1.1) resulted in slow conversion of **64** and good yields could be obtained only after 24 h.. The effect of substituent R^3 in aryl aldehydes was also studied, and despite the absence of any influence on the condensation/epoxidation sequence, the cyclization step was determined to be favoured by the presence of electron rich aryl groups. Electron poor aryl substituents such as trifluorotoluoyl hampered the cyclization step (entry 6, Table 1.1), maybe because of the more challenging generation of carbocation species at benzylic positions.

Table 1.1 – 3HQs preparation through one-pot Knoevenagel condensation/epoxidation of cyanoacetanilides followed by decyanative epoxide-arene cyclization – substrate scope

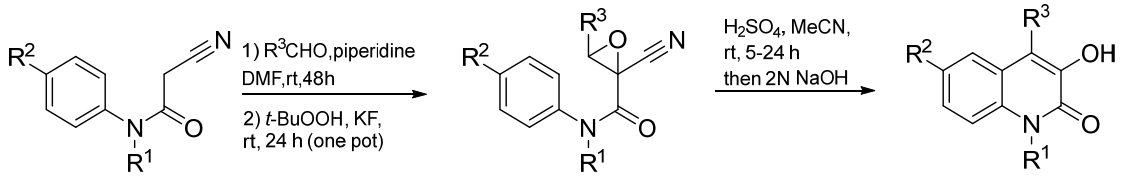

63 **64** **65**

entry	R^1	R^2	R^3	64 yield,(%)[a]	65 (yield,%)[b]
1	PMB	Me	Ph	49	99
2	PMB	Br	Ph	88	85[c]
3	Me	Cl	Ph	69	92[c]
4	Me	H	4-$MeOC_6H_4$	70	89
5	Me	H	1-naphthyl	87	90
6	Me	H	4-CF_3 C_6H_4	78	0

[a] isolated yields in two steps from **63**.[b] isolated yield from **64**. [c] were consumed in 24h

Despite the salient features of this methodology, it suffers from some disadvantages as it still depends on the synthesis of cyanoacetanilides as starting materials, and the cyclization of the epoxide requires use of H_2SO_4 that leads to the formation of the extremely poisonous and flammable hydrogen cyanide during the reaction

α-Hydroxylation and Intramolecular cyclization of N-phenylacetoacetamides

In 2013 Zhao's group presented a new strategy for the construction of the 3-hydroxyquinolin-2(1*H*)-ones. The reaction involved the conversion of *N*-phenylacetoacetamides in α-hydroxyanilide using iodobenzene I,I-bis(trifluoroacetate). The reaction proceeds through an hypervalent iodine reagent-mediated α-hydroxylation and converts to the cyclized product with 10 equiv. of concentrated H_2SO_4 yielding up to 88 % the final products (Table 1.2).[88]

Table 1.2 –Synthesis of 3HQs derivatives.

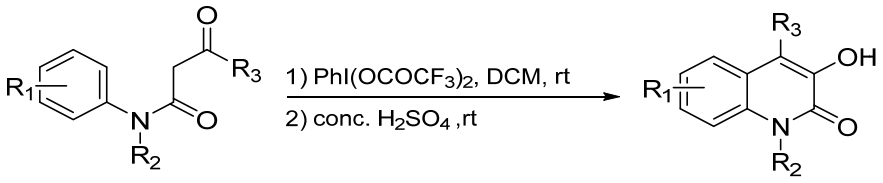

66 **67**

Entry	R^1	R^2	R^3	67 Yield (%)
1	H	Me	Me	88
2	H	Me	Ph	25
3	H	Ph	Me	82
4	H	H	Me	70
5	F	H	Me	74
6	Me	H	Me	50
7	2-Cl	H	Me	40
8	*para*-OMe	H	Me	35
9	*orto*-OMe	H	Me	30

The reaction scope was studied by decorating the starting material with different substituents on the aromatic ring R^1, on the nitrogen atom R^2 and on the carbonyl of the ketone R^3. Twenty examples of new 3HQ derivatives were synthetized in modest to good yields. A detrimental effect on the cyclization was observed when replacing the R^3 substituent from an alkyl to a phenyl, resulting in a yield dropping from 88 % to 25 % (entries 1and 2, Table 1.2).

On the other hand, replacing the methyl group on R^2 with a bulkier group as phenyl did not affect the yield of the reaction (entry 3). When the authors applied the method to synthesise a series of 3HQ resembling viridicatin, without substituents in the anilide (R^1=H) and unsubstituted nitrogen, the desired products were obtained in good yields (entries 4, 5). *Orto*-substituted substrates, especially with methoxy group, afforded products in low yields. A possible explanation for the yield erosion could be the formation of an array of unidentified by-products as a result of over oxidations of the electron–rich aromatic ring (entries 8, 9). Beside the main advantages of this strategy, the ready availability of the substrates and the convenient protocol, the biological active viridicatin **31** was afforded only in 60% yield and the precursor of viridicatiol was achieved in a lower 40% yield.

Eistert Ring Expansion

The last route described here is the addition of diazo compounds to cyclic ketones.[89] This well-known reaction, was reported by Eistert *et al.* in the early sixties[90; 91] On his seminal work, Eistert found that the aldol reaction between isatin with ethydiazoacetate EDA , in the presence of a promoter, acids or zinc chloride, resulted in the ring expansion reaction with formation of 3HQ core **69** in 86% yield. Despite the good yield of reaction, this first attempt to synthetize the 3HQ core displayed a poor breadth of substrate compatibility and consequently was found not practical for preparation of derivative libraries.

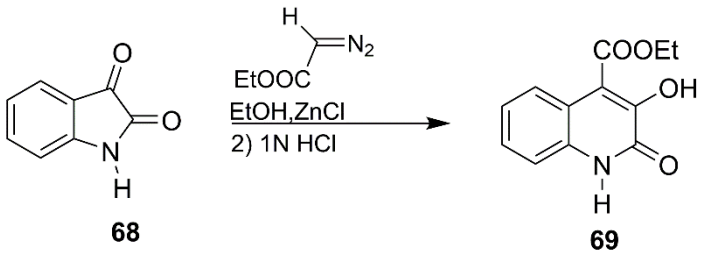

Scheme 1.17 – Eistert Ring Expantion.

Aware of these limitations, an extensive screening of Lewis acid as promoters for decomposition of isatin derived α-diazo-β-hydroxy ester **70** was recently performed by Pellicciari *et al.* (Table 1.3).The nature of the Lewis acid and the solvent polarity were observed to have a pivotal influence in the chemoselectivity of the decomposition. A cationic cascade mechanism or a concerted 1,2-aryl migration followed by dinitrogen release was suggested as possible paths for formation of the ring expanded product **69**. According to the proposed mechanism, hard Lewis acids such as BF_3•OEt_2 and $SnCl_4$ favor the cationic process, resulting in formation of products **73** derived from vinyl cation intermediate **72** after 1,2-aryl shift and subsequent trapping by the solvent. More polar and more nucleophilic solvents favored formation of **71** due to the increased stabilization of the vinyl cation intermediate **72**. Solvent adducts derived from dihalomethanes and nitriles were obtained in 12 – 40 % yields while acetylene compound **73** was the major product. Use of methanol as solvent in presence of BF_3•OEt_2 resulted in exclusive formation of **69** due to proton induced expansion by the in situ formed [BF3•OMe]-H^+. [92] Although the existing methods have their own merits in the preparation of certain 3-hydroxyquinolin-2(1*H*)-ones, finding a more general method applicable to the construction of more diverse structures regarding the aryl substitution patterns remains an open challenge.

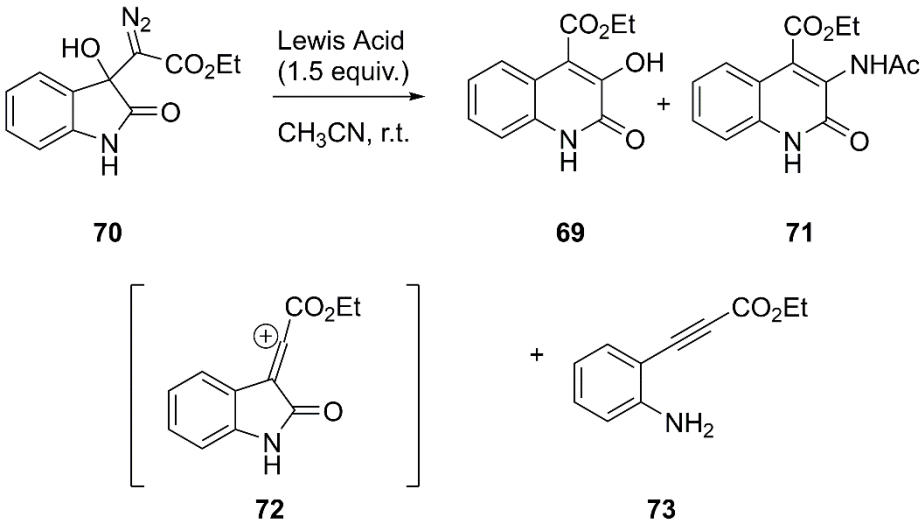

Scheme 1.18 Synthesis of compound **69** by Pellicciari *et al.*

Table 1.3 – Lewis Acids promoted ring expansion of α-diazo-β-hydroxy ester **70.**

Entry	Lewis Acid	ratio 69:71:73	Entry	Catalyst	ratio 69:71:73
1	BF_3•OEt_2	4:40:56	8	$InCl_3$	95:3:2
2	$SnCl_2$	100:0:0	9	$In(OTf)_3$	82:9:9
3	$Mg(ClO_4)_2$	100:0:0	10	$Yt(OTf)_3$	65:17:18
4	$Zn(OTf)_2$	100:0:0	11	$Al(OTf)_3$	43:26:31
5	$ZnCl_2$	100:0:0	12	$Sc(OTf)_3$	39:28:33
6	$ZnBr_2$	100:0:0	13	$SnCl_4$	0:40:60
7	$InBr_3$	99:0.5:0.5			

Chapter II

II. Synthesis of Viridicatin Alkaloids

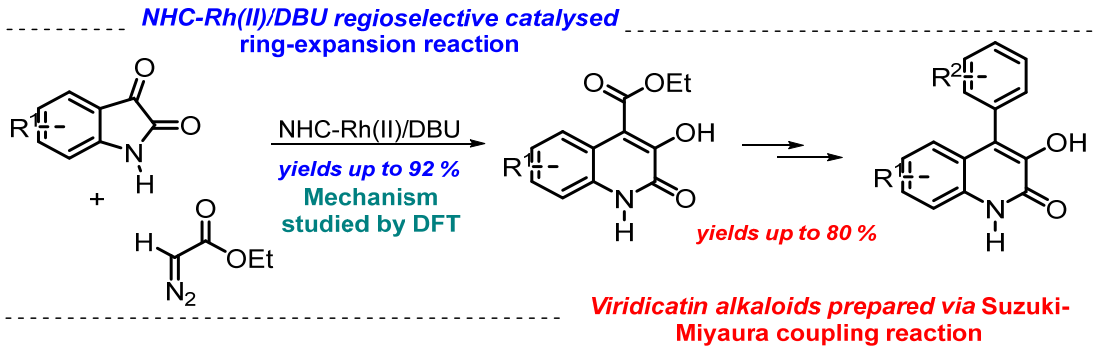

Abstract

An efficient and novel 4-step route for the synthesis of the viridicatin alkaloids via Suzuki-Miyaura coupling reaction of aryl-boronic acids with 3-hydroxy-4-bromoquinolin-2(1H)-ones prepared from 3-hydroxy-4-ethylesterquinolin-2(1H)-ones will be presented. The 3-hydroxy-4-arylquinolin-2(1H)-one core, include several natural products like viridicatin, viridicatol and 3-O-methyl viridicatin, which have been reported as very promising inhibitors against human immunodeficiency virus replication induced by tumour necrosis and as promising lead compounds for the development of new anti-inflammatory agents. We have developed a new one-pot NHC-dirhodium(II)/DBU catalysed Eistert ring expansion reaction of isatins with ethyl diazoacetate to afford the 3-hydroxy-4-ethylesterquinolin-2(1H)-one core regioselectively and in good to excellent yields. The DFT calculations performed on this system support a mechanism in which the key step is metallocarbene formation between the 3-hydroxyindole-diazo intermediate and the dirhodium(II) complex. Finally, vidicatin alkaloids were synthesised in yields up to 80 % via the abovementioned Suzuki-Miyaura cross coupling with aryl-boronic acids.

2.1 Introduction

2.1.1 Combining transition metal catalysis and organocatalysis: A new emerging concept

Historically, organic synthesis has been dominated by transition metal catalysis.[93] Through extensive efforts, chemists have continued to make remarkable achievements in relation to understanding metal properties, rational ligand design and applications of their versatile reactivity patterns in various transformations. Nevertheless, transition metal catalysts often suffer from being sensitive to air and moisture or are present as contaminants in products.[94] Therefore, chemists started to explore new kinds of catalytic reactions with the "absence of metals", in which small organic molecules (organo-catalysis) act as catalytically active species to facilitate chemical transformations. This novel type of catalysis has emerged as a major concept in organic chemistry, and after experiencing its "golden age", [95, 96] it is now a mature field of research. Organocatalysis has become one of the most popular and fundamental tools to target enantiomerically enriched compounds.

Despite this remarkable progress, organocatalysis suffers from a lack of efficient modes to activate relatively inert chemical bonds. In contrast to this, metal catalyst are known to activate a varied range of chemical bonds, particularly those inactive chemical bonds that organocatalysts are unable to cleave.[97] To overcome this limitation and develop more efficient approaches for the synthesis of complex molecule, the theoretical combination of these two distinct catalytic systems namely metal complex catalysis with organocatalysis, gave rise to Metal-organo-catalysed (MOC) systems.

With this new chemical tool chemists were able to develop unprecedented transformations[98] with good chemo- and stereo-selectivity inaccessible through the use of single specific catalytic systems.[99] For this reason, the concept of combining organocatalysis with transition metal complexes has attracted much interest, becoming a new research area. During the last decade, impressive developments in new types of catalyst combinations and new reaction types have been disclosed.[98, 100]

A variety of binary catalytic systems involving the use of metals such us Rh(II), Pd(0), Au(I), and Mg(II), and chiral organocatalysts, including chiral phosphoric acids and quinine-based bifunctional molecules allowed the execution of many unprecedented trasformations.[97]

In their last publication, "Combining transition metal catalysis and organocatalysis – an update", Du and Shao proposed a general classification for the combination of organo and metal catalysis from the catalytic cycle point of view, consisting in three main types (Figure 2.1):

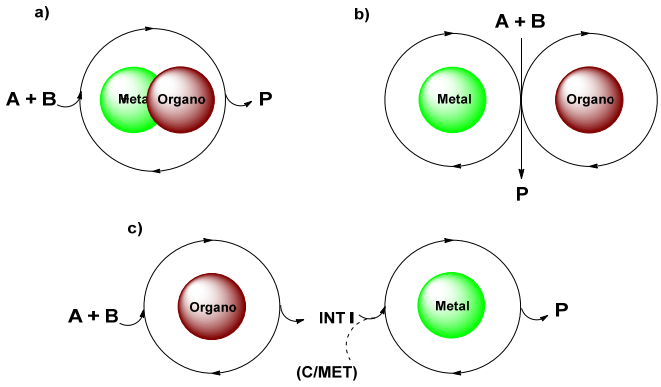

Figure 2.1- (a) The concept of cooperative catalysis. (b) The concept of synergistic catalysis. (c) The concept of sequential or relay catalysis.

1. **Cooperative catalysis (a):** the organocatalyst and the transition metal catalyst are involved in the same catalytic cycle to form a product.
2. **Synergistic catalysis (b):** the catalysts activate the two substrates (A and B) by two directly catalytic cycles; the substrates undergo both cycles to the formations of the final product.
3. **Sequential or relay catalysis (c):** the two different catalysts (the transition metal catalyst and the organocatalyst), that undergo two distinct catalytic cycles and consecutive reactions, whereby the substrates (A and B) first react to form an intermediate (**INT I**) in the first catalytic cycle, which can either be the organocatalytic cycle or the transition metal catalytic cycle. Subsequently, this intermediate is converted to the final product (P) by another independent catalyst.

The main challenge of combining transition metal and organocatalysed transformations is to ensure the compatibility of catalysts, substrates, intermediates and solvents throughout the whole reaction sequence. The key to overcome this challenge is the judicious selection of appropriate catalyst combinations. Often, the combination of a hard Lewis acid with a soft Lewis base or a soft Lewis acid with a hard Lewis base is able to avoid the deactivation of catalysts. In addition, the following strategies have also been adopted: the use of the site isolation or phase separation techniques, and sequential addition of catalysts and substrates.[99]

2.2 Generation of metallocarbenes from diazo compounds using di-rhodium dimers

Our approach towards the synthesis of 3HQs was built on the long-standing interest of the group on the use of dirhodium(II) complexes to promote transformations of diazo compound upon combination with the emerging MOC protocol.[101-106]

Dirhodium (II) catalysts have been widely used as tools in organic synthesis, ultimately resulting in myriads of transformations and formation of a variety of compounds.[107] Dirhodium complexes are bimetallic compounds with one metal-metal bond (Rh-Rh), four bridge ligands, and two axial ligands arranged in an octahedral geometry conferring a lantern-like structure.[108] Differently of when using metals such as copper and ruthenium, the presence of the Rh-Rh single bond plays an important role in the performance of these complexes and the formation and reactivity of metallocarbenes. The introduction of new bridge ligands coordinated to dirhodium(II) dimers gives distinct degrees of charge to the metal and it enables the tuning of the complex reactivity and selectivity by changing the nature of the bridge ligand - i.e. ligands such as amides generate catalysts that are less reactive in reactions involving diazo compounds than when using complexes featuring carboxylates bridging ligands. The two axial positions of di-rhodium dimers are electrophilic and are often occupied by solvent molecules that establish weaker bonds with rhodium

centers when compared with the bridge coordination. These labile ligands are easily displaced by the substrates in the reaction vessel, and their role in catalysis has been somehow overlooked. Recently, Gois et al. [109] showed how the reactivity of these di-rhodium (II) complexes could be effectively tuned by incrementing the electronic density of the terminal Rh atom by simple coordination of N-Heterocyclic carbenes (NHCs). These ligands offer good potential, they are neutral, and they are two electron donor (o-donating) ligands with negligible π-back bonding tendency.

The most common catalytic application of dirhodium complexes is the generation of metallocarbenes from diazo compounds that can undergo C-H bond[110] and heteroatom H insertion, cyclopropanation, and dipolar ylide cycloaddition (Figure 2.2).

The mechanism for C-H insertion starts by a solvent decomplexation from the catalyst axial position, followed by a nucleophilic attack of the diazo compound onto the metal generating an ylide, which upon nitrogen extrusion provides the metallocarbene. Then, an electrophilic attack from the metallocarbene to an electron-rich C-H bond (substrate R-H) furnishes the product, regenerating the catalyst.[111]

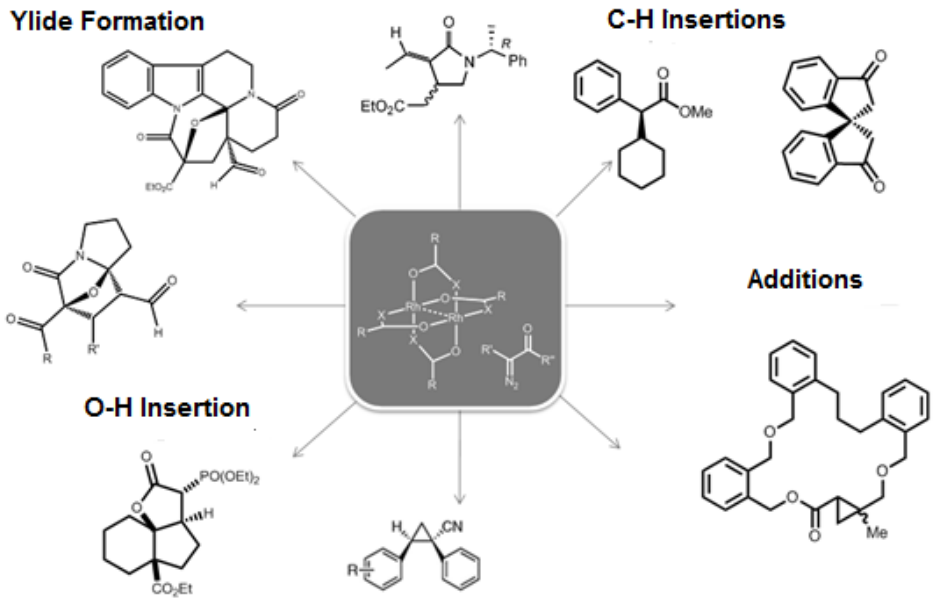

Figure 2.2 - General structure and reactivity of dirhodium(II) complexes.

Nakamura and co-workers studies[112] describe how the rate limiting step is the carbene coordination promoting nitrogen extrusion, and the C-H insertion is the rate limiting step of the insertion.[113] Moreover, they consider that only one of the two rhodium atoms works as a carbene binding site through out the reaction. The second rhodium atom acts as mobile ligand, so that the first one enhances the electrophilicy of the carbene moiety and facilitates the cleavage of the rhodium-carbon bond.

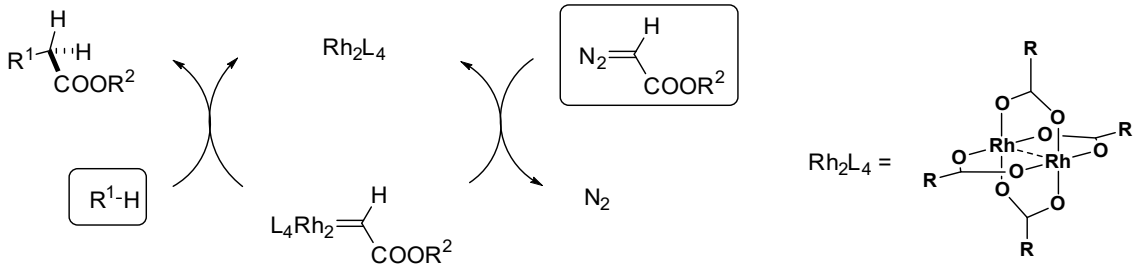

Scheme 2.1 - Schematic representation of the catalytic cycle of the di-Rhodium -catalyzed C-H bond activation/ C-C bond forming reaction of an α-diazoacetate with an Alkane.

For their exquisite reactivity, stability, and tolerance to water and oxygen, dirhodium(II) complexes are very desirable catalysts to include in MOC systems.

2.2.1 Exploring metal organo catalytic systems based on di-Rhodium complexes

In the context of dual catalysis, dirhodium complexes have an important role in the development of combined Brønsted acid and transition metal catalysed tandem reactions. Generally, Brønsted acids promote organocatalytic reactions through protonation to form an ion pair. In the reported work by Wenhao a*t al,*[114] di-Rh(II) complexes have been used in a MOC reaction based on the addition of ylides to aldehydes and imines. The role of the di-Rh(II) complex was to catalyse the ylide formation, while the chiral phosphoric acids mediated the enantioselective addition of this intermediate (Scheme 2.2).

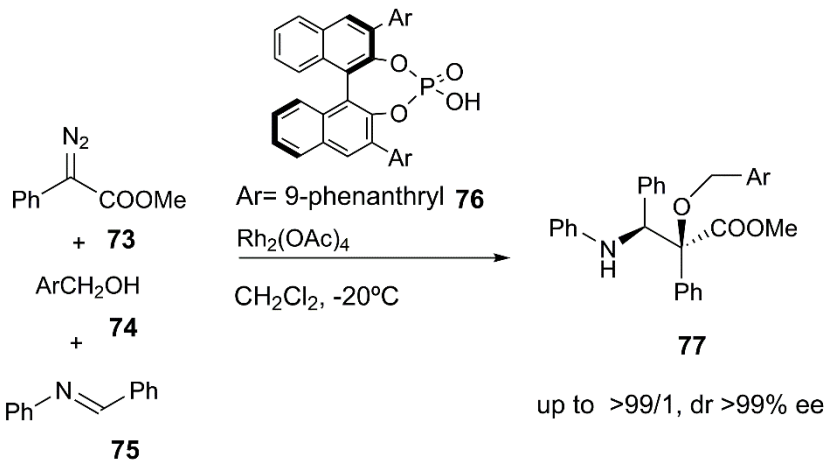

Scheme 2.2- Rhodium catalysed three component reaction using chiral Brønsted acids.

As aforementioned, the major challenge of developing a MOC system is the selection of appropriate catalyst combinations. Dirhodium complexes are quite well known as a Lewis acid, and the combination of this catalyst with an organic Lewis base, could lead to the deactivation of both catalysts. As far as our knowledge goes, only few examples covering the combination of these two types of catalysts in one single transformation can be found in the literature.[115, 116] In 2005 Doyle and co-worker[117] reported a first example of dual/cooperative catalysts strategy using di-Rhodium (Lewis acid) and a cinchona alkaloid as the organocatalyst (Lewis base). They reported a [2+2] cycloaddition reaction between ethyl glyoxylate **78** and trimethylsilylketene **79** catalyzed by a di-rhodium carboxamide (Scheme 2.3). To achieve the reaction with high enantioselectivity and to decrease significantly the time of the reaction, the authors chose a Lewis base cinchona alkaloid as co-catalyst due to its known activation of ketenes. The main problem to use cinchona Lewis base in this system was probably the inhibition of the dirhodium complex by Lewis base coordination of either the hindered tertiary amine or the quinoline nitrogen to the rhodium axial coordination sites. Nevertheless using this MOC catalytic system, the author obtained the desired product β-lactone in 68% yield and 90% *ee* in 20 h at room temperature. Despite the success, no information was provided regarding the putative reaction mechanism.

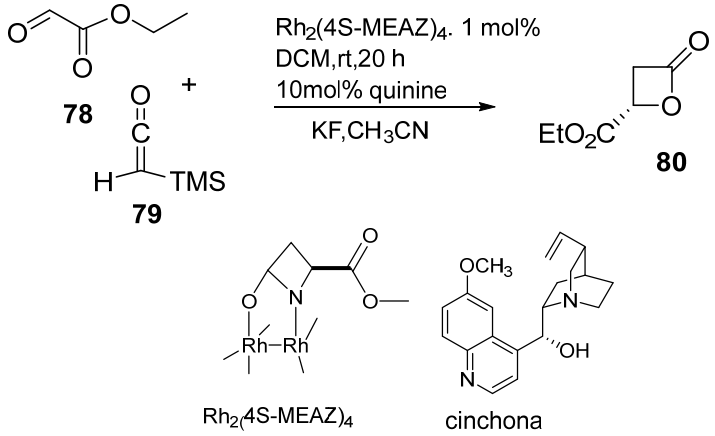

Scheme 2.3 - [2+2] cycloaddition reaction between ethyl glyoxylate and trimethylsilylketene catalyzed by a di-Rhodium carboxamide

Another example of the use of this MOC catalytic system (dirhodium(II) compounds and cinchona alkaloids) is the asymmetric N-H insertion of phenyldiazoacetate with anilines reported by Hashimoto et al. The catalytic system based on di-rhodium(II) tetrakis(triphenylacetate)($Rh_2(TPA)_4$) and dihydrocinchonine provided phenylglycine derivatives in up to 71% *ee*. These studies clearly demonstrated that this catalytic system is effective for the enantiocontrol in the intermolecular N–H insertion reaction of phenyldiazoacetates with anilines (Scheme 2.4).

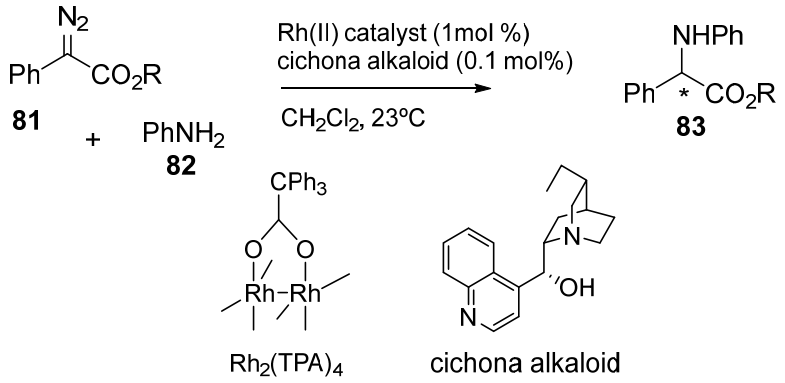

Scheme 2.4 - Cooperative metal-organo-catalysed reactions based on di-Rh(II) and Lewis base organo-catalysts

These examples of MOC systems prompted us to study new catalytic systems based on di-rhodium catalysts and organic Lewis bases as a useful strategy to find new ways to access interesting biological cores. Despite the outstanding ability of di-Rh(II) metal complexes to stabilize carbenes via formation of the corresponding metallocarbene, such complexes are also known Lewis acids.[118] The design of cooperative metal-organo-catalysed reactions based on a Lewis acid and a Lewis base organocatalyst is considerable more challenging due to the potential mutual catalyst inhibition as the Lewis base adds to the di-Rh(II) axial coordination sites (Scheme 2.5).

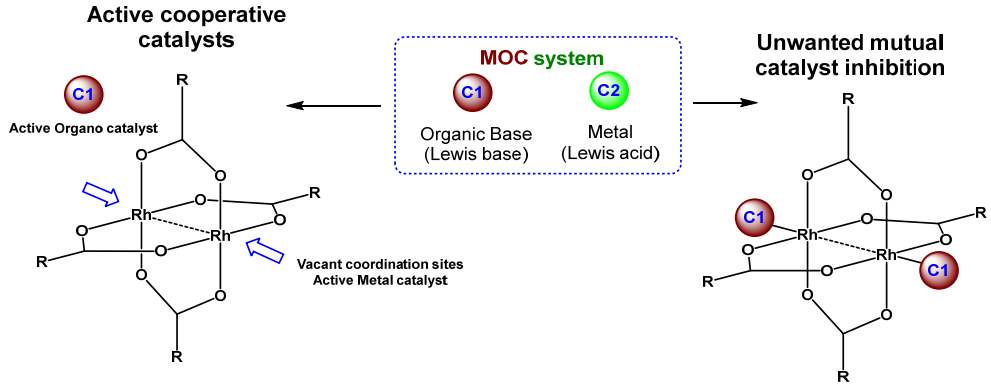

Scheme 2.5 - Potential di-Rh(II) inhibition when used in combination with Lewis base organocatalysts.

To tackle the development of new cooperative MOC protocols based on the Lewis base/di-Rh(II) concept, we studied the combination of di-Rh(II) complexes with organic bases and ring expansion protocols (Scheme 2.6) aiming at the synthesis of biologically active molecules. The ring expansion (RE) strategy using diazo compounds has been extensively used in synthetic organic synthesis to prepare valuable compounds such as: benzo-azepines, quinolinones, cyclic ketones and many other small heterocycles.[89] This reaction typically involves two steps, the first being the installation of the diazo moiety in the substrate via aldol-type nucleophilic addition of ethyl diazoacetate (EDA) to a ketone (Scheme 2.6). After this, the ring expansion is promoted using HCl, Lewis acid catalysts, temperature or photochemical irradiation.[119] Bearing this in mind we envisioned that by using a MOC system this reaction could be carried out more efficiently in one-pot, using an organic base to

catalyse the addition of the EDA and a metal catalyst to promote the ring expansion via the generation of a rhodium-carbenoid.

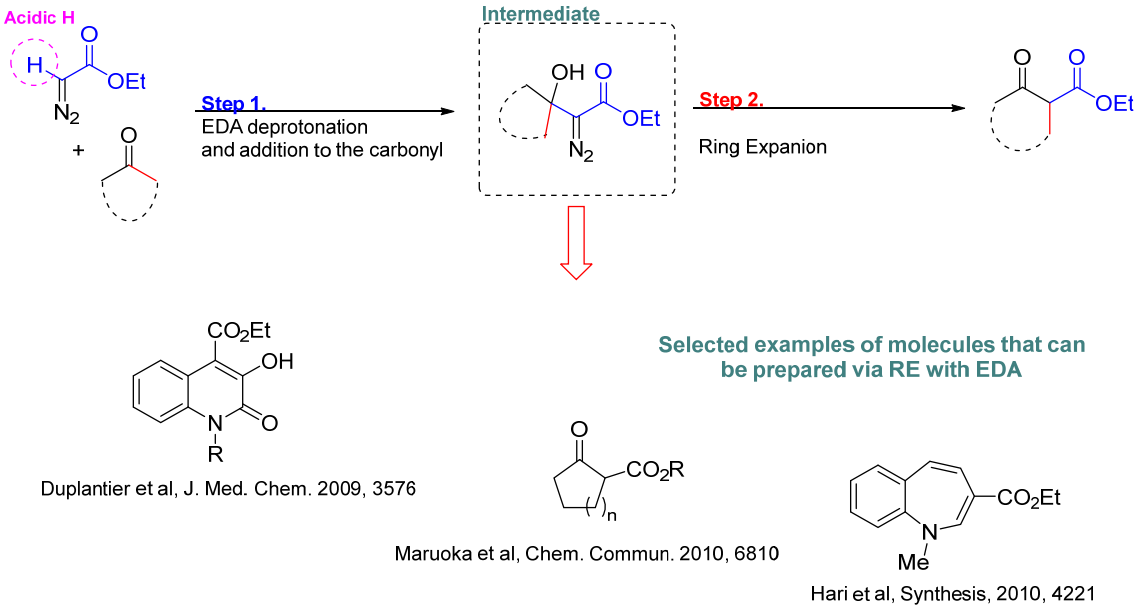

Scheme 2.6 - Molecules that can be prepared via a ring expansion strategy.

To obtain a MOC system that may efficiently catalyse the ring expansion reaction using EDA, the organic base and the metal catalyst should not react between them. This is a troublesome step as it requires the discovery of a compatible Lewis base and Lewis acid pair that may still catalyse the reaction. In addition to this, the metal complex should react solely with the diazo intermediate and not undergo metallocarbene formation upon reaction with ethyl diazoacetate (Scheme 2.7).

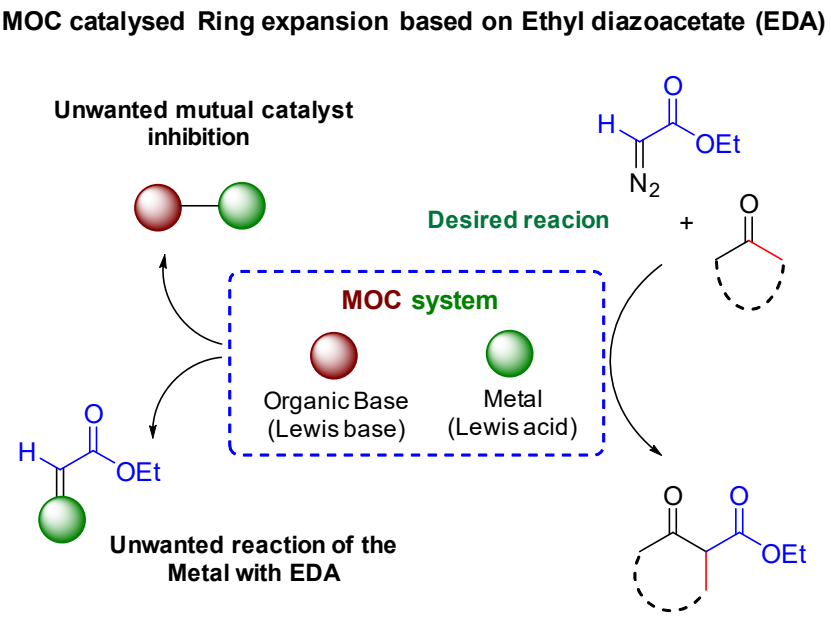

Scheme 2.7 - Unwanted reaction in the Metal-Organo-Catalysed ring expansion using EDA.

2.2.2 Preliminary Results

With the aim to discover a MOC system that would smoothly achieve a regioselective ring expansion reaction obtained *via* the formation of a metallocarbene using di-Rh(II) complexes, we carefully planned the first experiments.

Initial studies were performed to synthetize intermediate diazo compound **70,** typically prepared via addition of ethyl diazoacetate to isatin in the presence of diethyl amine in ethanol (1 eq, rt, 2 days). After synthetizing compound **70,** we tested the ring expansion reaction using a catalytic amount of $Rh_2(OAc)_4$ in dichloromethane (DCM). To our delight, under these conditions compound **70** rapidly underwent ring expansion to afford the 3-hydroxy-4-ethylesterquinolin-2(1*H*)-ones **69** in 81% yield, which precipitated in the reaction medium. Motivated by this interesting result we further improved the reaction by using ethanol instead of DCM as solvent, and we added 0.5 mol% of $Rh_2(OAc)_4$. In these conditions, compound **69** was isolated in 90 % yield after simple filtration (Scheme 2.6). The product of the reaction was

characterized through NMR techniques and the results are in agreement with the literature.[77] The assignment of the NMR spectra reveals the presence of a triplet at 1.32 ppm and the quadruplet at 4.40 ppm from the ethyl ester moiety and the singlet of the OH in position C-3 of the 3HQ core at 10.28 ppm in ^{1}H NMR (Appentix C, Figure C1) .

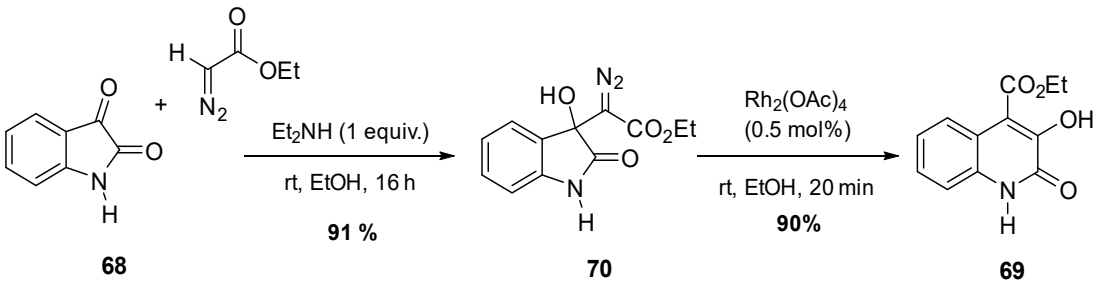

68 **70** **69**

Scheme 2.8 –EDA addition to isatin followed by Eistert ring expansion reaction catalysed by $Rh_2(OAc)_2$

Also in ^{13}C NMR can be found the characteristic value of the carbonyl of the ester at 165.39 ppm (Appendix C, Figure C1) and further confirmed by X-ray crystallography (Figure 2.3).

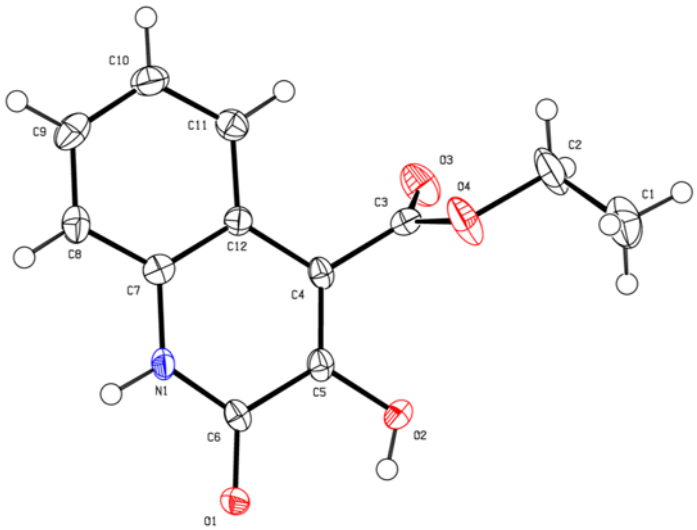

Figure 2.3 – X-ray crystallography of **69.**

2.2.3 **Rh(II) recycling**

The enormous synthetic value of dirhodium complexes has been proven over the years, as they are able to catalyse a wide range of transformations. These complexes are usually prepared from exchange of $Rh_2(OAc)_4$ ligands with carboxylic acids or from the reduction of $RhCl_3$ in the presence of the corresponding carboxylic acid. Therefore scarce industrial applications of these complexes have been reported.[107]

Rhodium supply depends mostly on South Africa (82%) and Russia (14%) and its primary use is in the catalytic converters in automobiles. Since this metal is one of the rarest on Earth (rhodium's annual production is some 1% of gold's) the price performance becomes very unpredictable and extremely dependent on automobile industry demands. For instance, after a 20-fold increase from 2003 to 2008 in rhodium average price, it fell by more than 90% in 2009 as a result of the sharp decline of the global automobile industry and followed by global crisis. Nowadays, rhodium is sold at 23 USD g−1 some 50% less than gold and 5% more than platinum, and the annual consumption is around 22 tons. Although relatively cheap at the moment, the high cost of the metal and the difficulty in recovering and recycling it are still the major factors that limit the application of dirhodium complexes at an industrial scale. Furthermore, the tight legislation on metal contamination of active pharmaceutical ingredients imposes the development of efficient methods for metal removal.Reutilisation of metal complexes can be achieved by several methods, based on heterogeneous and homogeneous strategies.[120] Each of these methods has some intrinsic drawbacks and advantages that should be considered depending on the type of catalyst and the reaction in focus. Taking in consideration this background and impressed by the efficiency of this transformation, the ring expansion reaction was repeated with the objective of recycling the catalyst used. Therefore, after filtration of **69** which precipitates in the reaction medium, the ethanolic solution containing the dirhodium(II) complex was charged with more diazo compound **84** and was efficiently converted into **69**. The catalytic system was then reused for 6 cycles with an average isolated yield of 90 % (Scheme 2.9).

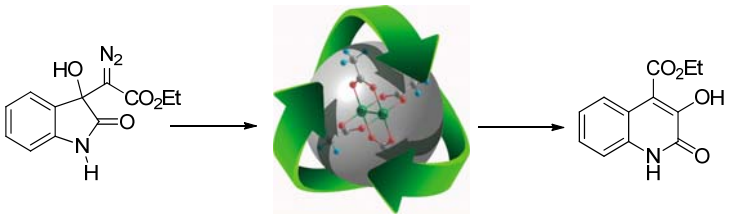

Cycle	Yield
1	90 (%)
2	90 (%)
3	88 (%)
4	93 (%)
5	92 (%)
6	90 (%)

Scheme 2.9 - Recycling dirhodium(II) complex ring expansion-reaction.

2.2.4 **Implementation of MOC system.**

After confirming that $Rh_2(OAc)_4$ was indeed an efficient catalyst for the Eistert ring expansion reaction, we turned our attention towards the possibility of implementing a one-pot metal-organo-catalysed protocol for the preparation of 3-hydroxy-4-ethylesterquinolin-2(1*H*)-ones as shown in Scheme 2.10. As mentioned in the introduction of this chapter, one of the main challenges on developing one-pot metal-organo-catalysed systems is to prevent the self-quenching of both metal and organo catalysts (see Scheme 2.3 section 2.1.2). To verify the practicability of the projected route, initial studies focused on the choice of catalytic base for the formation of diazo compound **84** were executed. Among the different bases studied for catalytic addition of EDA to isatin (Table 2.1), 1,8-Diazabicyclo[5.4.0]undec-7-ene (DBU) was found to be the most efficient. Using DBU in 15 mol % (entry 4), compound **68** was obtained in 78% yield after 24 h at room temperature and purification by flash chromatography.

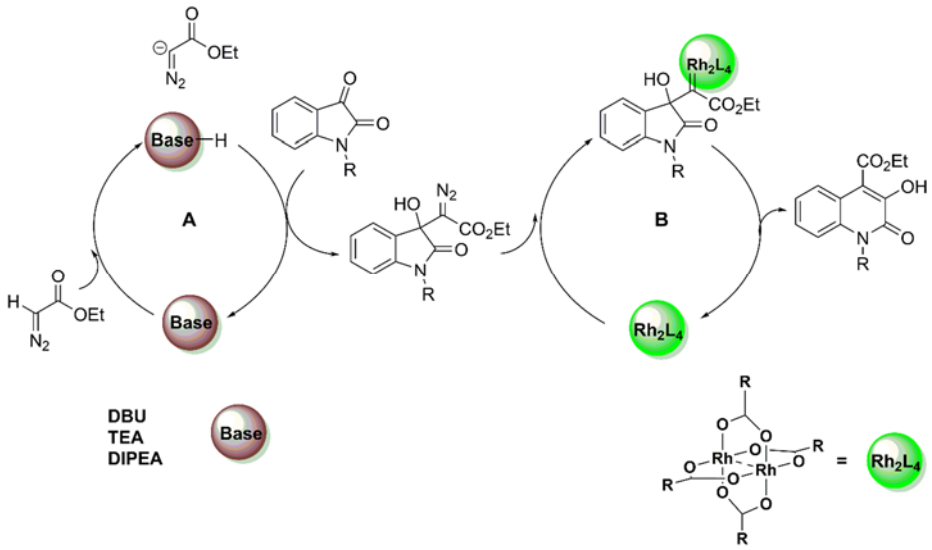

Schema 2.10 - A metal-organo-catalytic system for the synthesis of 3HQs

Lower yields or traces of compound **70** were obtained with other organic bases such as trimethylamine (TEA), diethylamine, diisopropyl ethyl amine (DIPEA) (Table 2.1, entries 1-4) or with *t*-BuOK inorganic base (Table 2.1, entry 5).

Table 2.1- Screening of base for the aldol-type addition of EDA[a]

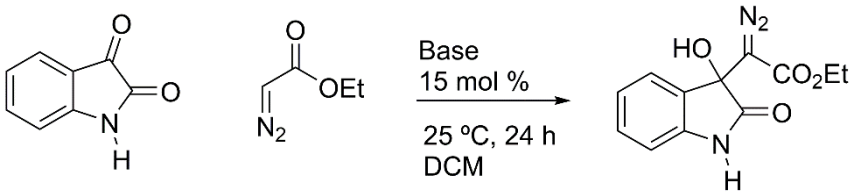

68 **70**

Entry	Base	Yield %[b]
1	Triethylamine	<14
2	Diethylamine	15
3	Diisopropyl ethyl amine	Traces
4	1,8-Diazabicyclo[5.4.0]undec-7-ene	78
5	*t*-BuOK	17

[a] **Reaction conditions**: isatin (0.3 mmol), EDA (1.2 eq.), DBU (15 mol %) and DCM (1.5 mL), rt, 24 h.; [b] isolated yield

The analysis of the NMR spectra are in agreement with structure of the compound and further X-ray crystallography (Figure 2.4) confirm the structure of the diazo intermediate **70**.

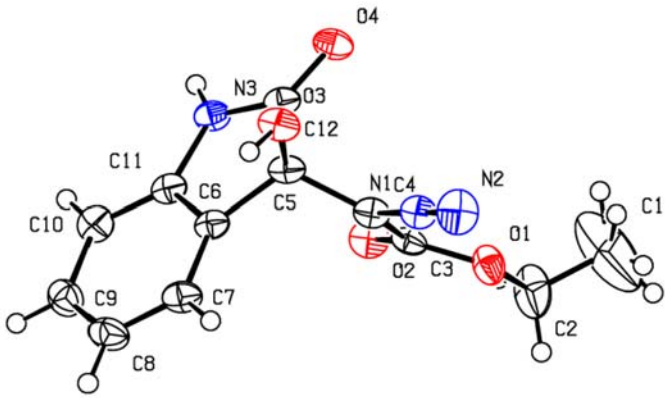

Figure 2.4 – X-ray crystallography of **70.**

Following these preliminary results, DBU was selected to investigate the effect of different reaction solvents (Table 2.2).

Table 2.2- Solvent screening for DBU catalysed aldol-type addition of EDA to isatin[a]

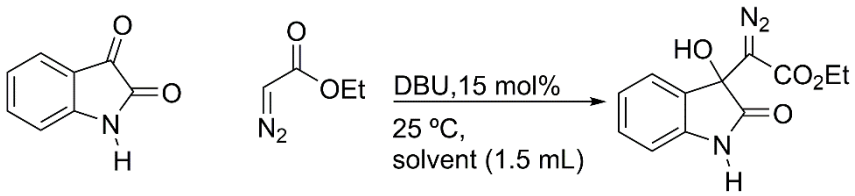

68 **70**

Entry	Solvent	Time (h)	Yield %
1	DCM	2	<25
2	Toluene	2	51
3	Chlorobenzene	2	47
4	Et_2O	2	68
5	THF	2	38
6	EtOH	2	73
7	EtOH	3	82

Reaction conditions: isatin (0.3 mmol), EDA (1.2 eq.), DBU (15 mol %)

Despite the good yield observed in DCM after 24 h reaction time (Table 2.2, entry 4), less than 25 % of product was obtained after 2 h in the same reaction conditions (Table 2.2, entry 1).Aromatic solvents, such as toluene and chlorobenzene, allowed the formation of the desired product in ca. 50 % yields after 2 h. Considering more polar ether solvents, diethyl ether was superior to tetrahydrofuran (THF), leading to formation of **70** in 68 % yield. Ethanol was nevertheless the best solvent system tested, resulting in formation of the desired compound in 78 and 82 % yields after 2 and 3 h, respectively (Table 2.2, entries 5 and 6).Smaller amounts of base were considered and observed to have a detrimental effect on the reaction yield (Table 2.3).

Table 2.3- Effect of the amount of DBU in the ring expansion reaction in ethanol[a]

DBU mol %	**Time** (h)	**Yield %**
15 [a)]	2	73
15	3	82
10	6	77
5	3	59

[a] **Reaction conditions**: isatin (0.3 mmol), EDA (1.2 eq.), DBU, and EtOH (1.5 mL), rt.

2.2.5 Eistert Ring expansion of isatins with EDA using a sequential DBU/$Rh_2(OAc)_4$ system

After optimizing the EDA addition to isatin, the compatibility between $Rh_2(OAc)_4$ and DBU was tested by adding 1 mol% of this complex to the reaction mixture. Pleasantly, the sequential protocol afforded the compound 3-hydroxy-4-ethylesterquinolin-2(1*H*)-ones **69** in 63 % yield confirming the possibility to combine in the same pot both catalysts (Scheme 2.10). With this promising result in hand, we started to investigate the scope of this reaction under the optimized reaction conditions [DBU (15 mol %) in EtOH, 25 ºC followed by addition of $Rh_2(OAc)_4$ 1 mol %], and the results are shown in table 2.4.

Table 2.4 – Eistert ring expansion of isatins with EDA using a sequential DBU/$Rh_2(OAc)_4$ system.

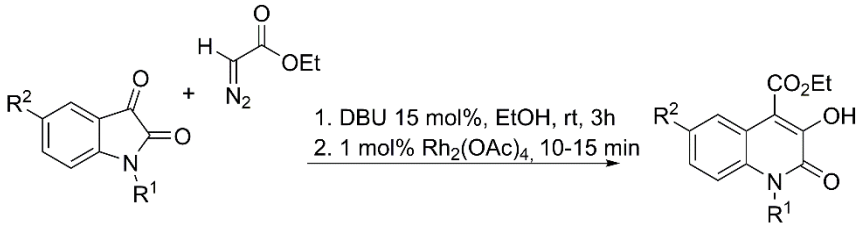

Entry	R^1	R^2	Compound	Yield %
1	H	H	**69**	63
2	H	F	**84**	64
3	H	Cl	**85**	92
4	H	Br	**86**	90
5	H	CF_3O	**87**	74
6	Me	H	**88**	75
7	Me	F	**89**	75
8	Me	Cl	**90**	81
9	Me	Br	**91**	78
10	Me	CF_3O	**92**	81
11	Bn	H	**93**	73
12	Bn	F	**94**	93
13	Bn	Cl	**95**	87
14	Bn	Br	**96**	72

reaction conditions: isatin (0.3 mmol), EDA (1.2 eq.), DBU (15 mol %) and EtOH (1.5 mL). 1 mol % of $Rh_2(OAc)_4$ was added to the reaction mixture after 3 h

Commercially substituted isatins were used bearing electron withdrawing groups on the indoline-2,3-dione nucleus (R^2) and different substituents on the nitrogen (R^1). *N*-Methyl and *N*-benzyl isatins were synthetized when necessary from commercial isatin (see experimental section). The methodology, shown in Table 2.4, was quite tolerant to the substituents present in the aromatic ring. Furthermore, good to excellent yields were obtained when using *N*-unsubstituted (Table 2.4, compounds **69; 84-87**), *N*-methyl (Table 2.4, compounds **88-92**) and *N*-benzyl (Table 2.4, **93-96**) isatins. The NMR data of all the compounds are in agreement with the chemical structure in addition to the X-ray crystallography of compound **93** (Figure 2.5).

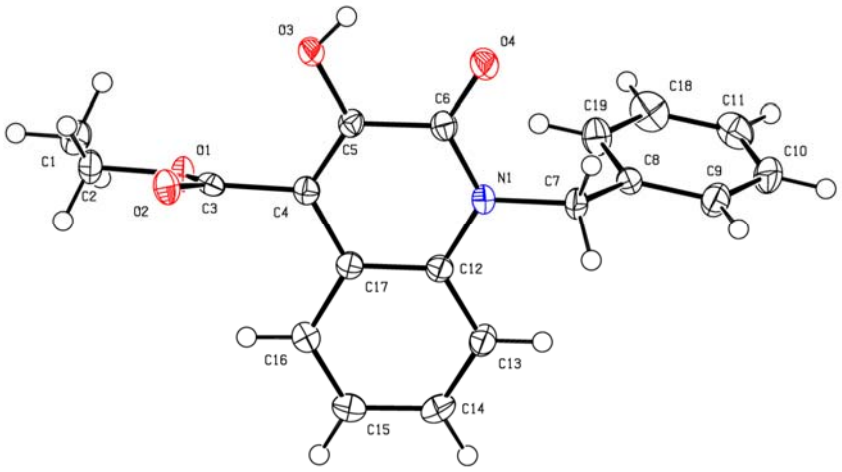

Figure 2.5 – X-ray crystallography of **93.**

2.2.6 Eistert ring expansion of isatins with EDA using a one-pot relay DBU/$Rh_2(OAc)_4$ system.

Once established the sequential transformation, we considered the possibility to have both catalysts present in one-pot from the on-set of the reaction, and assess the eventuality of self-quench of the catalytic system or the competitive metallocarbene formation of di-Rh(II) complex with EDA. The first attempt to performed the one pot relay system was carried out using *N*-methyl-isatin with EDA in the presence of 15 mol% DBU and $Rh_2(OAc)_4$ in DCM (Scheme 2.11). Aware of the potential difficulties already described when performing a one pot reaction, the reaction yielded compound **88** in just 30 % after 3h of reaction (Table 2.4, entry 1).

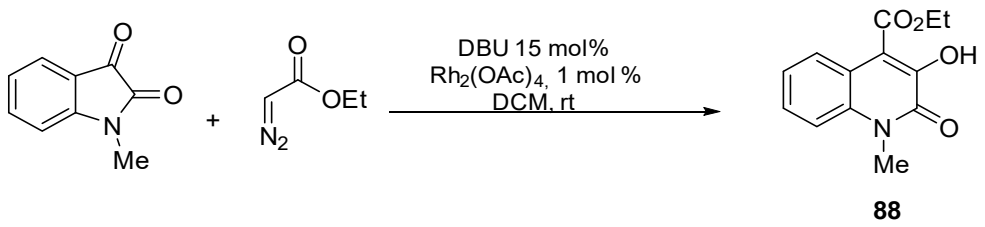

88

Scheme 2.11 – One-pot reaction using *N*-methyl-isatin with EDA in the presence of DBU 15 mol% and $Rh_2(OAc)_4$ in DCM

One of the most important characteristics of dirhodium(II) complexes is the fact that they are easily tunable in their electrophilicity profile by replacement of the ligands (Scheme 2.12), which dramatically reflects on the catalyst reactivity and selectivity as demonstrated by Doyle et al.[121]

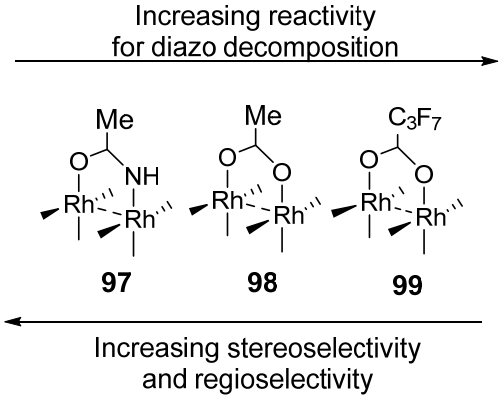

Scheme 2.12 – Ligands influence on the electrophilicity of dirhodium(II) complexes

As depicted in Scheme 2.12, dirhodium(II) perfluorobutyrate ($Rh_2(pfb)_4$, **99**), whose ligands are strongly electron withdrawing, showed high reactivity for diazo decomposition comparable to that for CuOTf, although in low stereo- and regiocontrol. In contrast, dirhodium(II) carboxamidates, including dirhodium acetamidate ($Rh_2(acam)_4$, **97**),[122] and di-rhodium caprolactamate ($Rh_2(cap)_4$, **98**)[123] exhibited lower reactivity and higher selectivity.[124, 125] For this reason, different Rh(II) catalysts with diverse electronic characters and different ligand were tested in the one-pot ring expansion reaction (Scheme 2.13). Recently, our group reported that dirhodium(II) complexes coordinated in one of their axial positions with N-heterocyclic carbenes (NHCs) generate metallo-carbenes from diazo substrates giving a distinct reactivity from the parent $Rh_2(OAc)_4$ complex.[126] Based on this, the catalytic activity of dirhodium(II) complexes **97, 110**-**104** were evaluated aiming at reducing the interaction of DBU with the metal complex.

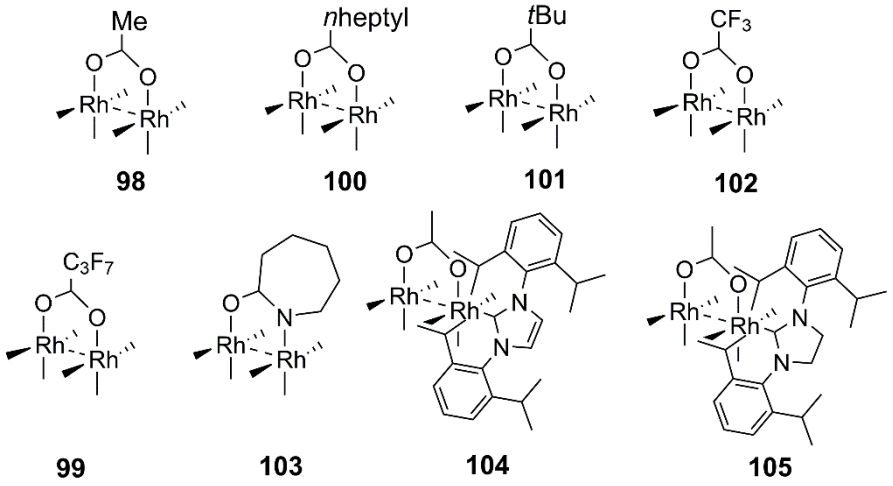

Scheme 2.13 – Dirhodium(II) catalysts evaluated in the one-pot Eistert ring expansion of isatins with EDA.

Considering the conversions determined based on the ^{1}H-NMR reaction crude mixture, (Table 2.4) complex **104** containing an electron-donating axial NHC ligand,[21a,24 109, 127] was found to be the most efficient catalyst.

Table 2.4 – Eistert ring expansion of isatins with EDA using a one-pot DBU/$Rh_2(OAc)_4$ system.[a]

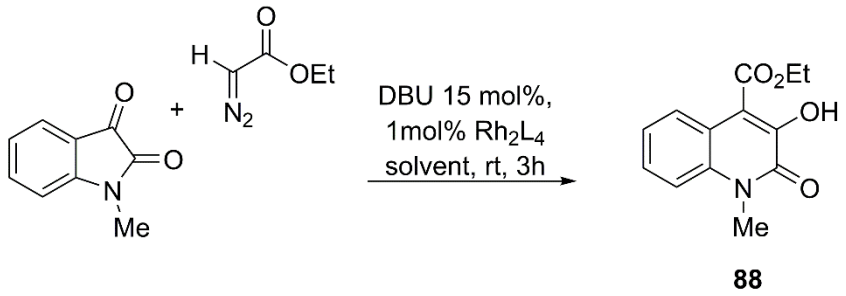

88

Entry	Solvent	Catalyst	Product(%)	Diazo(%)	Isatin(%)
1	DCM	98	32	<16	51
2	DCM	100	35	<14	50
3	DCM	101	25	<7	67
4	DCM	102	35	<17	47
5	DCM	99	46	<19	34
6	DCM	103	43	<20	35
7	DCM	104	44	<9	45
8	DCM	105	35	13	53
9	Toluene	104	51	3	44
10	DCE	104	49	2	44
11	EtOH	104	80	1	19
12	DME	105	45	10	43

N-methyl isatin (0.3 mmol), EDA (1.2 eq.), DBU (15 mol %), dirhodium complex (1 mol %), solvent (1.5 mL)

This complex promoted the formation of product **88** in 44 %, while avoiding the build-up of the diazo intermediate which was detected in only 9 % (Table 2.4, entry 7). Analogously to the sequential protocol, ethanol was the best solvent for the one-pot protocol affording the desired product **88** in 80 % yield (Table 2.4, entries 9-12). Once optimized the reaction conditions, the protocol was extended to other substrates with similar or better yields than the ones observed when performing the reaction in a sequential manner (Table 2.5)

Table 2.5 - Eistert Ring expansion of isatins with EDA using a one-pot relay DBU/$Rh_2(OAc)_4$ system.

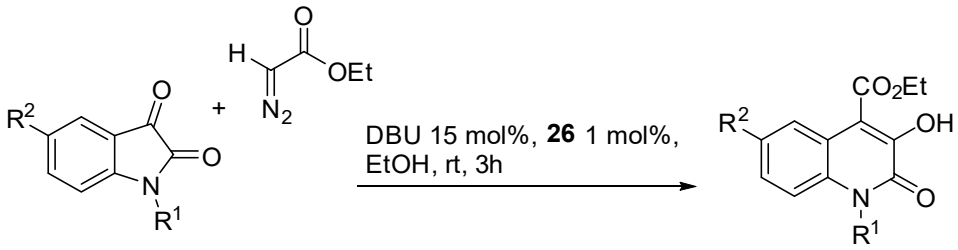

Entry	Compound	R^1	R^2	Yield
1	**69**	H	H	63 %
2	**92**	CH_3	CF_3O	81 %
3	**90**	CH_3	Cl	92 %
4	**91**	CH_3	Br	90 %
5	**93**	CH_2Ph	H	85 %
6	**95**	CH_2Ph	Cl	68 %

2.2.7 **Computational Study**

After establishing the ring expansion protocol, we addressed the complex preference for the decomposition of the isatin-diazo intermediate instead of EDA. In order to understand this and get further insight on the reaction mechanism, the ring expansion reaction catalyzed by dirhodium complexes was studied by Density Functional Theory (DFT).[128] This study was performed by Dr. Nuno Candeias.

For the calculation model reactant, we use the diazo compound resultant from the addition of EDA to isatin (**70**), and the mechanism explored starting from the formation of the metallocarbene and subsequent ring expansion. The free energy profiles obtained are represented in Figure 2.6- 2.8 and a general working model of the mechanism is show in Figure 2.9.

The metallocarbene formation proceeds through a concerted mechanism in which the transition state (**ts1**) accounts for the C-Rh formation with synchronous release of a nitrogen molecule (Figure 2.6). This aspect is evident by the C-Rh decrease from 2.39 Å in the optimal **70**-**$Rh_2(OAc)_4$** pair to 2.10 Å in **ts1**, whilst the Wiberg index increases from 0.17 to 0.43. Consequently, after the liberation of N_2, the metallocarbene is formed by strengthening the C-Rh bond as shown by the C-RH distance (1.98 Å) and the Wiberg index (0.71) in **mc1**.

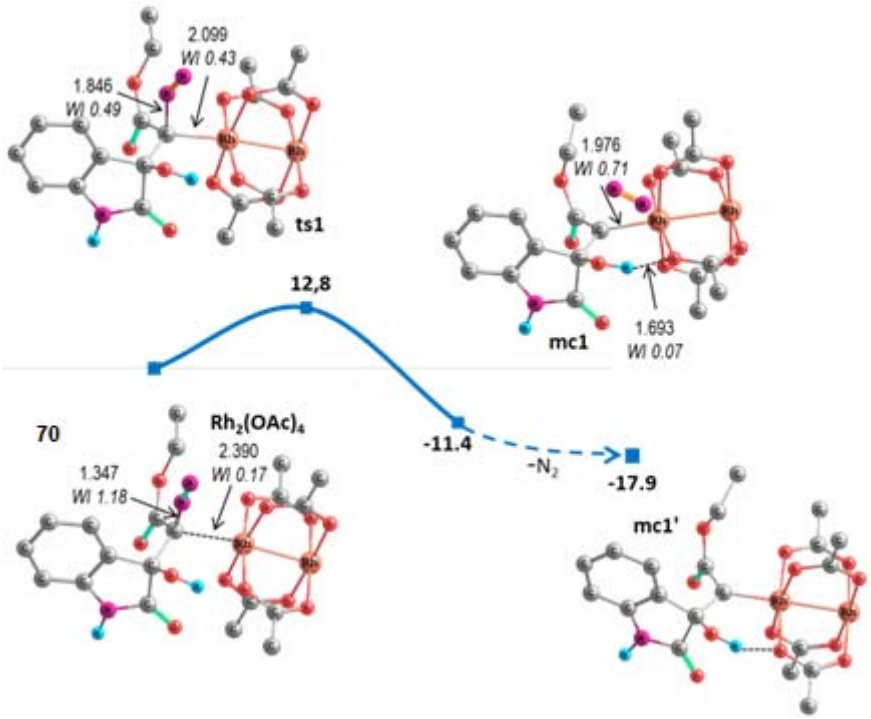

Figure 2.6 - Energy profiles calculated for the metallocarbene formation between the 3-substituted 3-hydroxy-oxindole (**70**). The relevant bond distances (Å) are indicated, as well as the respective as well as the respective Wiberg indices (WI, italics)

An intramolecular H-bond formed between the hydroxyl group of the oxindole moiety and one of the carboxylates of the metallic complex is observed, stabilizing the represented conformation of **mc1'** in 7 kcal/mol compared with the conformer

in which the O-H bond is kept away from the carboxylate ligands of the dirhodium complex (Appendix, Figure A1) For the one pot version of this transformation to be successful, ethyl diazoacetate cannot react with $Rh_2(OAc)_4$ to form the corresponding metallocarbene. After the observation of the preferential formation of the ethyl diazoacetate addition to isatin, the mechanism for the formation of the metallocarbene derived from that diazo compound was studied, for comparison purposes. Analogously to the formation of the metallocarbene derived from **70**, the one derived from ethyl diazoacetate also proceeds through a concerted nitrogen extrusion and C-Rh bond formation as indicated by the strengthening of the C-Rh bond and weakening of the C-N bond from the **eda+Rh$_2$(OAc)$_4$** pair to **ts$_{eda}$** (Figure 2.7).

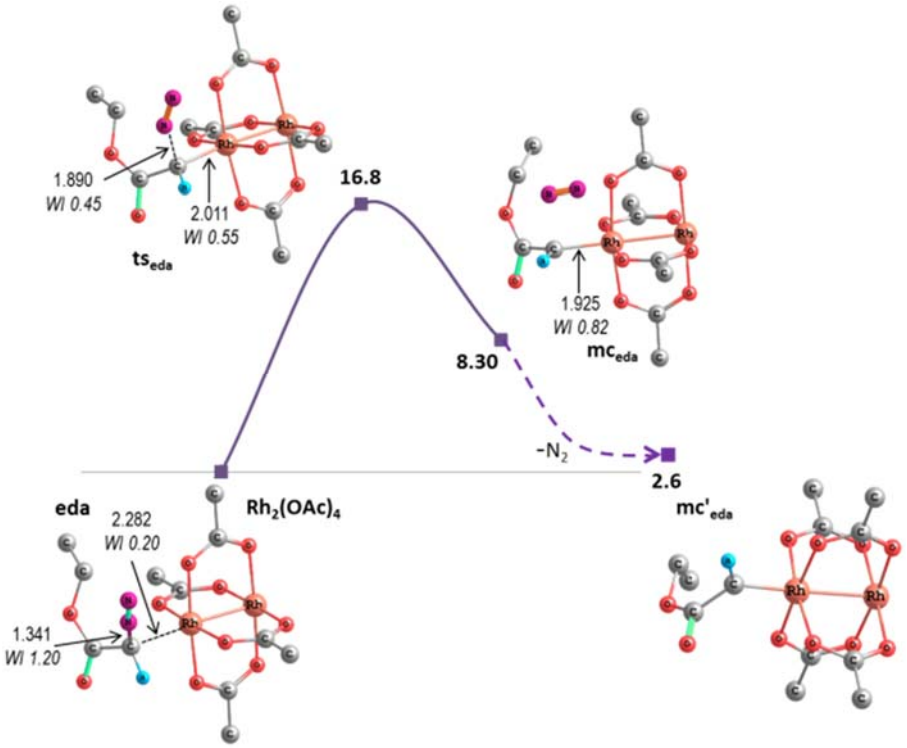

Figure 2.7 - Energy profiles calculated for ethyl diazoacetate (eda) and dirhodium(II) tetraacetate. The relevant bond distances (Å) are indicated, as well as the respective as well as the respective Wiberg indices.

However, this process is thermodynamically unfavorable (ΔG_{298} = 2.6 kcal/mol) and has an energy barrier 4 kcal/mol higher than the one previously discussed (Figure 2.6), which corroborates the selectivity of the dirhodium catalyst towards reaction with oxindole starting material. After formation of the metallocarbene (Figure 2.8 and

Figure 2.9), this rearranges from **mc1** to **mc2**, with a concomitant weakening of the Rh–C bond, as shown by the corresponding Wiberg indices, 0.7 in **mc1** and 0.4 in **mc2**. The geometry changes that occurred from **mc1** to **mc2** allows migration of the aryl ring that will happen in the next step, through transition state **ts2**. This transformation occurs through a three-membered ring in which the bond that is being formed and the one that is broken have similar distances and Wiberg indices around 1.6 Å and 0.7, respectively. On the other hand, the other C-C bond of the three-membered ring is kept unchanged during the process. The C_{aryl}-C bond migration step, from **mc2** to **mc3**, is thermodynamically favorable by over 18 kcal/mol.

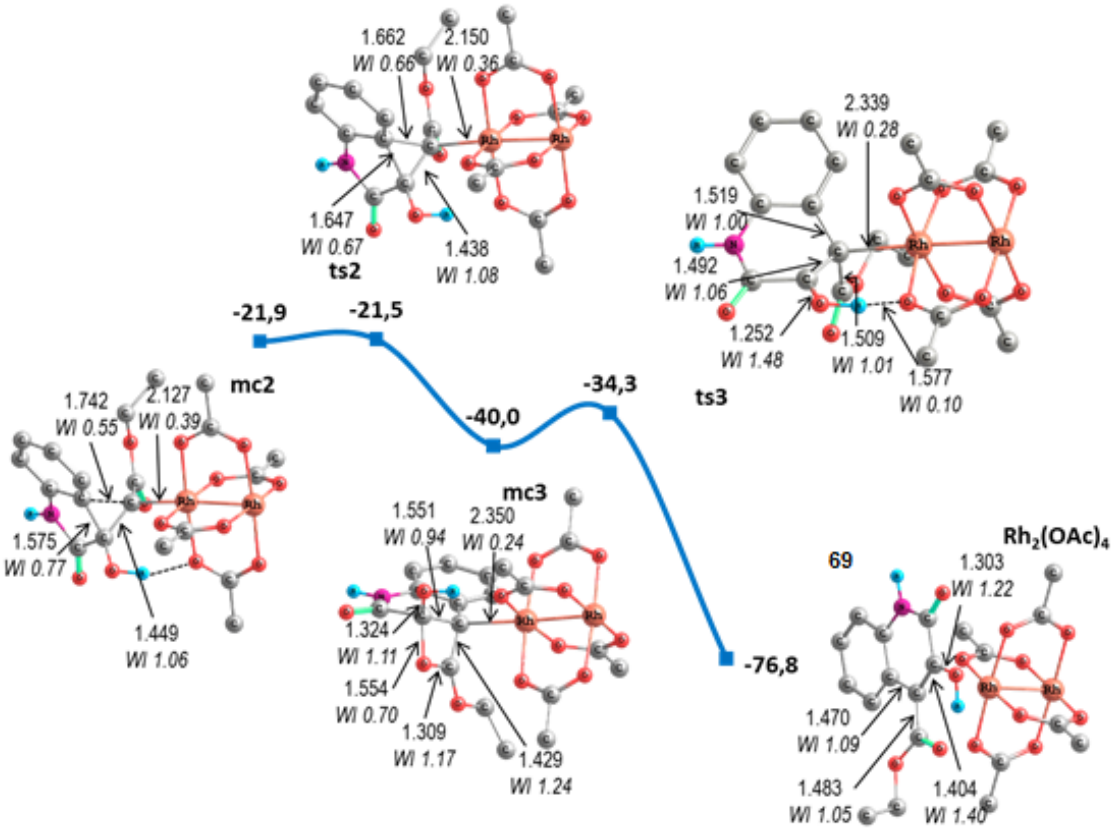

Figure 2.8 – Energy profiles calculated for the 1,2-aryl migration of the metallocarbene formed between the 3-substituted 3-hydroxy-oxindole and dirhodium(II) tetraacetate. The relevant bond distances (Å) are indicated, as well as the respective Wiberg indices.

Intermediate **mc3** is characterized by the presence of a fused four-membered ring, that is formed by the interaction of the free electron pair of the carbonyl oxygen with

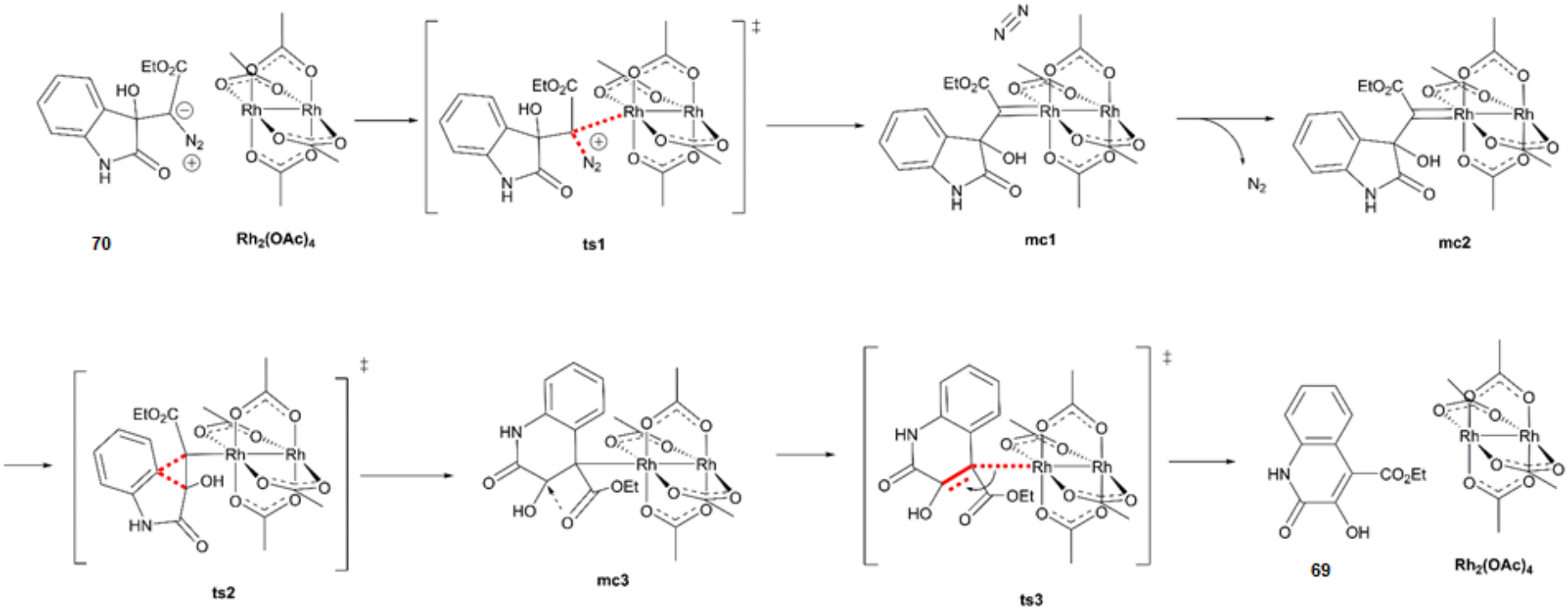

Figure 2.9 – Mechanistic representation of the dirhodium catalyzed ring expansion reaction of 3-hydroxy oxindole.

the 3-carbon of the quinolone moiety in order to stabilize the electronic deficiency of that position. Interestingly, whilst the dirhodium catalyst is determinant to extrude the molecular nitrogen and consequently form the metallocarbene, its role along the pathway is diminished. Probably due to the bulkiness of the quinolone ring, the C-Rh bond length is kept longer than 2.3 Å after this stage, being accompanied by a low Wiberg index (WI 0.2 for Rh-C of **mc3**) when compared with **mc1** (C-Rh WI 0.7). The following step in the mechanism corresponds to the C-Rh bond cleavage and synchronous formation of the C=C bond, going through transition state **ts3**, with an energy barrier of 6 kcal/mol. After the product formation, an intramolecular hydrogen bond between the hydroxyl group at the 3 position and the carboxylic ester stabilizes the product whilst the dirhodium complex is liberated to reenter in the catalytic cycle. A very weak interaction of the final product with the metal complex is observed and the conformation obtained for **69** (Figure 2.8) is in strong agreement with the X-ray structure determined for the product (with deviations smaller than 0.06 Å). The mechanism discussed above represents a thermodynamically favorable process (ΔG_{298} = –77 kcal/mol) with metallocarbene formation as the rate determining step (i.e., is the first one) and an energy barrier of 13 kcal/mol. The metallocarbene formation has been previously determined to be the rate determining step in Rh-carbenoid C–H insertions.[129]

Lewis acids are known to catalyze the ring expansion of 3-hidroxyindoles bearing a diazoethoxycarbonyl at the 3-position, as previously reported by Pellicciari and co-workers.[130] Taking this into consideration, and despite the rather weak Lewis acidity of dirhodium complexes,[23] we explored alternative mechanisms for the ring expansion reaction. This was achieved considering coordination of the substrate to Rh through the carbonyl group of carboxylic ester moiety or by the carbonyl of the 3-oxindole function. In both cases, substrate coordination yielded a stabilization of the initial pair of reactants. However, the mechanisms calculated for those starting species are not competitive with the one presented above (Appendix A for complete energetic profiles).

In addition, alternative mechanisms accounting for the product formation without the intervention of the dirhodium complex were also considered (Appendix A for

complete energetic profiles). Two paths were envisaged, one proceeds via a free carbene intermediary and the other is a concerted 1,2-aryl migration with nitrogen extrusion. In both cases the calculated energy barriers are considerably higher than the ones associated with the mechanism discussed above.

2.2.8 **Synthesis of Viridicatin alkaloids**

Once established the efficient regioselective ring expansion reaction of isatins with ethyl diazoacetate, we evaluated the possibility of synthesising the viridictin core *via* a Suzuki-Miyaura coupling reaction of aryl-boronic acids with 3-hydroxy-4-bromoquinolin-2(1*H*)-ones.

Suzuki cross coupling reaction of aryl halides with organoboronic acids proved to be the most efficient method for the construction of biaryl or substituted aromatic moieties.[131, 132]

In cross-coupling Suzuki-Miyaura reaction (SMC), the catalytic cycle is thought to follow a sequence involving the oxidative addition of an aryl halide to a Pd(0)complex to form an arylpalladium(II) halide intermediate. Transmetalation with a boronic acid and reductive elimination from the resulting diarylpalladium complex affords the corresponding biaryl and regenerates the Pd(0) complex (Figure 2.10).[133] Although not yet clear, the role of the base has been suggested to encompass the facilitation of the otherwise slow transmetalation of the boronic acid, by forming a more reactive boronate species that can interact with the Pd center and transmetalate in an intramolecular fashion.[134]. Alternatively it has been proposed that the base replaces the halide in the coordination sphere of the palladium complex and facilitates the intramolecular transmetalation.[135]

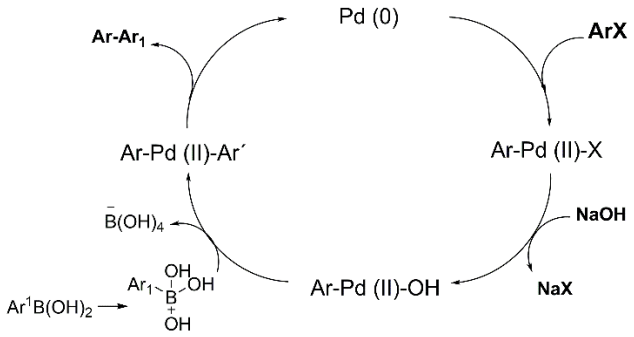

Figure 2.10 - General catalytic cycle for Suzuki-Miyaura couplings.

For the subsequent palladium-catalysed Suzuki cross coupling reaction the activated bromide **105** was prepared. The 3-hydroxy-4-bromoquinolin-2(1*H*)-ones **105** was simply set by decarboxylation of the ester moiety of compound 6 in basic medium followed by acidification with 2 N HCl solution yielding **9** in 92%. After that, compound **9** was reacted with N-bromosuccinimide in DMF according to the protocol described in the literature to provide the halide in 90 % yield.[77]

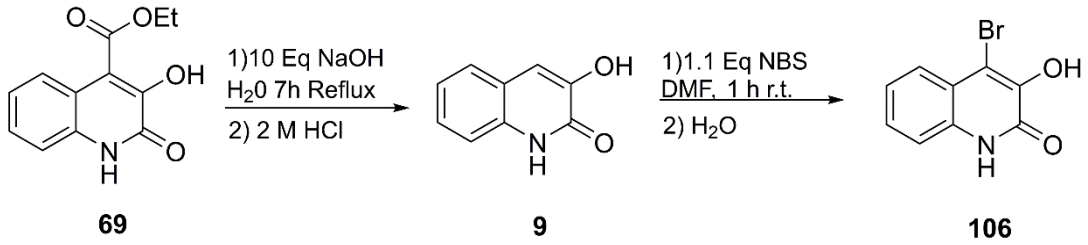

69 **9** **106**

Scheme 2.14- Synthesis of 3-hydroxy-4-bromoquinolin-2(1*H*)-one **106**

We carried out the the first coupling reaction in refluxing dimethoxyethane (DME) for 24h using $Pd(dba)_3$ (3 mol%), $P(Ph)_3$ (12 mol %) and Na_2CO_3 aqueous solution as base. With these reaction conditions we were able to isolate viridicatin **31** in 50 % yield after purification by flash chromatography

Table 2.5 - Catalyst screening for Suzuki-Miyaura coupling of **106** and phenylboronic acid

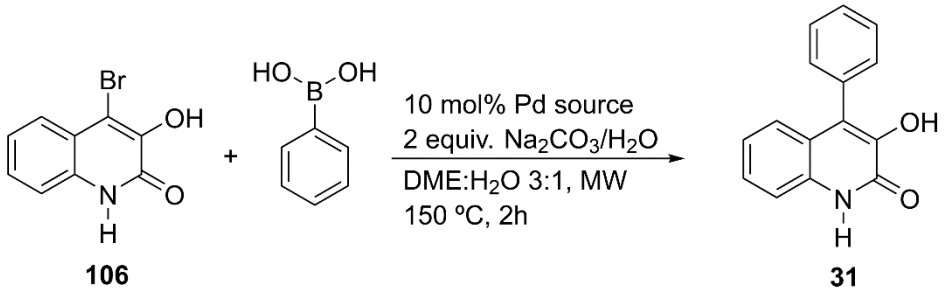

106 **31**

Pd source	mol%	Isolated Yield (%)
$Pd_2(dba)_3$	5 mol%	47
$Pd(dppf)Cl_2 \cdot CH_2Cl_2$	10 mol%	66
$Pd(PPh_3)_4$	10 mol%	80
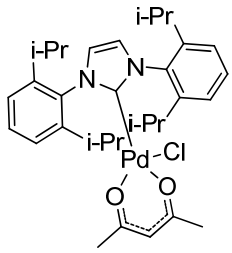	10 mol%	50
$PdCl_2$	10 mol%	59

It is well-known that the Suzuki coupling and other transition-metal-catalysed reaction can be significantly shortened by direct in-core microwave heating.[136] Taking advantage of the rapid automated processing features of modern microwave reactor instrumentation,[137] the Suzuki reaction was quickly optimized probing different catalyst/solvent/base combinations in addition to varying reaction time and temperature. The best conversions and isolated product yields were achieved by using tetrakis(triphenylphosphine)palladium(0) as catalyst. A 3:1 mixture of DME and water proved to be the optimal solvent combination, together with sodium carbonate as base. The optimal temperature/time was found to be 150 °C/2h by microwave.

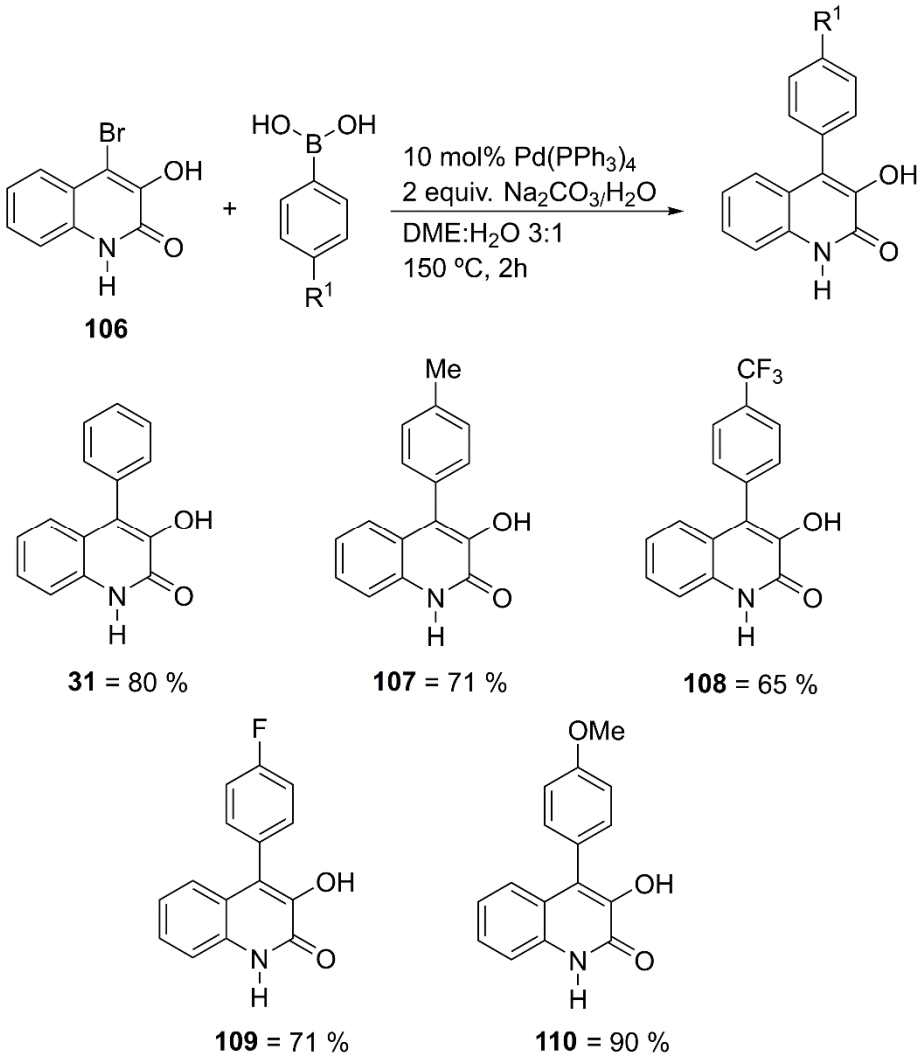

Scheme 2.15 – Synthesis of viridicatin alkaloid derivatives based on the Suzuki-Miyaura coupling reaction of aryl-boronic acids with 3-hydroxy-4-bromoquinolin-2(1H)-ones **106**.

Biologically active viridicatin was obtained in 80 % yield after flash chromatography purification and further characterised through NMR techniques. The NMR chemical shifts data assigment (Appendix C, Figure C2) are in agreement with the chemical structure of the compound and with the previously reported data.[87] The optimized reaction conditions were successfully used in the coupling of 3-hydroxy-4-bromoquinolin-2(1*H*)-one with arylboronic acids featuring electron-withdrawing and electron-donating substituents yielding viridicatin derivatives **107**-**110** from good to exelent yields. All the derivatives were characterized by NMR techniques (Section 6.6).

2.2.9 **Conclusion**

An efficient synthesis of viridicatin alkaloids based on a Suzuki-Miyaura coupling reaction of aryl-boronic acids with 3-hydroxy-4-bromoquinolin-2(1*H*)-ones prepared from 3-hydroxy-4-ethylesterquinolin-2(1*H*)-ones was developed. The 3-hydroxy-4-ethylesterquinolin-2(1*H*)-one was simply prepared by a regioselective ring expansion reaction of isatins with ethyl diazoacetate catalysed by dirhodium(II) complexes. The reaction mechanism was studied by DFT calculations that highlighted the metallocarbene formation between the 3-hidroxyindole-diazo intermediate and the dirhodium(II) complex as the key step of the mechanism.

The discovered compatibility of the NHC-dirhodium(II) complex **104** and DBU, enabled the implementation of the one-pot addition of ethyl diazoacetate to isatin followed by the NHC-dirhodium(II) catalyzed ring expansion reaction, ultimately leading to preparation of 3-hydroxy-4-ethylesterquinolin-2(1*H*)-ones in yields up to 92 %. Finally, the 3-hydroxy-4-bromoquinolin-2(1*H*)-one core was simply coupled with aryl-boronic acid to afford the expected vidicatin alkaloids in up to 80 % yield.

Chapter III

III. Synthesis of 4-Substituted-3-Hydroxyquinolin-2(1*H*)-ones and Anticancer Activity Evaluation

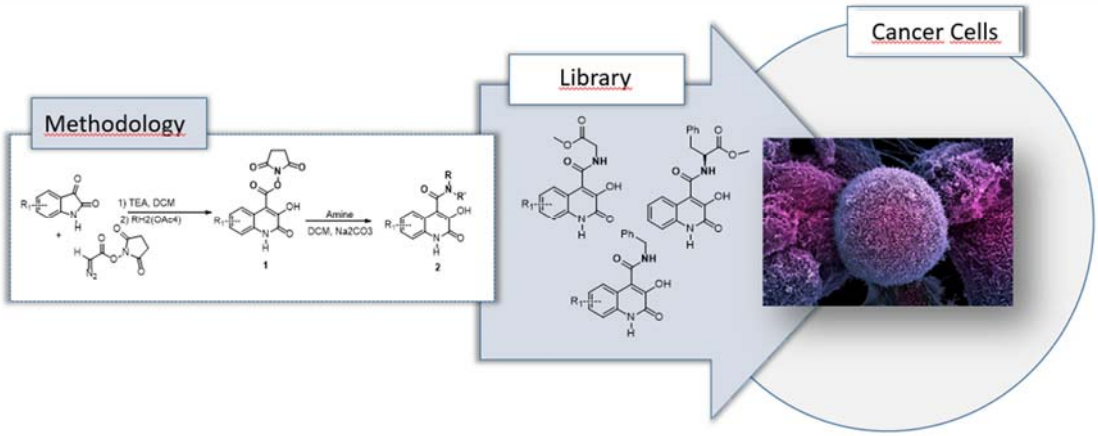

Abstract

Herein we shown that the 3-hydroxyquinolin-2(1H)-one (3HQ) core is a suitable platform to develop new compounds with anticancer activity against MCF-7 (IC50s up to 4.82 μM), NCI-H460 (IC50s up to 1.80 μM) and HT-29 (IC50s up to 11.37 μM) cancer cell lines. The ring-expansion reaction of isatins with diazo esters catalysed by di-rhodium(II) complexes proved to be a simple and effective strategy to synthesise 4-carboxylate-3HQs (yields up to 92%). 4-Carboxamide-3HQs were more efficiently prepared using NHS-diazoacetate, and this innovative methodology enabled the construction of "peptidic-like" 3HQs in yields up to 88%. Among this series, the L-leucine-4-carboxamide-3HQ induced the cell death of MCF-7 (IC50 of 15.12 μM), NCI-H460 (IC50 of 2.69 μM) cancer cell lines without causing any appreciable cytotoxicity against the non-cancer cell model (CHOK1).

3.1 Cancer hallmarks

Cancer is a burden of our days. An estimated 14.1 million new cancer cases and 8.2 million cancer deaths occurred in 2012 worldwide.[138] According to GLOBOCAN 2012 statistic, among the many cancers, lung, breast and colorectum cancer are the most frequently diagnosed and are the leading causes of cancer death in both sex and in developed and less developed countries (Figure 3.1).[139] Currently, as suggested from World Health Organization (WHO), primary prevention strategies such as tobacco control, vaccination (for liver and cervical cancers), early detection, and the promotion of physical activity and healthy dietary patterns are the strategies for intervention in cancer control.[140] Despite the availability of improved drugs and targeted cancer therapies, it is expected that the new cases of cancer will jump to 19.3 million worldwide by 2025. Unfortunately, cancer remains a highly unmet medical need and discovery and development of remarkable chemotherapeutic agents having a limited toxicity profile are still needed.[138]

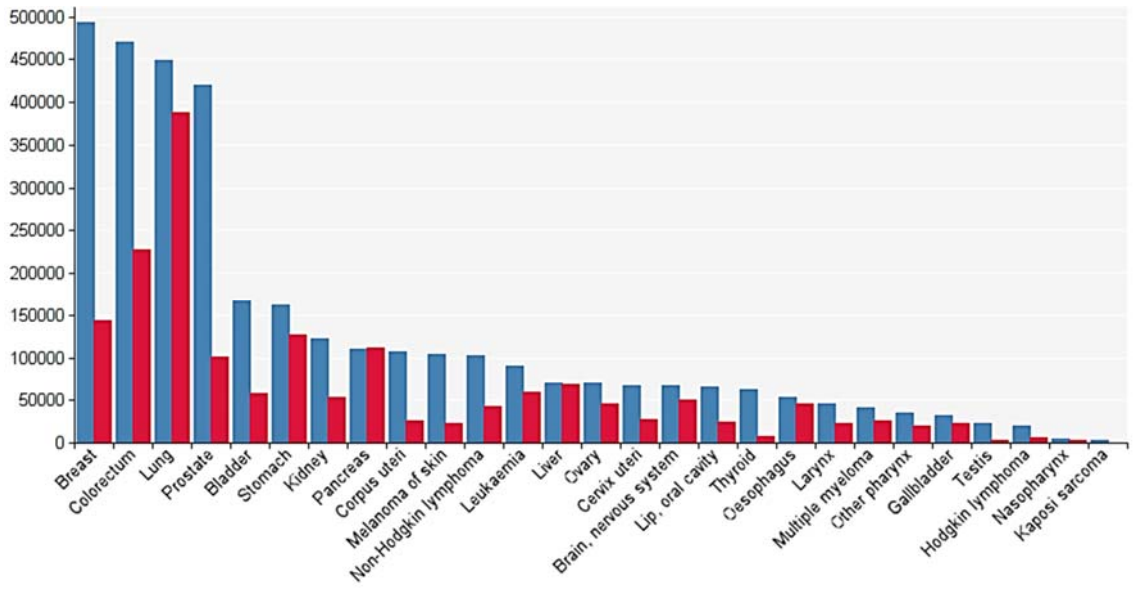

Figure 3.1 - Incidence (blue) and mortality (red) of cancer worldwide. GLOBALCAN 2012 (IARC).

Heterocyclic quinolin-2(1*H*)-one analogues were already reported as anticancer agents in literature. Novel active anti tumour agent as Zanestra **7** and linomide **16** showed the biological potential of quinolin-2(1*H*)-ones core and inspired us to explore further the 3HQs derivatives. Despite the important biological activities of 3HQ compounds, the use of this scaffold in the construction of anti-proliferative agents remains mostly unexplored. However, while developing new inhibitors of the HIV-1 reverse transcriptase associated RNase H activity, Bailly et *al* observed that a series of 4-substituted 3HQs were significantly cytotoxic against non-cancer MT-4 cells, and this precluded their further use as antiviral agents.[72] Keeping these observations, we envisioned that a 3HQs library could be further explored as a valuable platform to prepare innovative anti-proliferative agents. In continuation of our work we envisioned the synthesis of 4-carboxylate and 4-carboxamides substituted 3HQs and their anticancer screening studies.

3.2 Anti-proliferative activity and chemical modifications of the 3-hydroxyquinolin-2-ones lead core

3.2.1 Preliminary anti-proliferative screening

Aiming to test our hypothesis, we first set out to prepare a small library of 4-carboxylate 3HQs derivatives. The synthesis of the 4-carboxylate-substituted-3HQs was achieved using the sequential protocol already described in chapter II. As shown in Scheme 3.1, exploring our recently described Eistert ring-expantion reaction of isatins with diazo acetate (EDA) catalysed by di-rhodium (II) complexes, 4-carboxylate-3HQs **69** and **84-96** were synthesised in good to excellent yields.

Once prepared, this set of compounds was evaluated against a panel of different s cancer cell lines namely: breast cancer cells (MCF-7), human non-small lung cancer cells (NCI-H460) and human colorectal adenocarcinoma cells (HT-29) (Table 3.1).

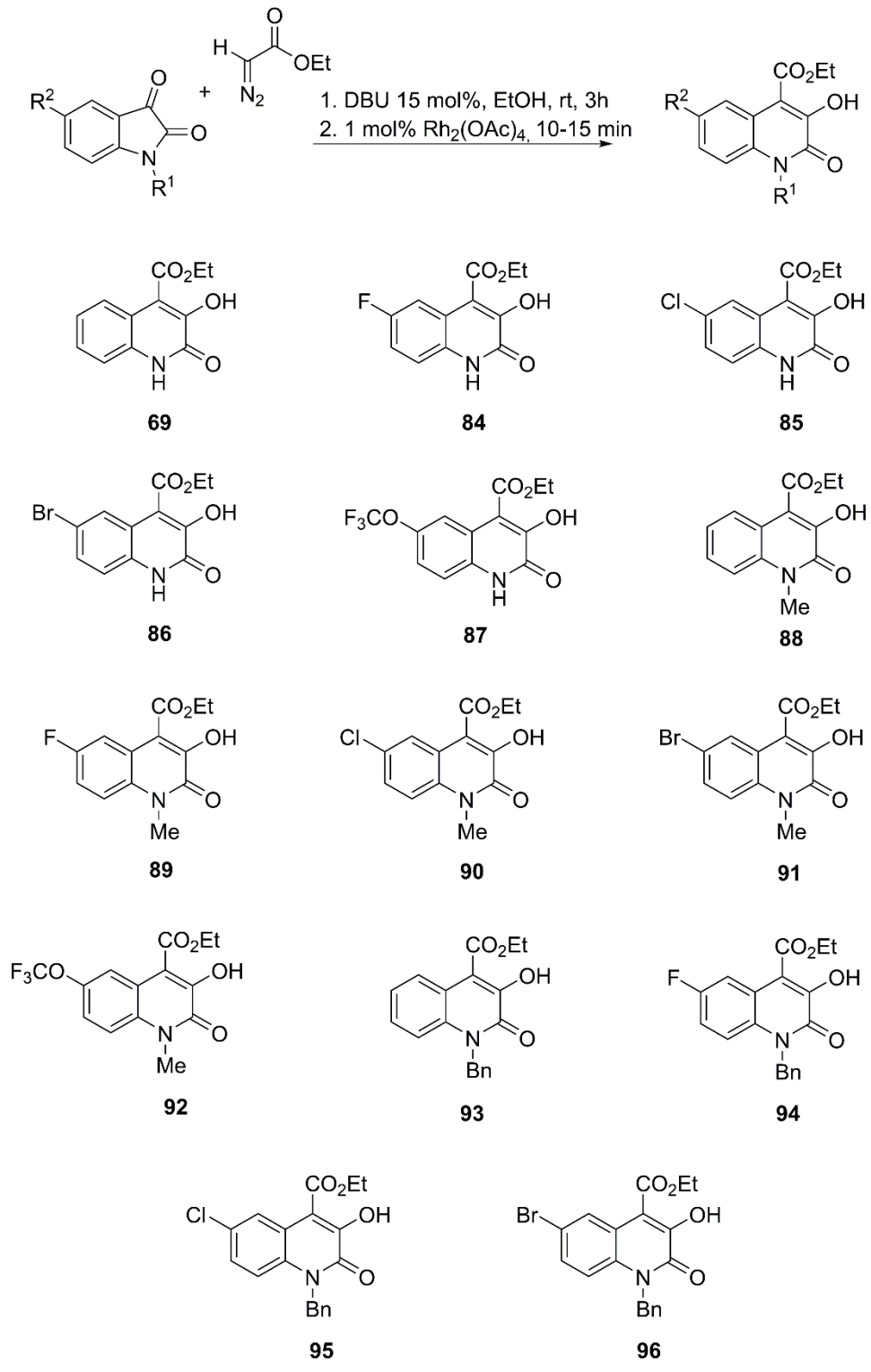

Scheme 3.1 Synthesis of 4-carboxylate substituted 3HQs **69**, **84**-**96** based on an Eistert ring expantion reaction of isatins with diazo acetate (EDA) catalysed by di-rhodium complexes.

Table 3.1 reports the biological data of anti-proliferative activity for this series of 3HQs. This assay revealed that 4-carboxylate-3HQs were generally non-active against the three cancer lines tested, though the 6-trifluoromethyl-4-ethylacetate-3HQ **87** was able to reduce the viability of the NCI-H460 cells in 48% at the concentration of 20 μM. Encouraged by this result we directed our attention to the 7-trifluoromethyl-4-ethylacetate-3HQ core and some structural modifications were performed.

Table 3.1 – Anti-proliferative evaluation of compounds **69** and **84**-**96** against MCF-7, NCI-H460 and HT-29 cancer cell lines.

ENTRY	COMPOUND	20 μM		
		MCF-7	NCI-H460	HT-29
1	**69**	NA	NA	87%
2	**84**	NA	NA	NA
3	**85**	NA	NA	NA
4	**86**	86%	NA	NA
5	**87**	95%	52%	74%
6	**88**	NA	82%	NA
7	**89**	NA	NA	NA
8	**90**	NA	NA	NA
9	**91**	NA	NA	NA
10	**92**	NA	NA	NA
11	**93**	NA	NA	NA
12	**94**	NA	NA	NA
13	**95**	NA	NA	NA
14	**96**	NA	NA	NA

Percentage of cell-viability; NA – Non-active at the concentration of 20 μM

3.2.2 **Structural modifications on the 3-hydroxyquinolin-2-one lead core 87.**

Once compound **87** was identified as lead, we performed some synthetic modifications of the compound. First we modified position C-4 of **87** by hydrolysis of the ester and further decarboxylation (Scheme 3.2). Product **111** was synthetized in 75 % yield and characterized by NMR spectroscopy. The assignment of the NMR spectra revels the absence of the typical signals of the ester moiety namely the quartet

of CH_2 at 4.49 ppm and triplet of CH_3 at 1.41 ppm and the presence of a singlet with a chemical shift of 7.42 ppm corresponding to the hydrogen in position C-4 of the 3HQ core.

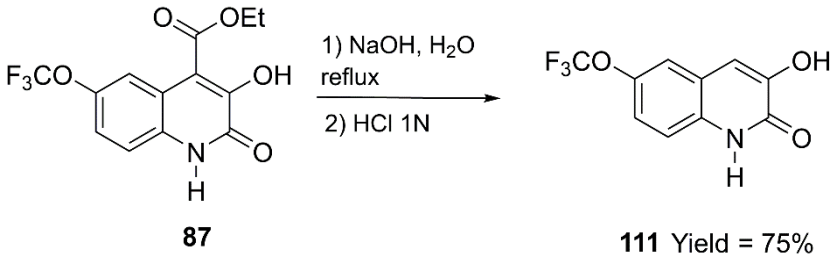

Scheme 3.2 – Synthesis of compound **111**

The second modification was the installation of a benzyl group in the nitrogen atom of the trifluoromethoxy quinolinone (Scheme 3.3). To perform this, the described Eistert ring expansion reaction of isatins with EDA catalysed by di-rhodium (II) complexes (see chapter II) was performed. With this protocol we were able to obtain compound **112** in moderate yield. Compound **112** was characterized by ^{1}H-NMR, ^{13}C-NMR and the results are in agreement with the chemical structure of the compound. With these two new hydroquinone derivatives in hand, their biological activity against the three cancer cell lines was determined and compared with the lead compound **87** (Table 3.2).

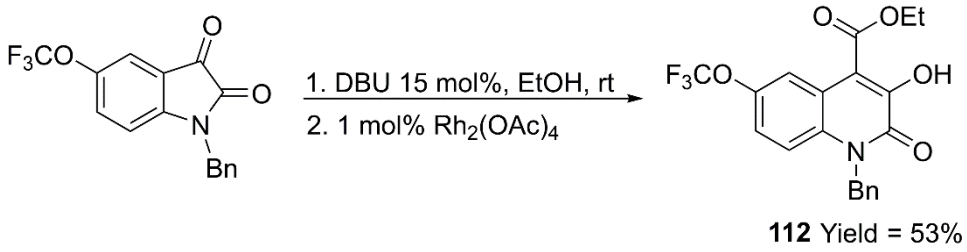

Scheme 3.3 Synthesis of compound **112** based on an Eistert ring expansion reaction of isatins with EDA catalysed by di-rhodium complexes.

Unfortunately, these structural modifications, namely the decarboxylated **111** and *N*-benzylated **112** resulted in the loss of the observed activity against the 3 cancer cell lines (Table 3.2).

Table 3.2. Anti-proliferative evaluation of compounds **111-112** against MCF-7, NCI-H460 and HT-29 cancer cell lines.

ENTRY	COMPOUND	MCF-7	NCI-H460	HT-29
1	**87**	95%	52%	74%
2	**111**	NA	NA	NA
3	**112**	NA	NA	NA

Percentage of cell-viability; NA – Non-active at the concentration of 20 μM

From an early structural relationship (SAR) point of view of our investigation, we addressed the influence of the substituent at the position C-4 on the activity of the heterocycle. For this reason, with the objective to perform structural modifications on position C-4 of the 6-F_3CO-3HQ core, a series of diazoacetate compounds were prepared and used in the Eistert ring expansion reaction of the 5-trifluoromethoxy-isatin.

Diazo acetates **113-115** were prepared in moderate to high yields as previously reported by Fukuyama and co-workers (Scheme 3.4),[141] by treatment of bromoacetates with *N*,*N*'-ditosylhydrazine (TsNHNHTs). All diazo acetates were characterized by ^{1}H-NMR, ^{13}C-NMR and the results are in agreement with the literature.

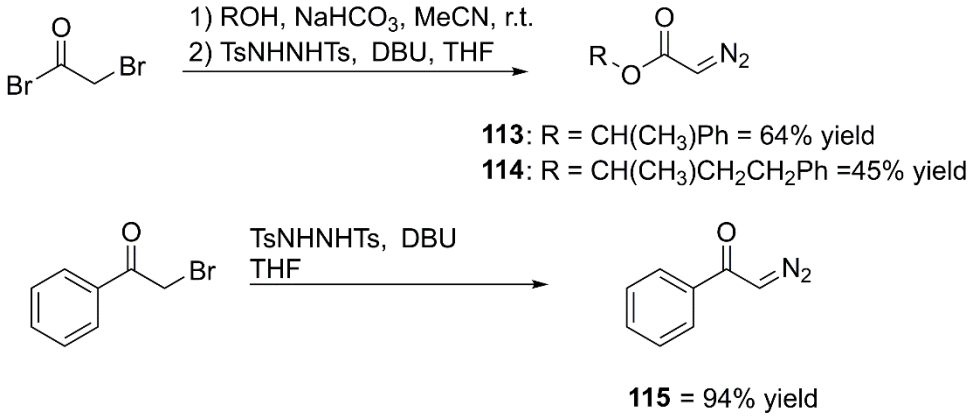

Scheme 3.4 – Synthesis of diazo acetates **113-115**

With the new α-diazo carbonyl compounds in hand, a new series of ester 3HQ derivatives were synthetized as shown in Scheme 3.5, this simple protocol afforded 3HQ **115-120** in yields ranging from 71 to 86%. All new derivatives were characterized by ^{1}H-NMR, ^{13}C-NMR and the results are in agreement with the chemical structure of the compounds. Once prepared, the 3HQs were evaluated against the aforementioned panel of cancer cell lines.

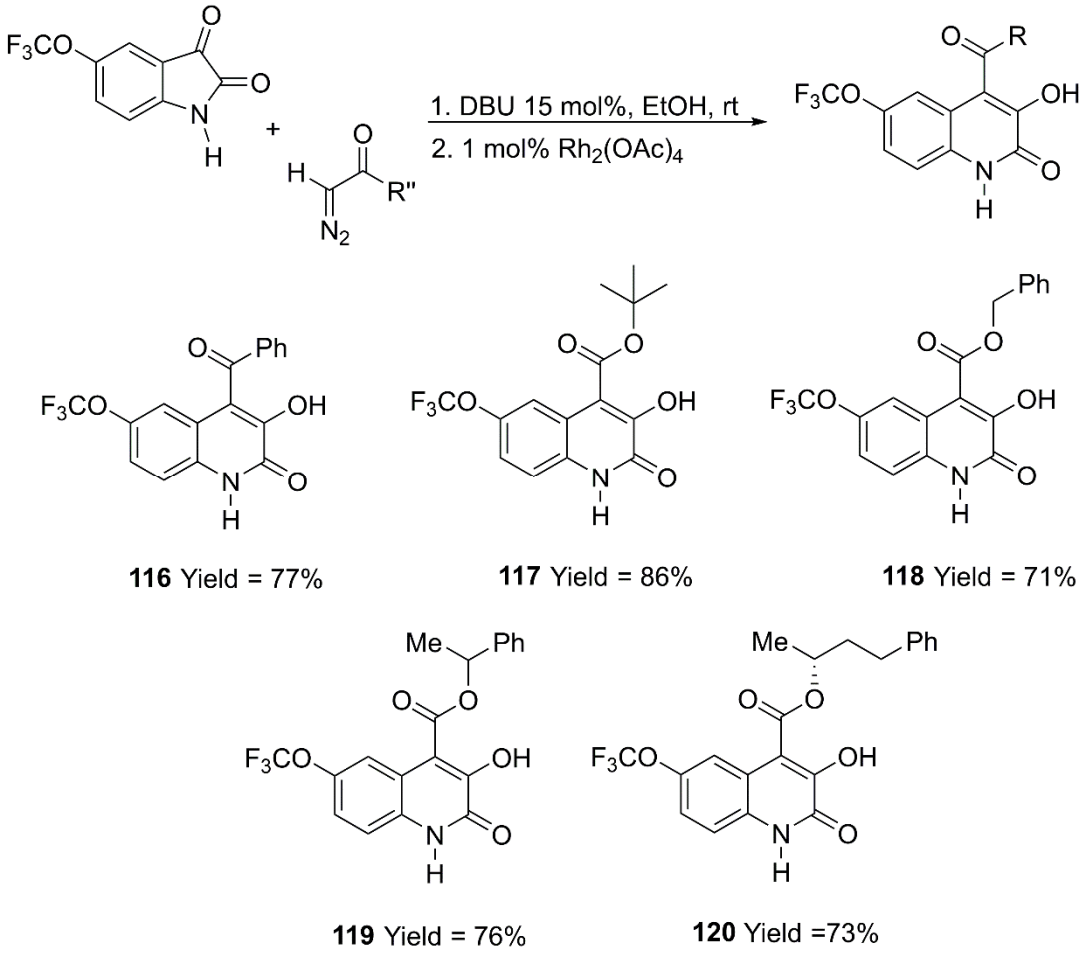

Scheme 3.5 Synthesis of 4-carboxylate substituted 3HQs **116-120** based on an Eistert ring expansion reaction of isatins with different diazo compounds, catalysed by di-rhodium complexes.

As shown in Table 3.3, the operated structural modifications had a profound impact on the heterocycles activity. Promisingly, the introduction of a benzyl ester on compound **118,** resulted in an increased activity against the 3 cancer cell lines with an IC_{50} as low as 1.8 μM, against the NCI-H460 cells. Analogously, the 3HQ **120** featuring a slightly longer alkyl chain also showed an IC_{50} of 2.10 μM against the same

cell line. However, the indiscriminate activity observed for these molecules, suggested the possibility of these 3HQs beeing also significantly toxic against non-cancer cell lines. To study this, compound **118** was evaluated against the non-cancer Chinese hamster ovary cells (CHOK1), and as expected, the 3HQ **118** proved to be quite cytotoxic on this model (IC_{50} of 5.65±1.05 μM). The incorporation of alkyl esters at position C-4 clearly induced a higher anti-proliferative effect against cancer cells but regrettably, also a significant toxicity towards non-cancer cell lines. Therefore, to improve the toxicity profile of these compounds, we studied the anti-proliferative properties of 6-trifluoromethoxy-4-carboxamide-3HQs.

Table 3.3 – Anti-proliferative evaluation of compounds **116-120** against MCF-7, NCI-H460 and HT-29 cancer cell lines

ENTRY	COMPOUND	μM		
		MCF-7	**NCI-H460**	**HT-29**
1	**116**	10.75±1.12	10.36±1.86	NA
2	**117**	13.39±2.50	6.05±1.05	NA
3	**118**	10.11±2.10	1.80±1.15	11.37±1.10
4	**119**	12.07±1.00	7.34±1.22	NA
5	**120**	15.99±1.16	2.10±1.10	NA

This study was initiated with the synthesis of 4-carboxamides-3HQs following reported protocols, in which the ethyl ester is typically hydrolysed to the acid under basic conditions, converted into the acyl chloride and then coupled with primary and secondary amines, as shown in Scheme 3.6. Unfortunately, and despite our many attempts, when starting with 6-trifluoromethoxy-4-ethylacetate-3HQ **88**, this simple protocol invariably resulted in the decarboxylation of the corresponding acid to yield compound 6-F_3CO-3HQ. Interestingly, the reported synthesis of 4-carboxamides-3HQs using this method also proceeds in yields not higher than 40%.[72] Based on this, we conceived that a more direct route to prepare 4-carboxamide-3HQs, avoiding the carboxylic acid intermediate would be to perform the Eistert ring expansion reaction with NHS-diazo acetate,[142] followed by a simple amidation step (Scheme 3.7).

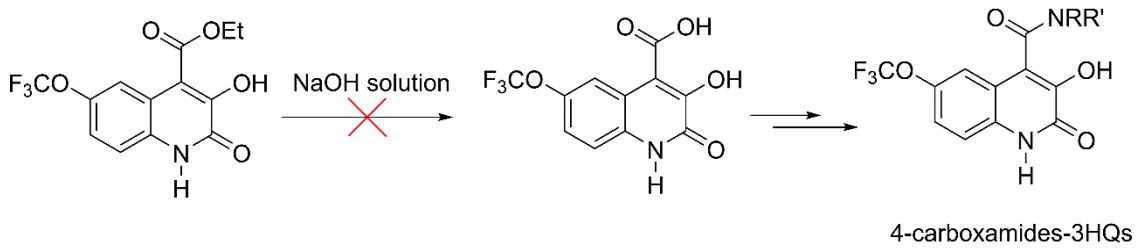

Scheme 3.6- Synthesis of 4-carboxamides-3HQs.

In order to synthesise the NHS diazo compound , firstly Mukherjee and co-worker's protocol was attempted.[143] *p*-Toluenesulfonylhydrazide was condensed in acid conditions with glyoxylic acid yielding 2-(2-tosylhydrazono)acetic acid **122** in 60% yield and its purity was assessed by melting point determination (white solid; mp: 150-152ºC).

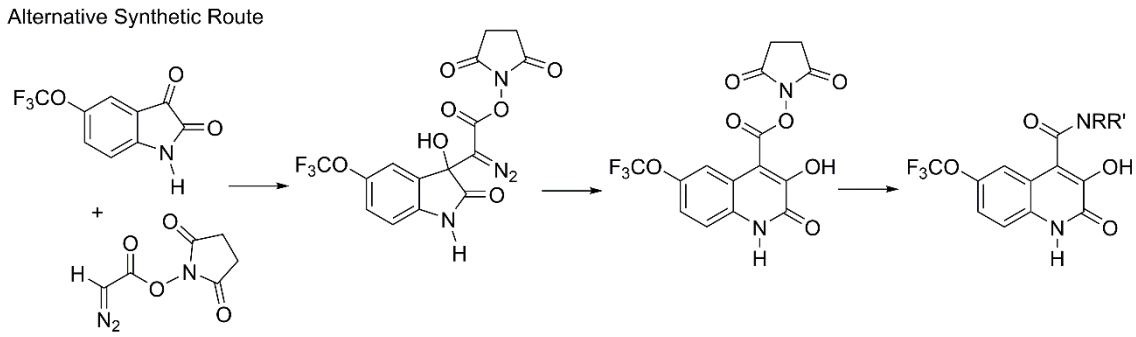

Scheme 3.7 Alternative synthetic route for synthesis of 4-carboxamides-3HQs

The coupling reaction of **122** in presence of *N*,*N*'-Dicyclohexylcarbodiimide (DCC) and NHS to unveil the α-diazo carbonyl compound failed despite our many attempts (Scheme 3.8, Method A). To avoid this inconvenience (Scheme 3.8, Method B), carboxylic acid **122** was converted into the corresponding acyl chloride **123** by treatment with thionyl chloride[144] to afford the desired compound as pale yellow prism crystals (m.p. 101-112ºC). The acyl chloride was finally converted into the desired compound **124** in 40 % yield, as reported by Doyle and co-workers.[4] The activated succinimidyl diazoacetate **124** was then tested in the amidation with *N*-benzyl-isatin under different conditions. Various source of bases, organic and inorganic, and solvents were examined and the results observed are summarized in (Table 3.4).

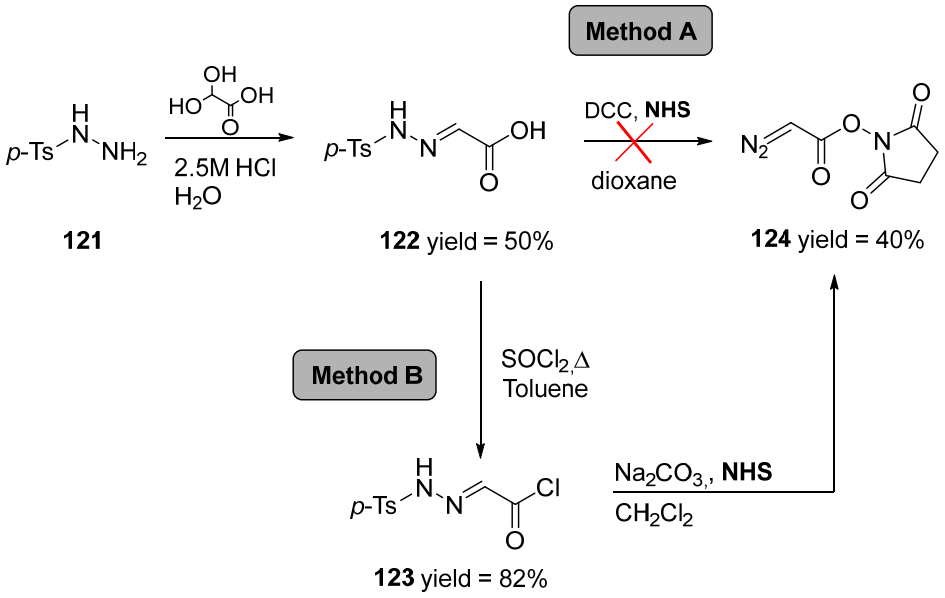

Scheme 3.8 Preparation of succinimidyl diazoacetate **124**.

We started by screening different amounts of base in THF, which regardless the base strength provided only traces of product. Assuming a weaker basicity of the alfa carbonyl positions of **124** than EDA, NaH was then used to screen different solvents as 1-4 dioxane and dichloromethane. Upon unsuccessful formation of the desired product we hypothesized that the aldol type reaction was incomplete due to the reversibility of the process. Hence, the solvent was changed to ethanol and using only 20 mol% of triethylamine the product precipitation was visible in the reaction medium. This procedure allowed the formation of the product in 88 % yield after 3h, as the equilibrium was shifted towards the product. Furthermore, this allowed the product isolation by simple filtration of the reaction mixture while avoiding any chromatography. The analysis of ^{1}H and ^{13}C NMR data allowed to confirm the formation of the intermediate **125** and the assignment all protons and carbons, with exception of the carbon attached to the diazo moiety, which was not observed in the ^{13}C NMR (Appendix C, Figure C3 a).

Table 3.4 – Optimization of reaction conditions of NHS-diazo addition on *N*-benzyl-isatin.

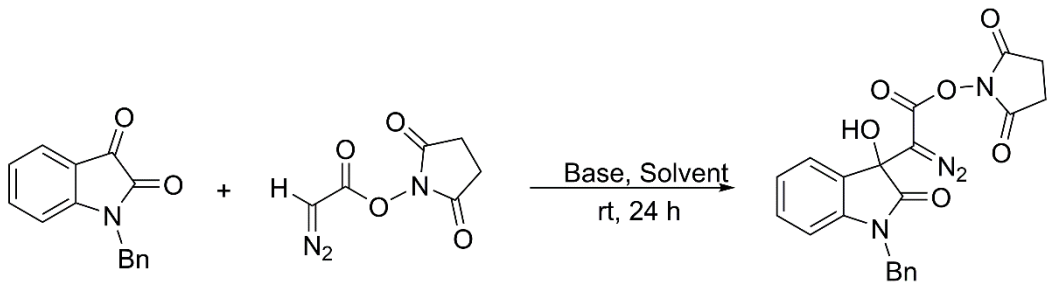

124 **125**

Entry	Base (Eq)		Solvent	Time	Yield
1	NaH	1.0	CH_2Cl_2	24 h	Traces
2	NaH	1.0	dioxane	24 h	No reaction
3	NaH	2.0	THF	24 h	Traces
4	*t*BuOK	2.0	THF	24h	> 3 %
5	DBU	2.0	THF	24 h	No reaction
6	LHMDS	2.0	THF	24 h	No reaction
7	*t*BuOK	2.0	*i*-PrOH	24 h	> 7 %
8	DBU	0.2	THF	24 h	Traces
9	DBU	1.0	THF	24 h	Traces
10	TEA	0.2	THF	24 h	Traces
11	DBU	0.2	THF	24 h	Traces
12	DIPEA	0.2	THF	24 h	No reaction
13	TEA	0.2	CH_2Cl_2	24 h	Traces
14	TEA	0.2	EtOH	3h	88 %
15	TEA	0.2	EtOH	24h	80%
16	TEA	0.2	EtOH	24h	75 % yield

Furthermore, the presence of a ^{1}H singlet at 2.73 ppm, corresponding to four protons and a ^{13}C signal with δ_c 25.75 corresponding to two carbon, corroborates the introduction of the NHS-diazo moiety. After that, the diazo intermediate **125** was then submitted to the ring expansion reaction catalysed by 0.5 mol% of $Rh_2(OAc)_4$. The reaction proceeded smoothly in EtOH, and compound **126** was isolated by filtration in 84% yield. The product of the reaction was characterized by NMR spectroscopy, and elemental analysis. The assignment of NMR spectra reveals the apparence of a ^{13}C signal with δ_c 110.49 corresponding to C-4 and ^{13}C signal with δ_c 145.87 corresponding to the C-3 linked to OH of the 3HQ core (Appendix C, Figure C3 b). After obtained the key intermediate **126** (Scheme 3.9) the benzylamine was

added in the presence of sodium carbonate, and this afforded the targeted 4-carboxamide 3HQ **127** in good yield (Scheme 3.10).

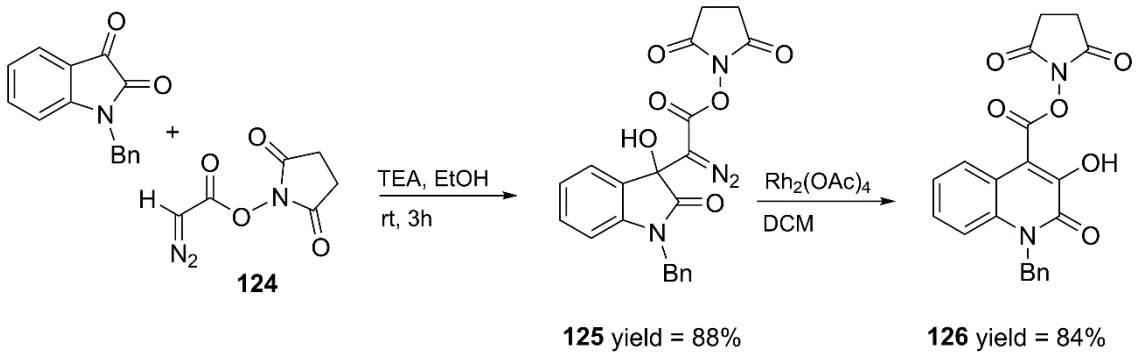

Scheme 3.9 Synthesis of 4-NHS -3HQs based on Eistert ring expansion reaction of protected isatins with NHS-diazo acetate, followed by an amidation step.

Notably, this method proved to be compatible with more complex amines, and L-glycine and L-phenylalanine afforded the peptidic-like[6] 4-carboxamides-3HQs **128** and **129** in 79% and 70% yields respectively.

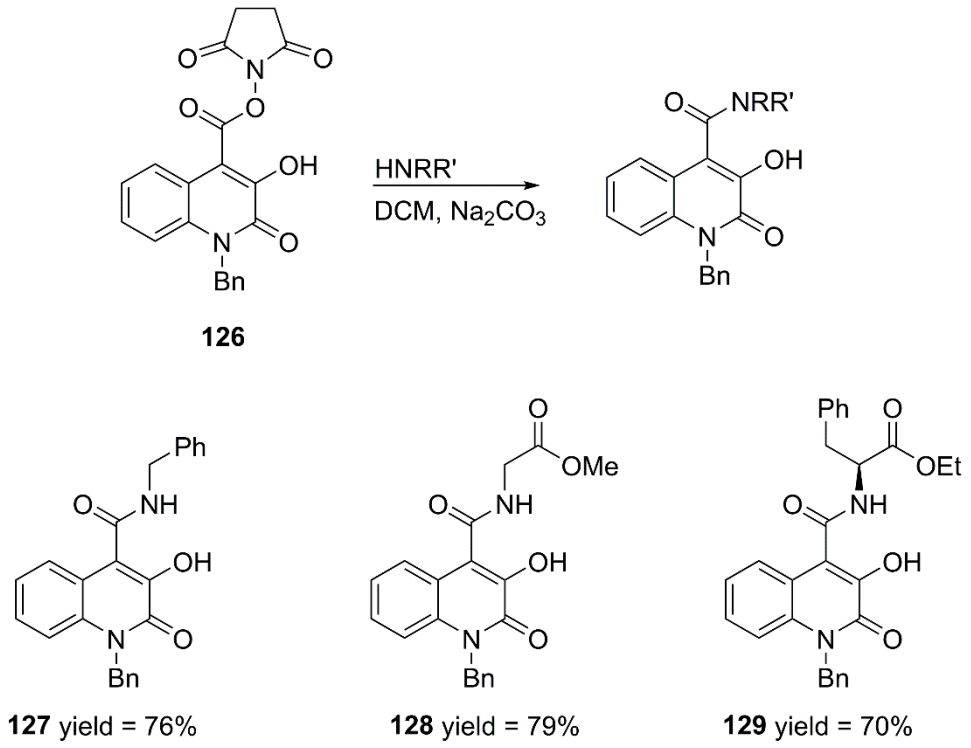

Scheme 3.10 Synthesis of 4-carboxamide-3HQs **127-129**

All the 4-carboxamides-3HQs were characterized by NMR techniques, elemental analysis (section 6.9). The results are in good agreement with the chemical structure of the compounds. Once demonstrated the feasibility of this synthetic scheme, the same protocol was used to functionalize the 6-trifluoromethoxy-isatin (Scheme 3.11).

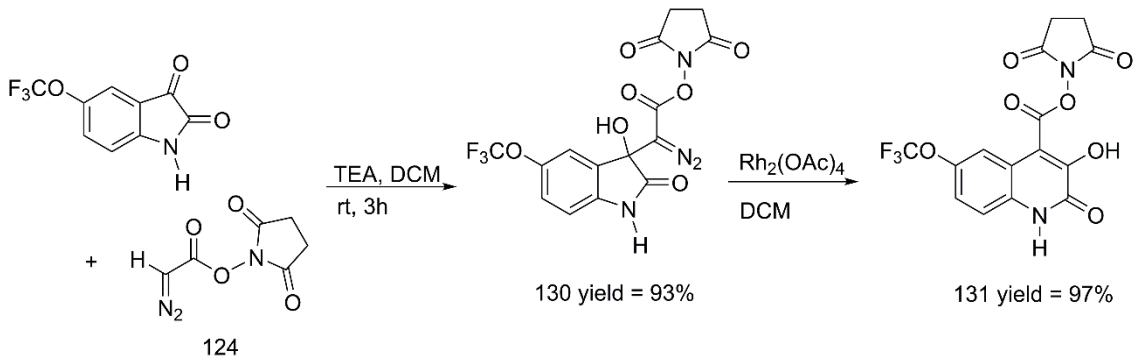

Scheme 3.11 Synthesis of 6-F_3CO-4-NHS -3HQs based on Eistert ring expansion reaction of protected isatins with NHS-diazo acetate, followed by an amidation step.

The presence of an unprotected amide group was not detrimental for the preparation of the diazo intermediate **130** which was obtained in 93% yield. The analysis of ^{1}H and ^{13}C NMR data confirmed the formation of the intermediate **130** and all protons and carbons, were assigned with exception of the carbon attached to the diazo moiety, which was not observed in the ^{13}C spectrum (Appendix C, Figure C4 a). After, compound **130** underwent in ring expansion reaction, afford the 3HQ heterocycle **131** almost quantitatively using 0.5 mol% of $Rh_2(OAc)_4$. As expected, primary and secondary amines also reacted smoothly with the 6-trifluoromethoxy-4-NHS-3HQ **131** to yield the carboxamides **132-137** in yields up to 90%. The reaction was performed in DCM, where **131** proved to be quite insoluble. However, the addition of the amines deprotonates the nitrogen of the 3-HQ it becames soluble. With the progress of the reaction, the concentration of H^+ increases in the solution, the nitrogen protonates and the product of the reaction precipitates from the reaction medium. Similarly, the 6-trifluoromethoxy-4-NHS-3HQ **131** reaction with protected amino acids also afforded the 4-carboxamides-3HQs **138-143** in good to excellent yields without any chromatographic step.

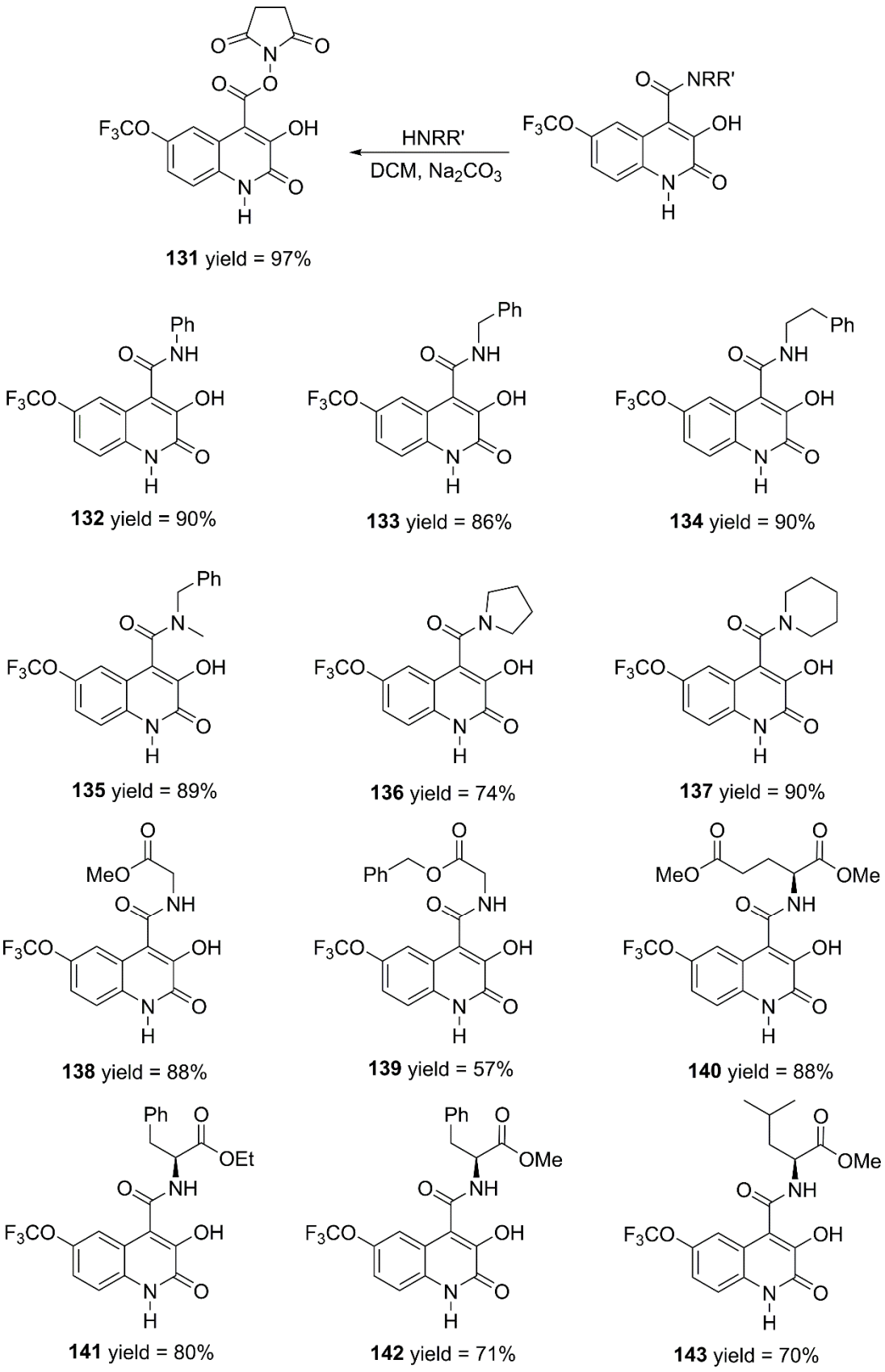

Scheme 3.12 Synthesis of 4-carboxamide-3HQs based on Eistert ring expansion reaction of 6-trifluoromethoxy-isatin with NHS-diazo acetate, followed by an amidation step.

The products of both reactions were characterized by NMR spectroscopy. The assignments of the NMR spectra are in good agreement with the chemical structure of the compounds.

The anti-proliferative activity of compounds **132-143** was evaluated. Considering the results depicted on Table 3.9, the assayed 4-carboxamides-3HQs were shown to be less toxic against the non-cancer cell model (CHOK1) than the 4-carboxylate-3HQs series. For instance, compound **133** which was only slightly less potent towards MCF-7 and NCI-H460 cancer cell lines then the matching 4-carboxylate-3HQ **118**, was clearly less toxic to CHOK1 cells at a concentration of 20 μM (Table 3.3, Entry 2). This profile was even more pronounced in the case of compounds **134** and **136** that showed a good selectivity towards the MCF-7 (IC_{50} of 4.82 μM) and NCI-H460 (IC_{50} of 7.27 μM) cancer cell lines respectively (Table 3.3, Entries 3 and 6), maintaining a low toxicity towards the CHOK1 cells.

Table 3.3 Anti-proliferative evaluation of compounds **132-143** against MCF-7, NCI-H460, HT-29 AND CHOK1 cell lines.

Entry	Compound	μM			
		MCF-7	**NCI-H460**	**HT-29**	**CHOK1**
1	**132**	NA	NA	NA	NA
2	**133**	12.03±1.04	9.46±1.20	NA	NA
3	**134**	4.82±1.24	NA	NA	NA
4	**135**	17.50±2.40	NA	NA	NA
5	**136**	NA	NA	NA	ND
6	**137**	NA	7.27±1.25	NA	NA
7	**138**	NA	NA	NA	ND
8	**139**	12.57±1.11	NA	NA	NA
9	**140**	NA	NA	NA	ND
10	**141**	9.44±7.52	8.40±1.67	NA	NA
11	**142**	9.49±1.02	11.35±1.11	NA	NA
12	**143**	15.12±1.91	2.69±1.38	NA	NA

Determined IC_{50} of the compounds in MCF-7, NCIH460 and HT-29 cancer cell lines and CHOK1 non-cancer cell model after 48 hours incubation; NA – Non-active at the concentration of **20μM;** ND - not determined.

The peptidic-like 4-carboxamides-3HQs **138-143** were also active against the MCF-7 and NCI-H460 cell lines. In particular, compound **143** elicited an IC_{50} of 2.69 μM against the NCI-H460 cells (Table 3.3, Entry 12), which compares well with the best

result obtained with the 4-carboxylate-3HQ series (Table 3.3, Entry 5). Furthermore, due to their interesting activity both in NCI-H460 and MCF-7 cells, compound **120** and **143** were further tested as to their ability to induce cell death in these cell lines by LDH release. Interestingly, exposure to compound **120** or **143**, at IC_{50} and 2x IC_{50}, significantly increased general cell death in both cell lines, confirming the anticancer potential of these compounds.

3.2.3 Conclusion

In this study the cytotoxic potential of 3HQs was addressed for the first time. The Eistert ring expansion reaction of isatins with diazo compounds catalysed by $Rh_2(OAc)_4$ was shown to be a versatile methodology to prepare 3HQs. The direct addition of structurally diverse diazo compounds to isatins enabled the construction of a series of 4-carboxylate-3HQs (in yields up to 86%) which were shown to possess anti-proliferative activity against a panel of MCF-7, NCI-H460 and HT-29 cancer cell lines. Regrettably, this series of compounds also induced severl cytotoxicity against a model of non-cancer cell lines (CHOK1, IC_{50} of 5.65±1.05 μM) and this motivated the evaluation of 4-carboxamide-3HQs. These compounds troublesome preparation was simplified by performing the ring expansion reaction of isatin derivatives with NHS-diazo acetate. This methodology afforded the targeted 4-carboxamides-3HQs in yields up to 90%, and this series of cytotoxic 3HQs were shown to have an improved selectivity towards MCF-7 (3HQ **132**, IC_{50} of 4.82 μM) and NCI-H460 (3HQ **135**, IC_{50} of 7.27 μM) cancer cell lines.

Chapter IV

IV. Phenylalanine Hydroxylase Activation Studies

Abstract

Phenylketonuria (PKU) is caused by an inborn mutation in human phenylalanine hydroxylase (hPAH). Most missense mutations on PAH gene result in a misfolding of PAH enzyme leading to a loss-of-fuction of it. PAH enzyme is required to metabolise L-Phenylalanine to L-Tyrosine, the deficiency of the enzyme leads to a toxic accumulation of Phe and its metabolites in tissues and body fluids. Herein we report the discovery of new modulators of hPAH inspired on the structure of its substrate and regulator L-Phenylalanine and 3HQs core. These new hPAH modulators were simply prepared based on ring-expansion reaction of isatins with NHS-diazoacetate catalysed by di-rhodium(II) complexes yielding 4-Carboxamide-3HQs in good-to-excellent yields. 7-trifluoromethyl-4-carboxamide-3HQs C14, was identified as the most efficient hPAH modulator, with an apparent binding affinity nearly identical to the natural allosteric activator L-Phenylalanine.

4.1 Phenylketonuria: an introduction.

Phenylketonuria (PKU; OMIM #261600) is the most common inborn error of amino acid metabolism.[145] This genetic disease was first described by the Norwegian physician Asbjorn Folling in 1934.[146] Approached by a mother of two impaired siblings, Dr Asbjorn Folling studied a sample of her children's urine to understand if that overwhelming smell of the urine was related to the observed intellectual impairment. Those urines, were characterized by a strange musty odor and after addition of ferric chloride, a normal procedure to reveal the presents of ketones in urine of diabetic patients, a strange dark-green color was developed. This unusual result encouraged Dr Folling to proceed with additional chemical assays which also involved extraction and purification procedures to isolate the responsible compound. Finally, he postulate that the observed unusual color was due to the presence of phenylpyruvic acid.[147] Therefore, in his paper from 1934, he speculated that Phenylpyruvic Oligophrenia (now known as PKU) was caused by an inherited error in the metabolism of the essential amino acid L-phenylalanine (L-Phe), which had a chemical structure almost identical to that of phenylpyruvic acid.

The incidence of PKU is ≈ 1:10000 live births in Europe[148] and if left untreated, this disorder is accompanied by progressive mental retardation, brain damage, epilepsy, and neurological and behavioral problems caused by the neurotoxic effect of hyperphenylalaninemia (HPA).[149] It is now known that this high level of L-Phe concentration in plasma is related to a deficient activity of phenylalanine hydroxylase (PAH; EC # 1.14.16.1). On the basis of blood L-Phe concentrations, PAH deficiency can be classified into classical PKU (L-Phe >1200 μmol/L), mild PKU (L-Phe = 600–1200 μmol/L) and mild HPA, where blood L-Phe level (<600 μmol/L) is elevated above upper reference range (120 μmol/L).[150] The decrease in PAH activity found in most forms of PKU and HPA are caused by mutations in the *PAH* gene. To date, more than 900 *PAH* gene mutations (as annotated in the Phenylalanine Hydroxylase Gene Locus-Specific Database PAHvdb; http://www.biopku.org) have been reported (May 23, 2016), of which 60% represent missense mutations leading to single

amino acid substitutions.[151-153] At present, a lifelong dietary restriction of L-Phe is the recommended approach for PKU treatment. Therefore, patients must follow a low protein diet L-Phe-free, which often leads to malnutrition and psychosocial complications.

4.2 **Phenylalanine Hydroxylase**

Phenylalanine is an essential amino acid and it is obtained exclusively by diet or by intracellular proteolysis. This amino acid is important for the synthesis of proteins, as well as for the synthesis of L-tyrosine (L-Tyr, **146**) and its derivatives, namely dopamine, norepinephrine and melanin. The metabolic pathway of L-Phe is initiated by PAH that catalyzes the *para*-hydroxylation of L-Phe to L-Tyr (Figure 1.4). This is the rate-limiting step in the catabolic degradation of L-Phe, and under physiological conditions about 75% of the L-Phe from the diet, is degraded by this pathway.

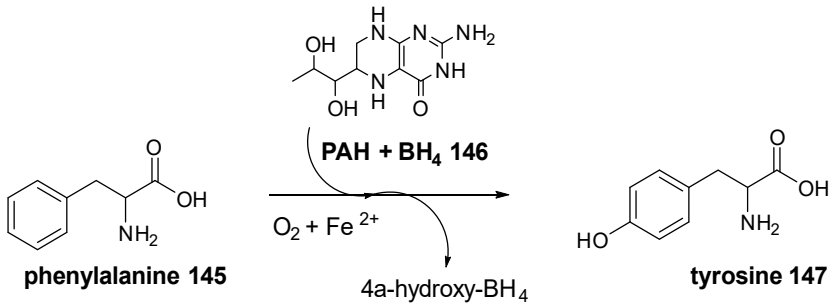

Figure 4.1 - conversion of L-Phe to L-Trr is via a pathway involving the para-hydroxylation of the benzene by PAH, the cofactor BH_4 snf molecular oxygen.

Human PAH (hPAH) belongs to the family of aromatic amino acid hydroxylases, which includes PAH, tyrosine hydroxylase (TH) and tryptophan hydroxylase (TPH).[147] These monooxygenases are tetrahydropterin (BH_4) and non-haem Fe (II)-dependent, and therefore, they catalyse the hydroxylation of the respective substrate (L-Phe, Tyr or Tryptophan) in the presence of the cofactor BH_4 and a non-heme mononuclear iron ion, with oxygen as co-substrate (Figure 4.1). The catalytic

mechanism of hPAH has been studied with experimental and computational tools.[147] This mechanism seems to occur by O_2 binding and activation via a Fe–O–O–BH_4 bridge, followed by heterolytic cleavage of the O–O bond to form the Fe(IV)=O hydroxylation intermediate, whose existence was proven experimentally, and subsequent hydroxylation of the amino acid substrate (Scheme 4.1).[154]

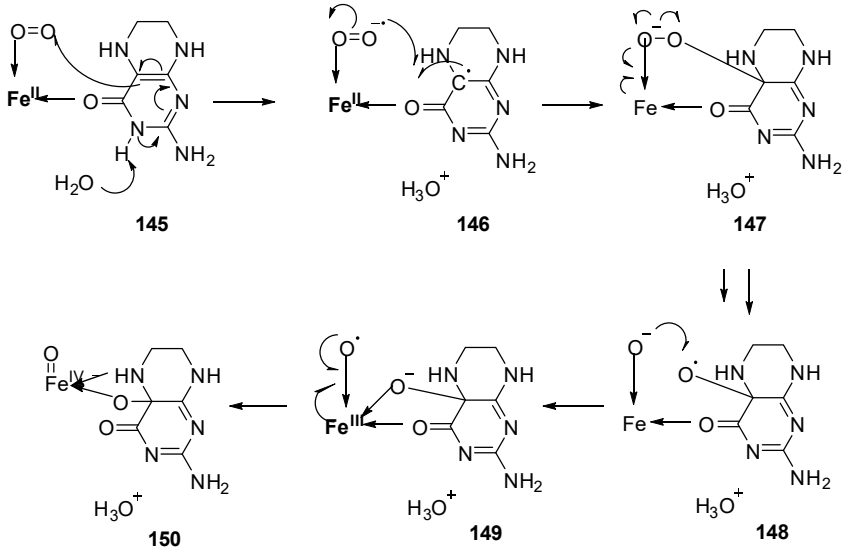

Scheme 4.1 - Catalytic mechanism of catalytic mechanism of PAH and its intervenients: Fe (II), O_2 and BH_4.[155]

4.2.1 Regulation of phenylalanine hydroxylase

The normal product of the *PAH* gene (located on chromosome 12q23.2) is the PAH protein, containing 452 amino acids. *In vitro* PAH can exist in an equilibrium of homotetramers and homodimers, although the tetramers have been considered the biological active forms.[149] Each monomer is about 50 kDa in size and presents three structural and functional domains: i) an N-terminal regulatory domain (RD) (Figure 4.2, yellow), containing the serine residue which is thought to be involved in activation by phosphorylation (Ser16 in hPAH); ii) the catalytic domain (Figure 4.2, green),

containing the non-heme iron atom; and iii) the C-terminal domain, which consist in a dimerization and tetramerization motif (Scheme 4.2, blue).[154]

Regulation of PAH activity is known to occur at several levels, including allosteric activation by the substrate L-Phe, inhibition by the cofactor BH_4 and also activation by phosphorylation of Ser16 (as mentioned before). Some of these regulatory properties are mediated by the N-terminal RD. In particular L-Phe has been proposed to bind not only to the catalytic domain, but also to an allosteric site localized in the hPAH N-terminal RD. Notably, the hPAH-RD contains the ACT (Aspartate kinase, Chorismate mutase and TyrA) domain, a structural motif found in a variety of allosteric proteins involved in the binding of small activator molecules, usually amino acids and pyrimidines. Recent studies supported an allosteric regulation of hPAH, which involve the stabilization of this ACT domain upon binding of L-Phe during the enzyme activation.[156]

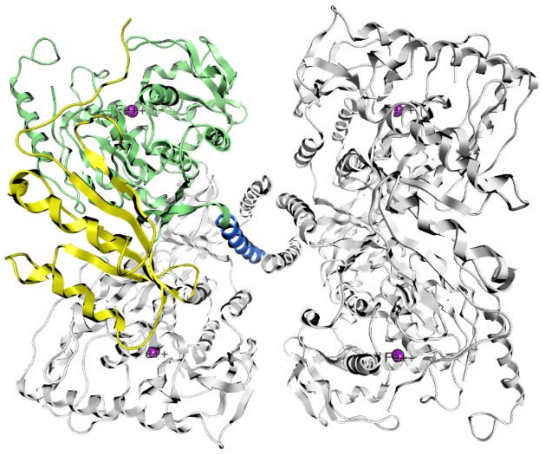

Figure 4.2 - The domain structure of hPAH. Each hPAH subunit is classified into three structural and functional domains which are involved in regulation, catalytic activity, and oligomerization. Regulatory domain (yellow), catalytic domain (green) and tetramerization domain (blue) of the hPAH.

Recently, Patel et *al.* provided, for the first time, a structural evidence that a L-Phe binding site exists in the hPAH RD, and its binding, results in dimerization of hPAH-RD (Figure 4.3). In fact, the report crystal structure of hPAH-RD bound with L-Phe

(PDB 5FII; 1.8 Å resolution), revealed that the ACT domain forms homodimers, being the L-Phe bound at the dimer interface..

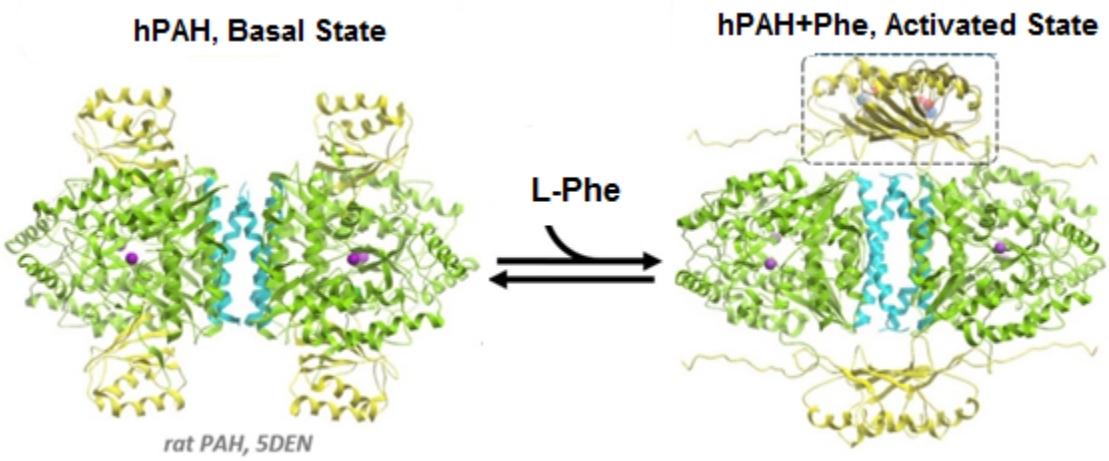

Figure 4.3 - Proposed model of PAH activation by Phenylalanine.

Therefore, these data support the emerging model of an PAH allosteric regulation, whereby L-Phe binds to the hPAH-RD mediating the dimerization of the regulatory modules that would induce conformational changes to activate the enzyme.[151]Moreover this important discovery open a new rationale for the structure-guided drug design of small molecules, using the hPAH-RD as a target for protein activation

4.2.2 **Treatment and emerging PKU therapies**

As already mentioned, more than 900 *PAH* gene mutations have been identified in PKU patients. The majority of these DNA changes consist in missense mutations resulting in single amino acid substitutions in the translated protein leading to impaired stability and folding of the hPAH variants. In general, misfolded proteins can form aggregates which present a cytotoxic function (gain-of-function) or alternatively, the misfolded protein is recognized by the cellular protein quality control machinery and targeted for degradation (loss-of-function).[157] It is now accepted that

the majority of misfolded hPAH variants are degraded leading to low intracellular levels and as such PKU is considered a conformational disorder with loss-of-function.

The *PAH* mutations are very prominent and through newborn screening tests, it is possible to prevent the major manifestation of the disease, including mental retardation, by initiating the adequate therapy as soon as possible after birth. A rigid low L-Phe diet is still, at present, the main therapeutic approach available. This dietetic restriction has, as major advantage, applicability towards all mutations with and adequate outcome. However, and despite the recent improvement of low-Phe dietetic products, this rigid long-term diet can lead to social boundary and malnutrition. Therefore, there is an urgent need for alternative pharmacological therapies to partially or totally substitute the low–Phe diet.

BH_4 supplementation, has been demonstrated to reduce plasma L-Phe levels, in the short and long term, and increase L-Phe tolerance mainly in patients presenting the mild PKU phenotype. The efficacy and safety of BH_4 supplementation treatment using the commercial form of the synthetic BH_4, i.e. Kuvan™ (sapropterin dihydrochloride, BioMarin Pharmaceuti-cal Inc, USA) has been demonstrated in clinical trials. About 40% of mild PKU patients reach a stable reduction of >30% of plasma L-Phe levels with this treatment, increasing their dietary L-Phe tolerance. Also, the use of supplementation with large neutral amino acid (LNAA), has led to reduced cerebral concentrations of L-Phe. Both these supplementations with sapropterin and LNAA may allow less (but still) restrictive L-Phe diets.

Currently, two therapeutic strategies, that envision a complete substitution of the classic low-Phe diet, has been developed, namely gene therapy and enzyme replacement therapy. Over the last decade, different groups could demonstrate promising results in murine PKU animal models using adeno-associated virus.[158] Recombinant *PAH* gene, targeted into liver or skeletal muscle, allowed a decrease in blood L-Phe in animal models.[159, 160] However, translation into a clinical setting in humans has not yet been accomplished, since according to "clinicaltrials.gov" no clinical trials for gene therapy of PKU have been conducted.[158] Regarding enzyme

replacement therapy a PEG-modified phenylalanine ammonia lyase (PEG-PAL) has recently finished Phase II clinical trials. PEG-PAL administration allowed a reduction of blood Phe levels of PKU patients. However immunogenic side effects have been reported.

One emerging therapeutic approach to treat conformational disorders is the use of pharmacological chaperones (PCs). These small molecular weight compounds usually resemble natural ligands of the target proteins, and can rescue the misfolded conformers of these proteins by stimulating their renaturation or scaffolding the final folded structure. In the case of PKU, the cofactor BH_4 is a natural ligand, and can be considered a PC when given as therapeutic supplementation for BH_4 –responsive HPA/PKU patients. In 2008, Pey *et al*[161] performed a high-throughput ligand screening for the identification of PCs to treat PKU (Scheme 4.2). From the over 1000 pharmacological agents tested, they identified 4 compounds (Scheme 4.2) that improved the thermal stability of hPAH and did not show substantial inhibition of hPAH activity.

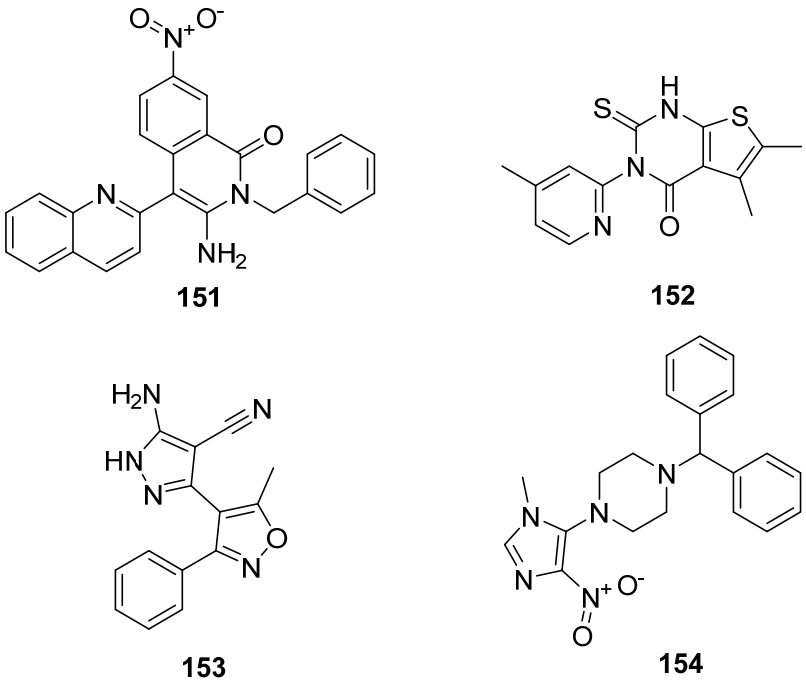

Scheme 4.2 - Chemical structure of compound with potential pharmacological chaperone ability hits from Pey *at al.* [161]

Specially, they found that compounds **153** and **152** stabilized the functional tetrameric conformation of recombinant wild-type hPAH (WT-hPAH) and some hPAH variants. Moreover, these compounds also significantly increased the activity and the steady-state hPAH protein levels in cells transiently transfected with either WT-hPAH or the hPAH variants. Furthermore, PAH activity in mouse liver increased after a 12-day oral administration of low doses of compounds **151** and **152**. Interesting results were also found with compound **154,** which mimic the binding mode of BH_4 to hPAH.[162]

Another important study for the development of PCs by virtual screening approach, was performed by Santos–Sierra *et al.*[163] The authors used BH_4 as query structure for shape-focused virtual screening of NCI structural data base and identified 84 candidates with the potential to bind the active site of hPAH.

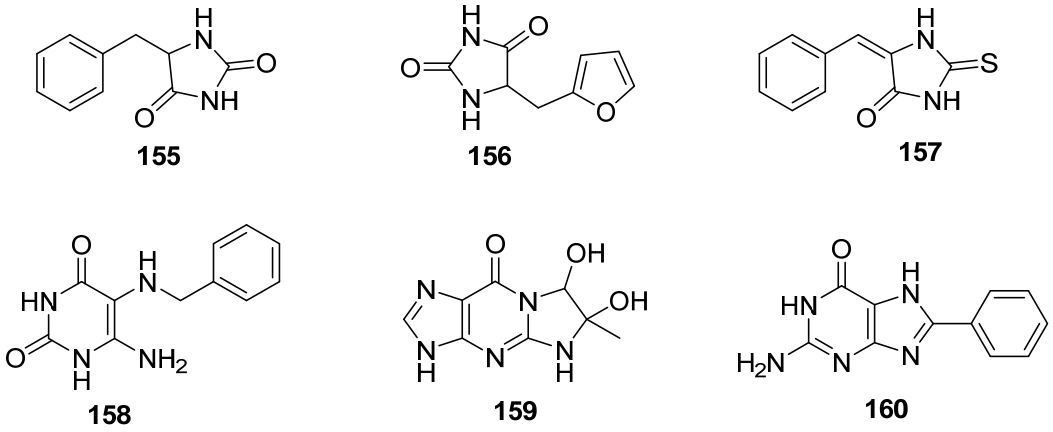

Scheme 4.3 - Compounds with potential pharmacological chaperone ability. Hits from Santos-Sierra *et al.* [163]

The physical interaction of selected compounds with hPAH was screened using surface plasmon resonance (SPR) and led to the selection of 6 compounds (Scheme 4.3). The scaffolds found presented different structural basis. Three of the compounds (**155, 156**, **157**) are based on a (thio)hydantoin scaffold with a short linker to a phenyl or furan moiety. Other compounds are based on uracil (**158**) and guanine (**159**, **160**) scaffolds. In the literature hydantoin derivatives can be found in the urine

of PKU patients and relates with hydantoin-based compounds such as **155**, which showed inhibitory activity on hPAH[164]. Compounds related to **158,** such as pyrimidines, have been identified and investigated with regard to their function as cofactors of hPAH.[163] The *in vitro* evaluation of these six compounds suggested that they were able to restore the enzymatic activity of the unstable rat PAH (rPAH) V106A variant and to increase its stability against proteolytic degradation (cell-based assays). *In vivo* studies allowed to demonstrate that two (**155** and **158**) of the six compounds, substantially improved the *in vivo* L-Phe oxidation and blood L-Phe concentrations on PKU mice models (*Pah*^{enu1}). Notably, benzylhydantoin (**157**) was twice as effective as tetrahydrobiopterin.

As already mentioned an important study of Patel *at al.*[165] concerning the allosteric regulation by L-Phe binding to the hPAH-RD, disclose the possibility to develop a new generation of PCs that specifically target the RD domain in order to activate the variant hPAH proteins.[151] The possibility to synthetize L-Phe-like molecules that could act in such manner would be also an opportunity to target the allosteric domain as a stabilization strategy. Recently our group reported the synthesis of L-Phe-like modulators[166] with an apparent binding affinity as L-Phe substrate, for the active site of hPAH. The most effective activator of hPAH was compound **161** prepared with L-Phe, para-methoxy-salylaldehyde and phenyl boronic acid. This compound showed to improve hPAH activity by 1.8-fold ($P < 0.0001$), maintaining a high apparent binding affinity ($C_{0.5}$ of 14.8 ± 4.9 μM).

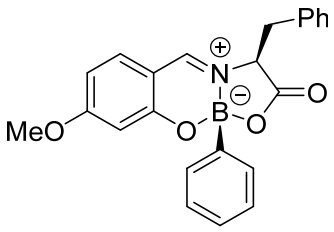

161

Scheme 4.4 - Structure of compound **161,** a Phe-like modulator with affinity to the active site of *h*PAH.

4.3 Phenylanlanine Hydroxylase Activation

Based on this knowledge we hypothesized that 3HQ derivatives could be a useful platform to design new hPAH modulators. 3-HQs, as already describe in chapter I, have a unique set of properties which are ideal to develop modulators of the hPAH protein: they can complex metallic centers and they are an isoster of glycine (Figure 4.4). As already mentioned, hPAH is an iron-dependent enzyme, presenting an atom of Fe in the catalytic domain.

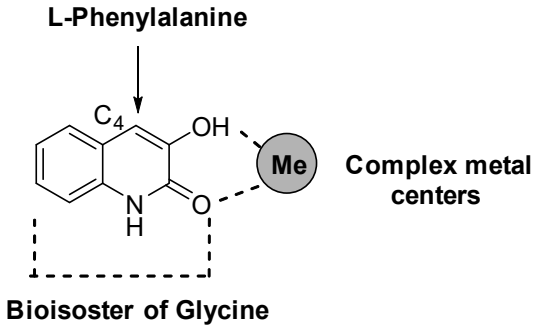

Figure 4.4 - Rational for the design of new PAH modulators

The possibility to chelate this center by the 3HQ core, namely with the OH group in position C3 of the quinolone and the oxygen of the lactamic function, could rise to a stability of the hPAH tetramer, preventing misfolding, aggregation and proteolytic degradation. Furthermore, since L-Phe is the hPAH substrate, the molecules were design to incorporate L-Phe in position C4 of the 3HQs core. The incorporation of L-Phe into the 3HQ core, lead to the construction of a "peptidic-like" structure that can also effectively target the more solvent exposed regulatory domain. To test this idea, L-Phe-3HQ compounds **141**,**165, 166,** and **167**, depicted in Scheme 4.5, were prepared.

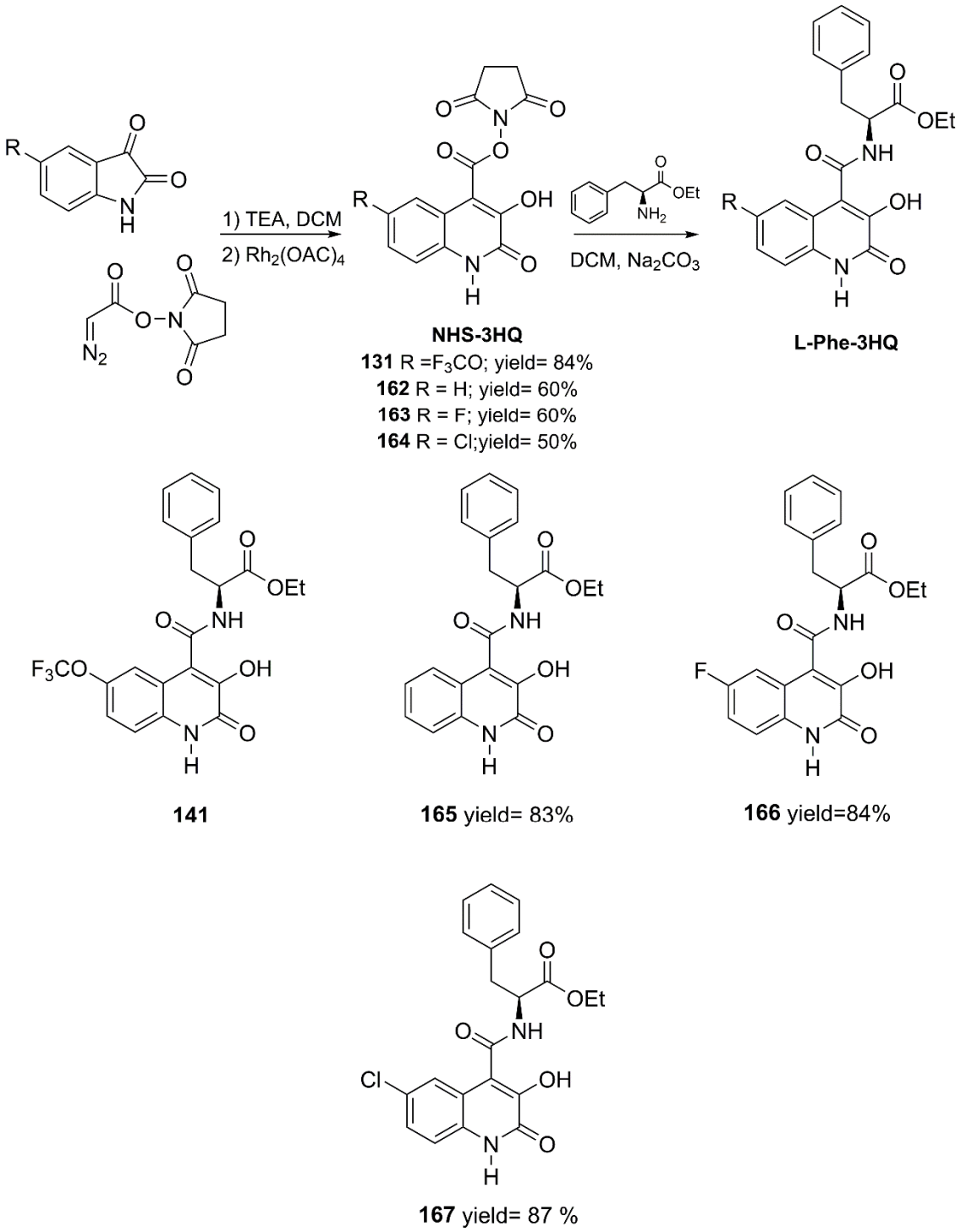

Scheme 4.5 - Synthesis of 4-L-Phe-3HQs **141** and **165-167.**

These compounds were easily achieved using our sequential protocol based on Ring-Expansion reaction of isatins with NHS-diazoacetate catalysed by dirhodium(II) complexes yielding NHS-3HQ derivatives in moderate yields. After that, by a simple amidation with L-Phenylalanine ester, NHS-3HQ were converted in L-Phe-3HQ

derivatives in good yields. All L-Phe-3HQ derivatives were characterized by NMR spectroscopy and the assignment of the NMR spectra are in good agreement with the chemical structure of the compounds.

Once prepared, compounds **141** and **165-167** were evaluated for their effect on stabilizing the tetrameric wild-type hPAH enzyme and for their effect over the hPAH enzymatic activity. One of the methods used to monitor the stabilizing effect of small molecules is the Thermal shift or Thermofluor® stability assay. This method, uses differential scanning fluorimetry (DSF), and is based on the fact that low-molecular-weight ligands can bind and stabilize purified proteins. The coupling between the binding molecule and the protein, lead to an increase in the mid-point denaturation temperature (T_m) of the protein.[167] The experimental procedure is rapid and relatively economic. After mixing the compounds with the protein and a fluorescent probe (Figure 4.5a) the temperature is slowly increased and the thermal unfolding is then measured by the increase in fluorescence (Figure 4.5b).

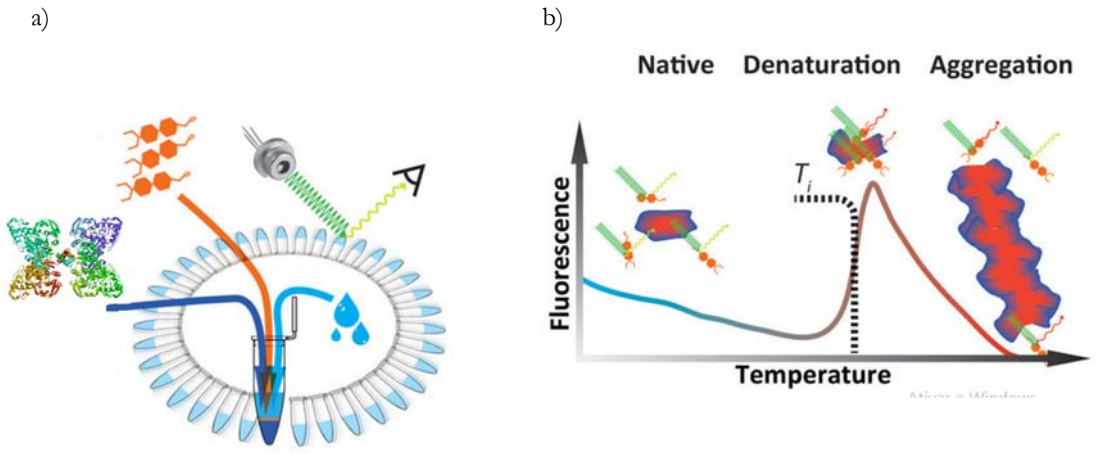

Figure 4.5 – Differential scanning fluorimetry (DSF) assay

This assay can be performed in a conventional instrument for real-time PCR. The fluorescent probe (usually SYPRO Orange) must have an affinity for hydrophobic residues, as such at low temperatures, when the protein is folded hydrophobic residues are not exposed and the fluorescence of the probe is quenched by water

(Figure 4.5b). When the temperature is increased, and the protein starts to unfold, the fluorescent probe will interact with the exposed hydrophobic patches of the protein and become unquenched. Thus, when appropriate scaling and baseline correction are applied, the fluorescence intensity allows to calculate the fraction of unfolded protein and the apparent *Tm* can then easily be obtained. The difference in the temperature (ΔT_m) of this midpoint in the presence and absence of ligand is related to the binding affinity of the small molecule, with a decrease and increase being related to a destabilizing and stabilizing effect, respectively The native hPAH enzyme presents an unfolding mechanism with two denaturation transitions associated with the unfolding of the regulatory (T_{m1} = 43.4 ± 0.7 ºC) and catalytic domains (T_{m2} = 53.5 ± 0.5 ºC) (Figure 4.6).

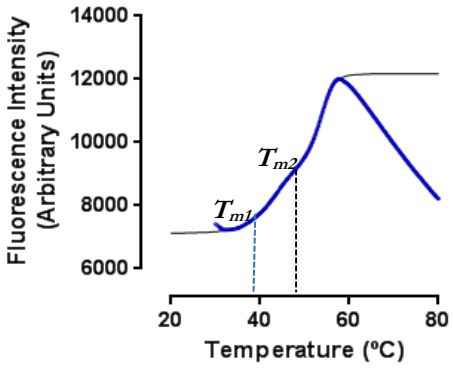

Figure 4.6 – Thermal denaturation of hPAH followed by differential scanning fluorimetry (DSF). Assay Conditions: recombinat hPAH WT tetramer: 1 mg/ml hPAH (2.5× SYPRO Orange) CFX96 Touch Real-Time system (Bio-Rad); FRET channel Melting curve: 20 to 70 ºC with increasing steps of 0.2 ºC with 1 s incubation time, using the for fluorescence acquisition

Our library of compounds was tested by this technique and all compounds which increase the melting temperature by more than a selected threshold value (2 °C) where regarded as hits in the screening. Tests for statistical significance were also performed using 1-way ANOVA by comparing the compound data to the DMSO control assay for DSF studies. Data was considered statistical different when $P < 0.01$

The Figure 4.7, shows the effect of compounds **141** and **165-166** on T_m of the regulatory (T_{m1}) and catalytic domain (T_{m2}) of hPAH. As depicted, compound **141**

(Figure 4.7a) binds to the regulatory domain and lead to an increase of 8.3 ºC in T_{m1} ($P < 0.0001$). Similarly, compound **166** exhibited the same ability to bind to the regulatory domain as compound **141.** However, for this compound an increment of only 2.6 ºC was observed for T_{m1} ($P < 0.01$). Interestingly, compounds **165** and **167** (as shown in Figure 4.7a) are strong destabilisers of the regulatory domain. Concerning the catalytic domain (T_{m2}, Figure 4.7b), we found that compound **166** exhibited not only a stabilizing effect on the regulatory domain, but also on the catalytic domain as it increased the T_{m2} in 4.2 ºC ($P < 0.001$). Compound **141** was not able to increase the stability of the catalytic domain, while compound **165** increased T_{m2} in 2.4 ºC ($P < 0.01$). Additionally, compound **167** still persist as a destabiliser of the hPAH enzyme. Data obtained with this first screening suggest that the observed different stabilizing properties are related with the withdrawing group present on compounds **141** and **166**.

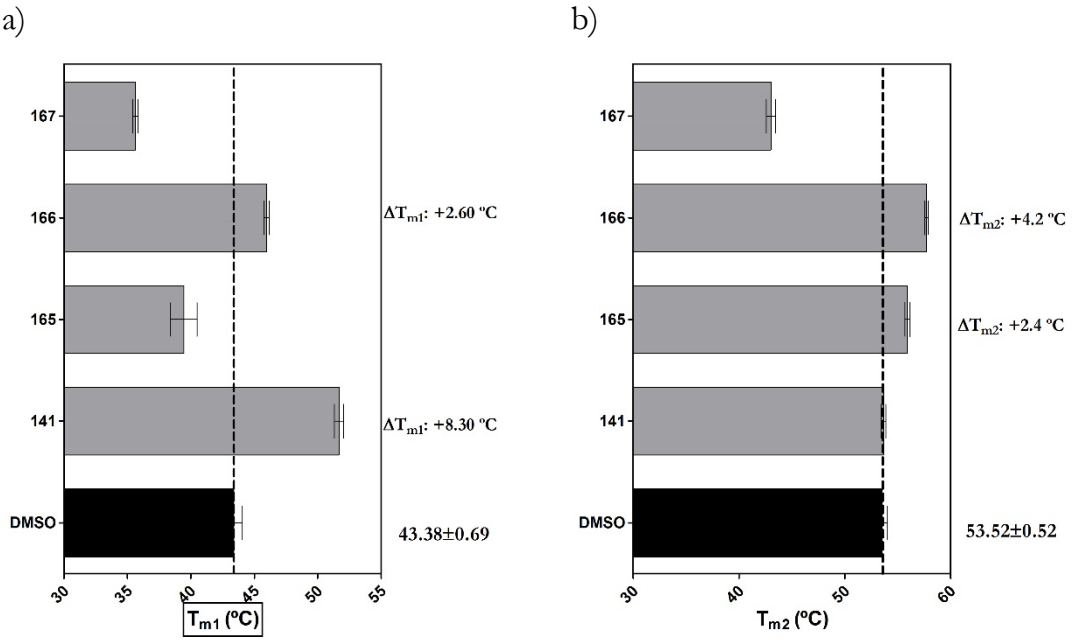

Figure 4.7 - DSF analysis of compounds **141** and **165-167** on the mid-point denaturation temperature of the a) regulatory domain (T_{m1}) and b) catalytic domain (T_{m2}) of hPAH.

After the DSF assay, we evaluated this set of compounds for their effect on the activity of tetrameric WT-hPAH, employing three experimental conditions. The first condition (I) the assay was performed adding the substrate L-Phe and L-Phe-3HQs

simultaneously, at time zero without pre-incubation step to avoid the stability effect that can activate the enzyme ('non-activated' condition). The second condition (II) involved pre-incubation with the tested L-Phe-3HQs alone, to establish its ability to pre-activate the enzyme, mimicking L-Phe-promoted pre-activation ('compound-activated' condition). The third and last condition (III) of the assay, involved pre-incubation of hPAH with substrate L-Phe and compound L-Phe-3HQs to evaluate the competition between them ('substrate-activated' condition). Control assays with each L-Phe-3HQ alone and omitting L-Phe were performed to rule out L-Phe release from the L-Phe-3HQ bearing this moiety and consequent conversion to L-Tyr. We tested the activity of compounds **141** and **165**-**167** (Figure 4.8), and we found that all of them were able to activate the tetrameric hPAH enzyme in the "non-activated condition" assay (assay I).

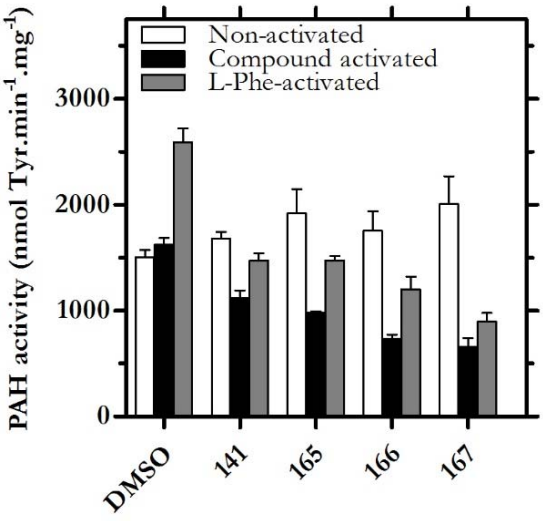

Figure 4.8 Activity of compound **20-22 and 2** in hPAH enzyme assay.

In contrast, for what concern the 'compound-activated' condition (assay II), all compounds inhibit the enzyme and clearly do not demonstrate any ability to mimic L-Phe-promoted pre-activation effect. Nevertheless, compounds **165** and **141** were less effective in the inhibition of the enzyme than compounds **166** and **167**. In the last condition of the assay, 'substrate-activated' condition, only compound **141** and **165** showed a mild inhibition of the enzyme. Based on these results, and the statistical analysis performed in the DSF assay, we found that compounds **141** and **165** were the

most suitable compounds to pick as hits for the development of new hPAH modulators. For this reason, we embarked on a modification campaign to optimize the structure of these two lead L-Phe-3HQs compounds. The first modification performed in the scaffolds was to alkylate, with a benzyl group, the NH of the 3HQ moiety, aiming to understand if the NH position is important for their activity. We synthetized compound **129** and **169** using the protocol already describe in Chapter 3 (Scheme 4.6).

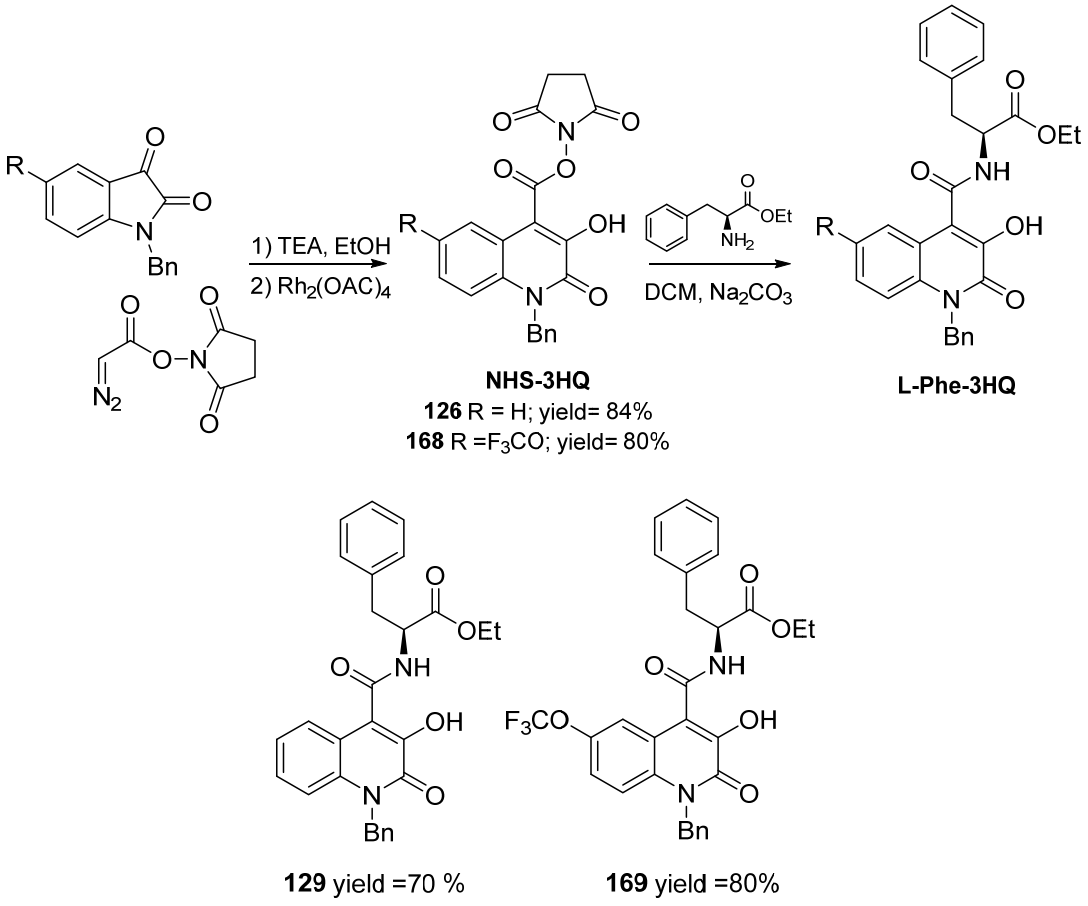

Scheme 4.6 - Synthesis of 4-L-Phe-3HQs **129** and **166.**

The two compounds were synthetized in good yield and both reaction products were characterized by NMR spectroscopy. The assignment of the NMR spectra are in good agreement with the chemical structure of the compounds. Once prepared, compounds **129** and **169** were tested by DSF (Figure 4.9). Only compound **129** showed for the capacity to stabilize the regulatory domain as it increased the T_{m1} of WT-hPAH in 7.7 ºC (Figure 4.9a). No stabilizing capacity was found for compound

169, showing that free NH could be important for the effect of that series of compounds. Furthermore, these two compounds were evaluated for their effect on the enzymatic activity of tetrameric WT-hPAH. Unluckily, both compounds showed to strong inhibit the enzyme (Figure 4.9b).

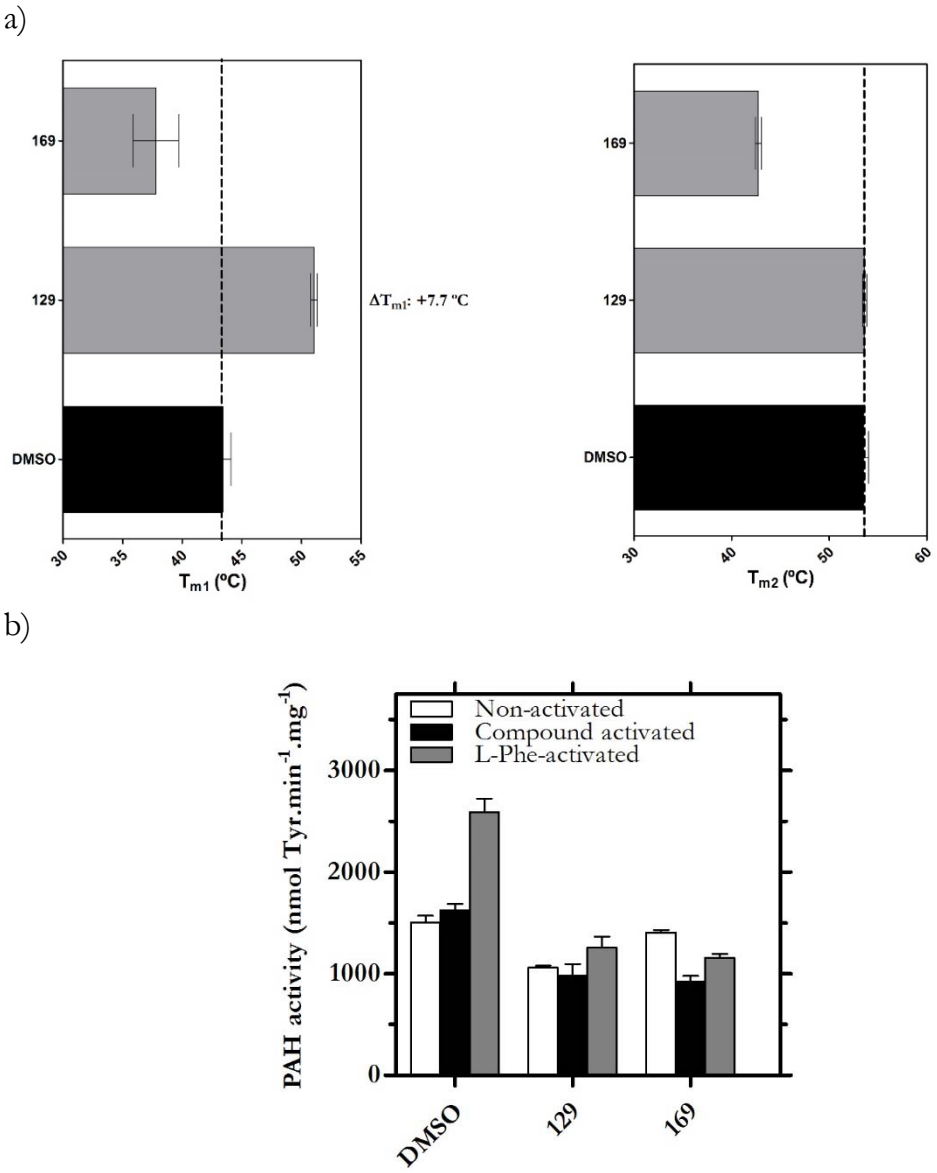

Figure 4.9 - a) DSF analysis of compounds **129** and **169** on the mid-point denaturation temperature of the regulatory (T_{m1}) and catalytic domain (T_{m2}) of WT-hPAH. **b)** Results of the activity assay for compounds **129** and **169**.

After these unsuccessful modifications, we focus our attention on compound **141** which showed the most interesting result on the DSF and the activity assays. To improve the properties of these compounds, we studied the possibility to modify position C-4 of the F_3CO-3HQ core (Scheme 4.7).

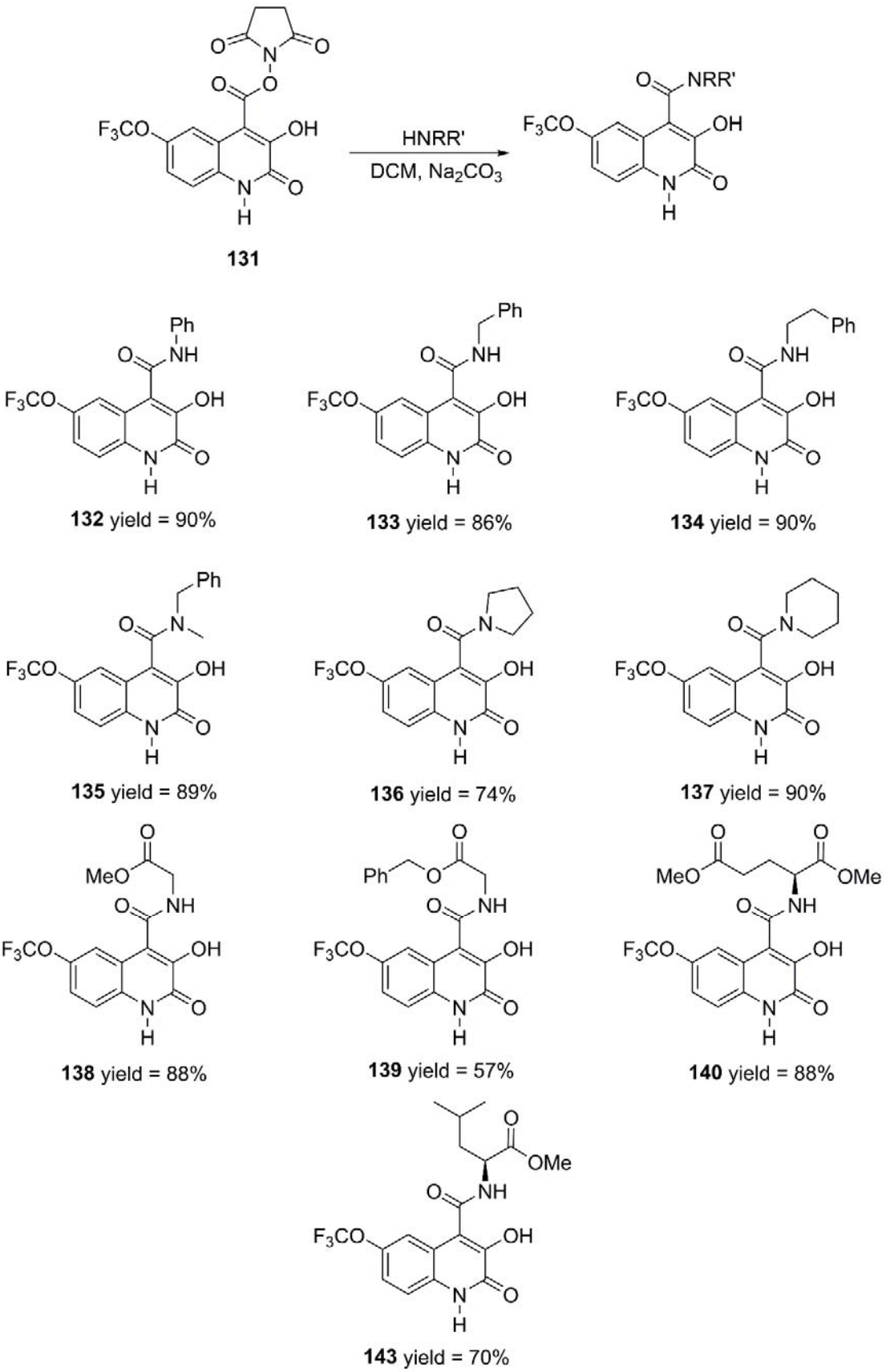

Scheme 4.7 - Compounds 7-trifluoromethyl-4-carboxamide-3HQs.

In position C-4, different amines were installed, namely primary and secondary amines and different amino acids (L-isoleucine, L-glycine and L-glutamate) instead of the L-Phe. These compounds were synthetized following the protocol already discussed in Chapter III in good yields.

All compounds were evaluated for their effect on the hPAH thermal stability (DSF) and enzymatic activity using the three experimental conditions already described. The different amines introduced in the 6-F_3CO-3HQ core showed, mostly in DSF assay, no significant stabilizing effect (Scheme 4.10) for the two domains of hPAH. Nevertheless, with compounds **132** and **133** no thermographs were possible to obtain and as such it was not possible to calculate the respective T_{ms}. From this last set of compounds, only one interesting result was found. Compound **138,** holding a L- glycine in position C-4, increase the T_{m1} of 4.0 ºC suggesting a stabilization of the regulatory domains.

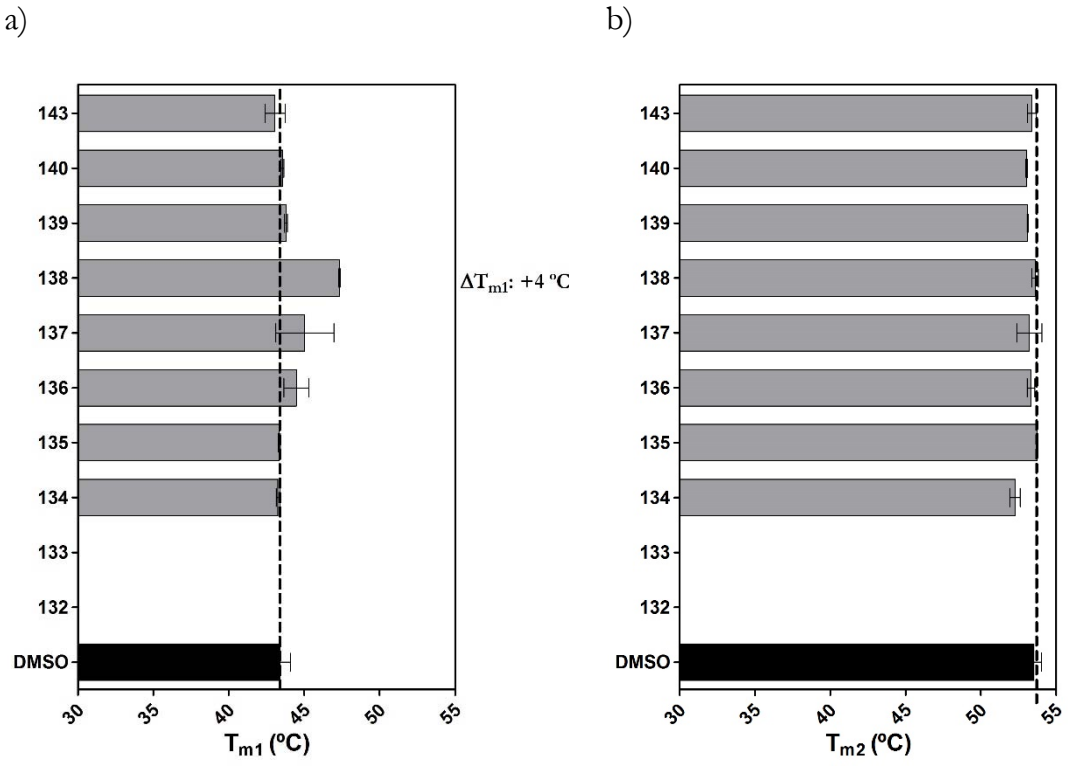

Figure 4.10 – Results of 7-trifluoromethyl-4-carboxamide-3HQs in DSF assay.

In the activity assay, all compounds were tested using the previous assay conditions: non-activated, compound-activated and L-Phe- activated (Figure 4.10). An interesting result was found for compound **138**, which showed the capacity to stabilize the regulatory domain. The compound showed to be a strong inhibitor of the enzyme, suggesting to be a strong competitor of L-Phe amino acid, but enabled L-Phe activation. Tertiary amide **135** showed to inhibit the enzyme and being a strong competitor of L-Phe amino acid. Cyclic amine, pyrolidine **136** and piperidine **137** that showed in the DSF assay to stabilize the regulatory domain proved to be strong inhibitors in the enzymatic assay. The best result was found for compound **134** featuring a phenethyamine moiety. This compound showed in the DSF assay not have any relevant stabilizing effect on both the regulatory and catalytic domains, maintaining both T_m similar to those obtained in the absence of compounds. However, in the activity assay **134** showed a mild inhibition in the non-activated and compound activated assays.

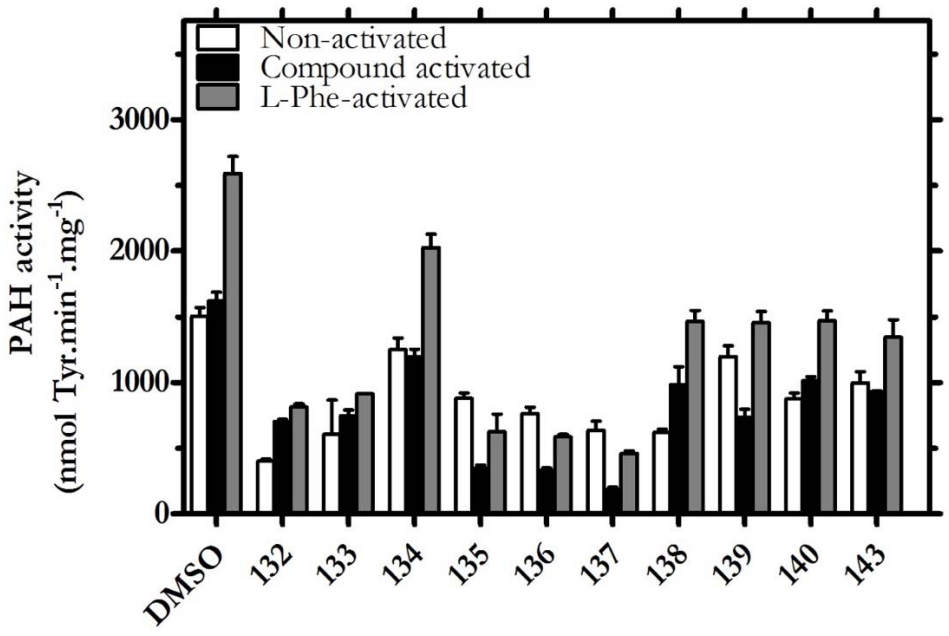

Figure 4.11 – Activity assay of compounds on tetrameric wild-type *h*PAH enzyme.

However, in condition III (substrate activated) the compound allowed the hPAH protein to respond to L-Phe activation, thus without competing with the amino acid

substrate. Moreover, statistica evidence was found for this compound ($P<0.001$). Finally, for what concerned the last peptide like compounds **139**, **140**, **143** they exhibit only mild inhibition for the L-Phe activated assay.

4.4 **Conclusion**

In this study, we have evaluated the biological properties of 3HQ derivatives as new modulators of PAH enzyme activity and stability. Starting with the idea to incorporate L-Phenylalanine in the 3HQs core to modulate the capacity to bind to the hPAH enzyme, either on its regulatory domain and/or active site, we synthetized a short library of L-Phe-3HQ derivatives. From this library, compound **141** showed the most interesting results, stabilizing the regulatory domain and furthermore with a low inhibition effect on hPAH activity assay. For this reason, compound **141** was selected as a hit. To improve the biological properties of this lead, different amines were introduced in position C-4 of the 3HQs core. A new library of 4-carboxamide-F_3CO-3HQs compounds was synthetized and evaluated for their effect on the hPAh thermal stability (DSF) and enzymatic activity. From this library of 4-carboxamide-F_3CO-3HQs compound **134**, featuring a phenethylamine moiety, was identified as the most effective compound, able to directly increment hPAH activity by a pre-activation mechanism similar to the one induced by the substrate L-Phe.

Chapter V

V. General Discussion and Conclusions

5.1 Introduction

The 3-hydroxyquinolin-2(1H)-one (3HQ) **9** core is an important motif that is present in the structure of viridicatin **31**, viridicatol **32** and 3-O-methyl viridicatin **33** naturally occurring products.[3, 4, 70] These metabolites, isolated from penicillium species, have been shown to inhibit the replication of human immunodeficiency virus and to be promising lead compounds for the development of new anti-inflammatory agents.[5, 6] Furthermore, this unique heterocycle was recognized to be a valuable bioisoster of α-amino acids showing similar binding interaction as the co-crystalized amino acid in DAOO enzyme.[7, 8, 9] In addition, recent publications found this pharmacophore to bind metal cofactors present in viral enzymes, namely HRNase H associated to RT [72] and Influenza A Endonuclease,[73] showing to be a potent inhibitor. Based on this important property of this core we decided to initiate a line of research to discover a methodology to synthetize 3HQ derivatives in a highly efficient regioselective way with the aforementioned MOC concept.

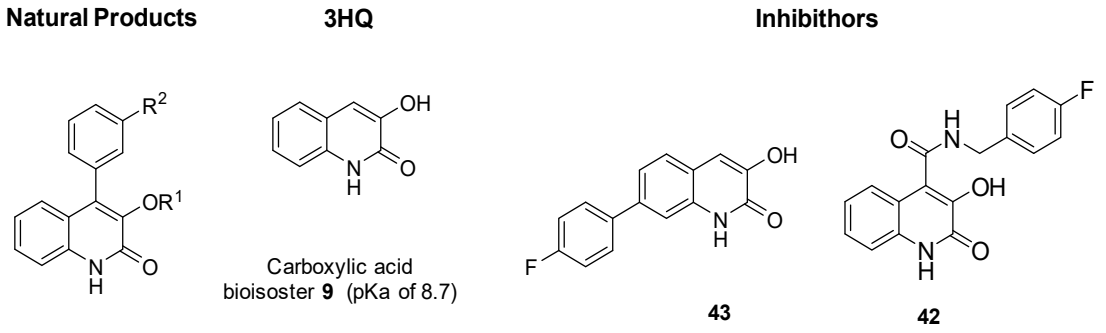

Scheme 5.1 - The 3-hydroxyquinolin-2(1H)-one (3HQ) core present in the structure of natural occurring compounds, as a carboxylic acid bioisoster and as an enzyme inhibitor.

5.2 Synthesis of 3HQs derivatives

3HQs derivatives, 4-carboxylate-3HQs, were synthesized through an efficient regioselective Eistert ring expansion reaction using the new emergent MOC methodology. According to the route depicted in Scheme 5.2., reaction of isatins with diazo compounds catalysed by dirhodium(II) complex and DBU enabled the generation of 3-hydroxy-4-ethylesterquinolin-2(1*H*)-ones **69**. The scope of the reaction was investigated using the sequential protocol. The methodology was quite tolerant with substituents present in the aromatic ring of isatins, namely withdrawing groups as F, Cl, Br, and F_3OC, and also when using N-substituted isatins as N-CH_3 and N-CH_2Ph. Furthermore, all the products were easily isolated by simple filtration, avoiding any chromatography yielding the desired compounds from good to excellent yields (Table 2.4 compounds **69**, **84**-**96**). One-pot protocol of the ring expansion reaction of isatin and EDA was also performed. A NHC-dirhodium(II) complex/ DBU was found to be the best system to implement the one-pot addition of EDA to isatins followed by ring exapansion of **69**. Analogously to the sequential protocol, the scope of the reaction was extended to other substrates with similar or better yields than the ones obtained by the sequential method (Table 2.5 compounds **69**, **90**-**93**, **95**). The ring expansion reaction catayzed by dirhodium complexes was studied by DFT calculations. The study indicated the formation of metallocarbene between the product of the addition of diazo compounds in isatins **74** and the dirodium complex as the rate-limiting step of the mechanism.

The ring expansion reaction of isatins, catalysed by di-rhodium (II) complexes, was also performed with different diazo esters, proving to be an effective strategy to synthesize 4-Ester-3HQs (Scheme 3.4, compounds **115**-**119**). Viridicatin **31** and derivatives **107-110** were synthesized from intermediate **106** after decarboxylation of **69** and subsequently reaction with NBS**.** Suzuki-Miyaura coupling of **106** in the presence of phenyl boronic acids, 10 mol% $Pd(PPh_3)_4$ using microwave irradiation yield viridicatin **31**. Expected compound **31** was obtained in 80% yield and viridicatin

derivatives **107-110** could also be obtained in good yields using different aryl boronic acids.

For the synthesis of 4-carboxamide-3HQs (Scheme 5.2) it was necessary to firstly synthesize NHS-diazo acetate and to further perform the Eistert ring-expansion reaction with isatins catalysed by 0.5 mol% of $Rh_2(OAc)_4$ using TEA as base.

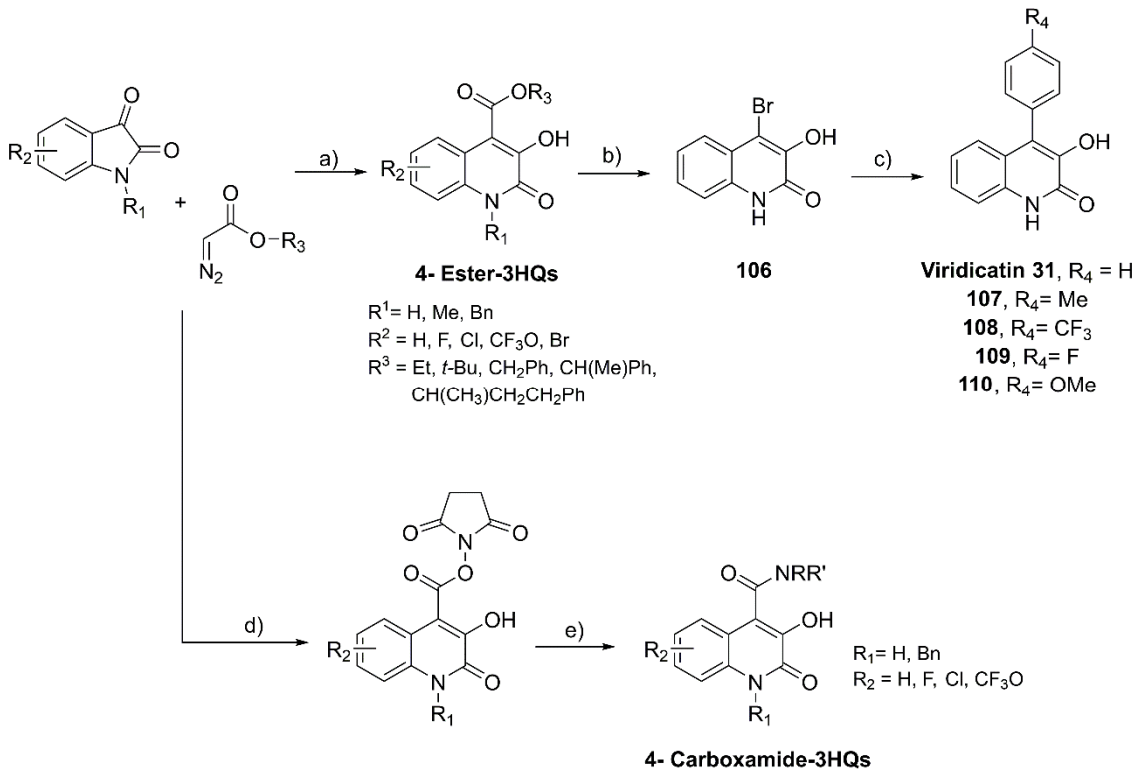

Scheme 5.2 - Synthesis of 4-Ester-3HQs, 4-Carboxamide-3HQs and viridicatin derivatives 31. a) DBU, dirhodium complex (1 mol%), absolute EtOH, r.t., 3h; b) (i) NaOH, H_2O, reflux, 7h; (ii) aq HCl; (iii) NBS, DMF; c) 10 mol% $Pd(PPh_3)_4$, Na_2CO_3/H_2O, DME:H_2O 3:1, MW, 150ºC, 2h; f) TEA, $Rh_2(OAc)_4$ (1 mol%), DCM, r.t.; g)HNRR', Na_2CO_3, DMF, r.t., overnight.

The methodology proved to be a simple and effective strategy to synthetize 4-NHS-3HQs, by simple filtration in yields up to 97%. Finally, reaction of 4-NHS-3HQs with different type of amines, namely primary and secondary amines in DCM and in presence of Na_2CO_3 proceeded smoothly to yield the 4-Carboxamide-3HQs **127**, **132-143**. Additionally, protected amino acids were used in the reaction with 4-NHS-3HQs affording the 4-Carboxamide-3HQs "peptide like" **128-129**, **138-143** in

good to excellent yields without any chromatographic step. Structures of all key intermediates and final compounds were establish on the basis of NMR techniques.

5.3 Biological evaluation of 3-HQs

5.3.1 *In vitro* Anticancer Activity SAR

The synthesized 3HQs derivatives (Table 3.1, compounds **69**, **84**-**96**) were evaluated *in vitro* for their anticancer activity against MCF-7, NCI-H460 and HT-29 cancer cell lines. 4-carboxylate-3HQs series shown to be generally not active against the three cancer cell lines. However, there is an evidence that an electro withdrawing group (F_3CO) in position 7 of the 4-carboxylate-3HQ **87** was able to reduce the viability of the NCI-460 cells in 48% at the concentration of 20 μM. Based on this result compound **87** was chosen as lead compound to perform structural modifications with the aim to increase the anti-proliferative activity.

Decarboxylation of ester moiety in C-4 position of compound **87** giving compound **111** and N-benzylated **112** resulted in a loss of activity. This results clearly indicate that the presence of free N-H is a requirement for the anti-proliferative activity and the reason could be addressed to the ability of NH group to perform a hydrogen bond. Furthermore, the replacement of the ethyl ester group in position C-4 of hydroquinone **87**, remarkably reduced the anti-proliferative activity against the cancer cells enabling the substitutents' importance in that position.

Different esters were introduced at position C-4 of compound **87**, leading to an increased activity against the 3 cancer cells line. Compound **118** with a benzyl ester in position C-4 resulted in an IC_{50} of 1.80 μM against NCI-H460. Analogously, compound **120** holding a three carbons chain showed an IC_{50} of 2.10 μM against NCI-H460. The introduction of more steric bulky esters was also evaluated for the anti-proliferative activity. Compounds **117** and **119,** showed to be less active compared to compounds **118** and **120** in the NCI-H460 cancer cell line showing IC_{50} of 6.05 μM and 7.34 μM respectively**.** The presence of a phenyl ketone instead of an ester group

was also evaluated. Compound **116** showed to be active against both cancer cell lines with an IC_{50} of 10.75 μM for MCF-7 and 10.36 μM for NCI-H460. Because of the indiscriminate activity of compound **118** in the three cancer cells lines, this compound was evaluated against a non-cancer CHOK1 and proved to be quite toxic on this model (5.6±1.0 μM). From a SAR point of view, incorporation of alkyl esters in position C-4 in **87** core clearly induced higher anti-proliferative effect against cancer cell but unfortunately a significant toxicity was also detected. This effect could be addressed to metabolic issues since esters can be rapidly cleaved in vivo. The 6-trifluoromethoxy-4-carboxamide-3HQs derivatives were found to be active against MCF-7, NCI-H460 and not against HT-29 cancer cell lines and less toxic. The introduction of benzyl amide on compound **133** resulted in a less anti-proliferative activity compared to the isosteric compound **118** with a benzyl ester group. Compound **133** showed an IC_{50} of 12.0 μM in MCF-7 and 9.5 μM in NCI-H460 moreover it shown to be less cytotoxic towards the CHOK1 cells. A slightly longer alkyl chain (two carbons) featuring in compound **134** showed more selectivity towards MCF-7 (IC_{50} 4.8 μM), while the introduction of aniline in the core **132** results in a loss of activity. Methylated benzyl amide **135** showed to be significantly more selective against MCF-7 than the parent compound **133,** nevertheless a no activity was found. Cyclic amines were introduced, namely pyrolidine **136** and piperidine **137** but only compound **137** showed to be active and selective against NCI-H460 with an IC_{50} 4.8 μM.

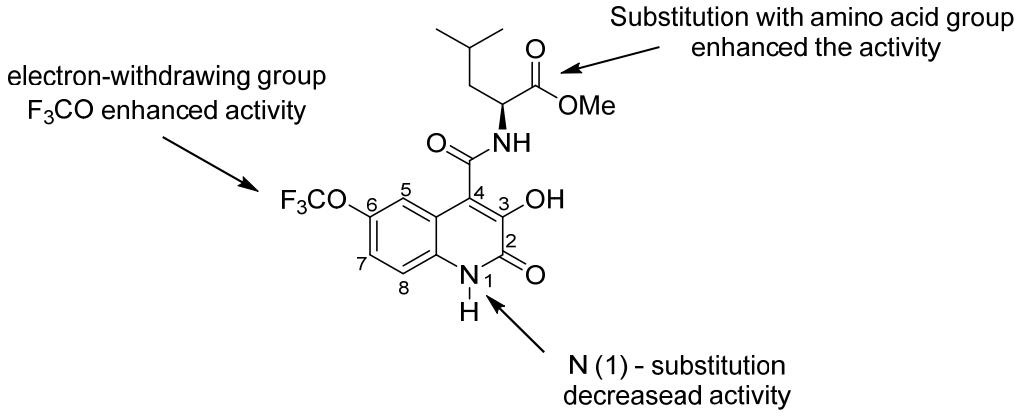

Scheme 5.3 – Structure-activity-relationship of compound **143** towards cancer cells.

The peptide-like 4-carboxamides -3HQs **140**-**143** were also evaluated showing some activity against MCF-7 and NCI-H460 cancer cell lines. Between the two peptide-like holding L-Glycine amino acid, only compound **137** showed selectivity against the MCF-7 cell line (IC_{50} 12.6 μM) while compound **136** was not active. Among this series of peptide-like L-leucine-4-carboxamide-3HQ **143** (Scheme 5.3) showed an interesting activity against NCI-H460 cell line with an IC_{50} of 2.7 μM.

Table 5.1 – Anti-proliferative activity of 7-OCF_3-3HQ series against MCF-7, NCIH460 and HT-29 cancer cell lines and CHOK1 non-cancer cell lines.

Entry	Compound	μM			
		MCF-7	**NCI-H460**	**HT-29**	**CHOK1**
1	**87**	95%*	52%*	74%*	NA
2	**111**	NA	NA	NA	NA
3	**112**	NA	NA	NA	NA
4	**116**	10.75±1.12	10.36±1.86	NA	ND
5	**117**	13.39±2.50	6.05±1.05	NA	7.59±1,33
6	**118**	10.11±2.10	1.80±1.15	11.37±1.10	5.6±1.05
7	**119**	12.07±1.00	7.34±1.22	NA	ND
8	**120**	15.99±1.16	2.10±1.10	NA	ND
9	**132**	NA	NA	NA	NA
10	**133**	12.03±1.04	9.46±1.20	NA	NA
11	**134**	4.82±1.24	NA	NA	NA
12	**135**	17.50±2.40	NA	NA	NA
13	**136**	NA	NA	NA	ND
14	**137**	NA	7.27±1.25	NA	NA
15	**138**	NA	NA	NA	ND
16	**139**	12.57±1.11	NA	NA	NA
17	**140**	NA	NA	NA	ND
18	**141**	9.44±7.52	8.40±1.67	NA	NA
19	**142**	9.49±1.02	11.35±1.11	NA	NA
20	**143**	15.12±1.91	2.69±1.38	NA	NA

***** Percentage of cell-viability; NA – Non-active at the concentration of 20 μM; Determined IC_{50} of compounds in MCF-7, NCIH460 and HT-29 cancer cell lines and CHOK1 non-cancer cell model after 48 hours incubation; NA- Non-active at the concentration of 20 μM; ND- Not determined.

5.3.2 **Biochemical studies of PAH modulators**

The 3HQs derivatives **141**, and **165-167** featuring L-Phenylalanine in position C-4 were synthetized (Scheme 4.5) and evaluated for their activity against hPAH protein either upon the stabilization of the regulatory and/or catalytic domain or upon an effect on the catalytic activity. From the first screening of the library, compound **141** holding a F_3CO group on 3HQ moiety displayed the most interesting results and for this reason was selected as hit for further modifications.

The first modification performed on the hit **141**, was the introduction of a benzyl group in the quinolinic nitrogen of the F_3OC-3HQ (Scheme 4.6) and compound **169** was evaluated by DSF and enzymatic activity assays. This modification resulted in the loss of the stabilizing effect on the regulatory domain of hPAH and furthermore compound **169** showed to be a strong inhibitor of the protein. From a structural relationship (SAR) point of view, we found that the free NH of this series of compounds is detrimental for the stabilizing capacity effect on the regulatory domain on hPAH enzyme.

With the objective of improving the biological activity of these compounds we performed structural modification on C-4 of the 6-F_3OC-3HQ core. Different amines in position C-4 namely primary, secondary amines and different amino acids were installed. From this 6-F_3CO-carboxamide-3HQ, compound **134** (scheme 5.4) showed to be the only compound able to rescue the hPAH activity in the substrate compound activated assay (condition III). The compound allowed the protein to respond to L-Phe activation, thus without competing with the amino acid substate.

As a result we now have in hands to sets of chemical structures to be further improved. The first set of compounds will be derived from **141** and aims to restore the stability of the hPAH protein, thus acting as pharmacological chaperones. It is currently accepted that reversible competitive inhibitors of misfolded enzymes can

act as pharmacological chaperones as long as they present low affinity for the enzyme.[168] Binding of the inhibitor to the misfolded enzyme is expected to stabilize the protein preventing its premature degradation by the protein quality control system of the cell. To this end the designed compounds should be characterized concerning the inhibitory constants (Ki). A different approach to restore the activity of deficient enzymes is to identify compounds that could act as enzyme activators. In this prespective, the second set of compounds, derived from **134**, could act as hPAH activators.

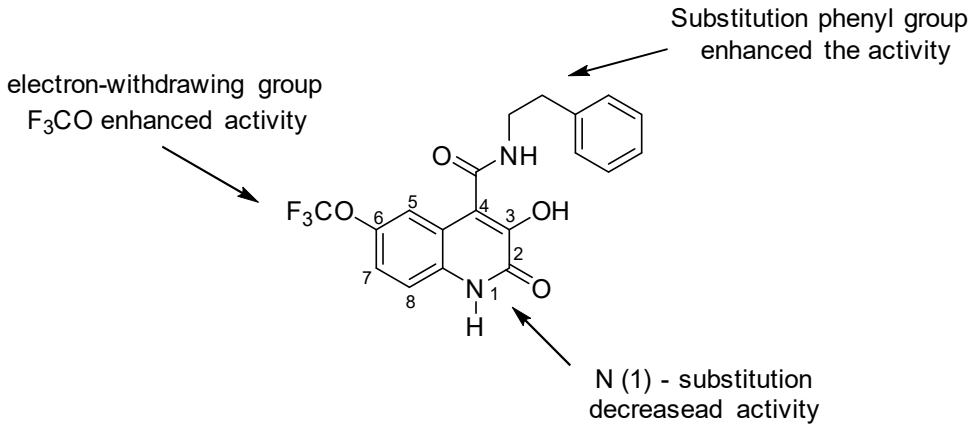

Scheme 5.4 – Structure-activity relationships (SAR) of 6-F_3OC-carboxamide-3HQ over hPAH.

5.4 Conclusions

The main objective of this project was to synthesise, in an efficient way using the new emergent MOC methodology, novel derivatives of 3-hydroxyquinolin-2(1*H*)-ones and test their biological activity as antiproliferative agents and as modutators of phenylalanine hydroxylase enzyme

The synthesisis of the 3-hydroxy-4-ethylesterquinolin-2(1*H*)-one and its derivatives was achived by a regioselective ring expansion reaction of isatins with ethyl diazoacetate catalysed by dirhodium(II) complexes. The reaction mechanism, was studied by DFT calculations, and highlighted the metallocarbene formation between

the 3-hidroxyindole-diazo intermediate and the dirhodium(II) complex as the key step of the mechanism.

Moreover, we also discovered an efficient cooperative system, NHC-dirhodium(II) complex and DBU, which was able to catalyze, in one-pot, the Eistert ring expansion of isatins with ethyl diazoacetate. This system showed to overcome the self-quench of the catalytic system and any competitive metallocarbene formation of di-Rh(II) complex with EDA . Therefore, the one pot reaction catalyzed by NHC-dirhodium(II) complex and DBU was able to afford 3-hydroxy-4-ethylesterquinolin-2(1H)-one and its derivatives. Using the 3-hydroxy-4-ethylesterquinolin-2(1H)-one as a plataform, we were also able to synthesize viridicatin alkaloids in a 4-steps route, via Suzuki-Miyaura coupling reaction of aryl-boronic acids with 3-hydroxy-4-bromoquinolin-2(1H)-ones prepared from 3-hydroxy-4-ethylesterquinolin-2(1H)-ones.

The ring-expansion reaction of isatins catalysed by di-rhodium(II) complexes was also extended to synthesize a series of 4-carboxylate-3HQs by direct addition of structurally diverse diazo compounds to isatins. This series of compounds were tested for the first time against a panel of MCF-7, NCI-H460 and HT-29 cancer cell lines. Unfortunately, a severe cytotoxic against a model of non-cancer cell lines was also found. Instead, 4-carboxamides-3HQs, simply prepared by ring expansion reaction of isatin derivatives with NHS-diazo acetate, showed an improved selectivity towards MCF-7 and NCI-H460 cancer cell lines and no cytotoxic against the same model of a non-cancer cell lines.

In this study, was also evaluated the biological properties of 3HQ derivatives as new modulators of PAH enzyme activity. We synthetized a small library of L-Phe-3HQ derivatives which was tested for PAH enzyme activity. From this library, compound **141** showed the most interesting results, stabilizing the regulatory domain and furthermore with a low inhibition effect on hPAH activity assay. A new library of 4-carboxamide-F_3CO-3HQs compounds was synthetized and evaluated for their effect on the hPAH thermal stability (DSF) and enzymatic activity. Compound **134**,

featuring a phenethylamine moiety, was identified as the most effective compound, able to directly increment hPAH activity by a pre-activation mechanism similar to the one induced by the substrate L-Phe.

Overall, 3HQs scaffold has been confirmed as usefull scaffold to development new agents active against tumor cancer cell lines and also as potential lead structures for the development of new modulator of PAH enzyme.

Chapter VI

VI. Material and Methods

"An experiment is a question which science poses to Nature, and a measurement is the recording of Nature's answer"

Max Planck

'The Meaning and Limits of Exact Science', Science (30 Sep 1949), 110, No. 2857, 325.
Advance reprinting of chapter from book Max Planck, Scientific Autobiography (1949), 110

6.1 General

6.1.1 Chemicals

Reagents were purchased from **Aldrich Chemical Company LDTd** or **Alfa Aesar Thermo Fisher Scientific** and were used as received from commercial suppliers unless otherwise stated.

Dichloromethane (DCM) Dimethoxyethane (DME) as reaction solvent was freshly distilled over calcium hydride while Ethanol and DMF were used without any purification. All reactions were performed in oven-dried glassware. Microwave reactions were carried out in oven dried 10 mL reaction vessels. Reaction mixtures were analysed by thin layer chromatography using Merck silica gel 60F254 aluminium plates and visualized by UV light and with phosphomolybdic acid solution. In column chromatography it was silica gel 60 M purchased from MN (Ref. 815381).

6.1.2 Instrumentation

Nuclear Magnetic Resonance (NMR): NMR spectra were record in a Bruker ultrashield 400 MHz (9.4 T) spectrometer equipped with a 5 mm Quad Nuclear Probe (QNP), operating at 400.1 MHz for ^{1}H NMR and 100.6 MHz for ^{13}C NMR (Faculty of Science, University of Lisbon) or recorded in a Bruker ultrashield 300 MHz (7.05 T) spectrometer (Avance-300) equipped with a 5 mm single-axis Zgradient quattro nucleus probe, operating at 300.1 MHz for ^{1}H NMR and 75.5 MHz for ^{13}C NMR (School of Pharmacy and Pharmaceutical Sciences, University of Lisbon) using $CDCl_3$, $(CD_3)_2SO$ as deuterated solvents. Chemical Shifts (δ) are reported in parts per million (ppm), using solvent as internal reference, tetramethylsilane (TMS). All coupling constants are expressed in Hz Data are reported using the following convention: s (singlet), d (doublet), dd (double doublet), dt (double triplet), t (triplet), td (triple triplet), tt (triple triplet), q (quartet), quint (quintuplet) and m (multiplet).

Mass spectrometry (MS): Mass spectra were recorded in a mass spectrometer (Micromass Quattro Micro API, Waters, Ireland) with a Triple Quadrupole (TQ) and with an electrospray ion source (ESI) operating in positive mode.

High Resolution Mass Spectrometry (HRMS): The utilized instrument was a LTQ Orbitrap XL mass spectrometer (Thermo Fischer Scientific, Bremen, Germany) controlled by *LTQ Tune Plus 2.5.5* and *Xcalibur 2.1.0*. The capillary voltage of the electrospray ionization (ESI) was set to 3000 V. The capillary temperature was 275ºC. The sheath gas flow rate (nitrogen) was set to 5 (arbitrary unit as provided by the software settings). The capillary voltage was 36 V and the tube lens voltage 110 V. Performed in U. Porto CEMUP centro de materiais de Universidade do Porto

Elemental analysis (EA): Elemental analysis was performed in a Flash 2000 CHNS-O analyzer (ThermoScientific, UK).

Microwave reactions: were performed using a Discover SP CEM microwave.

6.1.3 Methods

Thin-layer chromatography (TLC): Reactions were followed by thin-layer chromatography using coated silica gel plates (Merck, aluminum sheets, silica gel 60 F254, 200 μm layer-thickness, 25 μm particle size) or in aluminium oxide matrix (60 Å medium pore diameter and 200 μm layerthickness) with fluorescent indicator in PET support.

Colum chromatography: Flash column chromatography was performed using silica gel 60 (230-400 mesh, Merck and co.).

6.2 General method for the tandem synthesis of 3-hydroxy-2(1H)-oxoquinoline-4-ethylesters :

A round bottom flask equipped with a magnetic stirrer was charged with a solution of isatin (0.3 mmol) in absolute ethanol (1.5mL), ethyl diazoacetate (1.2 eq), 1,8-Diazabicyclo[5.4.0]undec-7-ene (DBU) (15 mol %) and $Rh_2(OAc)_4$ (1 mol %). The mixture was then stirred for 3 hours at room temperature after which the reaction mixture was centrifuged and the product isolated by filtration. The collected solid was washed with water, Et_2O, and dry under reduced pressure to furnishing the expected 3-hydroxy-4-ethylesterquinolin-2-(1*H*)-ones

6.3 General method for the sequential synthesis of 3-hydroxy-4-ethylesterquinolin-2-(1H)-ones

Ethyl diazoacetate (1.2 eq) and DBU (15 mol %) were added to a stirred solution of isatin (0.3 mmol) in absolute ethanol (1.5 ml). The reaction mixture was stirred for 3 hours at room temperature and then $Rh_2(OAc)_4$ (1 mol%) was added to afford the ring expansion product, which readily precipitated from the reaction mixture and was isolated by filtration. The collected solid was washed with Et_2O, and dry under reduced pressure to furnish the expected 3-hydroxy-4-ethylesterquinolin-2-(1H)-ones.[5]

Experimental data

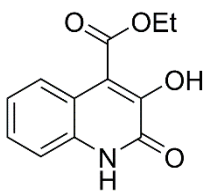

Compound 69[77] was obtained in 63 % yield (using the sequential or the tandem protocols).

^{1}H NMR (400 MHz, DMSO): 12.34 (s, 1H), 10.28 (s, 1H), 7.25 – 7.42 (m, 3H), 7.20 (t, J = 7.4 Hz, 1H),) 4.40 (q, J = 7.1 Hz, 2H), δ 1.32 (t, J = 7.1 Hz, 3H);

^{13}C NMR (100 MHz, DMSO): 165.39, 157.97, 143.70, 133.04, 127.07, 123.30, 122.77, 117.16, 116.95, 115.48, 61.37, 14.16.

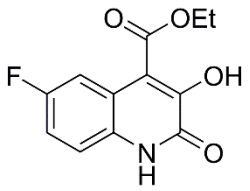

Compound 84[72] was obtained in 64% yield (using the sequential protocol).

^{1}H NMR (400 MHz, DMSO): δ 12.41 (s, 1H), 10.57 (s, 1H), 7.34 (dd, *J* = 9.0, 5.1 Hz, 1H), 7.25 (td, *J* = 8.7, 2.6 Hz, 1H), 7.18 (dd, *J* = 10.1, 2.4 Hz, 1H), 4.40 (q, *J* = 7.1 Hz, 2H),1.32 (t, *J* = 7.1 Hz, 3H);

^{13}C NMR (100 MHz, DMSO): 158.37, 144.10, 133.44, 127.47, 123.70, 123.17, 117.56, 117.35, 115.88, 108.75, 108.50, 61.53, 14.11

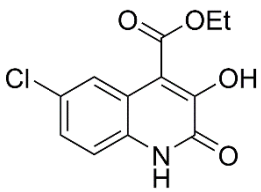

Compound 85[72] was obtained in 92% yield as white solid. (using the sequential procedure).

^{1}H NMR (400 MHz, DMSO): δ 12.48 (s, 1H), 7.20 – 7.56 (m, 3H), 4.40 (q, J = 6.8 Hz, 2H), 1.31 (t, J = 6.7 Hz, 3H).

^{13}C NMR (100 MHz, DMSO): δ 165.41, 158.23, 146.04, 132.07, 127.16, 122.65, 119.12, 117.73, 115.58, 61.91 14.52.

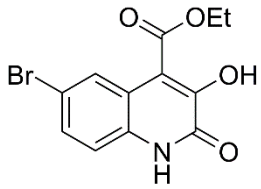

Compound 86 was obtained in 90% yield as white pure solid (using the sequential procedure);

^{1}H NMR (400 MHz, DMSO): 12.46 (s, 1H), 10.64 (s, 1H), 7.53 (s, 2H); 7.26 (d, *J* = 9.0 Hz, 1H), 4.40 (dd, *J* = 13.9, 7.0 Hz, 2H) 1.31 (t, *J* = 6.9 Hz, 3H);

^{13}C NMR (100 MHz, DMSO): δ 164.97, 157.79, 145.46, 132.02, 129.52, 125.17, 119.15, 117.60, 115.14, 114.62, 114.29, 61.53, 14.14;

HRMS EI^{+}: *m/z* [M+H]$^{+}$ Calculated for $C_{12}H_{10}BrNO_4^{+}$: 310.9793 **found** 310.9795

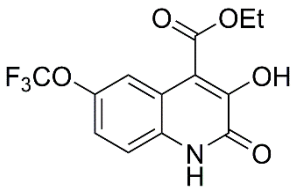

Compound 87 was obtained in 74% as white pure solid;

^{1}H NMR (400 MHz, DMSO): δ 12.53 (s, 1H), 10.71 (s, 1H), 7.39 (t, *J* = 12.5 Hz, 3H), 4.40 (q, *J* = 7.1 Hz, 2H), 1.31 (t, *J* = 7.1 Hz, 3H);

^{13}C NMR (100 MHz, DMSO): δ 164.84, 157.80, 145.83, 143.31, 131.85, 121.47 (d, *J* = 263.21 Hz), 120.22, 118.92, 117.28, 115.42, 61.54, 14.06;

LRMS (ESI): *m/z* $[M+H]^+$ 318, 319

Elemental analysis calculated. (%) for $C_{13}H_{10}F_3NO_5$: C 49.22, H 3.18, N 4.42; **found** (%): C 49.36, H 3.33, N 4.39

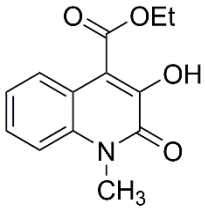

Compound 88 was obtained in 75% yield (using the sequential procedure).

^{1}H NMR (400 MHz, CDCl3 8.46 (s, 1H),): 7.85 (dd, J = 8.1, 1.1 Hz, 1H), 7.50 – 7.43 (m, 1H), 7.37 (d, J = 8.1 Hz, 1H), 7.27 – 7.33 (m, 1H), 4.53 (q, J = 7.1 Hz, 2H), 3.82 (s, 3H), 1.46 (t, J = 7.1 Hz, 3H),

^{13}C NMR (100 MHz, CDCl3): δ 166.24, 158.61, 144.75, 134.30, 127.88, 125.50, 123.80, 118.20, 114.57, 113.92, 30.85, 14.39.

LRMS (ESI): *m/z* $[M+H]^+$ 248;

Elemental analysis calculated. (%) for $C_{14}H_{16}NO_4$: C, 63.15; H, 5.30; N, 5.67; **found** (%): C, 63.51; H, 5.52; N, 5.65;

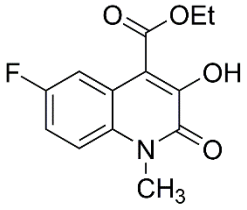

Compound 89 was obtained in 75% yield as pale yellow solid (using the sequential procedure);

^{1}H NMR (400 MHz, $CDCl_3$): 7.70 (dd, *J* = 10.3, 2.8 Hz, 1H), 7.33 (dd, *J* = 9.2, 4.7 Hz, 1H), 7.15– 7.23 (m, 1H), 4.53 (q, *J* = 7.1 Hz, 2H), 3.80 (s, 3H), 1.47 (t, *J* = 7.1 Hz, 3H);

^{13}C NMR (100 MHz, $CDCl_3$): δ 166.34, 158.83 (d, *J*= 240.7 Hz), 157.96, 147.27, 130.59, 119.32 (d, *J* = 9.5 Hz), 115.91 (d, *J* = 8.7 Hz), 115.32, 115.08, 111.49, 111.23, 62.43, 31.07, 14.24.

HRMS EI$^+$: *m/z* **[M+H]$^+$** calculated for $C_{13}H_{12}FNO_4^+$: 265.0750 **found** 265.0741

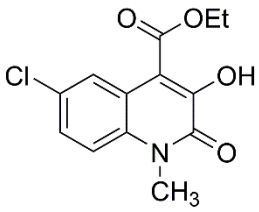

Compound 90 was obtained in 81% (using the sequential procedure) or 92% yield (using the tandem procedure) as a yellow solid;

^{1}H NMR (400 MHz, $CDCl_3$): 7.92 (d, *J* = 2.2 Hz, 1H), 7.39 (d, *J* = 9.2 Hz, 1H), 7.32 – 7.22 (m, 1H), 4.53 (q, *J* = 7.1 Hz, 2H), 3.78 (s, 3H), 1.47 (t, *J* = 7.1 Hz, 3H);

^{13}C NMR (100 MHz, $CDCl_3$): δ 166.23, 158.20, 146.91, 132.72, 129.43, 127.70, 124.99, 119.36, 115.86, 112.16, 62.56, 31.05, 14.33;

LRMS (ESI): *m/z* ([M-H]$^-$): 280; 266; 252

Elemental analysis calculated. (%) for $C_{13}H_{12}ClNO_4$: C 55.43, H 4.29, N 4.97; **found** (%): C 50.72, H 3.96, N 4.85

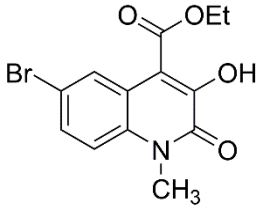

Compound 91 was obtained in 78% (sequential procedure) or (tandem procedure) as a yellow solid;

^{1}H NMR (400 MHz, $CDCl_3$): 8.10 (d, *J* = 2.1 Hz, 1H), 7.55 (dd, *J* = 9.0, 2.2 Hz, 1H), 7.20 – 7.30 (m, 1H), 4.56 (q, *J* = 7.1 Hz, 2H), 3.80 (s, 3H), 1.49 (t, *J* = 7.1 Hz, 3H);

^{13}C NMR (100 MHz, $CDCl_3$): δ 166.22, 158.21, 146.85, 133.15, 130.52, 128.00, 119.77, 117.02, 116.13, 112.07, 62.59, 31.03, 14.34;

LRMS (ESI): *m/z* [M-H]$^-$: 324.3; 310

Elemental analysis calculated. (%) for $C_{13}H_{12}BrNO_4$: C 47.87, H 3.71, N 4.29; **found** (%): C 47.41, H 3.96, N 4.58;

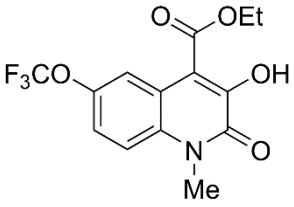

Compound 92 was obtained in 81% yield as pale yellow solid (using the sequential or the tandem procedures);

^{1}H NMR (400 MHz, $CDCl_3$): 7.92 (d, *J* = 1.6 Hz, 1H), 7.37 (d, *J* = 9.2 Hz, 1H), 7.31 (d, *J* = 1.9 Hz, 1H), 4.53 (q, *J* = 7.1 Hz, 2H), 3.80 (s, 3H), 1.46 (t, *J* = 7.1 Hz, 3H);

^{13}C NMR (100 MHz, $CDCl_3$): δ 166.62, 158.07, 148.37, 144.91, 132.51, 121.78 (d, *J* = 263.21 Hz), 120.31, 119.05, 117.72, 115.74, 111.60, 62.56, 31.03, 14.08;

LRMS (ESI): *m/z* [M-H]⁻:330; 302

Elemental analysis calculated. (%) for $C_{14}H_{12}F_3NO_5$: C 50.76, H 3.65, N 4.23; **found** (%): C 50.72, H 3.96, N 4.85;

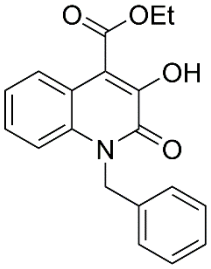

Compound 93 was obtained in 73% (sequential procedure) or 85% yield (tandem procedure) as a pale yellow solid;

^{1}H NMR (400 MHz, $CDCl_3$): 8.33 (s, 1H), 7.83 (dd, *J* = 8.0, 0.9 Hz, 1H), 7.12 – 7.40 (m, 8H), 5.63 (s, 2H), 4.56 (q, *J* = 7.1 Hz, 2H), 1.48 (t, *J* = 7.1 Hz, 3H);

^{13}C NMR (100 MHz, $CDCl_3$): δ 166.01, 158.84, 144.17, 135.19, 133.57, 128.96, 127.82, 127.66, 126.51, 125.41, 123.74, 118.29, 115.40, 114.48, 62.26, 47.26, 14.30;

LRMS (ESI): *m/z* $[M+H]^+$ 324;

Elemental analysis calculated. (%) for $C_{19}H_{17}NO_4$: C 70.58, H 5.30, N 4.33; **found** (%): C 70,08, H 5,26, N 4.41.

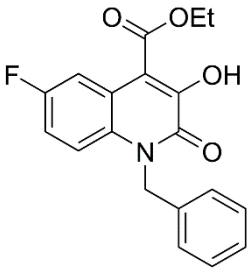

Compound 94 was obtained in 93% yield as a yellow solid (using the sequential procedure);

^{1}H NMR (400 MHz, $CDCl_3$): 7.68 (dd, *J* = 10.2, 2.8 Hz, 1H), 7.37 – 7.21 (m, 5H), 7.17 (d, *J* = 7.1 Hz, 2H), 7.05 (d, *J* = 7.1 Hz, 1H), 5.61 (s, 2H), 4.56 (q, *J* = 7.1 Hz, 2H), 1.49 (t, *J* = 7.1 Hz, 3H);

^{13}C NMR (100 MHz, $CDCl_3$**):** 166.29, 158.9 (d, J= 241 Hz), 158.53, 146.81, 135.09, 130.03, 129.15, 127.90, 126.58, 119.72, 117.03 (d, *J* = 8.6 Hz), 115.43 (d, *J* = 23.1 Hz),111.59 111.34, 62.60, 47.68, 14.38;

LRMS (ESI): *m/z* $[M+H]^+$ 342;

Elemental analysis calculated. (%) for $C_{19}H_{16}FNO_4$: C 66.86, H 4.72, N 4.10; **found** (%):C 66.11, H 4.79, N 4.18;

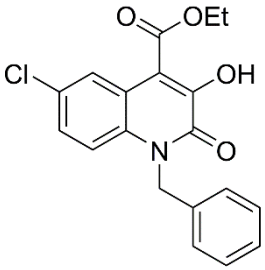

Compound 95 was obtained in 87% (sequential procedure) or 68% yield (tandem procedure) as a yellow solid;

^{1}H NMR (400 MHz, $CDCl_3$): δ 7.92 (d, *J* = 2.2 Hz, 1H), 7.37 – 7.24 (m, 6H), 7.21 (d, *J* = 9.1 Hz, 1H), 5.60 (s, 2H), 4.56 (dt, *J* = 7.1, 5.8 Hz, 2H), 1.41 – 1.54 (m, 3H);

^{13}C NMR (100 MHz, $CDCl_3$): δ 166.10, 158.68, 146.46, 134.96, 132.06, 129.51, 129.15, 127.93, 127.76, 126.57, 125.03, 119.73, 116.82, 112.95, 62.61, 47.54, 14.37;

LRMS (ESI): *m/z* $[M+H]^+$ 358;

Elemental analysis calculated. (%) for $C_{19}H_{16}ClNO_4$: C 63.78, H 4.51, N 3.91; **found** (%): C 63.89, H 4.67, N 3.98;

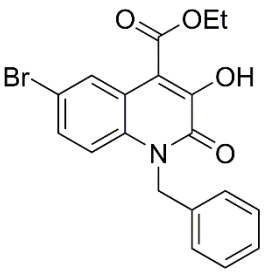

Compound 96 was obtained in 72% yield as a yellow solid (using the sequential procedure);

^{1}H NMR (400 MHz, $CDCl_3$): 8.06 (d, *J* = 2.2 Hz, 1H), 7.22 – 7.45 (m, 5H), 7.07 – 7.22 (m, 3H), 5.59 (s, 2H), 4.56 (q, *J* = 7.1 Hz, 2H), 1.49 (t, *J* = 7.1 Hz, 3H);

^{13}C NMR (100 MHz, $CDCl_3$): δ 166.07, 158.63, 146.34, 134.92, 132.51, 130.59, 129.17, 128.04, 127.95, 126.56, 120.08, 117.09, 112.86, 62.66, 47.51, 14.37;

LRMS (ESI): *m/z* $[M+H]^+$: 404;

Elemental analysis calculated. (%) for $C_{19}H_{16}BrNO_4$: C 56.73, H 4.01, N 3.48; **found** (%): C 56.74, H 4.17, N 3.65;

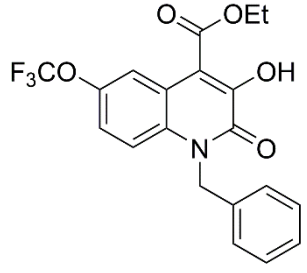

Compound **112** was obtained in 53% yield as white solid (using the sequential procedure);

^{1}H NMR (400 MHz, $CDCl_3$) δ 7.85 (s, 1H), 7.31 – 7.14 (m, 5H), 7.11 (d, J = 6.8 Hz, 3H), 5.54 (s, 2H), 4.49 (q, J = 7.1 Hz, 2H), 1.41 (t, J = 7.1 Hz, 3H).

^{13}C NMR (101 MHz, $CDCl_3$) δ 166.41, 158.45, 147.76, 144.92, 134.81, 131.88, 129.07, 127.85, 126.48, 121.75, 120.39, 119.33, 117.78, 116.67, 112.31, 62.64, 47.58, 14.12.

LRMS (ESI): *m/z* $[M+H]^+$ 404;

Elemental analysis calculated (%), C, 58.97; H, 3.96; F, 13.99; N, 3.44; **found** (%): C, 58.27; H, 4.44; N, 3.52.

6.4 Synthesis of 3-hydroxyquinolin-2(1H)-one 9.

Compound **69** (5 mmol) was added to a solution of NaOH (10 mmol) in H_2O (50mL). The reaction was then stirred at reflux for 7 h. The formed precipitate after acidification until pH 1-2 with aqueous HCl solution (2 M), was filtered, washed with water and dried under reduced pressure to yield the 3-hydroxyquinolin-2-(1H)-one in 92% (74.4 mg).

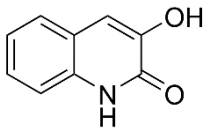

Compound 9[72] was obtained in 92% yield as a white solid.

^{1}H NMR (400 MHz, $(CD_3)_2SO$) δ 12.01 (s, 1H), 9.46 (s, 1H), 7.48 (d, J = 7.6 Hz, 1H), 7.27 (dd, J = 6.1, 1.3 Hz, 2H), 7.18 – 7.05 (m, 2H);

^{13}C NMR (101 MHz, $(CD_3)_2SO$): δ, 159.01, 146.65, 133.98, 126.70, 126.23, 122.49, 121.15, 115.18, 112.89

.

6.5 Synthesis of 4-bromo-3-hydroxyquinolin-2(1H)-one

Compound **106** was performed according with the protocol described in the literature: Sit, Sing-Yuen; Ehrgott, Frederick J.; Gao, Jinnian; Meanwell, Nicholas A**.** Bioorganic & Medicinal Chemistry Letters, **1996**, 6, 499 - 504.

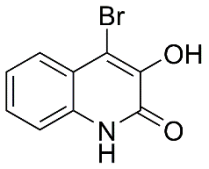

Compound 106[72] was obtained in 72% yield as a gray solid.

^{1}H NMR (400 MHz, $(CD_3)_2SO$) δ 12.32 (s, 1H), 10.40 (d, *J* = 14.5 Hz, 1H), 7.70 (d, *J* = 8.0 Hz, 1H), 7.44 – 7.15 (m, 3H);

^{13}C NMR (101 MHz, $(CD_3)_2SO$): 157.11, 145.45, 132.93, 127.93, 125.66, 123.42, 120.19, 115.74, 109.75.

6.6 Optimization of the microwave-assisted Suzuki-Mayura reaction.

An oven dried 10 mL microwave reaction vessel was charged with 4-bromo-3-hydroxyquinolin-2(1H)-one (0.4 mmol), phenyl-boronic acid (2.2 equiv.) and freshly dried DME (1.1 ml). Then a Pd source and a solution 2 M of Na_2CO_3/ H_2O (0.4 mL) were added to the reaction mixture. The vessel was capped and the mixture was stirred for 5 minutes at room temperature. The sealed vessel was then heated by microwave irradiation at 150 C for 2 hours. After cooling to the room temperature, the resulting dark-colored mixture was purified by flash chromatography using a Combiflash Rf teledyne isco system and 1:1 mixture of Hexane/EtOAc to afford 3-hydroxy-4-phenylquinolin-2(1H)-one.

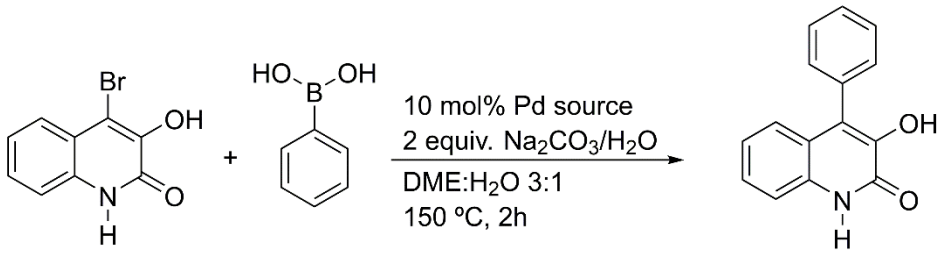

Pd source mol%	Yield (%)
$Pd_2(dba)_3$ 5mol%	47
Pd ferroceno 10mol%	65.7
Pdtetrakis 10mol%	80
Pd NHC 10mol%	50
PdCl2 10mol%	59

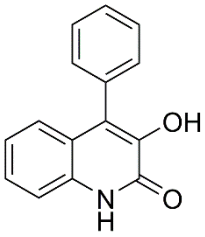

Compound 31[87] obtained as a white solid 80 %.

^{1}H NMR (400 MHz, $(CD_3)_2SO$): δ 12.24 (s, 1H), 9.21 (s, 1H), 7.51 (dd, *J* = 7.4, 7.2 Hz, 2H), 7.45 (d, *J* = 7.4 Hz, 1H) 7.26 – 7.39 (m, 4H), 7.03 – 7.06 (m, 2H),

^{13}C NMR (100 MHz, $(CD_3)_2SO$): δ 158.32, 142.47, 133.78, 133.19, 129.88, 128.37, 127.69, 126.46, 124.33, 123.98, 122.16, 120.93, 115.30;

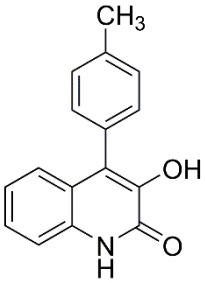

Compound 107 was obtained in 71% yield as a white solid;

^{1}H NMR (400 MHz, $(CD_3)_2SO$): δ 12.20 (s, 1H), 9.14 (s, 1H), 7.37–7.26 (m, 4H), 7.21 (d, *J* = 8.0 Hz, 2H), 7.10 –7.02 (m, 2H), 2.38 (s, 3H);

^{13}C NMR (100 MHz, $(CD_3)_2SO$): δ 170.8, 168.4, 163.2, 138.9, 137.0, 128.3, 122.3, 120.8, 120.3, 110.3, 106.0, 62.8, 23.4, 13.7;

HRMS EI$^+$: *m/z* **[M+H]$^+$** calculated for $C_{16}H_{13}NO_2{}^+$: 251.0946 **found** 251.0945

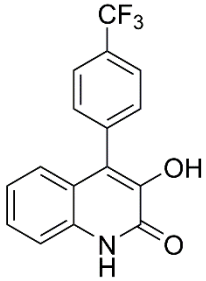

Compound 108 was obtained in 65% yield as a white solid;

^{1}H NMR (400 MHz, $(CD_3)_2SO$): δ 12.29 (s, 1H), 9.50 (s, 1H), 7.88 (d, *J* = 7.2 Hz, 2H), 7.59 (d, *J* = 7.2 Hz, 2H), 7.36 (s, 2H), 6.86-7.22 (m, 2H);

^{13}C NMR (100 MHz, $(CD_3)_2SO$): δ 158.57, 143.25, 138.76, 133.67, 131.38, 128.57, 127.12, 125.79, 124.78 (d, *J* = 275 Hz), 124.46, 123.00, 122.83, 120.77, 115.85.

HRMS EI$^+$: *m/z* **[M+H]$^+$** calculated for $C_{16}H_{10}F_3NO_2{}^+$: 305.0664 **found** 305.0665

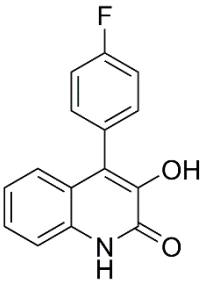

Compound 109 was obtained in 65% yield as a white solid;

^{1}H NMR (300 MHz, $(CD_3)_2SO$): δ12.24 (s, 1H), 9.30 (s, 1H), 7.44– 7.26 (m, 6H) , 7.13– 7.00 (m, 2H);

^{13}C NMR (75 MHz, $(CD_3)_2SO$): δ 162.07 (d, J = 245 Hz) 158.66, 143.16, 133.61, 132.47, 130.43, 126.96, 124.63, 123.41, 122.68, 121.31, 115.92, 115.76.

HRMS EI$^+$: m/z $[M+H]^+$ Calculated for $C_{15}H_{10}FNO_2^+$: 255.0696 **found** 255.0685

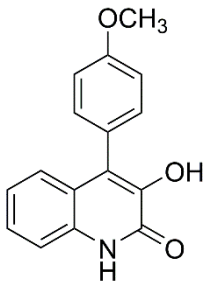

Compound 110 was obtained in 72% yield as a white solid;

^{1}H NMR (400 MHz, $(CD_3)_2SO$): δ 12.19 (s, 1H), 9.11 (s, 1H), 7.44 – 7.21 (m, 4H), 7.09 (m, 4H), 3.82 (s, 3H);

^{13}C NMR (100 MHz, $(CD_3)_2SO$): δ 206.97, 159.17,158.78, 142.95, 133.65, 131.59, 126.85, 126.08, 124.89, 124.17, 122.54, 121.62, 115.73, 114.27, 55.59

HRMS EI$^+$: m/z $[M+H]^+$ Calculated for $C_{16}H_{13}NO_3^+$ 267,0895 **found** 267.0945.

Single crystal X-ray diffraction for compounds 70, 69 and 93:

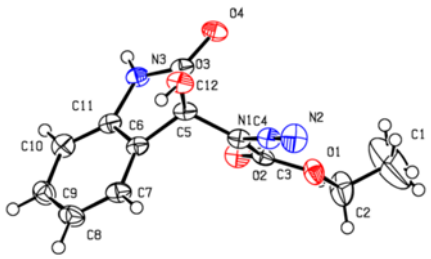

Crystals of **70**, **69** and **93** suitable for X-ray diffraction studies were mounted on a loop with protective oil. X-ray data were collected at 150K on a Bruker AXS-KAPPA APEX II diffractometer using graphite monochromated Mo-Kα radiation (λ=0.71069 Å) and operating at 50kV and 30 mA. Cell parameters were retrieved using Bruker SMART software and refined using Bruker SAINT[169] on all observed reflections. Absorption corrections were applied using SADABS[170]. Structure solution and refinement were performed using direct methods with program SIR97[171] and SHELXL97[172], both included in the package of

programs WINGX-Version 1.80.05[173]. A full-matrix least-squares refinement was used for the non-hydrogen atoms with anisotropic thermal parameters. All hydrogen atoms connected to carbons were inserted in idealized positions and allowed to refine riding in the parent carbon atom; hydrogen atoms bonded to nitrogen atoms were located in a difference map.

Crystallographic data for compound **70** (CCDC 939410): $C_{12}H_{11}N_3O_4$, fw=261.24, monoclinic, space group $P2_1/c$, a=19.2024(16) Å, b=11.8604(8) Å, c=11.0525(10) Å, β= 105.828(4) °, V =2421.8(3) Å^3, Z=8, T=150K, d_{calc}=1.433 mg.m^{-3}, μ =0.110 mm^{-1}, F(000)=1088, yellow block crystal (0.22 x 0.10 x 0.08 mm). Of 19885 reflections collected, 5328 were independent (R_{int}= 0.0430); 345 variables refined with 5328 reflections to final R indices $R_1(I > 2\sigma(I))$=0.0472, $wR_2(I > 2\sigma(I))$=0.1163, R_1(all data)=0.0724, wR_2(all data)=0.1255, GOF= 1.054. A disorder model was applied to one methyl group.

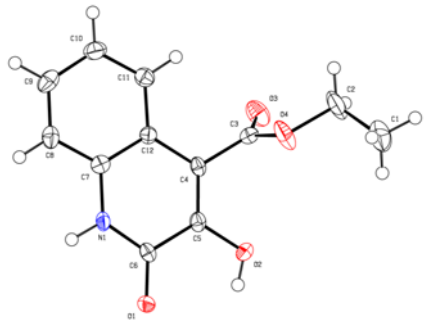

Crystallographic data for compound **69** (CCDC 939411): $C_{12}H_{11}NO_4$, fw=233.22, trigonal, space group *R*-3, a=25.034(5) Å, b=25.034(5) Å, c=8.926(5) Å, V =4856(3) Å^3, Z=18, T=150K, d_{calc}=1.435 mg.m^{-3}, μ =0.109 mm^{-1}, F(000)=2196, colourless needle (0.2 x 0.02 x 0.02 mm). Of 10137 reflections collected, 1972 were independent (R_{int}= 0.1573); 158 variables refined with 1972 reflections to final R indices $R_1(I > 2\sigma(I))$=0.0483, $wR_2(I > 2\sigma(I))$=0.0795, R_1(all data)=0.1650, wR_2(all data)=0.0938, GOF= 0.749.

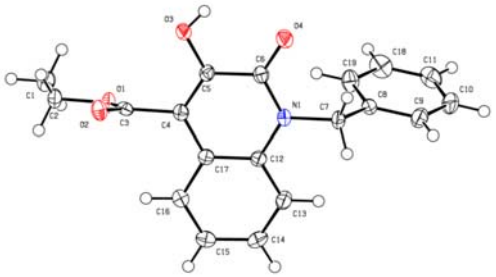

Crystallographic data for compound **93** (CCDC 939640): $C_{19}H_{17}NO_4$, fw=323.34, triclinic, space group *P*-1, a=6.8034(6) Å, b=10.6251(8) Å, c=11.2680(8) Å, α= 92.853(4), β= 102.984(4) °, γ= 95.613(4), V = 787.73(11) $Å^3$, Z=2, T=150K, d_{calc}=1.363 $mg.m^{-3}$, μ =0.096 mm^{-1}, F(000)=340, colourless block crystal (0.20 x 0.04 x 0.02 mm). Of 9515 reflections collected, 3236 were independent (R_{int}= 0.0413); 219 variables refined with 3236 reflections to final R indices $R_1(I > 2\sigma(I))$=0.0451, $wR_2(I > 2\sigma(I))$=0.1123, R_1(all data)=0.0807, wR_2(all data)=0.1255, GOF= 1.059.

Synthesis of 3-hydroxyquinolin-2(1H)-one 111:

Compound **69** (5 mmol) was added to a solution of NaOH (10 mmol) in H_2O (50mL). The reaction was stirred at reflux for 7 h and acidified until pH 1-2 with aqueous HCl solution (2 M). The formed precipitate was filtered, washed with water and dried under reduced pressure to yield the 3-hydroxyquinolin-2-(1*H*)-one in 75% yield.

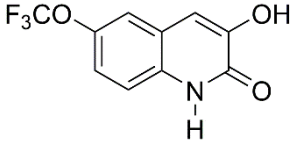

^{1}H NMR (300 MHz, $(CD_3)_2SO$): δ 12.52 (s, 1H), 10.43 (s, 1H), 7.89 – 7.81 (m, 2H), 7.66 (t, J = 7.4 Hz, 1H), 7.50 (t, J = 7.6 Hz, 2H), 7.42 (d, J = 9.0 Hz, 1H), 7.37 – 7.29 (m, 1H), 6.90 (d, J = 1.6 Hz, 1H).

^{13}C NMR (13C NMR (75 MHz, $(CD_3)_2SO$) δ 158.69, 147.69, 143.45, 132.69, 122.10, 119.94, 118.96, 118.17, 116.78, 112.26.

HRMS EI$^+$ *m/z* [M+H]$^+$: Calculated $C_{10}H_7F_3NO_3^+$: 246,0373 **found** 246.03706.

6.7 Preparation of α-Diazo carbonyl compounds

Diazo acetates **113**-**115** were prepared as previously reported by Fukuyama and co-workers, according to the following scheme.

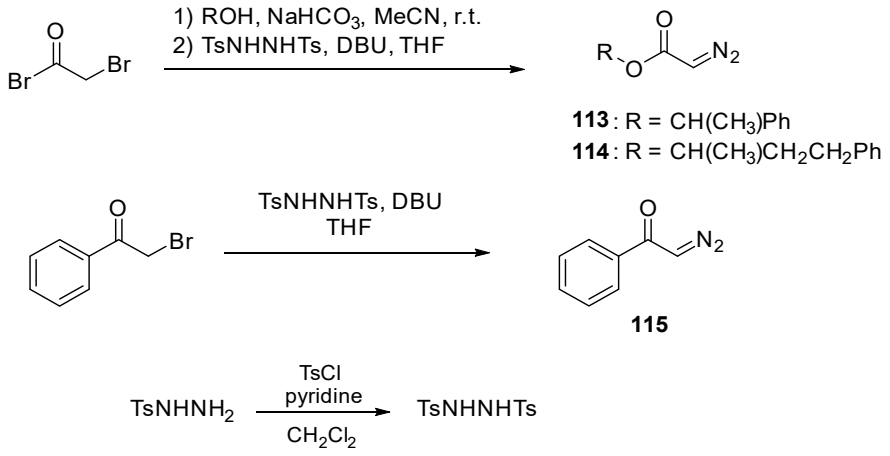

Synthesis of *N,N'*-ditosylhydrazine

A flame-dried, 50mL, round-bottomed flask fitted with a magnetic stir bar was charged with p-toluenesulfonyl hydrazide (3.47 g, 18.4 mmol) and p-toluenesulfonyl chloride (5.27 g, 27.06 mmol) in 18.4 mL of anhydrous CH_2Cl2. The suspension was stirred at room temperature while pyridine (3.2 mL, 27.06 mmol) was added dropwise over 1 min. During the addition, the reaction mixture became homogenous and turned yellow. White precipitate was observed within 3 min and the reaction mixture was stirred for 1.5 h. Et2O (20 mL) and H2O (10 mL) were added and stirred at 0 °C for 15 min. The suspension was filtered through a Büchner funnel and washed with Et2O (10 mL). The solid thus obtained was dissolved in boiling MeOH (40 mL), which precipitated after cooling to room temperature. The mixture was concentrated to half volume by rotary evaporation and cooled to 0 °C. The precipitate was collected

by filtration in a Büchner funnel and washed with cold MeOH (10 mL) and Et2O (50 mL) to give *N*,*N*'-ditosylhydrazine (5.24 g, 72%);

^{1}H NMR (300 MHz, $(CD_3)_2SO$) δ 9.59 (s, 1H), 7.65 (d, J = 8.3 Hz, 2H), 7.39 (d, J = 8.0 Hz, 2H), 2.39 (s, 3H).

^{13}C NMR (100 MHz, $(CD_3)_2SO$) δ 143.7, 135.7, 129.7, 128.0, 21.3;

Preparation of diazo acetates 113 - 114

The secondary alcohol (150 mg, 1.0 mmol) and $NaHCO_3$ (252 mg, 3.0 mmol) were dissolved in acetonitrile (5.0 mL) and bromoacetyl bromide (131 μL, 1.5 mmol) was added slowly at 0 °C. After stirring 10 min at that temperature, the reaction was quenched with H_2O (5.0 mL). The solution was extracted with CH_2Cl_2 (3 x 5 mL). The organic phase was washed with brine and dried over Mg_2SO4. The solvent was evaporated, and the residue was used in the next reaction without purification. The bromoacetate thus obtained and *N*,*N*'-ditosylhydrazine (681 mg, 2.0 mmol) were dissolved in THF (5.0 mL) and cooled to 0 °C. DBU (750 mL, 5.0 mmol) was added dropwise and stirred at that temperature for 10 minutes. After the quenching of the reaction by addition of saturated $NaHCO_3$ solution (5.0 mL), this was extracted with Et_2O (3 x 5 mL). The organic phase was washed with brine, dried over Mg_2SO4 and concentrated under vacuum. The desired product was obtained after purification by flash chromatography in silica gel.

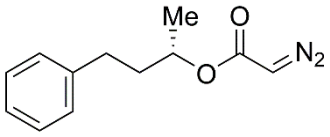

4-Phenyl-2-butanyl 2-diazoacetate

99.1 mg, 45% Yield

^{1}H NMR (300 MHz, $CDCl_3$) δ 7.34 – 7.10 (m, 5H), 5.13 – 4.92 (m, 1H), 4.72 (s, 1H), 2.77 – 2.51 (m, 2H), 2.04 – 1.90 (m, 1H), 1.90 – 1.75 (m, 1H), 1.28 (d, J = 6.3 Hz, 3H);

^{13}C NMR (100 MHz, $CDCl_3$) δ 166.3, 141.3, 128.3, 128.2, 125.8, 71.0, 46.1, 37.6, 31.6, 20.1;

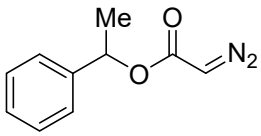

1-Phenylethyl 2-diazoacetate

42.7 mg, 64% Yield

^{1}H NMR ($CDCl_3$, 400 MHz) δ 7.44-7.30 (m, 5H), 5.97 (q, J = 6.4 Hz, 1H), 4.76 (s, 1H), 1.56 (d, J = 6.4 Hz, 3H);

^{13}C NMR ($CDCl_3$, 100 MHz) δ 166.0, 141.4, 128.4, 127.8, 125.9, 72.6, 46.3, 22.2;

Preparation of α-Diazoacetophenone 115

α-Bromoacetophenone (199 mg, 1.0 mmol) and *N*,*N*'-ditosylhydrazine (681 mg, 2.0 mmol) were dissolved in THF (5.0 mL) and cooled to 0 °C. DBU (750 μL, 5.0 mmol) was added dropwise and the reaction was stirred at that temperature for 10 minutes. After the quenching of the reaction by the addition of saturated $NaHCO_3$ solution (5.0 mL), the mixture was extracted with Et_2O (3 x 5.0 mL). The organic phase was washed with brine, dried over Mg_2SO4 and concentrated under reduced pressure. The obtained residue was purified by flash chromatography in silica gel to give pure α-diazoacetophenone as a yellow solid (68.3mg, 94%).

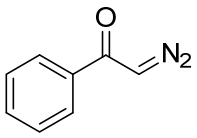

^{1}H NMR ($CDCl_3$, 400 MHz) δ 7.77 (d, J = 7.3 Hz, 2H), 7.55 (m, 1H), 7.46 (m, 2H), 5.91 (s, 1H).

^{13}C NMR ($CDCl_3$, 100 MHz) δ 186.3, 136.6, 132.7, 128.6, 126.6, 54.2;

Preparation of succinimidyl diazoacetate 124

Compound **122** was prepared according to literature procedures and its purity assessed by melting point determination (white solid; mp: 150-152ºC). Compound

123 was also prepared according to literature procedures and its purity assessed by melting point determination (Pale yellow prism crystals; m.p. 101-112ºC).

Compound **124** was prepared as described by Doyle and co-workers[142], and obtained as light yellow crystals with the following spectral characterization:

^{1}H NMR (300 MHz, $CDCl_3$) δ 5.21 (s, 1H), 2.84 (s, 4H).

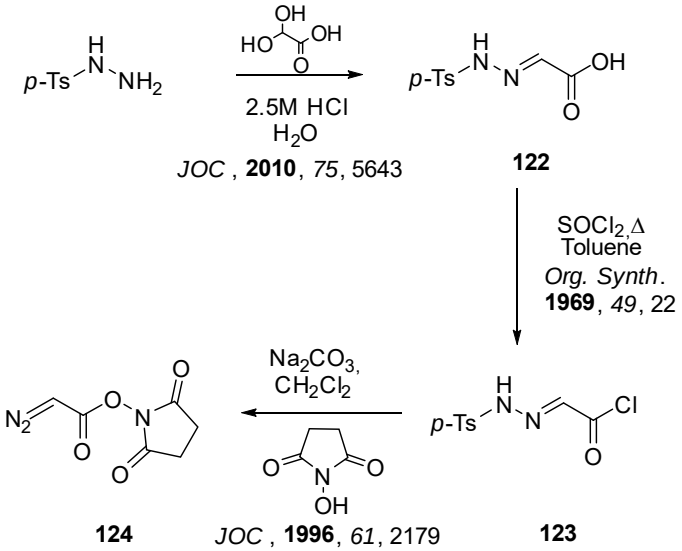

6.8 General synthesis of 4-carboxylate-3HQs:

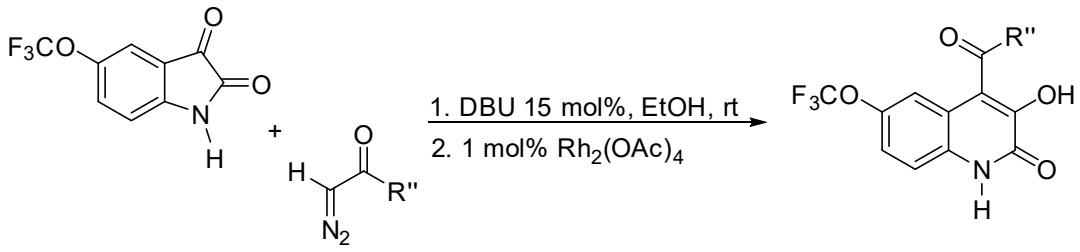

Synthesis compounds (116 - 120): Appropriate diazo compound (1.2 eq) and DBU (15 mol%) were added to a stirred solution of 5-(trifluoromethoxy)isatin (0.3 mmol) in absolute ethanol (1.5 mL) at room temperature. The reaction mixture was stirred for 3 hours, the solvent was removed under reduced pressure and the diazo intermediate purified by flash chromatography. The diazo intermediate and $Rh_2(OAc)_4$ (1 mol %) were dissolved in absolute ethanol and stirred at room

temperature for 20 minutes to afford the ring expansion product, which readily precipitated from the reaction mixture and was isolated by filtration. The collected solid was washed with Et_2O, and dried under reduced pressure to furnish the expected 4-substituted 3-hydroxy-quinolin-2-(1H)-ones.

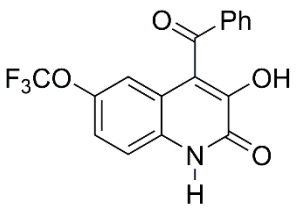

Compound **116** was obtained in yield 77% as white solid;

^{1}H NMR (300 MHz, $(CD_3)_2SO$): δ 12.52 (s, 1H), 10.43 (s, 1H), 7.89 – 7.81 (m, 2H), 7.66 (t, J = 7.4 Hz, 1H), 7.50 (t, J = 7.6 Hz, 2H), 7.42 (d, J = 9.0 Hz, 1H), 7.37 – 7.29 (m, 1H), 6.90 (d, J = 1.6 Hz, 1H).

^{13}C NMR (75 MHz, $(CD_3)_2SO$): δ 194.24, 157.94, 144.66, 143.24, 143.21, 143.18, 136.01, 132.46, 125.18, 121.79, 120.78, 119.20, 118.40, 115.01,

LRMS (ESI): *m/z* $[M+H]^+$: 349.6; 337.9.

Elemental analysis calculated (%),C, 58.46; H, 2.89; N, 4.01; **found**: 59.05; H, 3.01; N, 4.63;

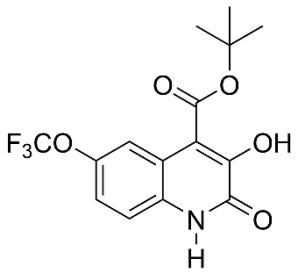

Compound **117** was obtained in 86% yield as white solid;

^{1}H NMR (400 MHz, $(CD_3)_2SO$) δ 12.49 (s, 1H), 10.57 (s, 1H), 7.40 (s, 2H), 7.24 (s, 1H), 1.56 (s, 9H).

^{13}C NMR (101 MHz, $(CD_3)_2SO$) δ 164.50, 158.36, 145.38, 143.70, 132.27, 121.88, 120.59, 118.54, 117.79, 117.06, 115.01, 83.28, 28.23;

LRMS (ESI): *m/z* ($[M+H]^+$): 385;

Elemental analysis calculated (%) $C_{15}H_{14}F_3NO_5$: C 59.37, H 5.24, N 14.58, **found**: C 59.48, H 5.55, N 14.25;

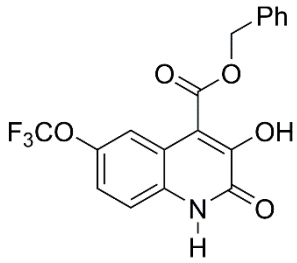

Compound **118** was obtained in 71% yield as white solid;

^{1}H NMR 1H NMR (300 MHz, $(CD_3)_2SO$) δ 12.53 (s, 1H), 10.78 (s, 1H), 7.59 – 7.21 (m, 8H), 5.44 (s, 2H).

^{13}C NMR (75 MHz, $(CD_3)_2SO$) δ 164.71, 157.74, 146.00, 143.26, 135.59, 131.88, 128.50, 128.45, 128.35, 121.82, 120.29, 118.12, 117.25, 115.63, 114.94, 67.03;

LRMS (ESI): *m/z* ([M+H]$^+$): 380;

Elemental analysis calculated (%) for $C_{18}H_{12}F_3NO_5$: C, 57.00; H, 3.19; N, 3.69; **found**: C, 56.87; H, 3.44; N, 3.77.

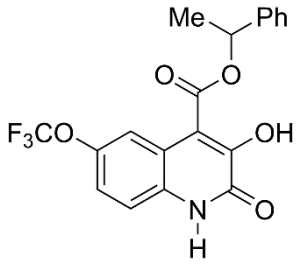

Compound **119** was obtained in 76% yield as orange pure solid;

^{1}H NMR (300 MHz, $CDCl_3$) δ 12.65 (s, 1H), 11.31 (s, 1H), 8.22 (s, 1H), 7.36-7.22 (m, 6H), 7.22 (s, 1H), 6.29 (q, J = 6.3 Hz, 1H), 1.80 (d, J = 6.6 Hz, 3H).

^{13}C NMR (75 MHz, $CDCl_3$) δ 168.32, 158.79, 145.20, 139.88, 130.65, 128.88, 128.75, 126.42, 126.42, 122.22, 120.95, 118.82, 118.08, 117.97, 117.72, 76.29, 21.99;

LRMS (ESI): *m/z* M+H]$^+$: 394; 337.9; 289.6; 104.7.

Elemental analysis calculated (%) for: $C_{19}H_{14}F_3NO_5$: C, 58.02; H, 3.59; N, 3.56; **found**: C, 57.93; H, 3.86; N, 3.58:

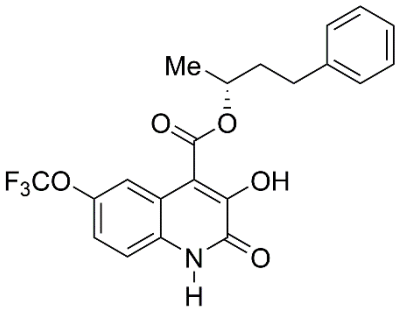

Compound **120** was obtained in 77% yield as orange solid;

^{1}H NMR (300 MHz, $CDCl_3$) δ 12.74 (s, 1H), 8.12 (s, 1H), 7.46 (d, J = 8.7 Hz, 1H), 7.31 – 6.92 (m, 6H), 5.32 (dd, J = 12.1, 6.6 Hz, 1H), 2.82 – 2.59 (m, 2H), 2.16 - 2.12 (m, J = 14.6, 7.3 Hz, 1H), 2.04 – 1.90 (m, 1H), 1.44 (d, J = 6.2 Hz, 3H).

^{13}C NMR (75 MHz, $CDCl_3$) δ 168.76, 158.90, 152.97, 145.25, 140.88, 130.88, 128.63, 128.40, 126.25, 122.38, 120.87, 118.21, 117.55, 111.77, 74.59, 37.48, 31.86, 20.15;

LRMS (ESI): *m/z* $[M+H]^+$ 422; 289.6;132.7.

Elemental analysis calculated (%) for $C_{21}H_{18}F_3NO_5$: C, 59.86; H, 4.31; N, 3.32; **found**: C, 60.50; H, 4.54; N, 3.54

6.9 Synthesis of 4-NHS-3HQs 125-126, 130-131

A round bottom flask equipped with a magnetic stirrer was charged with isatin derivative (0.3 mmol), absolute ethanol (1.5 mL), NHS-diazoacetate (1.2 equiv) and triethylamine (20 mol%). The mixture was stirred for 3 hours at room temperature until formation of a precipitated. The reaction mixture was centrifuged to recover the solid which was then washed with hexane. The isolated diazo compound was then dissolved in 2.5 mL of dry DCM and reacted with $Rh_2(OAc)_4$ (1 mol%) at room temperature over a period of 20 minutes. The ring expansion product precipitated from the reaction mixture and was collected by filtration and then washed with hexane.

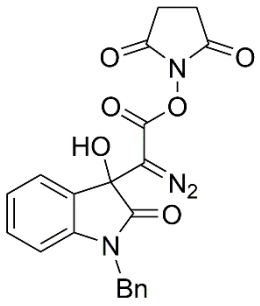

Compound **125** was obtained in 88% yield as grey solid;

^{1}H NMR: (300 MHz, $CDCl_3$) δ 7.52 (dd, J = 7.5, 0.8 Hz, 1H), 7.30 – 7.19 (m, 6H), 7.05 (td, J = 7.6, 0.9 Hz, 1H), 6.67 (d, J = 7.7 Hz, 1H), 4.86 (AB q, J = 15.8 Hz, 2H), 4.51 (s, 1H), 2.73 (s, 4H).

^{13}C NMR: (75 MHz, $CDCl_3$) δ 174.37, 169.18, 159.58, 142.53, 134.89, 131.12, 129.01, 127.94, 127.38, 125.31, 123.93, 110.18, 71.25, 44.39, 25.55;

HRMS EI$^-$: *(m/z)* $[M]^-$Calculated for $C_{21}H_{16}N_2O_5^-$ 415,0912; **found** 415,09006.

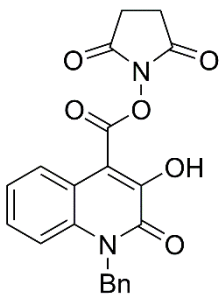

Compound **126** was obtained in 84 % yield as grey solid;

^{1}H NMR (300 MHz, $(CD_3)_2SO$) δ 11.29 (s, 1H), 7.89 (d, J = 7.2 Hz, 1H), 7.51 – 7.38 (m, 2H), 7.48-7.24 (m, 6H), 5.65 (s, 2H), 2.94 (s, 4H).

^{13}C NMR (75 MHz, $(CD_3)_2SO$) δ 170.25, 161.22, 157.73, 145.87, 136.00, 133.21, 128.79, 127.73, 127.30, 126.53, 123.95, 123.51, 117.32, 115.83, 110.49, 46.04, 25.72;
LRMS (ESI): *m/z* $[M+H]^+$ 310;
Elemental analysis calculated (%) for $C_{21}H_{16}N_2O_6$: C, 64.28; H, 4.11; N, 7.14, **found**: C, 64.28; H, 4.11; N, 7.14.

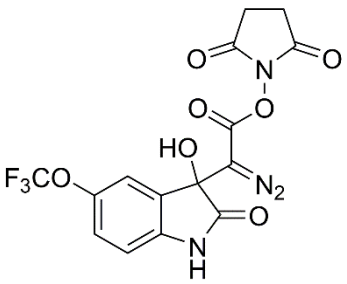

Compound **130** was obtained in 93% yield as grey solid;
^{1}H NMR (300 MHz, $(CD_3)_2SO$) δ 10.79 (s, 1H), 7.69 (s, 1H), 7. 58 (m, 1H), 7.28 (d, J = 1.6 Hz, 1H), 6.91 (d, J = 8.5 Hz, 1H), 2.73 (s, 4H).
^{13}C NMR (75 MHz, $(CD_3)_2SO$) δ 175.96, 170.59, 159.51, 143.84, 141.84, 131.12, 124.16, 120.62 (d, J =255.6 Hz), 119.64, 70.24, 61.23, 25.76;
Elemental analysis calculated (%) for C, 43.49; H, 2.19; N, 13.52 **found**: C, 43.49; H, 2.79; N, 12,82.

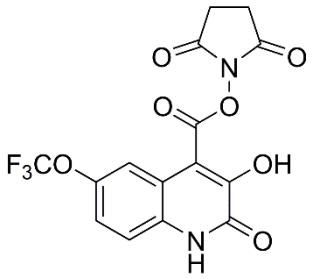

Compound **131** was obtained in 97% yield as grey solid;
^{1}H NMR (300 MHz, $(CD_3)_2SO$) δ 12.67 (s, 1H), 7.85 (s, 1H), 7.42 (s, 2H), 2.90 (s, 4H).
^{13}C NMR (75 MHz, $(CD_3)_2SO$) δ 170.31, 160.77, 157.19, 149.00, 143.59, 131.77, 120.63 (d, J =255.6 Hz), 118.48, 117.65, 117.51, 115.75, 109.39, 25.69.
LRMS (ESI): *m/z* $[M+H]^+$ 386.9; 355.2; 338.2;303.9.
Elemental analysis calculated (%) for $C_{15}H_9F_3N_2O_7$ + 0,33H_2O: C, 46.00; H, 2.48; N, 7.15, **found**: C, 45.93; H, 2.48; N, 7.14.

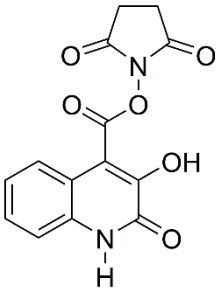

Compound **162** was obtained in 60% yield as grey solid;

^{1}H NMR (300 MHz, $(CD_3)_2SO$) δ 12.41 (s, 1H), 7.83 (s, 1H), 7.38 – 6.99 (m, 3H), 2.89 (s, 4H).

^{13}C NMR (75 MHz, $(CD_3)_2SO$) δ 172.26; 162.92; 157.13; 142.49; 136.95; 132.55; 127.69; 123.20; 122.97; 120.22; 115.64; 25.73.

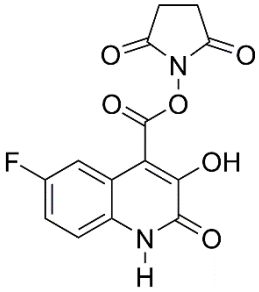

Compound **163** was obtained in 60% yield as grey solid;

^{1}H NMR (300 MHz, $(CD_3)_2SO$) 12.47(s, 1H); 7.69 (dd, 1H); 7.34 (dd, 1H), 7.26 (td, 1H); 2.9 (s, 4H);

^{13}C NMR (75 MHz, $(CD_3)_2SO$) δ 170.81, 161.20, 159.90, 157.32, 156.75, 149.11, 129.94, 118.15, 116.82, 116.50, 109.34, 108.99, 25.66

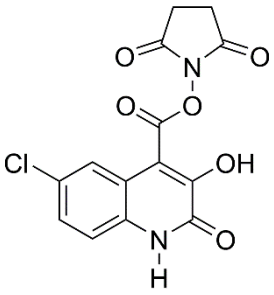

Compound **164** was obtained in 50% yield as grey solid;

^{1}H NMR (300 MHz, $(CD_3)_2SO$) δ 12.59 (s, 1H), 7.92 (d, J = 2.1 Hz, 1H), 7.43 (d, J = 2.2 Hz, 1H), 7.35 (d, J = 8.7 Hz, 1H), 2.92 (s, 4H).

^{13}C NMR (75 MHz, $(CD_3)_2SO$) δ 170.34, 160.85, 157.25, 149.27, 131.46, 127.13, 126.96, 122.44, 118.32, 117.48, 108.77, 25.69.

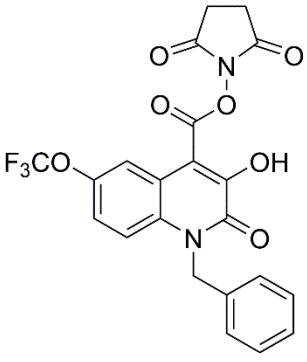

Compound **168** was obtained in 80% yield as grey solid;

^{1}H NMR (300 MHz, $(CD_3)_2SO$) δ 7.93 (s, 1H), 7.54 (d, J = 9.3 Hz, 1H), 7.44 (dd, J = 9.3, 1.8 Hz, 1H), 7.38 – 7.30 (m, 2H), 7.26 (t, J = 5.8 Hz, 3H), 5.64 (s, 2H), 2.93 (s, 4H).

^{13}C NMR (75 MHz, $(CD_3)_2SO$) δ 173.37, 161.56, 158.92, 146.88, 143.72, 136.69, 133.07, 129.23, 127.74, 126.90, 123.10, 121.01120.81 (d, J =255.6 Hz, 119.95, 118.99, 117.08, 112.17, 46.13, 25.65.

Synthesis of 4-carboxamide-3HQ 127-129 and 132-143:

The appropriate amine (1.1 equiv) and Na_2CO_3 (10 equiv) were added to a stirred solution of 4-NHS-3HQ **15** or **20** (87 μmol) in dry DCM (1 mL). The mixture was stirred overnight at room temperature after which the volatiles were evaporated under reduced pressure and the crude mixture acidified with HCl (2 N). The precipitate was then centrifuged and collected by filtration. Finally, the isolated solid was thoroughly washed with H_2O to furnish targeted 4-carboxamide-3HQs.

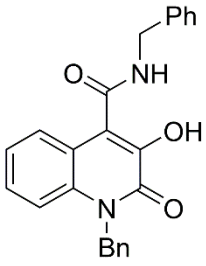

Compound **127** was obtained in 76% yield as grey pure solid

^{1}H NMR (300 MHz, $(CD_3)_2SO$) δ 9.96 (s, 1H), 9.10 (t, J = 6.1 Hz, 1H), 7.53 – 7.09 (m, 14H), 5.63 (s, 2H), 4.54 (d, J = 6.0 Hz, 2H);

^{13}C NMR (75 MHz, $(CD_3)_2SO$) δ 173.24, 164.75, 159.03, 141.46, 139.61, 136.88, 133.92, 129.14, 128.75, 127.75, 127.69, 127.55, 127.30, 127.00, 125.02, 123.34, 121.28, 119.54, 115.76, 45.95, 42.75.

HRMS EI$^+$: *m/z* $[M + H]^+$ Calculated for $C_{24}H_{21}N_2O_3^+$ 385.1547 ; **found** 385.15437

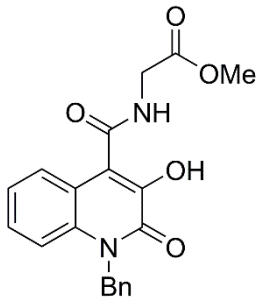

Compound **128** was obtained in 79% yield as grey pure solid

^{1}H NMR 1H NMR (300 MHz, $(CD_3)_2SO$) δ 9.96 (s, 1H), 9.07 (t, J = 5.6 Hz, 1H), 7.71 (d, J = 7.5 Hz, 1H), 7.44 – 7.20 (m, 9H), 5.63 (s, 2H), 4.08 (d, J = 5.8 Hz, 2H), 3.72 (s, 3H).

^{13}C NMR (75 MHz, $(CD_3)_2SO$) δ 170.62, 165.52, 158.99, 141.49, 136.88, 133.88, 129.16, 127.70, 127.59, 126.99, 125.44, 123.31, 120.86, 119.60, 115.65, 52.34, 45.96, 25.69;

LRMS (ESI): *m/z* $[M+H]^+$ 367;

Elemental analysis calculated (%) for: $C_{20}H_{18}N_2O_5$ + 0.5H_2O: C, 63,99; H, 5,10; N, 7.46,

found: C, 64.35; H, 5,00; N, 7.61.

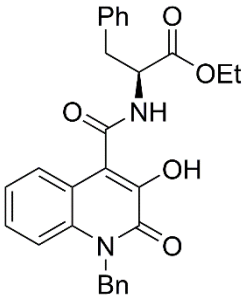

Compound **129** was obtained in 70% yield as grey pure solid

^{1}H NMR (300 MHz, DMSO) δ 12.45 (s, 1H), 9.28 (d, J = 5.7 Hz, 1H), 7.39 – 6.79 (m, 13H), 5.55 (s, 2H), 4.65 (s, 1H), 4.03 (s, 2H), 3.04 (s, 2H), 1.10 (s, 3H);

^{13}C NMR (75 MHz, DMSO) δ 172.93, 169.75, 164.25, 162.38, 137.98, 137.65, 129.91, 129.76, 128.97, 128.74, 127.28, 126.86, 124.98, 122.09, 121.71, 114.62, 60.45, 54.51, 46.23, 38.41, 14.51;

HRMS EI$^+$: *m/z* [M + H]$^+$Calculated for $C_{28}H_{27}N_2O_5$: 471,1914, **found** 471,19091

Elemental analysis calculated (%) for $C_{28}H_{26}N_2O_5$ + $2H_2O$: C, 66.39; H, 5.97; N, 5.53 **found**: C, 66.61; H, 5.16; N, 5.83

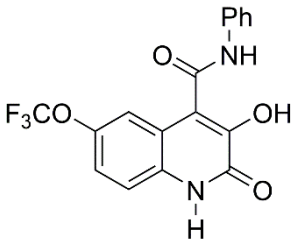

Compound **132** was obtained in 90% yield as grey pure solid;

^{1}H NMR (300 MHz, $(CD_3)_2SO$) δ 12.49 (s, 1H), 10.59 (s, 1H), 7.74 (d, J = 7.6 Hz, 2H), 7.47 – 7.29 (m, 5H), 7.13 (t, J = 7.4 Hz, 1H);

^{13}C NMR (75 MHz, $(CD_3)_2SO$) δ 162.47, 158.28, 143.93, 143.31, 138.82, 132.05, 128.92, 123.97, 121.87, 120.06, 119.72, 119.49, 119.14, 117.18, 115.54;

HRMS EI$^+$: *m/z* [M + H]$^+$ Calculated for $C_{17}H_{11}F_3N_2O_4^+$ 365,0744; **found** 365,07405

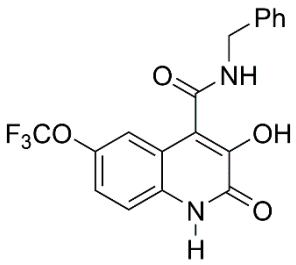

Compound **133** was obtained in 86% yield as grey pure solid;

^{1}H NMR (300 MHz, $(CD_3)_2SO$) δ 12.43 (s, 1H), 10.25 (s, 1H), 9.09 (t, J = 6.1 Hz, 1H), 7.50 – 7.18 (m, 8H), 4.51 (d, J = 6.0 Hz, 2H);

^{13}C NMR (75 MHz, $(CD_3)_2SO$) δ 163.90, 158.23, 143.54, 143.19, 139.20, 132.01, 128.28, 127.22, 126.89, 121.86, 119.96, 119.78, 119.39, 118.47, 117.04, 115.62:

LRMS (ESI): *m/z* $[M+H]^+$ 379;

Elemental analysis calculated (%) for $C_{18}H_{13}F_3N_2O_4$ + 1,50 H_2O: C, 53.34; H, 3.98; N, 6.91; **found**: C, 53.65; H, 3.64; N, 6.96;

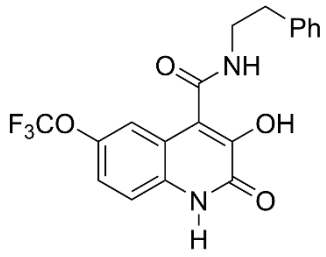

Compound **134** was obtained in 90% yield as grey pure solid;

^{1}H NMR (300 MHz, $(CD_3)_2SO$) δ 12.42 (s, 1H), 8.71 (d, J = 6.9 Hz, 1H), 7.42 (d, J = 8.9 Hz, 1H), 7.37 – 7.17 (m, 6H), 7.14 (d, J = 2.6 Hz, 1H), 3.54 (q, J = 6.8 Hz, 2H), 2.84 (t, J = 7.2 Hz, 2H).

^{13}C NMR (75 MHz, $(CD_3)_2SO$) δ 163.80, 158.35, 143.93, 143.13, 139.28, 131.85, 128.72, 128.27, 126.11, 121.87, 119.58, 119.49, 118.48, 116.88, 115.91, 35.06;

LRMS (ESI): *m/z* $[M+H]^+$ 393; 338.1; 142.9.

Elemental analysis calculated (%) for $C_{19}H_{15}F_3N_2O_4$ + H_2O: C, 55.61; H, 4.18; N, 6.83; **found**: C, 55.38; H, 3.84; N, 6.75;

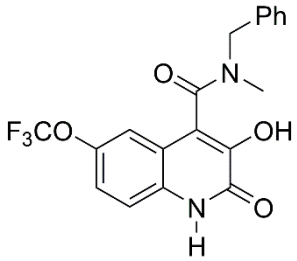

Compound **135** was obtained in 89% yield as grey pure solid;

^{1}H NMR mix of rotamers (300 MHz, $(CD_3)_2SO$) δ 12.45 (s, 0.61H), 12.45 (s, 0.39H), 10.47 (s, 0.35H), 10.45 (s, 0.65H), 7.49 – 7.04 (m, 8H), 4.77 (dd, J = 50.2, 14.8 Hz, 1.3H), 4.43 (dd, J = 35.2, 15.6 Hz, 0.70H), 2.94 (s, 1H), 2.80 (s, 2H).

^{13}C NMR: (75 MHz, $(CD_3)_2SO$) δ 170.12, 164.57, 143.17, 138.15, 128.55, 127.51, 126.84, 125.20, 124.85, 122.07, 118.69, 115.34, 111.93, 111.18, 110.92, 53.86, 49.29, 34.89, 31.80;

HRMS EI$^+$: *m/z* $[M + Na]^+$ Calculated for $C_{19}H_{15}F_3N_2NaO_4^+$ 415,0876; **found** 415,08725

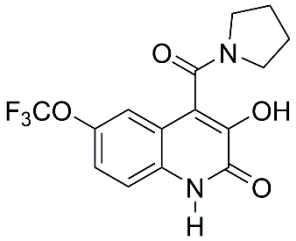

Compound **136** was obtained in 74% yield as grey pure solid;

^{1}H NMR (300 MHz, $(CD_3)_2SO$) δ 12.41 (s, 1H), 10.30 (s, 1H), 7.49 – 7.30 (m, 2H), 7.14 (s, 1H), 3.60-3.45 (m, 2H), 3.07 (dd, *J* = 10.5, 6.0 Hz, 2H), 1.99 – 1.60 (m, 4H).

^{13}C NMR (75 MHz, $(CD_3)_2SO$) δ 162.66, 158.13, 143.28, 142.59, 132.32, 121.86, 120.08, 118.71, 118.47, 117.07, 115.62, 46.24, 45.09, 25.29, 24.08.

HRMS EI$^+$: *m/z* [M + H]$^+$ Calculated for $C_{15}H_{14}F_3N_2O_4^+$ 343.0900; **found** 343.08973.

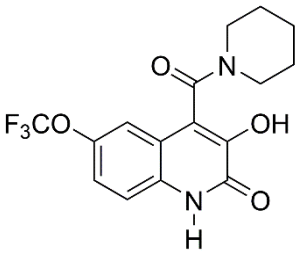

Compound **137** was obtained in 90% yield as grey pure solid;

^{1}H NMR (300 MHz, $(CD_3)_2SO$) δ 12.45 (s, 1H), 10.22 (s, 1H), 7.56 – 7.27 (m, 2H), 7.07 (s, 1H), 3.85 (d, J = 10.8 Hz, 1H), 3.49 (d, J = 12.1 Hz, 1H), 3.21 (br. s, 2H), 1.58 (br. s, 5H), 1.24 (br. s, 1H).

^{13}C NMR (75 MHz, $(CD_3)_2SO$) δ 162.59, 157.91, 143.20, 142.54, 132.38, 121.89, 120.05, 118.97, 118.90, 117.19, 115.30, 46.92, 41.61, 26.44, 25.54, 23.97.

HRMS EI$^+$: *m/z* [M + H]$^+$ Calculated for $C_{16}H_{16}F_3N_2O_4^+$ 357.1057; **found** 357.10538.

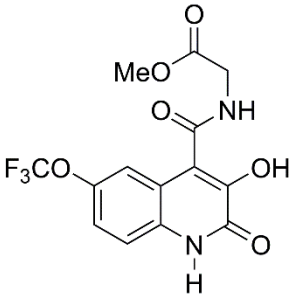

Compound **138** was obtained in 88% yield as grey pure solid;

^{1}H NMR (300 MHz, $(CD_3)_2SO$) δ 12.43 (s, 1H), 10.23 (s, 1H), 9.14 – 8.90 (m, 1H), 7.60 (m, 1H), 7.56 – 7.27 (m, 2H), 4.19 – 3.95 (m, 2H), 3.75 (s, 3H).

^{13}C NMR (75 MHz, $(CD_3)_2SO$) δ 170.05, 164.64, 158.13, 143.51, 143.25, 131.98, 121.90, 119.95, 119.45, 118.51, 116.87, 116.28, 51.82, 40.89.

HRMS EI$^-$: *m/z* $[M]^-$ Calculated for $C_{14}H_{10}F_3N_2O_6^-$ 359,0496; **found** 359,04977.

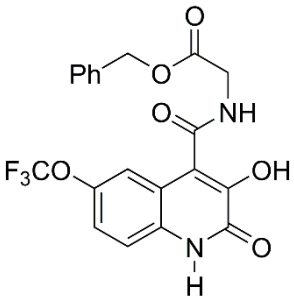

Compound **139** was obtained in 57% yield as grey pure solid;

^{1}H NMR (300 MHz, $(CD_3)_2SO$) δ 12.45 (s, 1H), 10.24 (s, 1H), 9.06 (t, J = 5.9 Hz, 1H), 7.63 (s, 1H), 7.44-7.33 (m, 7H), 5.21 (s, 2H), 4.12 (d, J = 5.8 Hz, 2H).

^{13}C NMR (75 MHz, $(CD_3)_2SO$) δ 169.57, 164.68, 158.15, 143.63, 143.28, 135.88, 131.96, 128.44, 128.12, 128.03, 121.90, 119.92, 119.45, 116.87, 116.35, 66.08, 41.00;

HRMS EI$^+$: ***m/z*** $[M + Na]^+$ Calculated for $C_{13}H_{17}NO_3Na$ 258.1101; **found** 258.1074

Elemental analysis calculated (%) for: $C_{20}H_{15}F_3N_2O_6 + 2H_2O$: C, 50.85; H, 4.05; N, 5.93; **found**:C, 50.40; H,3.74; N, 5.87.

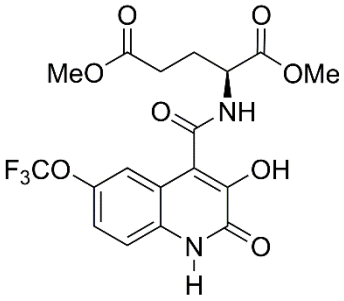

Compound **140** was obtained in 57% yield as grey pure solid;

^{1}H NMR (300 MHz, $(CD_3)_2SO$) δ 12.43 (s, 1H), 10.21 (s, 1H), 9.04 (d, J = 7.0 Hz, 1H), 7.59 – 7.27 (m, 3H), 4.48 (d, J = 2.4 Hz, 1H), 3.70 (s, 3H), 3.60 (s, 3H), 2.50 (2H, overlapped with solvent peaks), 2.18 – 1.81 (m, 2H).

^{13}C NMR (75 MHz, $(CD_3)_2SO$) δ 172.40, 171.53, 164.04, 157.90, 143.31, 142.97, 131.74, 119.75, 119.26, 119.17, 118.27, 116.67, 115.74, 51.76, 51.25, 51.19, 29.32, 25.33;

LRMS (ESI): *m/z* $[M+H]^+$ 446.8 ; 414.8; 347.8; 338.1; 142.9

Elemental analysis calculated (%) for: $C_{18}H_{17}F_3N_2O_8$ + H_2O: C, 44.82; H, 4.39; N, 5.81; O, 33.17; **found**: C, 44.44; H, 3.99; N, 6.05.

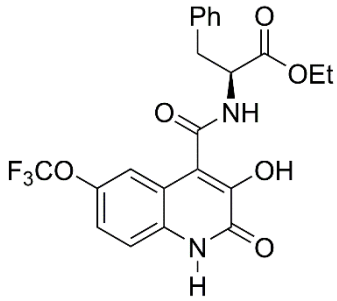

Compound **141** was obtained in 57% yield as grey pure solid;

^{1}H NMR (300 MHz, $(CD_3)_2SO$) δ 12.27 (d, J = 5.9 Hz, 1H), 11.58 (s, 1H), 9.21 (s, 1H), 7.39 – 7.07 (m, 7H), 6.86 (d, J = 6.8 Hz, 1H), 4.63 (q, J = 6.6 Hz, 1H), 4.01 (q, J = 6.9 Hz, 2H), 3.08 – 2.92 (m, 2H), 1.08 (t, J = 7.1 Hz, 3H).

^{13}C NMR (75 MHz, $(CD_3)_2SO$) δ 172.40, 169.28, 164.39, 163.01, 143.07, 137.43, 129.28, 128.28, 127.90, 126.48, 124.95, 115.88, 115.05, 113.28, 103.79, 60.06, 53.86, 37.95, 14.02;

HRMS EI$^+$: *(m/z)* [M+ Na]$^+$ Calculated for $C_{22}H_{19}F_3N_2NaO_6^+$ 487,1087; **found** 487,1082.

Elemental analysis calculated (%) for $C_{22}H_{19}F_3N_2O_6$ + $3H_2O$**:** C, 54.77; H, 4.39; N, 5.81; **found**: C, 54.51; H, 3.71; N, 6.18.

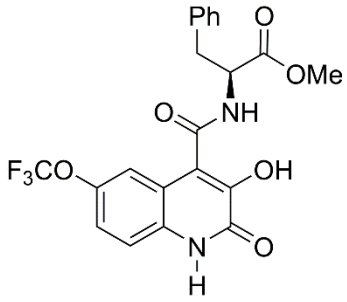

Compound **142** was obtained in 71% yield as grey pure solid;

^{1}H NMR (300 MHz, $(CD_3)_2SO$) δ 12.43 (d, J = 19.0 Hz, 1H), 9.13 (d, J = 7.4 Hz, 1H), 7.49 – 7.04 (m, 8H), 4.68 (ddd, J =9.5, 7.4, 5.3 Hz, 1H), 3.67 (s, 3H), 3.15-2.99 (m, 2H).

^{13}C NMR: (75 MHz, $(CD_3)_2SO$) δ 172.82, 171.72, 164.16, 158.16, 143.65, 143.15, 137.18, 131.90, 129.19, 128.25, 126.58, 119.84, 119.40, 116.80, 116.15, 53.99, 51.93, 36.35, 25.26.

LRMS (ESI): *m/z* [M+ Na]$^+$ 450.9; 419.1; 392.2; 338.17; 244.9.

Elemental analysis calculated (%) for: $C_{21}H_{17}F_3N_2O_6$ +0.5H_2O C, 54.91; H, 3.85; N, 6.10; **found**: C, 54.41; H, 3.75; N, 6.19

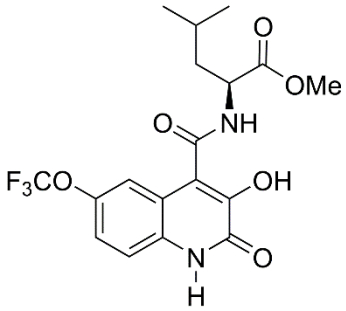

Compound **143** was obtained in 70% yield as grey solid;

^{1}H NMR (300 MHz, $(CD_3)_2SO$) δ 12.40 (s, 1H), 10.12 (s, 1H), 8.98 (s, 1H), 7.38 (s, 3H), 4.47 (s, 1H), 3.69 (s, 3H), 1.83 – 1.44 (m, 3H), 0.91 (s, 6H).

^{13}C NMR: (75 MHz, $(CD_3)_2SO$) δ 174.05, 169.40, 164.33, 163.13, 143.10, 127.95, 124.94, 122.12, 115.95, 115.18, 113.39, 103.91, 51.59, 50.13, 24.54;

LRMS (ESI): *m/z* [M+ Na]$^+$ 439**;** 416.9; 338.1; 142.9.

Elemental analysis calculated (%) for: $C_{18}H_{19}F_3N_2O_6$ + 0.5H_2O: C, 50.83; H, 4.74; N, 6.59; **found**: C, 49.46; H, 4.10; N, 6.25;

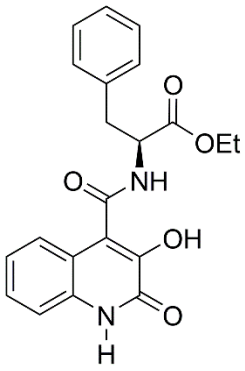

Compound **165** was obtained in 93% yield as grey solid;

^{1}H NMR (300 MHz $(CD_3)_2SO$) δ 12.03 (s, 1H), 9.71 (s, 1H), 7.60 – 6.82 (m, 33H), 4.86 – 4.50 (m, 3H), 4.09 (q J = 6.9 Hz, 2H), 3.04 (ddd, J = 22.8, 13.9, 7.6 Hz, 1H), 1.15 (t, J = 7.0 Hz, 11H).

^{13}C NMR: (75 MHz, $(CD_3)_2SO$) δ 171.66, 165.56, 160.02, 142.03, 137.36, 132.34, 129.37, 128.38, 126.62, 125.66, 124.12, 123.31, 122.08, 121.71, 119.50, 114.94, 60.64, 54.00, 14.08.

LRMS (ESI): *m/z* [M+ Na]$^+$ 403.69; 396,90; 193.88

Elemental analysis calculated (%) for: $C_{21}H_{20}N_2O_5$ + 0.5H_2O: C, 61.10; H, 5.76; N, 6.79; **found**: C, 60.87; H, 5.56; N, 6.65;

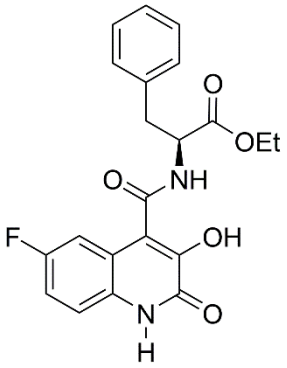

Compound **166** was obtained in 84% yield as grey solid;

^{1}H NMR (300 MHz, $(CD_3)_2SO$) δ 12.09 (s, 1H), 9.83 (s, 1H), 7.67 – 7.16 (m, 36H), 7.08 (t, J = 7.0 Hz, 4H), 4.65 (dd, J = 14.1, 7.7 Hz, 2H), 4.10 (q, J = 7.0 Hz, 2H), 3.04 (ddd, J = 22.8, 13.8, 7.5 Hz, 1H), 1.21 (t, J = 7.0 Hz, 3H)

^{13}C NMR: (75 MHz, $(CD_3)_2SO$) 13C NMR (75 MHz, DMSO) δ 172.00, 169.59, 164.21 (d, J = 248 Hz), 159.61, 156.42, 137.69, 130.03, 129.69, 128.69, 127.65, 127.01, 120.31, 119.43, 108.29, 106.24, 61.03, 54.43, 37.17, 14.57.

LRMS (ESI): *m/z* $[M+ H]^+$ 399.3

Elemental analysis calculated (%) for: $C_{21}H_{19}FN_2O_5$ + $0.7H_2O$: C, 61.37; H, 5.00; N, 6.82; **found**: C, 61.06; H, 5.09; N, 7.21;

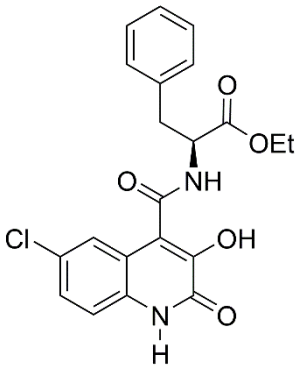

Compound **167** was obtained in 87% yield as grey solid;

^{1}H NMR (300 MHz, $(CD_3)_2SO$) δ 12.31 (s, 1H), 9.10 (s, 1H), 7.46 – 7.10 (m, 8H), 4.63 (q, J = 14.2, 8.0 Hz, 6H), 4.12 (q, J = 7.0 Hz, 2H), 3.04 (ddd, J = 23.1, 13.9, 7.6 Hz, 2H), 1.17 (t, J = 7.1 Hz, 3H).

^{13}C NMR: (75 MHz, $(CD_3)_2SO$) δ 171.60, 164.51, 164.47, 158.42, 143.73, 137.49, 132.07, 129.54, 128.60, 126.98, 126.84, 126.73, 123.22, 120.18, 119.57, 117.28, 61.06, 54.44, 14.36

LRMS (ESI): *m/z* $[M+ Na]^+$: 436,62;380.75; 193.88

Elemental analysis calculated (%) for: $C_{21}H_{19}ClN_2O_5$ + $1.1H_2O$: C, 58.03; H, 4.92; N, 6.45; **found**: C, 58.24; H, 4.87; N, 6.25;

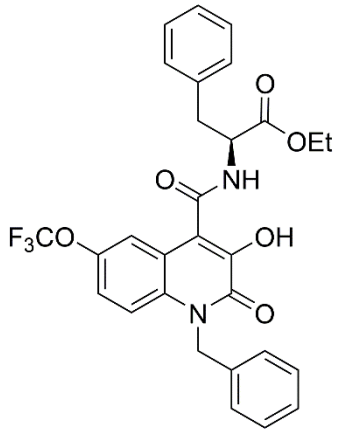

Compound **169** was obtained in 80% yield as grey solid;

^{1}H NMR (300 MHz, DMSO) δ 10.32 (s, 1H), 9.25 (s, 1H), 7.48 (d, *J* = 9.3 Hz, 1H), 7.38 – 7.07 (m, 12H), 5.63 (q, *J* = 16.2 Hz, 2H), 4.67 (dd, *J* = 14.7, 7.5 Hz, 1H), 4.12 (q, *J* = 7.1 Hz, 2H), 3.06 (ddd, *J* = 23.1, 13.9, 7.5 Hz, 2H), 1.17 (t, *J* = 7.1 Hz, 3H).

^{13}C NMR: (75 MHz, $(CD_3)_2SO$) δ 172.05, 169.40, 164.33, 163.13, 143.65, 143.15, 137.18, 131.90 130.10, 129.72, 129.15, 128.27, 127.36; 127.95, 124.94, 122.12, 115.95, 115.18, 113.39, 103.91, 77,11, 76. 54.99, 14.37

HRMS EI$^+$: *m/z* [M + Na]$^+$ Calculated for $C_{29}H_{26}F_3N_2NaO_6^+$ 555,1737; **found** 555,17270

Chapter VII

VII. References

1. Doweyko, A. M.; Doweyko, L. M. What is next for small-molecule drug discovery? *Future Medicinal Chemistry* **2009,** 1, 1029-1036.

2. Pharmaceuticals, B. Small and large molecules.

3. Cunningham, K. G.; Freeman, G. G. The Isolation and Some Chemical Properties of Viridicatin, a Metabolic Product of Penicillium-Viridicatum Westling. *Biochemical Journal* **1953,** 53, 328-332.

4. Luckner, M.; Mothes, K. On the Biosynthesis of 2,3-Dihydroxy-4-Phenyl-Quinoline (Viridicatin). *Tetrahedron Letters* **1962**, 1035-1039.

5. Heguy, A.; Cai, P.; Meyn, P.; Houck, D.; Russo, S.; Michitsch, R.; Pearce, C.; Katz, B.; Bringmann, G.; Feineis, D.; Taylor, D.; Tyms, A. Isolation and Characterization of the Fungal Metabolite 3-O-Methylviridicatin as an Inhibitor of Tumour Necrosis Factor α-Induced Human Immunodeficiency Virus Replication. *Antiviral Chemistry and Chemotherapy* **1998,** 9, 149-155.

6. Ribeiro, N.; Tabaka, H.; Peluso, J.; Fetzer, L.; Nebigil, C.; Dumont, S.; Muller, C. D.; Desaubry, L. Synthesis of 3-O-methylviridicatin analogues with improved anti-TNF-alpha properties. *Bioorganic & Medicinal Chemistry Letters* **2007,** 17, 5523-5524.

7. Ballatore, C.; Huryn, D. M.; Smith, A. B. Carboxylic Acid (Bio)Isosteres in Drug Design. *Chemmedchem* **2013,** 8, 385-395.

8. Poulie, C. B. M.; Bunch, L. Heterocycles as Nonclassical Bioisosteres of alpha-Amino Acids. *Chemmedchem* **2013,** 8, 205-215.

9. Duplantier, A. J.; Becker, S. L.; Bohanon, M. J.; Borzilleri, K. A.; Chrunyk, B. A.; Downs, J. T.; Hu, L. Y.; El-Kattan, A.; James, L. C.; Liu, S. P.; Lu, J. M.; Maklad, N.; Mansour, M. N.; Mente, S.; Piotrowski, M. A.; Sakya, S. M.; Sheehan, S.; Steyn, S. J.; Strick, C. A.; Williams, V. A.; Zhang, L. Discovery, SAR, and Pharmacokinetics of a Novel 3-Hydroxyquinolin-2(1H)-one Series of Potent D-Amino Acid Oxidase (DAAO) Inhibitors. *Journal of Medicinal Chemistry* **2009,** 52, 3576-3585.

10. Strashnova, S. B.; Kovalchukova, O. V.; Zaitsev, B. E.; Stash, A. I. Complexation of 2,3-dihydroxyquinaline with some bivalent d metals. Crystal and molecular structures of 2,3-dihydroxyquinoline. *Russian Journal of Coordination Chemistry* **2008,** 34, 775-779.

11. Quin, L. D.; Tyrell, J. A. Fundamentals of heterocyclic chemistry: importance in nature and in the synthesis of pharmaceuticals. John Wiley & Sons: 2010.

12. Larsen, R. D. Product class 4: quinolinones and related systems. *Science of Synthesis* **2005,** 15, 551–660

13. Albert, A.; Phillips, J. N. Ionization Constants of Heterocylic Substances .2. Hydroxy-Derivatives of Nitrogenous Six-Membered Ring-Compounds. *Journal of the Chemical Society* **1956**, 1294-1304.

14. Mason, S. F. The Tautomerism of N-Heteroaromatic Hydroxy-Compounds .1. Infrared Spectra. *Journal of the Chemical Society* **1957**, 4874-4880.

15. Michael, J. P. Quinoline, quinazoline and acridone alkaloids. *Natural Product Reports* **2001,** 18, 543-559.

16. Michael, J. P. Quinoline, quinazoline and acridone alkaloids. *Natural Product Reports* **2000,** 17, 603-620.

17. Michael, J. P. Quinoline, quinazoline and acridone alkaloids. *Natural Product Reports* **1999,** 16, 697-709.

18. Michael, J. P. Quinoline, quinazoline and acridone alkaloids. *Natural Product Reports* **1997,** 14, 605-618.

19. Abou-Raya, A.; Abou-Raya, S.; Sallam, N.; Helmii, M. Rebamipide in the Treatment of Xerostomia in Sjogren's Syndrome: Randomized Placebo-Controlled Study. *Annals of the Rheumatic Diseases* **2012,** 71, 212-212.

20. Takagi, K.; Hasegawa, T.; Ogura, Y.; Suzuki, R.; Yamaki, K.; Watanabe, T.; Kitazawa, S.; Satake, T. Comparative Studies on Interaction between Theophylline and Quinolones. *Journal of Asthma* **1988,** 25, 63-71.

21. Al-Amiery, A. A.; Al-Bayati, R. I. H.; Saour, K. Y.; Radi, M. F. Cytotoxicity, antioxidant, and antimicrobial activities of novel 2-quinolone derivatives derived from coumarin. *Research on Chemical Intermediates* **2012,** 38, 559-569.

22. Hewawasam, P.; Erway, M.; Moon, S. L.; Knipe, J.; Weiner, H.; Boissard, C. G.; Post-Munson, D. J.; Gao, Q.; Huang, S.; Gribkoff, V. K.; Meanwell, N. A. Synthesis and structure-activity relationships of 3-aryloxindoles: A new class of calcium-dependent, large conductance potassium (maxi-K) channel openers with neuroprotective properties. *Journal of Medicinal Chemistry* **2002,** 45, 1487-1499.

23. Hewawasam, P.; Fan, W. H.; Knipe, J.; Moon, S. L.; Boissard, C. G.; Gribkoff, V. K.; Starrett, J. E. The synthesis and structure-activity relationships of 4-aryl-3-aminoquinolin-2-ones: A new class of calcium-dependent, large conductance, potassium (maxi-K) channel openers targeted for post-stroke neuroprotection. *Bioorganic & Medicinal Chemistry Letters* **2002,** 12, 1779-1783.

24. Cappelli, A.; Pericot Mohr, G. l.; Gallelli, A.; Rizzo, M.; Anzini, M.; Vomero, S.; Mennuni, L.; Ferrari, F.; Makovec, F.; Menziani, M. C.; De Benedetti, P. G.; Giorgi, G. Design, Synthesis, Structural Studies, Biological Evaluation, and Computational Simulations of Novel Potent AT1 Angiotensin II Receptor Antagonists Based on the 4-Phenylquinoline Structure. *Journal of Medicinal Chemistry* **2004,** 47, 2574-2586.

25. Hewawasam, P.; Fan, W.; Ding, M.; Flint, K.; Cook, D.; Goggins, G. D.; Myers, R. A.; Gribkoff, V. K.; Boissard, C. G.; Dworetzky, S. I.; Starrett, J. E.; Lodge, N. J. 4-Aryl-3-(hydroxyalkyl)quinolin-2-ones: Novel Maxi-K Channel Opening Relaxants of Corporal Smooth Muscle Targeted for Erectile Dysfunction. *Journal of Medicinal Chemistry* **2003,** 46, 2819-2822.

26. Fang, Y. Q.; Karisch, R.; Lautens, M. Efficient syntheses of KDR kinase inhibitors using a Pd-catalyzed tandem C-N/Suzuki coupling as the key step. *Journal of Organic Chemistry* **2007,** 72, 1341-1346.

27. Angibaud, P. R.; Venet, M. G.; Filliers, W.; Broeckx, R.; Ligny, Y. A.; Muller, P.; Poncelet, V. S.; End, D. W. Synthesis routes towards the farnesyl protein transferase inhibitor ZARNESTRA (TM). *European Journal of Organic Chemistry* **2004**, 479-486.

28. Audisio, D.; Messaoudi, S.; Cegielkowski, L.; Peyrat, J. F.; Brion, J. D.; Methy-Gonnot, D.; Radanyi, C.; Renoir, J. M.; Alami, M. Discovery and Biological Activity of 6BrCaQ as an Inhibitor of the Hsp90 Protein Folding Machinery. *Chemmedchem* **2011,** 6, 804-815.

29. Cordi, A. A.; Desos, P.; Randle, J. C. R.; Lepagnol, J. Structure-Activity-Relationships in a Series of 3-Sulfonylamino-2-(1h)-Quinolones, as New Ampa Kainate and Glycine Antagonists. *Bioorganic & Medicinal Chemistry* **1995,** 3, 129-141.

30. Desos, P.; Lepagnol, J. M.; Morain, P.; Lestage, P.; Cordi, A. A. Structure-activity relationships in a series of 2(1H)-quinolones bearing different acidic function in the 3-position: 6,7-Dichloro-2(1H)-oxoquinoline-3-phosphonic acid, a new potent and selective AMPA/kainate antagonist with neuroprotective properties. *Journal of Medicinal Chemistry* **1996,** 39, 197-206.

31. Hewawasam, P.; Chen, N.; Ding, M.; Natale, J. T.; Boissard, C. G.; Yeola, S.; Gribkoff, V. K.; Starrett, J.; Dworetzky, S. I. The synthesis and structure-activity relationships of 3-amino-4-benzylquinolin-2-ones: discovery of novel KCNQ2 channel openers. *Bioorganic & Medicinal Chemistry Letters* **2004,** 14, 1615-1618.

32. Iyengar, J. S.; Nayak, Y. 2-Quinolones for antibacterial and antioxidant activity - A docking study. *Nitric Oxide-Biology and Chemistry* **2008,** 19, S50-S50.

33. Kudur, M. H.; Hulmani, M. Rebamipide: A Novel Agent in the Treatment of Recurrent Aphthous Ulcer and Behcet's Syndrome. *Indian Journal of Dermatology* **2013,** 58, 352-354.

34. Marcaccini, S.; Pepino, R.; Pozo, M. C.; Basurto, S.; Maria, G. V. B.; Torroba, T. One-pot synthesis of quinolin-2-(1H)-ones via tandem Ugi-Knoevenagel condensations. *Tetrahedron Letters* **2004,** 45, 3999-4001.

35. Mederski, W. W. K. R.; Osswald, M.; Dorsch, D.; Christadler, M.; Schmitges, C. J.; Wilm, C. 1,4-diaryl-2-oxo-1,2-dihyrdo-quinoline-3-carboxylic acids as endothelin receptor antagonists. *Bioorganic & Medicinal Chemistry Letters* **1997,** 7, 1883-1886.

36. Mitsos, C. A.; Zografos, A. L.; Igglessi-Markopoulou, O. An efficient route to 3-aryl-substituted quinolin-2-one and 1,8-naphthyridin-2-one derivatives of pharmaceutical interest. *J Org Chem* **2003,** 68, 4567-9.

37. Raitio, K. H.; Savinainen, J. R.; Vepsalainen, J.; Laitinen, J. T.; Poso, A.; Jarvinen, T.; Nevalainen, T. Synthesis and SAR studies of 2-oxoquinoline derivatives as CB2 receptor inverse agonists. *Journal of Medicinal Chemistry* **2006,** 49, 2022-2027.

38. Rekhter, M. A.; Radul, O. M.; Zhungietu, G. I.; Bukhanyuk, S. M. Synthesis of 2-quinolones from isatins and diketene. *Khimiya Geterotsiklicheskikh Soedinenii* **1998**, 1427-1429.

39. Takagi, K.; Kuzuya, T.; Horiuchi, T.; Nadai, M.; Apichartpichean, R.; Ogura, Y.; Hasegawa, T. Lack of Effect of Repirinast on the Pharmacokinetics of Theophylline in Asthmatic-Patients. *European Journal of Clinical Pharmacology* **1989,** 37, 301-303.

40. Yamada, N.; Kadowaki, S.; Takahashi, K.; Umezu, K. MY-1250, a major metabolite of the anti-allergic drug repirinast, induces phosphorylation of a 78-kDa protein in rat mast cells. *Biochemical Pharmacology* **1992,** 44, 1211-1213.

41. Yancopoulos, G. D.; Davis, S.; Gale, N. W.; Rudge, J. S.; Wiegand, S. J.; Holash, J. Vascular-specific growth factors and blood vessel formation. *Nature* **2000,** 407, 242-248.

42. Zhong, W.; Liu, H.; Kaller, M. R.; Henley, C.; Magal, E.; Nguyen, T.; Osslund, T. D.; Powers, D.; Rzasa, R. M.; Wang, H.-L.; Wang, W.; Xiong, X.; Zhang, J.; Norman, M. H. Design and synthesis of quinolin-2(1H)-

one derivatives as potent CDK5 inhibitors. *Bioorganic & Medicinal Chemistry Letters* **2007,** 17, 5384-5389.

43. McCormick, J. L.; McKee, T. C.; Cardellina, J. H.; Boyd, M. R. HIV Inhibitory Natural Products. 26. Quinoline Alkaloids from Euodia roxburghiana. *Journal of Natural Products* **1996,** 59, 469-471.

44. Mitscher, L. A.; Gracey, H. E.; Clark, G. W.; Suzuki, T. Quinolone Anti-Microbial Agents .1. Versatile New Synthesis of 1-Alkyl-1,4-Dihydro-4-Oxo-3-Quinolinecarboxylic Acids. *Journal of Medicinal Chemistry* **1978,** 21, 485-489.

45. Kesten, S. J.; Degnan, M. J.; Hung, J. L.; Mcnamara, D. J.; Ortwine, D. F.; Uhlendorf, S. E.; Werbel, L. M. Antimalarial-Drugs .64. Synthesis and Antimalarial Properties of 1-Imino Derivatives of 7-Chloro-3-Substituted-3,4-Dihydro-1,9(2h,10h)-Acridinediones and Related Structures. *Journal of Medicinal Chemistry* **1992,** 35, 3429-3447.

46. Malamas, M. S.; Millen, J. Quinazolineacetic Acids and Related Analogs as Aldose Reductase Inhibitors. *Journal of Medicinal Chemistry* **1991,** 34, 1492-1503.

47. Rowley, M.; Leeson, P. D.; Stevenson, G. I.; Moseley, A. M.; Stansfield, I.; Sanderson, I.; Robinson, L.; Baker, R.; Kemp, J. A.; Marshall, G. R.; Foster, A. C.; Grimwood, S.; Tricklebank, M. D.; Saywell, K. L. 3-Acyl-4-Hydroxyquinolin-2(1h)-Ones - Systemically Active Anticonvulsants Acting by Antagonism at the Glycine Site of the N-Methl-D-Aspartate Receptor Complex. *Journal of Medicinal Chemistry* **1993,** 36, 3386-3396.

48. Tedesco, R.; Shaw, A. N.; Bambal, R.; Chai, D. P.; Concha, N. O.; Darcy, M. G.; Dhanak, D.; Fitch, D. M.; Gates, A.; Gerhardt, W. G.; Halegoua, D. L.; Han, C.; Hofmann, G. A.; Johnston, V. K.; Kaura, A. C.; Liu, N. N.; Keenan, R. M.; Lin-Goerke, J.; Sarisky, R. T.; Wiggall, K. J.; Zimmerman, M. N.; Duffy, K. J. 3-(1,1-Dioxo-2H-(1,2,4)-benzothiadiazin-3-yl)-4-hydroxy-2(1H)-quinolinones, potent inhibitors of hepatitis C virus RNA-dependent RNA polymerase. *Journal of Medicinal Chemistry* **2006,** 49, 971-983.

49. Andersen, O.; Lycke, J.; Tollesson, P. O.; Svenningsson, A.; Runmarker, B.; Linde, A. S.; Astrom, M.; Gjorstrup, P.; Ekholm, S. Linomide reduces the rate of active lesions in relapsing-remitting multiple sclerosis. *Neurology* **1996,** 47, 895-900.

50. Karussis, D.; Lehmann, D.; Ovadia, H.; MizrachiKoll, R.; Gjorstup, P.; Linde, A.; Astrom, M.; Abramsky, O. Immunological evaluation in patients with secondary progressive multiple sclerosis treated with linomide. *Neurology* **1996,** 46, 3088-3088.

51. Shia, J. D.; Xiao, Z. L.; Ihnat, M. A.; Kamat, C.; Pandit, B.; Hu, Z. G.; Li, P. K. Structure-activity relationships studies of the anti-angiogenic activities of linomide. *Bioorganic & Medicinal Chemistry Letters* **2003,** 13, 1187-1189.

52. Vukanovic, J.; Isaacs, J. T. Linomide Inhibits Angiogenesis, Growth, Metastasis, and Macrophage Infiltration within Rat Prostatic Cancers. *Cancer Research* **1995,** 55, 1499-1504.

53. Vukanovic, J.; Passaniti, A.; Hirata, T.; Traystman, R. J.; Hartleyasp, B.; Isaacs, J. T. Antiangiogenic Effects of the Quinoline-3-Carboxamide Linomide. *Cancer Research* **1993,** 53, 1833-1837.

54. Karussis, D. M.; Lehmann, D.; Slavin, S.; Vourka-Karussis, U.; Mizrachi-Koll, R.; Ovadia, H.; Ben-Nun, A.; Kalland, T.; Abramsky, O. Inhibition of acute, experimental autoimmune encephalomyelitis by the synthetic immunomodulator linomide. *Annals of Neurology* **1993,** 34, 654-660.

55. Isaacs, J. T.; Pili, R.; Qian, D. Z.; Dalrymple, S. L.; Garrison, J. B.; Kyprianou, N.; Bjork, A.; Olsson, A.; Leanderson, T. Identification of ABR-215050 as lead second generation quinoline-3-carboxamide anti-angiogenic agent for the treatment of prostate cancer. *Prostate* **2006,** 66, 1768-78.

56. Karussis, D. M.; Lehmann, D.; Slavin, S.; Vourkakarussis, U.; Mizrachikoll, R.; Ovadia, H.; Kalland, T.; Abramsky, O. Treatment of Chronic-Relapsing Experimental Autoimmune Encephalomyelitis with the Synthetic Immunomodulator Linomide (Quinoline-3-Carboxamide). *Proceedings of the National Academy of Sciences of the United States of America* **1993,** 90, 6400-6404.

57. Diab, A.; Michael, L.; Wahren, B.; Deng, G. M.; Bjork, J.; Hedlund, G.; Zhu, J. Linomide suppresses acute experimental autoimmune encephalomyelitis in Lewis rats by counter-acting the imbalance of pro-inflammatory versus anti-inflammatory cytokines. *Journal of Neuroimmunology* **1998,** 85, 146-154.

58. Tian, W. Z.; Navikas, V.; Matusevicius, D.; Soderstrom, M.; Fredrikson, S.; Hedlund, G.; Link, H. Linomide (roquinimex) affects the balance between pro- and anti-inflammatory cytokines in vitro in multiple sclerosis. *Acta Neurologica Scandinavica* **1998,** 98, 94-101.

59. Wolinsky, J. S.; Narayana, P. A.; Noseworthy, J. H.; Lublin, F. D.; Whitaker, J. N.; Linde, A.; Gjorstrup, P.; Sullivan, H. C.; Texas-Houston, U.; Investigators, N. A. L. Linomide in relapsing and secondary progressive MS - Part II: MRI results. *Neurology* **2000,** 54, 1734-1741.

60. Noseworthy, J. H.; Wolinsky, J. S.; Lublin, F. D.; Whitaker, J. N.; Linde, A.; Gjorstrup, P.; Sullivan, H. C.; Investigators, N. A. L. Linomide in relapsing and secondary progressive MS - Part I: Trial design and clinical results. *Neurology* **2000,** 54, 1726-1733.

61. Jonsson, S.; Andersson, G.; Fex, T.; Fristedt, T.; Hedlund, G.; Jansson, K.; Abramo, L.; Fritzson, I.; Pekarski, O.; Runstrom, A.; Sandin, H.; Thuvesson, I.; Bjork, A. Synthesis and biological evaluation of new 1,2-dihydro-4-hydroxy-2-oxo-3-quinolinecarboxamides for treatment of autoimmune disorders: Structure-activity relationship. *Journal of Medicinal Chemistry* **2004,** 47, 2075-2088.

62. Burke, M. D.; Schreiber, S. L. A Planning Strategy for Diversity-Oriented Synthesis. *Angewandte Chemie International Edition* **2004,** 43, 46-58.

63. Schreiber, S. L. Target-Oriented and Diversity-Oriented Organic Synthesis in Drug Discovery. *Science* **2000,** 287, 1964.

64. Bagdi, A. K.; Hajra, A. Brønsted acidic ionic liquid catalyzed tandem reaction of 4-hydroxy-1-methyl-2-quinolone with chalcone: regioselective synthesis of pyrano[3,2-c]quinolin-2-ones. *RSC Advances* **2014,** 4, 23287.

65. Kulkarni, B. A.; Ganesan, A. Solution-phase combinatorial synthesis of 4-hydroxyquinolin-2(1H)-ones. *Chemical Communications* **1998**, 785-786.

66. Kutyrev, A.; Kappe, T. Methanetricarboxylates as key reagents for the simple preparation of heteroarylcarboxamides with potential biological activity .1. Reaction of methanetricarboxylates with indoline and 1,2,3,4-tetrahydroquinoline. *Journal of Heterocyclic Chemistry* **1997,** 34, 969-972.

67. Kappe, T.; Karem, A. S.; Stadlbauer, W. Synthesis of Benzo-Halogenated 4-Hydroxy-2(1h)-Quinolones. *Journal of Heterocyclic Chemistry* **1988,** 25, 857-862.

68. Coppola, G. M.; Hardtmann, G. E. The chemistry of 2H-3,1-benzoxazine-2,4(1H)dione (isatoic anhydride). 7. Reactions with anions of active methylenes to form quinolines. *Journal of Heterocyclic Chemistry* **1979,** 16, 1605-1610.

69. Beutner, G. L.; Kuethe, J. T.; Yasuda, N. A practical method for preparation of 4-hydroxyquinolinone esters. *Journal of Organic Chemistry* **2007,** 72, 7058-7061.

70. Austin, D. J.; Meyers, M. B. 3-0-Methylviridicatin New Metabolite from Penicillium Puberulum. *Journal of the Chemical Society* **1964**, 1197-&.

71. Rogolino, D.; Carcelli, M.; Sechi, M.; Neamati, N. Viral enzymes containing magnesium: Metal binding as a successful strategy in drug design. *Coordination Chemistry Reviews* **2012,** 256, 3063-3086.

72. Suchaud, V.; Bailly, F.; Lion, C.; Tramontano, E.; Esposito, F.; Corona, A.; Christ, F.; Debyser, Z.; Cotelle, P. Development of a series of 3-hydroxyquinolin-2(1H)-ones as selective inhibitors of HIV-1 reverse transcriptase associated RNase H activity. *Bioorganic & Medicinal Chemistry Letters* **2012,** 22, 3988-3992.

73. Sagong, H. Y.; Parhi, A.; Bauman, J. D.; Patel, D.; Vijayan, R. S. K.; Das, K.; Arnod, E.; LaVoie, E. J. 3-Hydroxyquinolin-2(1H)-ones As Inhibitors of Influenza A Endonuclease. *Acs Medicinal Chemistry Letters* **2013,** 4, 547-550.

74. Furukawa, H.; Singh, S. K.; Mancusso, R.; Gouaux, E. Subunit arrangement and function in NMDA receptors. *Nature* **2005,** 438, 185-192.

75. Kemp, J. A.; McKernan, R. M. NMDA receptor pathways as drug targets. *Nature Neuroscience* **2002,** 5, 1039-1042.

76. Meldrum, B. S. Glutamate as a neurotransmitter in the brain: Review of physiology and pathology. *Journal of Nutrition* **2000,** 130, 1007s-1015s.

77. Sit, S. Y.; Ehrgott, F. J.; Gao, J. N.; Meanwell, N. A. 3-hydroxy-quinolin-2-ones: Inhibitors of [H-3]-glycine binding to the site associated with the NMDA receptor. *Bioorganic & Medicinal Chemistry Letters* **1996,** 6, 499-504.

78. Kawazoe, T.; Park, H. K.; Iwana, S.; Tsuge, H.; Fukui, K. Human D-amino acid oxidase: an update and review. *Chemical Record* **2007,** 7, 305-315.

79. Thornber, C. W. Isosterism and Molecular Modification in Drug Design. *Chemical Society Reviews* **1979,** 8, 563-580.

80. Lima, L. M. A.; Barreiro, E. J. Bioisosterism: A useful strategy for molecular modification and drug design. *Current Medicinal Chemistry* **2005,** 12, 23-49.

81. Olesen, P. H. The use of bioisosteric groups in lead optimization. *Current opinion in drug discovery & development* **2001,** 4, 471-8.

82. Huntress, E. H.; Bornstein, J.; Hearon, W. M. An Extension of the Diels-Reese Reaction. *Journal of the American Chemical Society* **1956,** 78, 2225-2228.

83. Bergman, J.; Brimert, T. Synthesis of 5-and 7-nitro-3-hydroxyquinolin-2-ones. *Acta Chemica Scandinavica* **1999,** 53, 616-619.

84. White, J. D.; Dimsdale, M. J. Conversion of Cyclopenin into Viridicatin. *Journal of the Chemical Society D-Chemical Communications* **1969**, 1285-&.

85. Terada, A.; Yabe, Y.; Miyadera, T.; Tachikaw.R. Studies on Benzodiazepinooxazoles .4. Formation of Quinolones by Ring Contraction of a Benzo[6,7]-1,4-Diazepino[5,4-B]-Oxazole Derivative. *Chemical & Pharmaceutical Bulletin* **1973,** 21, 807-810.

86. Arshad, N.; Hashim, J.; Kappe, C. O. Synthesis of bisquinolone-based mono- and diphosphine ligands of the aza-BINAP type. *Journal of Organic Chemistry* **2008,** 73, 4755-4758.

87. Kobayashi, Y.; Harayama, T. A Concise and Versatile Synthesis of Viridicatin Alkaloids from Cyanoacetanilides. *Organic Letters* **2009,** 11, 1603-1606.

88. Yuan, Y. C.; Yang, R.; Zhang-Negrerie, D.; Wang, J. W.; Du, Y. F.; Zhao, K. One-Pot Synthesis of 3-Hydroxyquinolin-2(1H)-ones from N-Phenylacetoacetamide via PhI(OCOCF3)(2)-Mediated alpha-Hydroxylation and H2SO4-Promoted Intramolecular Cyclization. *Journal of Organic Chemistry* **2013,** 78, 5385-5392.

89. Candeias, N. R.; Paterna, R.; Gois, P. M. P. Homologation Reaction of Ketones with Diazo Compounds. *Chemical Reviews* **2016,** 116, 2937-2981.

90. Eistert, B.; Selzer, H. Umsetzungen einiger Diazoalkane mit Isatin, N-Methyl-isatin, Cumarandion und Thionaphthenchinon. *Chemische Berichte* **1963,** 96, 1234-1255.

91. Eistert, B.; Borggrefe, G.; Selzer, H. Synthesen von N-Hydroxy-carbostyrilen. *Justus Liebigs Annalen der Chemie* **1969,** 725, 37-51.

92. Gioiello, A.; Venturoni, F.; Marinozzi, M.; Natalini, B.; Pellicciari, R. Exploring the Synthetic Versatility of the Lewis Acid Induced Decomposition Reaction of alpha-Diazo-beta-hydroxy Esters. The Case of Ethyl Diazo(3-hydroxy-2-oxo-2,3-dihydro-1H-indol-3-yl)acetate. *Journal of Organic Chemistry* **2011,** 76, 7431-7437.

93. Beller, M.; Bolm, C. *Transition Metals for Organic Synthesis*. 2004; Vol. 1.

94. Rueping, M.; Koenigs, R. M.; Atodiresei, I. Unifying Metal and Bronsted Acid Catalysis-Concepts, Mechanisms, and Classifications. *Chemistry-a European Journal* **2010,** 16, 9350-9365.

95. Bertelsen, S.; Jorgensen, K. A. Organocatalysis--after the gold rush. *Chemical Society Reviews* **2009,** 38, 2178-89.

96. Dalko, P. I.; Moisan, L. In the golden age of organocatalysis. *Angewandte Chemie-International Edition* **2004,** 43, 5138-5175.

97. Chen, D.-F.; Han, Z.-Y.; Zhou, X.-L.; Gong, L.-Z. Asymmetric Organocatalysis Combined with Metal Catalysis: Concept, Proof of Concept, and Beyond. *Accounts of Chemical Research* **2014,** 47, 2365-2377.

98. Du, Z.; Shao, Z. Combining transition metal catalysis and organocatalysis - an update. *Chemical Society Reviews* **2013,** 42, 1337-1378.

99. Du, Z. T.; Shao, Z. H. Combining transition metal catalysis and organocatalysis - an update. *Chemical Society Reviews* **2013,** 42, 1337-1378.

100. Shao, Z.; Zhang, H. Combining transition metal catalysis and organocatalysis: a broad new concept for catalysis. *Chemical Society Reviews* **2009,** 38, 2745-2755.

101. Candeias, N. R.; Gois, P. M. P.; Afonso, C. A. M. Rh(II) catalysed intramolecular C-H insertion of diazo substrates in water: a simple and efficient approach to catalyst reuse. *Chemical Communications* **2005**, 391-393.

102. Candeias, N. R.; Gois, P. M. P.; Afonso, C. A. M. Rh(II)-catalyzed intramolecular C-H insertion of diazo substrates in water: Scope and limitations. *Journal Of Organic Chemistry* **2006,** 71, 5489-5497.

103. Gois, P. M. P.; Afonso, C. A. M. Regio- and stereoselective dirhodium(II)-catalysed intramolecular C-H insertion reactions of alpha-diazo-alpha-(dialkoxyphosphoryl)acetamides and -acetates. *European Journal of Organic Chemistry* **2003**, 3798-3810.

104. Gois, P. M. P.; Afonso, C. A. M. Dirhodium(II)-catalysed C-H insertion on alpha-diazo-alpha-phosphono-acetamides in an ionic liquid. *Tetrahedron Letters* **2003,** 44, 6571-6573.

105. Gois, P. M. P.; Candeias, N. R.; Afonso, C. A. M. Preparation of enantioselective enriched alpha-(dialkoxyphosphoryl) lactams via intramolecular C-H insertion with chiral dirhodium(II) catalysts. *Journal of Molecular Catalysis a-Chemical* **2005,** 227, 17-24.

106. Gomes, L. F. R.; Trindade, A. F.; Candeias, N. R.; Veiros, L. F.; Gois, P. M. P.; Afonso, C. A. M. Cyclization of Diazoacetamides Catalyzed by N-Heterocyclic Carbene Dirhodium(II) Complexes. *Synthesis-Stuttgart* **2009**, 3519-3526.

107. Candeias, N. R.; Afonso, C. A. M.; Gois, P. M. P. Making expensive dirhodium(ii) catalysts cheaper: Rh(ii) recycling methods. *Organic & Biomolecular Chemistry* **2012,** 10, 3357-3378.

108. Cotton, F. A.; Murillo, C. A.; Walton, R. A. *Multiple Bonds Between Metal Atoms*. Springer: 2005.

109. Trindade, A. F.; Gois, P. M. P.; Veiros, L. F.; Andre, V.; Duarte, M. T.; Afonso, C. A. M.; Caddick, S.; Cloke, F. G. N. Axial coordination of NHC ligands on dirhodium(II) complexes: Generation of a new family of catalysts. *Journal Of Organic Chemistry* **2008,** 73, 4076-4086.

110. Doyle, M. P.; Duffy, R.; Ratnikov, M.; Zhou, L. Catalytic Carbene Insertion into C-H Bonds. *Chemical Reviews* **2010,** 110, 704-724.

111. Trindade, A. F.; Coelho, J. A. S.; Afonso, C. A. M.; Veiros, L. F.; Gois, P. M. P. Fine Tuning of Dirhodium(II) Complexes: Exploring the Axial Modification. *Acs Catalysis* **2012,** 2, 370-383.

112. Nakamura, E.; Yoshikai, N.; Yamanaka, M. Mechanism of C-H bond activation/C-C bond formation reaction between diazo compound and alkane catalyzed by dirhodium tetracarboxylate. *Journal of the American Chemical Society* **2002,** 124, 7181-7192.

113. Wong, F. M.; Wang, J. B.; Hengge, A. C.; Wu, W. M. Mechanism of rhodium-catalyzed carbene formation from diazo compounds. *Organic Letters* **2007,** 9, 1663-1665.

114. Hu, W.; Xu, X.; Zhou, J.; Liu, W.-J.; Huang, H.; Hu, J.; Yang, L.; Gong, L.-Z. Cooperative Catalysis with Chiral Brønsted Acid-Rh2(OAc)4: Highly Enantioselective Three-Component Reactions of Diazo Compounds with Alcohols and Imines. *Journal of the American Chemical Society* **2008,** 130, 7782-7783.

115. Saito, H.; Uchiyama, T.; Miyake, M.; Anada, M.; Hashimoto, S.; Takabatake, T.; Miyairi, S. Asymmetric Intermolecular N-H Insertion Reaction of Phenyldiazoacetates with Anilines Catalyzed by Achiral Dirhodium(Ii) Carboxylates and Cinchona Alkaloids. *Heterocycles* **2010,** 81, 1149-1155.

116. Saito, H.; Iwai, R.; Uchiyama, T.; Miyake, M.; Miyairi, S. Chiral Induction by Cinchona Alkaloids in the Rhodium(II) Catalyzed O-H Insertion Reaction. *Chemical & Pharmaceutical Bulletin* **2010,** 58, 872-874.

117. Forslund, R. E.; Cain, J.; Colyer, J.; Doyle, M. P. Chiral Dirhodium(II) Carboxamidate-Catalyzed [2+2]-Cycloaddition of TMS-Ketene and Ethyl Glyoxylate. *Advanced Synthesis & Catalysis* **2005,** 347, 87-92.

118. Doyle, M. P. Perspective on Dirhodium Carboxamidates as Catalysts. *The Journal of Organic Chemistry* **2006,** 71, 9253-9260.

119. Zhang, Y.; Wang, J. Recent development of reactions with [small alpha]-diazocarbonyl compounds as nucleophiles. *Chemical Communications* **2009**, 5350-5361.

120. Trindade, A. F.; Gois, P. M. P.; Afonso, C. A. M. Recyclable Stereoselective Catalysts. *Chemical Reviews* **2009,** 109, 418-514.

121. Doyle, M. P.; Forbes, D. C. Recent advances in asymmetric catalytic metal carbene transformations. *Chemical Reviews* **1998,** 98, 911-935.

122. Doyle, M. P.; Bagheri, V.; Daniel, K. L.; Pearson, M. M.; Thomas, N. F. Electronic and Steric Control in Intramolecular Carbon-Hydrogen Insertion Reactions of Diazo-Compounds Catalyzed by Rhodium(Ii) Carboxylates and Carboxamides. *Abstracts of Papers of the American Chemical Society* **1990,** 199, 24-Catl.

123. Doyle, M. P.; Westrum, L. J.; Wolthuis, W. N. E.; See, M. M.; Boone, W. P.; Bagheri, V.; Pearson, M. M. Electronic and Steric Control in Carbon Hydrogen Insertion Reactions of Diazoacetoacetates Catalyzed by Dirhodium(Ii) Carboxylates and Carboxamides. *Journal of the American Chemical Society* **1993,** 115, 958-964.

124. Alonso, M. E.; Fernandez, R. Effect of Catalyst on Zwitterionic Intermediacy in Additions of Dimethyl Diazomalonate to Vinyl Ethers. *Tetrahedron* **1989,** 45, 3313-3320.

125. Maryanoff, B. E. Reaction of Dimethyl Diazomalonate and Ethyl 2-Diazoacetoacetate with N-Methylpyrrole. *Journal of Organic Chemistry* **1982,** 47, 3000-3002.

126. Gomes, L. F. R.; Trindade, A. F.; Candeias, N. R.; Gois, P. M. P.; Afonso, C. A. M. Intramolecular C-H insertion using NHC-di-rhodium(II) complexes: the influence of axial coordination. *Tetrahedron Letters* **2008,** 49, 7372-7375.

127. Gois, P. M. P.; Trindade, A. F.; Veiros, L. F.; Andre, V.; Duarte, M. T.; Afonso, C. A. M.; Caddick, S.; Cloke, F. G. N. Tuning the reactivity of dirhodium(II) complexes with axial N-heterocyclic carbene ligands: The arylation of aldehydes. *Angewandte Chemie-International Edition* **2007,** 46, 5750-5753.

128. Brauner-Osborne, H.; Bunch, L.; Chopin, N.; Couty, F.; Evano, G.; Jensen, A. A.; Kusk, M.; Nielsen, B.; Rabasso, N. Azetidinic amino acids: stereocontrolled synthesis and pharmacological characterization as ligands for glutamate receptors and transporters. *Organic & Biomolecular Chemistry* **2005,** 3, 3926-3936.

129. Wong, F. M.; Wang, J.; Hengge, A. C.; Wu, W. Mechanism of Rhodium-Catalyzed Carbene Formation from Diazo Compounds. *Organic Letters* **2007,** 9, 1663-1665.

130. Pellicciari, R.; Natalini, B.; Sadeghpour, B. M.; Marinozzi, M.; Snyder, J. P.; Williamson, B. L.; Kuethe, J. T.; Padwa, A. The Reaction of α-Diazo-β-hydroxy Esters with Boron Trifluoride Etherate: Generation and Rearrangement of Destabilized Vinyl Cations. A Detailed Experimental and Theoretical Study. *Journal of the American Chemical Society* **1996,** 118, 1-12.

131. Weng, Z.; Teo, S.; Hor, T. S. A. Metal Unsaturation and Ligand Hemilability in Suzuki Coupling. *Accounts of Chemical Research* **2007,** 40, 676-684.

132. Johansson Seechurn, C. C. C.; Kitching, M. O.; Colacot, T. J.; Snieckus, V. Palladium-Catalyzed Cross-Coupling: A Historical Contextual Perspective to the 2010 Nobel Prize. *Angewandte Chemie International Edition* **2012,** 51, 5062-5085.

133. Martin, R.; Buchwald, S. L. Palladium-Catalyzed Suzuki−Miyaura Cross-Coupling Reactions Employing Dialkylbiaryl Phosphine Ligands. *Accounts of Chemical Research* **2008,** 41, 1461-1473.

134. Braga, A. A. C.; Morgon, N. H.; Ujaque, G.; Maseras, F. Computational Characterization of the Role of the Base in the Suzuki−Miyaura Cross-Coupling Reaction. *Journal of the American Chemical Society* **2005,** 127, 9298-9307.

135. Miyaura, N. Cross-coupling reaction of organoboron compounds via base-assisted transmetalation to palladium(II) complexes. *Journal of Organometallic Chemistry* **2002,** 653, 54-57.

136. Kappe, C. O. Controlled Microwave Heating in Modern Organic Synthesis. *Angewandte Chemie International Edition* **2004,** 43, 6250-6284.

137. Stadler, A.; Kappe, C. O. Automated library generation using sequential microwave-assisted chemistry. Application toward the Biginelli multicomponent condensation. *Journal of Combinatorial Chemistry* **2001,** 3, 624-630.

138. Torre, L. A.; Bray, F.; Siegel, R. L.; Ferlay, J.; Lortet-Tieulent, J.; Jemal, A. Global cancer statistics, 2012. *CA Cancer J Clin* **2015,** 65, 87-108.

139. Ferlay, J.; Soerjomataram, I.; Dikshit, R.; Eser, S.; Mathers, C.; Rebelo, M.; Parkin, D. M.; Forman, D.; Bray, F. Cancer incidence and mortality worldwide: Sources, methods and major patterns in GLOBOCAN 2012. *International Journal of Cancer* **2015,** 136, E359-E386.

140. Jamison, D. T.; Breman, J. G.; Measham, A. R.; Alleyne, G.; Claeson, M.; Evans, D. B.; Jha, P.; Mills, A.; Musgrove, P. *Disease control priorities in developing countries*. World Bank Publications: 2006.

141. Toma, T.; Shimokawa, J.; Fukuyama, T. N,N'-Ditosylhydrazine: A Convenient Reagent for Facile Synthesis of Diazoacetates. *Organic Letters* **2007,** 9, 3195-3197.

142. Doyle, M. P.; Kalinin, A. V. Highly enantioselective intramolecular cyclopropanation reactions of N-allylic-N-methyldiazoacetamides catalyzed by chiral dirhodium(II) carboxamidates. *Journal of Organic Chemistry* **1996,** 61, 2179-2184.

143. Mukherjee, M.; Gupta, A. K.; Lu, Z.; Zhang, Y.; Wulff, W. D. Seeking Passe-Partout in the Catalytic Asymmetric Aziridination of Imines: Evolving Toward Substrate Generality for a Single Chemzyme. *The Journal of Organic Chemistry* **2010,** 75, 5643-5660.

144. Blankley, C. J. Crotyl Diazoacetate. *Org. Synth.* **1969,** 49.

145. Pey, A. L.; Stricher, F.; Serrano, L.; Martinez, A. Predicted effects of missense mutations on native-state stability account for phenotypic outcome in phenylketonuria, a paradigm of misfolding diseases. *American Journal of Human Genetics* **2007,** 81, 1006-1024.

146. Folling, I. The discovery of phenylketonuria. *Acta Paediatr Suppl* **1994,** 407, 4-10.

147. Fitzpatrick, P. F. Mechanism of Aromatic Amino Acid Hydroxylation. *Biochemistry* **2003,** 42, 14083-14091.

148. Blau, N.; van Spronsen, F. J.; Levy, H. L. Phenylketonuria. *Lancet* **2010,** 376, 1417-27.

149. Mitchell, J. J.; Trakadis, Y. J.; Scriver, C. R. Phenylalanine hydroxylase deficiency. *Genet Med* **2011,** 13, 697-707.

150. Williams, R. A.; Mamotte, C. D. S.; Burnett, J. R. Phenylketonuria: An Inborn Error of Phenylalanine Metabolism. *The Clinical Biochemist Reviews* **2008,** 29, 31-41.

151. Patel, D.; Kopec, J.; Fitzpatrick, F.; McCorvie, T. J.; Yue, W. W. Structural basis for ligand-dependent dimerization of phenylalanine hydroxylase regulatory domain. *Scientific Reports* **2016,** 6.

152. Wettstein, S.; Underhaug, J.; Perez, B.; Marsden, B. D.; Yue, W. W.; Martinez, A.; Blau, N. Linking genotypes database with locus-specific database and genotype-phenotype correlation in phenylketonuria. *Eur J Hum Genet* **2015,** 23, 302-9.

153. Blau, N. Genetics of Phenylketonuria: Then and Now. *Hum Mutat* **2016,** 37, 508-15.

154. Underhaug, J.; Aubi, O.; Martinez, A. Phenylalanine Hydroxylase Misfolding and Pharmacological Chaperones. *Current Topics in Medicinal Chemistry* **2012,** 12, 2534-2545.

155. Olsson, E.; Martinez, A.; Teigen, K.; Jensen, V. R. Formation of the Iron–Oxo Hydroxylating Species in the Catalytic Cycle of Aromatic Amino Acid Hydroxylases. *Chemistry – A European Journal* **2011,** 17, 3746-3758.

156. Lang, E. J. M.; Cross, P. J.; Mittelstädt, G.; Jameson, G. B.; Parker, E. J. Allosteric ACTion: the varied ACT domains regulating enzymes of amino-acid metabolism. *Current Opinion in Structural Biology* **2014,** 29, 102-111.

157. Gregersen, N.; Bross, P.; Vang, S.; Christensen, J. H. Protein misfolding and human disease. In *Annual Review of Genomics and Human Genetics*, Annual Reviews: Palo Alto, 2006; Vol. 7, pp 103-124.

158. Gessler, D. J.; Gao, G. Gene Therapy for the Treatment of Neurological Disorders: Metabolic Disorders. In *Gene Therapy for Neurological Disorders: Methods and Protocols*, Manfredsson, P. F., Ed. Springer New York: New York, NY, 2016; pp 429-465.

159. Ding, Z.; Georgiev, P.; Thony, B. Administration-route and gender-independent long-term therapeutic correction of phenylketonuria (PKU) in a mouse model by recombinant adeno-associated virus 8 pseudotyped vector-mediated gene transfer. *Gene Ther* **2006,** 13, 587-93.

160. Ding, Z.; Harding, C. O.; Rebuffat, A.; Elzaouk, L.; Wolff, J. A.; Thony, B. Correction of Murine PKU Following AAV-mediated Intramuscular Expression of a Complete Phenylalanine Hydroxylating System. *Mol Ther* **2008,** 16, 673-681.

161. Pey, A. L.; Ying, M.; Cremades, N.; Velazquez-Campoy, A.; Scherer, T.; Thöny, B.; Sancho, J.; Martinez, A. Identification of pharmacological chaperones as potential therapeutic agents to treat phenylketonuria. *The Journal of Clinical Investigation* **2008,** 118, 2858-2867.

162. Torreblanca, R.; Lira-Navarrete, E.; Sancho, J.; Hurtado-Guerrero, R. Structural and Mechanistic Basis of the Interaction between a Pharmacological Chaperone and Human Phenylalanine Hydroxylase. *ChemBioChem* **2012,** 13, 1266-1269.

163. Santos-Sierra, S.; Kirchmair, J.; Perna, A. M.; Reiss, D.; Kemter, K.; Roschinger, W.; Glossmann, H.; Gersting, S. W.; Muntau, A. C.; Wolber, G.; Lagler, F. B. Novel pharmacological chaperones that correct phenylketonuria in mice. *Hum Mol Genet* **2012,** 21, 1877-87.

164. Boscott, R. J.; Bickel, H. Detection of Some New Abnormal Metabolites in the Urine of Phenylketonuria. *Scandinavian Journal of Clinical and Laboratory Investigation* **1953,** 5, 380-382.

165. Yue, W. W. From structural biology to designing therapy for inborn errors of metabolism. *Journal of Inherited Metabolic Disease* **2016,** 39, 489-498.

166. Montalbano, F.; Leandro, J.; Farias, G. D. V. F.; Lino, P. R.; Guedes, R. C.; Vicente, J. B.; Leandro, P.; Gois, P. M. P. Phenylalanine iminoboronates as new phenylalanine hydroxylase modulators. *Rsc Advances* **2014,** 4, 61022-61027.

167. Vollrath, F.; Hawkins, N.; Porter, D.; Holland, C.; Boulet-Audet, M. Differential Scanning Fluorimetry provides high throughput data on silk protein transitions. *Scientific Reports* **2014,** 4, 5625.

168. Leandro, P.; Gomes, C. M. Protein misfolding in conformational disorders: rescue of folding defects and chemical chaperoning. *Mini Rev Med Chem* **2008,** 8, 901-11.

169. Bruker AXS: SAINT+, release 6.22. *Bruker Analytical Systems: Madison,WI* **2005**.

170. Bruker AXS:SADABS. Bruker Analytical Systems: Madison,WI **2005**.

171. Altomare, A.; Burla, M. C.; Camalli, M.; Cascarano, G. L.; Giacovazzo, C.; Guagliardi, A.; Moliterni, A. G. G.; Polidori, G.; Spagna, R. SIR97: a new tool for crystal structure determination and refinement. *Journal of Applied Crystallography* **1999,** 32, 115-119.

172. Sheldrick, G. M. A short history of SHELX. *Acta Crystallographica Section A* **2008,** 64, 112-122.

173. Farrugia, L. J. WinGX - Version 1.80.05. *J. Appl. Cryst.* **1999,** 32, 837-838.

Chapter VIII

VIII. Appendix

A. Computational details

All calculations were performed using the Gaussian 03 software package[1],and the PBE1PBE functional, without symmetry constraints. That functional uses a hybrid generalized gradient approximation (GGA), including 25 % mixture of Hartree-Fock[2]exchange with DFT[3]exchange-correlation, given by Perdew, Burke and Ernzerhof functional (PBE).[4]The optimized geometries were obtained with the lanl2dz basis set[5]augmented with a f-polarization function[6]for Rh, and a standard 6-31G(d,p)[7]for the remaining elements (basis b1). Transition state optimizations were performed with the Synchronous Transit-Guided Quasi-Newton Method (STQN) developed by Schlegel *et al*,[8]following extensive searches of the Potential Energy Surface. Frequency calculations were performed to confirm the nature of the stationary points, yielding one imaginary frequency for the transition states and none for the minima. Each transition state was further confirmed by following its vibrational mode downhill on both sides and obtaining the minima presented on the energy profile. The electronic energies (E_{b1})obtained at the PBE1PBE/b1 level of theory were converted to free energy at 298.15 K and 1 atm (G_{b1}) by using zero point

---

[1]*Gaussian 03*, Revision C.02, Frisch, M. J.; Trucks, G. W.; Schlegel, H. B.;Scuseria, G. E.; Robb, M. A.; Cheeseman, J. R.; Montgomery, Jr., J. A.; Vreven, T.; Kudin, K. N.; Burant, J. C.; Millam, J. M.; Iyengar, S. S.; Tomasi, J.; Barone, V.; Mennucci, B.; Cossi, M.; Scalmani, G.; Rega, N.; Petersson, G. A.; Nakatsuji, H.; Hada, M.; Ehara, M.; Toyota, K.; Fukuda, R.; Hasegawa, J.; Ishida, M.; Nakajima, T.; Honda, Y.; Kitao, O.; Nakai, H.; Klene, M.; Li, X.; Knox, J. E.; Hratchian, H. P.; Cross, J. B.; Adamo, C.; Jaramillo, J.; Gomperts, R.; Stratmann, R. E.; Yazyev, O.; Austin, A. J.; Cammi, R.; Pomelli, C.; Ochterski, J. W.; Ayala, P. Y.; Morokuma, K.; Voth, G. A.; Salvador, P.; Dannenberg, J. J.; Zakrzewski, V. G.; Dapprich, S.; Daniels, A. D.; Strain, M. C.; Farkas, O.; Malick, D. K.; Rabuck, A. D.; Raghavachari, K.; Foresman, J. B.; Ortiz, J. V.; Cui, Q.; Baboul, A. G.; Clifford, S.; Cioslowski, J.; Stefanov, B. B.; Liu, G.; Liashenko, A.; Piskorz, P.; Komaromi, I.; Martin, R. L.; Fox, D. J.; Keith, T.; Al-Laham, M. A.; Peng, C. Y.; Nanayakkara, A.; Challacombe, M.; Gill, P. M. W.; Johnson, B.; Chen, W.; Wong, M. W.; Gonzalez, C. &Pople, J. A. Gaussian, Inc., Wallingford CT, (2004).

[2]Hehre, W. J.; Radom, L.; Schleyer, P. v.R. &Pople, J. A. *Ab Initio Molecular Orbital Theory*, John Wiley & Sons, NY, (1986)

[3] Parr, R. G. & Yang, W. in *Density Functional Theory of Atoms and Molecules*; Oxford University Press: New York, (1989).

[4] (a) Perdew, J. P.; Burke, K.; Ernzerhof, M. *Phys. Rev. Lett.* **1997**, *78*, 1396. (b) Perdew, J. P. *Phys. Rev. B***1986**, *33*, 8822.

[5] (a) Dunning Jr., T. H.; Hay, P. J. *Modern Theoretical Chemistry*, Ed. Schaefer, H. F. III (Plenum, New York, **1976**), vol. 3, p. 1. (b) Hay P. J.; Wadt, W. R. *J. Chem. Phys.***1985**, *82*, 270. (c) Wadt W. R.; Hay, P. J. *J. Chem. Phys.***1985**, *82*, 284. (d) Hay P. J.; Wadt, W. R. *J. Chem. Phys.***1985**, *82*, 2299.

[6] Ehlers, A. W.; Böhme, M.; Dapprich, S.; Gobbi, A.; Höllwarth, A.; Jonas, V.; Köhler, K. F.; Stegmann, R.; Veldkamp A.; Frenking, G. *Chem. Phys. Lett.***1993**, *208*, 111.

[7] (a) Ditchfield, R.; Hehre W. J.; Pople, J. A. *J. Chem. Phys.***1971**, *54*, 724. (b) Hehre, W. J.; Ditchfield R.; Pople, J. A. *J. Chem. Phys.***1972**, *56*, 2257. (c) Hariharan, P. C.; Pople, J. A. *Mol. Phys.***1974**, *27*, 209. (d) Gordon, M. S. *Chem. Phys. Lett.***1980**, *76*, 163. (e) Hariharan, P. C.; Pople, J. A. *Theor. Chim.Acta***1973**, *28*, 213.

[8] (a) Peng, C.; Ayala, P.Y.; Schlegel, H.B.; Frisch, M.J. *J. Comp. Chem.*, **1996**, *17*, 49. (b) Peng, C.; Schlegel, H.B. *Israel J. Chem.*, **1994**, *33*, 449.

energy and thermal energy corrections based on structural and vibration frequency data calculated at the same level.

Single point energy calculations were performed using an improved basis set (basis b2) and the geometries optimized at the PBE1PBE/b1 level. Basis b2 consisted of the same base (b1) for Rh and a standard 6-311++G(d,p)[9] for the remaining elements. Solvent effects (ethanol) were considered in the PBE1PBE/b2//PBE1PBE/b1 energy calculations using the Polarizable Continuum Model (PCM) initially devised by Tomasi and coworkers[10]as implemented on Gaussian 03.[11] The molecular cavity was based on the united atom topological model applied on UAHF radii, optimized for the HF/6-31G(d) level.

The free energy values presented along the text (G_{b2}^{soln}) were derived from the electronic energy values obtained at the PBE1PBE/b2//PBE1PBE/b1 level, including solvent effects (E_{b2}^{soln}), according to the following expression:$G_{b2}^{soln} = E_{b2}^{soln} + G_{b1} - E_{b1}$

[9] (a) McClean, A. D.; Chandler, G. S. *J. Chem. Phys.***1980**, *72*, 5639. (b) Krishnan, R.; Binkley, J. S.; Seeger, R. Pople, J. A. *J. Chem. Phys.***1980**, *72*, 650.(c) Wachters, A. J. H. *J. Chem. Phys.***1970**, *52*, 1033. (d) Hay, P. J. *J. Chem. Phys.***1977**, *66*, 4377. (e) Raghavachari, K.; Trucks, G. W. *J. Chem. Phys.***1989**, *91*, 1062. (f) Binning Jr., R. C.; Curtiss, L. A. *J. Comp. Chem.*, **1990**, *11*, 1206. (g) McGrath, M. P.; Radom, L. *J. Chem. Phys.***1991**, *94*, 511. (h) Clark, T.; Chandrasekhar, J.; Spitznagel, G. W.; Schleyer, P. v. R. *J. Comp. Chem.***1983**, *4*, 294. (i) Frisch, M. J.; Pople, J. A.; Binkley, J. S. *J. Chem. Phys.***1984**, *80*, 3265.

[10](a) Cancès, M. T.; Mennucci, B.; Tomasi, J. *J. Chem. Phys.***1997**, *107*, 3032. (b) Cossi, M.; Barone, V.; Mennucci, B.; Tomasi, J. *Chem. Phys. Lett.***1998**, *286*, 253. (c) Mennucci B.; Tomasi, J. *J. Chem. Phys.***1997**, *106*, 5151.

[11](a) Tomasi, J.; Mennucci, B.; Cammi, R. *Chem. Rev.* **2005**, *105*, 2999. (b) Cossi, M.; Scalmani, G.; Rega, N.; Barone, V. *J. Chem. Phys.***2002**, *117*, 43.

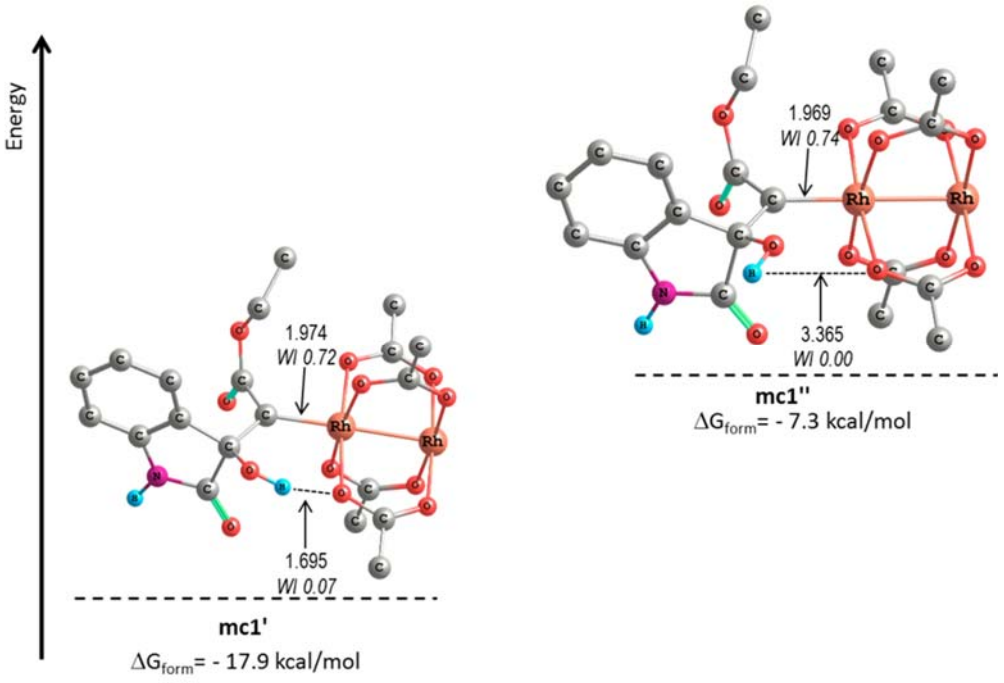

Figure A1 - Metallocarbene conformations with and without intramolecular hydrogen bond determined at PBE1PBE/b1//PBE1PBE/b2level of theory. The energy corresponds to Gibbs Free Energy in ethanol, after thermal correction and the energy values are referred to the **70** +**Rh$_2$(OAc)$_4$** pair of reactants. The relevant bond distances (Å) are indicated, as well as the respective Wiberg indices (WI, italics)

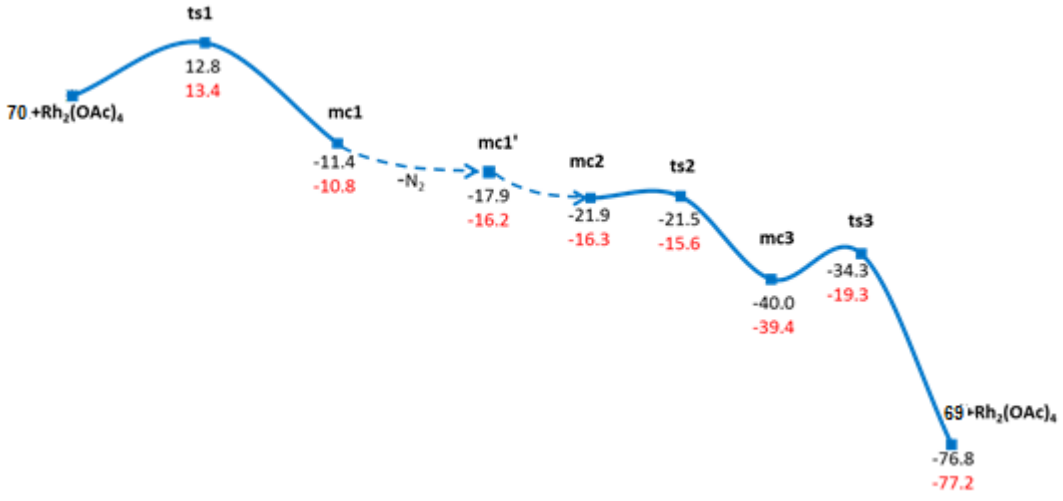

Figure A2 - Energy profiles calculated for the dirhodium catalyzed quinolone formation. The minima and the transition states were optimized and the energy values (kcal/mol) are referred to pair of starting materials (**70**+**Rh$_2$(OAc)$_4$**) after thermal correction to Gibbs Free Energy in ethanol (in black) or to Gibbs free energy in vacuum at the PBE1PBE/b1 level of theory (in red).

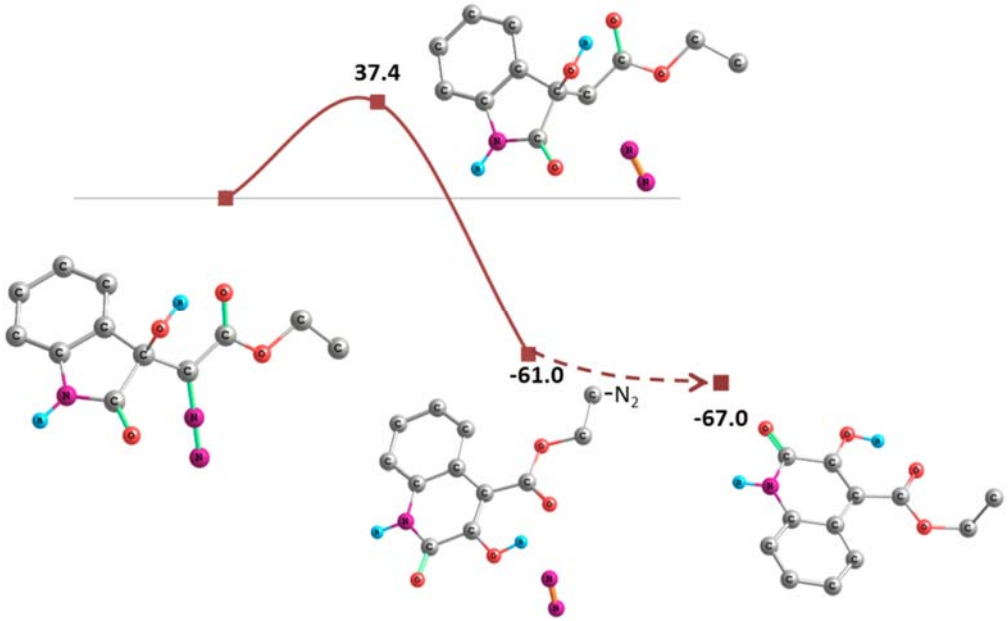

Figure A3 - Energy profiles calculated for rhodium free quinolone formation, via a concerted pathway. The minima and the transition states were optimized with at the pbe1pbe/6-31G** level of theory. The energy values (kcal/mol) are referred to the Gibbs Free Energyof the 3-hydroxy-oxindole (**70**) in the **A** conformation represented.

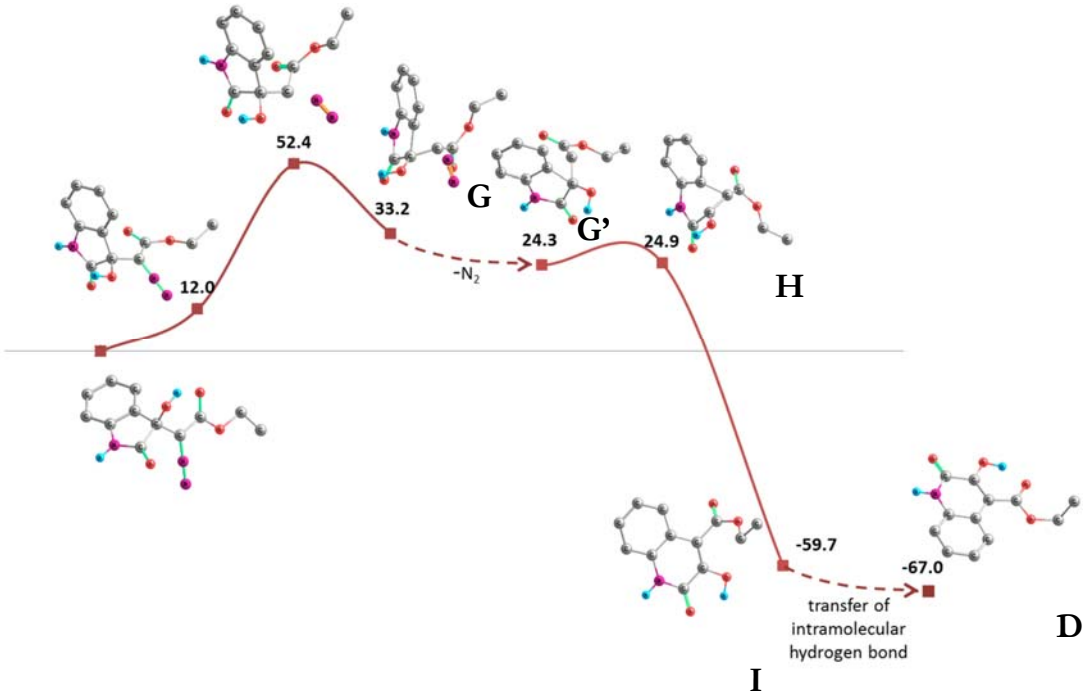

Figure A4 - Energy profiles calculated for rhodium free quinolone formation, via a free carbene pathway. The minima and the transition states were optimized at the pbe1pbe/6-31G** level of theory. The energy values (kcal/mol) are referred to the Gibbs Free Energyof the 3-hydroxy-oxindole (**70**) in the **A** conformation represented.

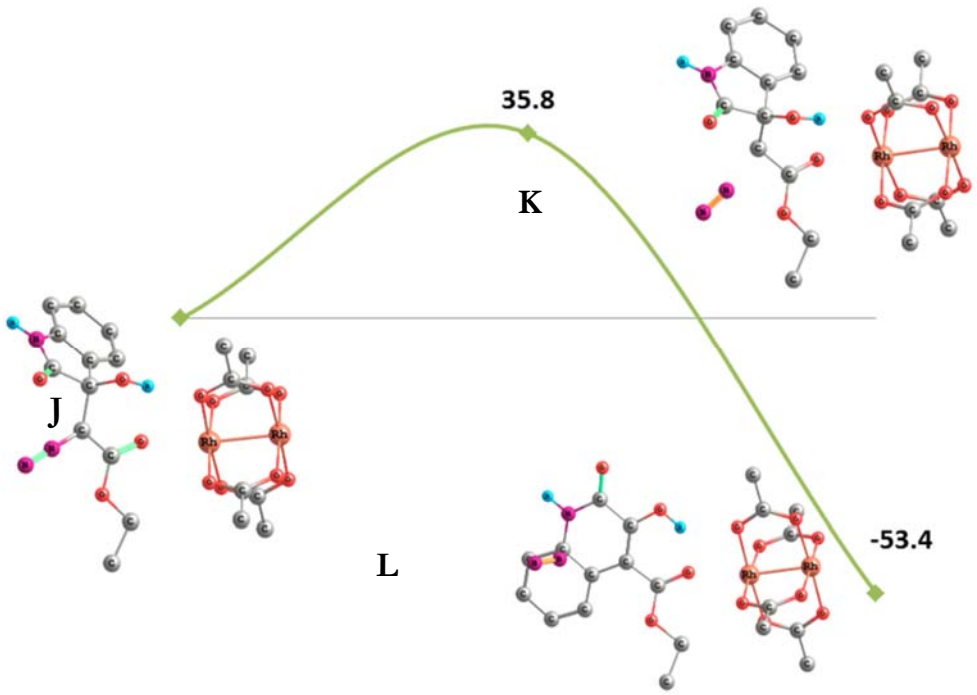

Figure A5 - Energy profiles calculated for the rhodium catalyzed quinolone formation, via coordination to the carbonylic ester of the 3-hydroxy-oxindole (**70**). The minima and the transition states were optimized at the PBE1PBE/b1level of theory. The energy values (kcal/mol) are referred to the Gibbs Free Energyof the pair of starting materials represented (**J**).

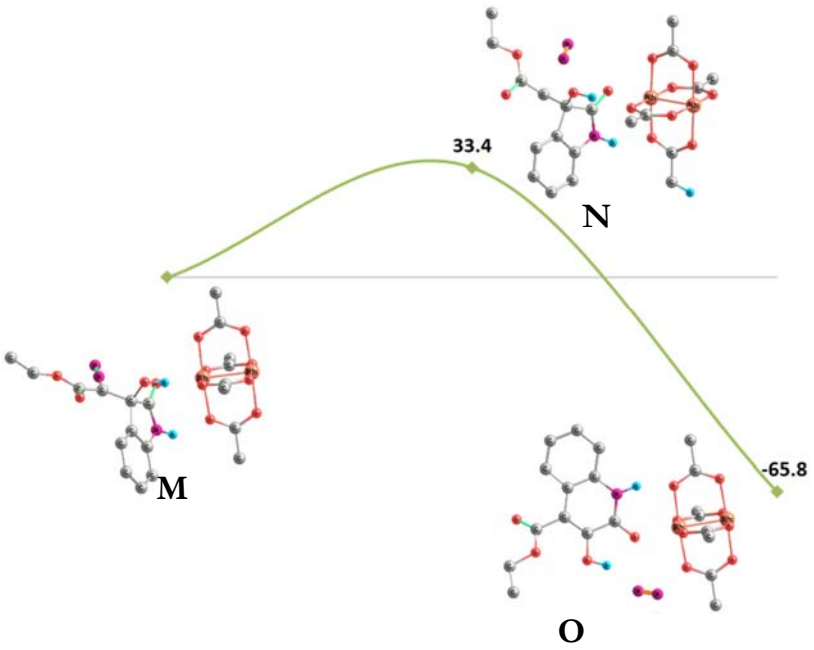

Figure A6 - Energy profiles calculated for the dirhodium catalyzed quinolone formation, via coordination to the carbonyl of the oxindole ring. The minima and the transition states were optimized at the PBE1PBE/b1level of theory. The energy values (kcal/mol) are referred to the Gibbs Free Energyof the pair of starting materials represented (**M**).

Atomic coordinates for all the optimized species (PBE1PBE/b2)

5-$Rh_2(OAc)_4$

45	1.574574	0.782673	-0.819868
45	-0.122120	-0.274816	0.491276
8	2.826632	0.480689	0.743026
1	3.030686	-1.001261	3.638526
1	-1.742121	1.792363	-3.765798
6	2.435027	-0.188272	1.743946
8	-1.441924	0.133299	-1.019416
6	-1.021390	0.701125	-2.065555
8	0.170618	1.092267	-2.277990
8	1.266751	-0.647666	1.923858
6	3.467474	-0.461383	2.798912
6	-2.007296	0.910227	-3.181642
1	3.899623	0.483994	3.136236
1	-1.972333	0.039989	-3.845137
8	1.919563	-1.066961	-1.646774
8	-0.511287	1.536061	1.334069
6	1.275807	-2.085691	-1.230698
6	0.144854	2.542247	0.949180
1	4.273426	-1.045320	2.346115
1	-3.018135	0.995790	-2.781854
8	1.054829	2.548464	0.060175
8	0.353960	-2.060143	-0.374153
6	1.671601	-3.409222	-1.816971
6	-0.168487	3.865076	1.591777
1	1.037058	-4.205446	-1.429784
1	-0.497591	4.573152	0.826046
1	2.717427	-3.603634	-1.562015
1	-0.945932	3.748684	2.346028
1	1.600219	-3.367292	-2.907165
1	0.739674	4.268888	2.047274
7	6.511186	0.213890	-1.565330
6	5.185744	-0.115883	-1.448493
8	4.724965	-0.955293	-0.713059
6	4.429002	0.638961	-2.598687
8	3.787769	-0.281413	-3.417828
6	5.572125	1.319198	-3.322693
6	5.588274	2.092319	-4.470744
6	6.802977	2.623049	-4.915163
6	7.976686	2.372539	-4.209154
6	7.976745	1.581730	-3.058769
6	6.763754	1.059087	-2.636098
6	3.391093	1.703359	-2.069989
8	4.896645	2.405269	-0.451791
6	3.963924	2.737687	-1.142083
8	3.490291	3.982278	-1.037050
6	2.107829	5.885470	-1.201309
6	2.422550	4.538839	-1.809704
7	2.660761	2.088049	-3.134034
7	2.029531	2.240478	-4.051109
1	7.204095	-0.159292	-0.937482
1	3.180619	-0.791187	-2.839300
1	4.678152	2.272787	-5.034970
1	6.831363	3.226782	-5.816609
1	8.914748	2.792365	-4.560702
1	8.896297	1.380376	-2.517935
1	1.309001	6.372814	-1.768033
1	2.988790	6.532282	-1.212965
1	1.780348	5.763295	-0.166225
1	2.750075	4.659626	-2.849383
1	1.546073	3.887755	-1.760126

ts1

45	1.667064	0.742218	-0.830296
45	-0.090372	-0.245142	0.510194
8	2.892175	0.355046	0.741904
1	3.057670	-1.175865	3.611830
1	-1.827533	2.107999	-3.476372
6	2.472678	-0.303561	1.741661
8	-1.408407	0.240013	-0.981032
6	-0.972882	0.786367	-2.026591
8	0.240500	1.110614	-2.253873
8	1.288333	-0.702857	1.930719
6	3.505872	-0.631051	2.781448
6	-1.952214	1.079473	-3.130046
1	3.966607	0.293689	3.138056
1	-1.741793	0.420347	-3.977618
8	1.917927	-1.125543	-1.649799
8	-0.358165	1.596012	1.354062
6	1.216355	-2.110859	-1.237907
6	0.348512	2.563026	0.967593
1	4.291889	-1.227681	2.310732
1	-2.972630	0.914217	-2.785821
8	1.246544	2.529813	0.062314
8	0.297583	-2.044619	-0.384154
6	1.543596	-3.447521	-1.838802
6	0.118672	3.900859	1.616374
1	0.872530	-4.213939	-1.452982
1	-0.285115	4.597494	0.875591
1	2.580154	-3.697298	-1.594752
1	-0.581825	3.805392	2.445336
1	1.465622	-3.392772	-2.928018
1	1.071264	4.305215	1.967463

7	6.487167	0.281092	-1.437653
6	5.195295	-0.168319	-1.384363
8	4.782897	-1.086631	-0.720332
6	4.394163	0.611594	-2.500880
8	3.807997	-0.311249	-3.362837
6	5.513490	1.373688	-3.187083
6	5.513570	2.167956	-4.320439
6	6.705144	2.774948	-4.728763
6	7.876075	2.579722	-4.002182
6	7.895955	1.766202	-2.868164
6	6.706271	1.166832	-2.483916
6	3.320799	1.525528	-1.857793
8	4.757260	2.438081	-0.362947
6	3.904975	2.721889	-1.177043
8	3.540987	3.989341	-1.337602
6	2.034665	5.801971	-1.513381
6	2.383818	4.435246	-2.054820
7	2.561206	2.019878	-3.465980
7	1.755046	1.924789	-4.219300
1	7.201151	-0.105999	-0.842098
1	3.189539	-0.843721	-2.819182
1	4.610005	2.307484	-4.904848
1	6.716696	3.395409	-5.619172
1	8.795452	3.059833	-4.324465
1	8.813650	1.603927	-2.311364
1	1.173440	6.206823	-2.053386
1	2.873808	6.492600	-1.630248
1	1.784763	5.735443	-0.451933
1	2.631301	4.498811	-3.120612
1	1.558407	3.736847	-1.898619

mc1

45	1.853666	0.747870	-0.615515
45	-0.168913	-0.071972	0.454641
8	2.833853	0.049118	1.022821
1	2.462620	-1.692949	3.747415
1	-1.015444	2.715962	-3.573668
6	2.209810	-0.582954	1.933229
8	-1.230419	0.697048	-1.115581
6	-0.612902	1.252110	-2.059783
8	0.650898	1.404863	-2.148207
8	0.969251	-0.805661	1.971464
6	3.060177	-1.092980	3.061684
6	-1.421840	1.766844	-3.219221
1	3.495718	-0.241844	3.592392
1	-1.357373	1.047437	-4.041516
8	1.983348	-1.108295	-1.488179
8	-0.270838	1.728770	1.414370
6	1.072704	-1.987625	-1.289759
6	0.586349	2.614943	1.164603
1	3.886337	-1.679436	2.652866
1	-2.466544	1.877770	-2.929245
8	1.554605	2.519209	0.338260
8	0.069105	-1.840377	-0.553125
6	1.247205	-3.286504	-2.022448
6	0.454181	3.933951	1.874878
1	0.474822	-3.995297	-1.726381
1	-0.201265	4.586818	1.288854
1	2.238924	-3.695038	-1.812290
1	-0.005178	3.783778	2.852586
1	1.187403	-3.100834	-3.099022
1	1.428154	4.414916	1.971059
7	6.735866	0.679350	-1.443602
6	5.561027	0.002865	-1.259929
8	5.361504	-0.963467	-0.574883
6	4.492789	0.676525	-2.255296
8	3.920569	-0.286682	-3.063733
6	5.396999	1.596689	-3.051641
6	5.124379	2.347197	-4.181192
6	6.146298	3.126248	-4.732059
6	7.412213	3.136170	-4.150667
6	7.703969	2.358312	-3.028249
6	6.681953	1.584655	-2.499502
6	3.559285	1.419286	-1.354561
8	4.868096	2.427204	0.231564
6	4.123460	2.628721	-0.704225
8	3.792835	3.847635	-1.098739
6	1.921549	5.126127	-1.858953
6	2.886131	4.017135	-2.202902
7	1.722085	0.540327	-5.213128
7	1.240664	-0.406465	-4.920221
1	7.573752	0.409985	-0.952079
1	3.284114	-0.802703	-2.528324
1	4.139900	2.309787	-4.638325
1	5.954889	3.719802	-5.620388
1	8.196599	3.749735	-4.583941
1	8.699470	2.351413	-2.595551
1	1.262454	5.320722	-2.710540
1	2.459686	6.047932	-1.621151
1	1.312905	4.839570	-0.999245
1	3.491257	4.265816	-3.080021
1	2.343491	3.083572	-2.398887

mc1'

45	1.854224	0.742528	-0.610380
45	-0.176490	-0.081672	0.441000
8	2.821858	0.063514	1.044602
1	2.405660	-1.565270	3.834187
1	-1.219103	2.783144	-3.383090
6	2.187256	-0.548127	1.961673

8 -1.218688 0.636446 -1.166878
6 -0.591568 1.195018 -2.102778
8 0.670005 1.375423 -2.163859
8 0.946041 -0.768778 1.991812
6 3.025258 -1.041333 3.107024
6 -1.381012 1.707041 -3.276659
1 3.524968 -0.191249 3.578771
1 -1.021118 1.230215 -4.192196
8 2.005749 -1.120709 -1.465695
8 -0.317409 1.735811 1.363391
6 1.113575 -2.013413 -1.247383
6 0.543620 2.621694 1.126322
1 3.804714 -1.703114 2.721024
1 -2.442077 1.501585 -3.139521
8 1.533117 2.520883 0.326221
8 0.102138 -1.868770 -0.520859
6 1.329312 -3.333645 -1.929882
6 0.388268 3.946403 1.821792
1 0.524914 -4.024889 -1.681553
1 -0.268337 4.585915 1.222499
1 2.291976 -3.747019 -1.616974
1 -0.081583 3.799932 2.795141
1 1.373256 -3.183361 -3.012198
1 1.355293 4.439428 1.926786
7 6.700171 0.594071 -1.552877
6 5.509754 -0.054243 -1.369178
8 5.294430 -1.037362 -0.713054
6 4.441944 0.687830 -2.315254
8 3.818686 -0.222280 -3.146833
6 5.356422 1.610572 -3.095565
6 5.084775 2.410342 -4.190865
6 6.117751 3.179556 -4.734721
6 7.394857 3.130767 -4.180458
6 7.685614 2.302908 -3.094197
6 6.651754 1.539999 -2.572839
6 3.553123 1.414791 -1.357469
8 4.919772 2.345381 0.224001
6 4.153526 2.591853 -0.683431
8 3.832647 3.829363 -1.024966
6 2.023477 5.218432 -1.732127
6 2.907560 4.053004 -2.104254
1 7.539013 0.284513 -1.087323
1 3.207690 -0.761921 -2.605286
1 4.090456 2.419139 -4.627373
1 5.926068 3.811405 -5.596157
1 8.188290 3.737177 -4.607256
1 8.689003 2.250594 -2.683379
1 1.348981 5.450922 -2.561825
1 2.623309 6.106690 -1.515364
1 1.427708 4.970408 -0.851764
1 3.500023 4.268227 -2.998783
1 2.305231 3.153472 -2.283579

mc1"

45 2.759227 -0.497778 -0.015293
45 1.581462 -2.118199 1.356740
8 4.424423 -1.033667 1.023941
1 5.531157 -3.036057 3.341671
1 -1.495659 0.704980 -1.263616
6 4.371617 -1.949462 1.904535
8 -0.144244 -1.589638 0.396048
6 -0.090302 -0.723223 -0.514087
8 0.951969 -0.102980 -0.905953
8 3.343731 -2.586894 2.259911
6 5.679033 -2.285699 2.565533
6 -1.365206 -0.379406 -1.235832
1 6.115322 -1.378078 2.989694
1 -1.293763 -0.728414 -2.270081
8 3.104316 -2.038161 -1.309877
8 1.303412 -0.628908 2.735937
6 2.633015 -3.190266 -1.063524
6 1.741681 0.524552 2.493234
1 6.374142 -2.658582 1.808439
1 -2.216887 -0.852668 -0.748114
8 2.338552 0.898800 1.430073
8 1.941255 -3.527268 -0.062129
6 2.942586 -4.249642 -2.086706
6 1.520552 1.584294 3.539451
1 2.512433 -5.205696 -1.789580
1 0.546437 2.054563 3.368250
1 4.026849 -4.338819 -2.192460
1 1.504645 1.128592 4.530273
1 2.542873 -3.942577 -3.056759
1 2.294249 2.350550 3.477130
7 6.704287 1.183995 -2.401040
6 5.842784 0.156208 -2.118677
8 6.121517 -0.968954 -1.807066
6 4.365793 0.730369 -2.389432
8 3.597089 -0.115464 -3.179744
6 4.698178 2.058922 -3.045351
6 3.872204 2.963996 -3.689758
6 4.434353 4.127048 -4.223728
6 5.803283 4.359980 -4.109516
6 6.650138 3.436962 -3.492231
6 6.077197 2.284213 -2.976552
6 3.783526 0.850787 -1.020297
8 5.398609 1.866242 0.254086
6 4.296638 2.002164 -0.234624
8 3.573032 3.095588 -0.051349
6 1.384041 3.974169 0.305240

6 2.264020 3.194392 -0.641016
1 7.699536 1.073249 -2.287147
1 4.081171 -0.266438 -3.998297
1 2.810346 2.757912 -3.790282
1 3.803579 4.849216 -4.732228
1 6.228177 5.270667 -4.521177
1 7.719581 3.612732 -3.431076
1 0.395343 4.116755 -0.141393
1 1.814201 4.957621 0.514092
1 1.270858 3.431077 1.245011
1 2.375477 3.714936 -1.597255
1 1.851464 2.194606 -0.822542

mc2

45 1.974712 0.689102 -0.936831
45 -0.235525 0.177243 -0.079968
8 2.627467 0.640333 0.992884
1 1.767431 -0.287149 3.965944
1 -0.824182 1.634602 -4.602598
6 1.809172 0.357082 1.924910
8 -0.934196 0.256750 -2.002843
6 -0.127645 0.507681 -2.935313
8 1.123361 0.725216 -2.814841
8 0.579585 0.111298 1.788931
6 2.374433 0.346412 3.318625
6 -0.679739 0.583066 -4.333892
1 2.354792 1.366821 3.715264
1 0.029087 0.150061 -5.042171
8 2.242515 -1.332331 -1.177578
8 -0.545528 2.186403 0.117978
6 1.311739 -2.139248 -0.822833
6 0.361364 2.983503 -0.237785
1 3.411886 0.009897 3.300128
1 -1.641715 0.073560 -4.388678
8 1.499507 2.670482 -0.719322
8 0.205424 -1.809959 -0.330833
6 1.608477 -3.600451 -1.006760
6 0.099742 4.455620 -0.061009
1 0.732414 -4.200787 -0.764239
1 0.486388 5.013285 -0.916313
1 2.442447 -3.877988 -0.355756
1 -0.967055 4.638089 0.067238
1 1.924976 -3.789304 -2.035840
1 0.629313 4.803672 0.831532
7 6.663552 1.087016 -2.787863
6 5.977169 -0.134754 -2.715869
8 6.488641 -1.216214 -2.684939
6 4.473370 0.192809 -2.696686
8 3.699057 -0.667471 -3.394210
6 4.468245 1.736013 -3.012226
6 3.459463 2.570829 -3.538608
6 3.812756 3.818197 -4.016884
6 5.158514 4.220700 -4.013216
6 6.186190 3.389613 -3.577961
6 5.839022 2.127203 -3.107657
6 3.999790 0.929044 -1.541496
8 5.527644 0.171055 0.046219
6 4.976277 1.142774 -0.418035
8 5.215635 2.348006 0.096134
6 4.026346 4.189869 1.030027
6 4.464593 3.518301 -0.251310
1 7.671446 1.115521 -2.825450
1 3.054420 -1.044327 -2.763876
1 2.432032 2.220629 -3.511444
1 3.052316 4.491942 -4.397167
1 5.413949 5.208523 -4.387430
1 7.223845 3.701228 -3.639393
1 3.501744 5.122753 0.799996
1 4.883265 4.421837 1.668415
1 3.347608 3.531844 1.578442
1 5.128776 4.166066 -0.834678
1 3.594537 3.258274 -0.852710

ts2

45 1.970649 0.686301 -0.953452
45 -0.245194 0.192381 -0.102539
8 2.613442 0.682481 0.979467
1 1.916708 -0.412692 3.876917
1 -0.798738 1.560374 -4.657393
6 1.790707 0.410565 1.910372
8 -0.929108 0.244652 -2.033434
6 -0.114802 0.462483 -2.966389
8 1.139448 0.667120 -2.844046
8 0.562700 0.157124 1.770856
6 2.340450 0.418769 3.310618
6 -0.658266 0.513348 -4.369473
1 2.034691 1.346074 3.805597
1 0.053270 0.066944 -5.066539
8 2.245654 -1.333185 -1.166401
8 -0.554807 2.205380 0.067332
6 1.312982 -2.132879 -0.801893
6 0.351154 2.996259 -0.303654
1 3.428725 0.362030 3.294410
1 -1.621414 0.005683 -4.420788
8 1.486269 2.674619 -0.787218
8 0.201883 -1.797045 -0.323543
6 1.614389 -3.597577 -0.947470
6 0.092925 4.471481 -0.148085
1 0.713327 -4.189837 -0.791499
1 0.453403 5.011553 -1.026001

1	2.369093	-3.875713	-0.205650
1	-0.969584	4.656936	0.007884
1	2.040537	-3.797279	-1.933364
1	0.650117	4.838225	0.719838
7	6.637608	1.118187	-2.822993
6	5.970045	-0.111656	-2.799002
8	6.494676	-1.186662	-2.839670
6	4.463891	0.171396	-2.705581
8	3.696970	-0.656458	-3.424263
6	4.427617	1.804294	-2.916692
6	3.420235	2.646553	-3.442998
6	3.775224	3.870292	-3.973684
6	5.126749	4.250888	-4.024894
6	6.151122	3.408919	-3.607969
6	5.800184	2.163275	-3.095057
6	4.016856	0.926554	-1.566669
8	5.549667	0.079299	-0.006112
6	4.992044	1.066466	-0.427470
8	5.233638	2.250536	0.138616
6	4.168756	4.124049	1.147356
6	4.475976	3.429136	-0.159576
1	7.642749	1.153449	-2.903926
1	2.964646	-0.946208	-2.846058
1	2.386956	2.324549	-3.364420
1	3.012298	4.545707	-4.345983
1	5.386955	5.223615	-4.433701
1	7.192238	3.693888	-3.721005
1	3.641295	5.063722	0.954162
1	5.084026	4.348154	1.702167
1	3.532860	3.485591	1.766056
1	5.090108	4.062444	-0.811457
1	3.549849	3.174685	-0.673477
45	1.970649	0.686301	-0.953452
45	-0.245194	0.192381	-0.102539
8	2.613442	0.682481	0.979467
1	1.916708	-0.412692	3.876917
1	-0.798738	1.560374	-4.657393
6	1.790707	0.410565	1.910372
8	-0.929108	0.244652	-2.033434
6	-0.114802	0.462483	-2.966389
8	1.139448	0.667120	-2.844046
8	0.562700	0.157124	1.770856
6	2.340450	0.418769	3.310618
6	-0.658266	0.513348	-4.369473
1	2.034691	1.346074	3.805597
1	0.053270	0.066944	-5.066539
8	2.245654	-1.333185	-1.166401
8	-0.554807	2.205380	0.067332
6	1.312982	-2.132879	-0.801893
6	0.351154	2.996259	-0.303654
1	3.428725	0.362030	3.294410
1	-1.621414	0.005683	-4.420788
8	1.486269	2.674619	-0.787218
8	0.201883	-1.797045	-0.323543
6	1.614389	-3.597577	-0.947470
6	0.092925	4.471481	-0.148085
1	0.713327	-4.189837	-0.791499
1	0.453403	5.011553	-1.026001
1	2.369093	-3.875713	-0.205650
1	-0.969584	4.656936	0.007884
1	2.040537	-3.797279	-1.933364
1	0.650117	4.838225	0.719838
7	6.637608	1.118187	-2.822993
6	5.970045	-0.111656	-2.799002
8	6.494676	-1.186662	-2.839670
6	4.463891	0.171396	-2.705581
8	3.696970	-0.656458	-3.424263
6	4.427617	1.804294	-2.916692
6	3.420235	2.646553	-3.442998
6	3.775224	3.870292	-3.973684
6	5.126749	4.250888	-4.024894
6	6.151122	3.408919	-3.607969
6	5.800184	2.163275	-3.095057
6	4.016856	0.926554	-1.566669
8	5.549667	0.079299	-0.006112
6	4.992044	1.066466	-0.427470
8	5.233638	2.250536	0.138616
6	4.168756	4.124049	1.147356
6	4.475976	3.429136	-0.159576
1	7.642749	1.153449	-2.903926
1	2.964646	-0.946208	-2.846058
1	2.386956	2.324549	-3.364420
1	3.012298	4.545707	-4.345983
1	5.386955	5.223615	-4.433701
1	7.192238	3.693888	-3.721005
1	3.641295	5.063722	0.954162
1	5.084026	4.348154	1.702167
1	3.532860	3.485591	1.766056
1	5.090108	4.062444	-0.811457
1	3.549849	3.174685	-0.673477

mc3

45	1.856744	0.873458	-1.214242
45	-0.305867	0.404890	-0.237732
8	2.278836	1.904772	0.514573
1	0.978365	2.750260	3.390772
1	-0.319583	-0.828398	-4.944507
6	1.403368	1.971454	1.439108
8	-0.812077	-0.639746	-1.918736
6	0.026814	-0.736779	-2.844504

8	1.199374	-0.223664	-2.822098
8	0.257277	1.454608	1.410727
6	1.795312	2.742229	2.670179
6	-0.344341	-1.500453	-4.081809
1	2.058252	3.766536	2.392323
1	0.391658	-2.288882	-4.260475
8	2.538191	-0.833453	-0.307091
8	-0.989280	2.120769	-1.102696
6	1.727228	-1.538768	0.371976
6	-0.199780	2.800388	-1.819061
1	2.682202	2.286505	3.119545
1	-1.339248	-1.931177	-3.976660
8	1.021852	2.540252	-2.049455
8	0.505378	-1.289674	0.570641
6	2.287363	-2.775773	1.020194
6	-0.758050	4.025383	-2.490169
1	1.572939	-3.595960	0.928232
1	-1.077026	3.756442	-3.502288
1	2.430110	-2.581832	2.088096
1	-1.623618	4.397321	-1.941367
1	3.244254	-3.045475	0.573648
1	0.013160	4.792570	-2.573566
7	5.776500	2.300847	-4.108820
6	5.369174	1.018106	-4.349281
8	5.897242	0.309451	-5.178034
6	4.178320	0.552716	-3.501313
8	3.242002	0.104003	-4.323469
6	4.272131	2.836030	-2.267250
6	3.752490	3.818464	-1.422728
6	4.158454	5.146550	-1.514112
6	5.088240	5.524119	-2.477339
6	5.607790	4.572010	-3.344052
6	5.208743	3.238626	-3.240079
6	3.918129	1.387324	-2.219846
8	4.785696	-0.526711	-2.563099
6	4.716307	0.369724	-1.612106
8	5.350732	0.145784	-0.514992
6	5.514361	0.462087	1.837562
6	5.353016	1.167015	0.515110
1	6.522659	2.608291	-4.717900
1	2.403613	-0.068405	-3.828760
1	3.018166	3.525792	-0.683215
1	3.739261	5.885914	-0.838348
1	5.406749	6.558810	-2.562944
1	6.329913	4.855653	-4.105932
1	5.566725	1.202454	2.641260
1	6.429383	-0.135651	1.860536
1	4.660060	-0.194597	2.020348
1	6.191154	1.835949	0.297886
1	4.414031	1.720080	0.469516

ts3

45	1.811490	0.926430	-1.221499
45	-0.347183	0.385898	-0.245499
8	2.107505	2.078131	0.449697
1	0.732239	2.965248	3.275462
1	-0.127484	-1.159595	-4.891996
6	1.214772	2.144873	1.355882
8	-0.765118	-0.796481	-1.877875
6	0.081289	-0.911455	-2.782621
8	1.239962	-0.341821	-2.750925
8	0.102636	1.557257	1.341309
6	1.535232	3.012958	2.540792
6	-0.212244	-1.760364	-3.981662
1	1.670891	4.045679	2.207272
1	0.528030	-2.562776	-4.048462
8	2.570733	-0.669813	-0.192915
8	-1.092857	2.017440	-1.232479
6	1.788920	-1.387836	0.506032
6	-0.330785	2.694186	-1.978783
1	2.476549	2.686521	2.990556
1	-1.213634	-2.181714	-3.907051
8	0.905605	2.481403	-2.189851
8	0.548048	-1.207678	0.667816
6	2.412773	-2.550278	1.228901
6	-0.933975	3.862744	-2.710264
1	1.718509	-3.391894	1.248819
1	-0.955064	3.642625	-3.781779
1	2.609745	-2.256382	2.265100
1	-1.947351	4.052902	-2.358086
1	3.353663	-2.832682	0.756162
1	-0.307071	4.746454	-2.571405
7	5.651267	2.457566	-4.242028
6	4.870652	1.458711	-4.722972
8	5.034090	0.903494	-5.787838
6	3.760065	1.026265	-3.760738
8	2.877239	0.364542	-4.353594
6	4.410751	2.775748	-2.179361
6	4.075160	3.659471	-1.150330
6	4.675226	4.908801	-1.023323
6	5.628266	5.324951	-1.945979
6	5.949239	4.494274	-3.009756
6	5.340218	3.245098	-3.128205
6	3.829624	1.378884	-2.313175
8	4.821783	-0.721364	-2.644562
6	4.706123	0.230283	-1.878520
8	5.416719	0.209861	-0.759345
6	5.651124	0.335235	1.591000
6	5.218823	1.088464	0.353561
1	6.393436	2.754073	-4.861040

1	2.127036	-0.010784	-3.711830
1	3.329690	3.351636	-0.430297
1	4.388293	5.558594	-0.201893
1	6.105500	6.295965	-1.854703
1	6.664474	4.812141	-3.764592
1	5.558696	0.980389	2.470457
1	6.691952	0.010179	1.509841
1	5.022049	-0.546815	1.734950
1	5.827738	1.985977	0.203401
1	4.169796	1.376614	0.422385

6-$Rh_2(OAc)_4$

45	1.746767	1.230702	-1.433779
45	-0.475910	0.953880	-0.637056
8	1.791538	3.019665	-0.456750
1	0.455289	4.650056	1.888616
1	0.130232	-2.278014	-4.066699
6	0.768201	3.395166	0.189676
8	-0.552371	-0.833282	-1.604475
6	0.460937	-1.203726	-2.266075
8	1.553752	-0.568035	-2.371858
8	-0.317900	2.753911	0.302587
6	0.846887	4.732201	0.872460
6	0.361374	-2.499713	-3.019939
1	0.213869	5.443332	0.333020
1	1.319141	-3.022028	-2.992662
8	2.399574	0.264502	0.252814
8	-1.153594	1.880462	-2.317600
6	1.537672	-0.117403	1.102193
6	-0.299314	2.287806	-3.159069
1	1.875049	5.094138	0.882062
1	-0.433731	-3.121032	-2.607718
8	0.959054	2.172958	-3.051277
8	0.284589	0.027676	1.010325
6	2.054771	-0.778437	2.350438
6	-0.811093	2.975293	-4.392518
1	1.365842	-1.560825	2.672405
1	0.010469	3.174348	-5.080485
1	2.109473	-0.029536	3.146933
1	-1.567504	2.348151	-4.870399
1	3.052551	-1.185385	2.184193
1	-1.297019	3.912478	-4.105900
7	3.941981	3.899008	-3.259283
6	3.597285	2.826291	-4.031452
8	3.197479	2.934726	-5.174720
6	3.816870	1.508768	-3.363167
8	3.608916	0.498537	-4.159375
6	4.604779	2.643988	-1.303336
6	5.026796	2.694090	0.035944
6	5.293557	3.897950	0.668051
6	5.134980	5.104932	-0.014190
6	4.690518	5.092251	-1.323912
6	4.416677	3.878016	-1.960561
6	4.283092	1.414762	-2.042480
8	4.508626	-0.938503	-2.343485
6	4.722886	0.054958	-1.647632
8	5.412886	-0.026205	-0.519790
6	7.154501	-1.710484	-0.795210
6	5.851156	-1.339657	-0.122472
1	3.806356	4.792266	-3.712749
1	3.810219	-0.321976	-3.621905
1	5.131800	1.771296	0.586027
1	5.623655	3.895150	1.702338
1	5.350991	6.049906	0.475279
1	4.545042	6.020829	-1.870406
1	7.507191	-2.672578	-0.411045
1	7.923061	-0.958875	-0.595187
1	7.018207	-1.802186	-1.874988
1	5.966739	-1.261812	0.961025
1	5.061011	-2.057526	-0.353621

eda-$Rh_2(OAc)_4$

45	1.699291	0.812298	-0.724886
45	-0.080423	-0.158835	0.531003
8	2.973705	0.198817	0.740959
1	3.025585	-1.490037	3.526303
1	-1.840113	2.560868	-3.128916
6	2.500374	-0.414011	1.747977
8	-1.360184	0.447801	-0.947087
6	-0.897043	1.052134	-1.951737
8	0.326991	1.346161	-2.150833
8	1.284764	-0.706875	1.937957
6	3.484860	-0.805130	2.814046
6	-1.864693	1.472627	-3.023601
1	3.815226	0.097426	3.336868
1	-1.555382	1.044971	-3.980886
8	1.950436	-0.984441	-1.662394
8	-0.315484	1.634049	1.473639
6	1.185333	-1.946994	-1.334886
6	0.439880	2.594214	1.152838
1	4.366479	-1.258435	2.356073
1	-2.874528	1.147341	-2.776387
8	1.353844	2.565925	0.269249
8	0.259761	-1.903243	-0.477170
6	1.432911	-3.261581	-2.021746
6	0.224936	3.904459	1.859175
1	0.563837	-3.911789	-1.923301
1	-0.430800	4.533393	1.248018
1	2.293617	-3.747833	-1.551671
1	-0.257858	3.737975	2.822367

1	1.676174	-3.096838	-3.072980
1	1.175727	4.424620	1.986042
6	3.512456	1.629670	-1.845384
8	4.906019	2.956448	-0.522458
6	3.991725	2.951840	-1.304197
8	3.416402	4.093786	-1.688822
6	1.463215	5.421720	-1.905320
6	2.162091	4.169896	-2.381362
7	3.146895	1.556174	-3.133230
7	2.770263	1.472175	-4.187753
1	4.179512	0.808464	-1.588152
1	0.519243	5.547859	-2.444294
1	2.082498	6.305799	-2.077662
1	1.251127	5.344285	-0.836546
1	2.363920	4.223549	-3.458743
1	1.548711	3.290697	-2.169416

ts_{eda}

45	1.724972	0.817032	-0.728287
45	-0.077093	-0.176871	0.535066
8	2.962617	0.197943	0.774955
1	2.982650	-1.399697	3.616429
1	-1.807555	2.516450	-3.173236
6	2.480608	-0.417169	1.779403
8	-1.347555	0.421316	-0.959741
6	-0.882544	1.022851	-1.959858
8	0.343710	1.329128	-2.150284
8	1.269735	-0.718856	1.961071
6	3.468715	-0.803809	2.844551
6	-1.836497	1.430379	-3.049238
1	3.891351	0.103480	3.285106
1	-1.519707	0.984547	-3.995921
8	1.991127	-0.979261	-1.657497
8	-0.317832	1.631281	1.462888
6	1.234444	-1.950471	-1.324620
6	0.429782	2.592012	1.140356
1	4.293672	-1.361526	2.394922
1	-2.849346	1.111333	-2.806307
8	1.352536	2.570440	0.260426
8	0.303044	-1.916813	-0.477026
6	1.512482	-3.263353	-2.004626
6	0.209116	3.908320	1.835285
1	0.664710	-3.938080	-1.887762
1	-0.347743	4.574541	1.168416
1	2.395395	-3.718096	-1.544460
1	-0.369758	3.760473	2.746792
1	1.735255	-3.101100	-3.060909
1	1.168101	4.379976	2.058131
6	3.343369	1.583031	-1.643775
8	4.839849	2.827002	-0.466786
6	3.928724	2.899830	-1.260424
8	3.453562	4.075182	-1.654290
6	1.572082	5.510153	-1.847034
6	2.196853	4.223587	-2.333325
7	2.900085	1.629223	-3.480079
7	2.252471	1.297014	-4.313065
1	4.147641	0.867498	-1.833058
1	0.631468	5.689387	-2.376832
1	2.236701	6.359964	-2.023063
1	1.365222	5.442809	-0.776467
1	2.397087	4.271120	-3.410483
1	1.543792	3.374200	-2.119647

mc_{eda}

45	1.835585	0.958666	-0.540107
45	-0.061293	-0.105578	0.536353
8	2.952957	0.242249	1.001788
1	2.784831	-1.512119	3.743400
1	-1.420998	2.776458	-3.231390
6	2.408393	-0.447315	1.924667
8	-1.258957	0.587793	-0.967209
6	-0.732789	1.255176	-1.891541
8	0.501164	1.569630	-1.987091
8	1.190895	-0.758044	2.001439
6	3.332042	-0.916696	3.013298
6	-1.614104	1.722844	-3.017423
1	3.786227	-0.048984	3.498943
1	-1.371457	1.152035	-3.919020
8	2.159607	-0.776862	-1.557524
8	-0.330384	1.650915	1.560580
6	1.366039	-1.756660	-1.355380
6	0.442278	2.620947	1.349662
1	4.141910	-1.505443	2.575095
1	-2.662957	1.570325	-2.764899
8	1.419615	2.647602	0.527329
8	0.380095	-1.772580	-0.573373
6	1.652890	-2.998331	-2.154682
6	0.191100	3.894333	2.110201
1	1.011449	-3.816598	-1.829296
1	-0.331687	4.601350	1.457747
1	2.705115	-3.271608	-2.045824
1	-0.432526	3.694570	2.981454
1	1.475248	-2.790048	-3.213954
1	1.137985	4.349442	2.405750
6	3.342742	1.770117	-1.420225
8	4.854827	2.957364	-0.333788
6	3.929587	3.073436	-1.112741
8	3.494442	4.228224	-1.573138
6	1.280008	5.069728	-1.982038
6	2.402640	4.213386	-2.514302

7 2.413071	0.784682	-4.613947
7 1.696570	-0.042737	-4.740498
1 3.941995	1.152295	-2.099337
1 0.473510	5.121120	-2.719881
1 1.628429	6.086248	-1.779775
1 0.889168	4.635332	-1.059391
1 2.804369	4.599692	-3.455966
1 2.053669	3.185044	-2.673271
6 2.905876	3.932736	-2.467219
1 4.070681	0.750975	-1.881574
1 1.071587	4.991473	-2.788757
1 2.243873	5.865754	-1.782798
1 1.348615	4.482632	-1.105930
1 3.392119	4.278755	-3.384242
1 2.483930	2.934538	-2.643692

mc'$_{eda}$

45 1.880615	0.810222	-0.451669
45 -0.189655	-0.048426	0.475525
8 2.798521	0.013231	1.179553
1 2.233621	-1.610380	3.947654
1 -1.113181	2.988246	-3.227404
6 2.118187	-0.609335	2.059016
8 -1.191516	0.726792	-1.125459
6 -0.533319	1.338376	-2.002943
8 0.728905	1.530641	-2.001785
8 0.873171	-0.795192	2.042132
6 2.904376	-1.169583	3.210823
6 -1.278333	1.908466	-3.179069
1 3.502946	-0.376305	3.664810
1 -0.887606	1.474730	-4.103418
8 2.109207	-0.958400	-1.434454
8 -0.369772	1.738746	1.464044
6 1.215059	-1.857094	-1.283141
6 0.511674	2.624220	1.313742
1 3.597670	-1.928588	2.837824
1 -2.343601	1.698526	-3.089802
8 1.548449	2.545170	0.571299
8 0.174549	-1.767655	-0.580473
6 1.459464	-3.148018	-2.015777
6 0.340001	3.920725	2.057231
1 0.573781	-3.781240	-1.973858
1 0.073842	4.710301	1.347550
1 2.301600	-3.668075	-1.549520
1 -0.449109	3.827281	2.802769
1 1.734689	-2.940808	-3.052235
1 1.283372	4.205839	2.527631
6 3.514027	1.448183	-1.243211
8 5.087609	2.507355	-0.110862
6 4.221167	2.691450	-0.942301
8 3.940168	3.867751	-1.465417
6 1.826141	4.879786	-2.004191

B. Biological Evaluation

Biological assay were performed in collaboration with Cellular Function and Therapeutic Targeting group of iMed.ULisboa of Professor Cecília Rodrigues.

Biochemical assay were performed in collaboration with Metabolism and Genetics group of iMed.ULisboa of Professor Ana Paula Leandro.

B1. Cell viability assays

Human cancer cell lines from breast (MCF-7), colon (HT-29) and lung (NCI-H460) were purchased from ATCC and cultivated in RPMI-1640 with L- glutamine and 10% fetal bovine serum (FBS) in a humidified atmosphere with 5% CO2 at 37 ºC. Cells were plated in 96-well plates with a density of 5x104 (NCI-H460), 1x105 (HT-29) and 1.5x105 (MCF-7) cells/well and cultured for 24 hours. Stock solutions of the compounds to be tested were prepared in DMSO and then diluted with the cell culture medium with 0.5% FBS (final concentration of organic solvent <1%). Cells were incubated with the compounds at 0-20 μM concentration for 48 hours. Cells were then washed with PBS and incubated with 0.5% FBS cell culture medium containing 50 μg/ml neutral red. Three hours later, cells were washed again with PBS and the amount of neutral red retained by the cells was extracted with an organic solution (20 ml distilled water, 20 ml ethanol and 400 μl glacial acetic acid). Absorbance of the samples was measured at 540 nm in a plate reader after gentle shaking. Viability was determined by the ratio of absorbance of treated and control cells. Two independent experiments were performed, each with 4 replicates for each experimental condition. IC_{50} were determined using GraphPad Prism 5.

B2. Cell death assays

For cell death assays**,** general cell death was evaluated using lactate dehydrogenase (LDH) Cytotoxicity Detection KitPLUS (Roche Diagnostics GmbH, Mannheim, Germany), by measuring the amount of cytosolic LDH released from plasma

membrane-damaged cells into the extracellular medium. Briefly, 50 μL of culture supernatant was collected from each well and added to a new 96-well plate to evaluate LDH release. In parallel, cells on the original plate were incubated for 15 min with lysis solution diluted in 50 μL of medium, to completely disrupt the remaining cells and release the intracellular LDH into medium. Subsequently, supernatant samples and total cell lysates were incubated with 50 μL of assay substrate for 10 to 30 min, at room temperature, protected from light. Absorbance readings were measured a t490 nm, with 620 nm reference wavelength, using a Model 680 microplate reader (Bio-Rad). Percentage of LDH release was determined as the ratio between the released LDH (supernatant) and total LDH (supernatant + cell lysate) in each well. Results are displayed as fold-change to vehicle (DMSO) control ± SEM

B3. Enzymatic activity assays

The hPAH activity was measured essentially as previously described in a 200 μL final volume reaction mixture, containing 100 μM L-Phe, 0.1 M Na-Hepes, pH 7, 0.1 mg·mL-1 catalase, 5 μg of recombinant wild-type hPAH tetramers, 100 μM of each compound or 1% DMSO (vehicle control). After 4 minutes of pre-incubation, 100 μM $(NH_4)_2Fe(II)SO_4$ was added and, unless otherwise stated, the reaction was started by addition of 75 μM BH_4 (together with 5 mM ascorbic acid) after 1 minute incubation with he iron (condition I in Figure C1; 'substrate-activated' condition). To study the specific activity of the non-activated hPAH, 100 μM L-Phe and 100 μM of each compound were added together with 75 μM BH4 at the start of the hydroxylation reaction (condition II in Figure C1; 'non-activated' condition). To evaluate pre-activation of the enzyme by the compound, hPAH was pre-incubated 4 minutes with each compound whereas the L-Phe substrate was only added at the start of the reaction, together with 75 μM BH_4 at the start of the reaction (condition III in Figure C1; 'compound-activated' condition. Blank reactions where the substrate L-Phe was omitted were also made for each compound. The amount of L-Tyr produced after 1 min was quantified by a HPLC method23 using a LiChroCART® 250-4 LiChrospher® 60 RP-select B (5 μm) column (Merck KGaA, Darmstadt, Germany),

a 5% ethanol mobile phase pumped at 0.7 mL·min-1 and fluorimetric detection (λexc= 274 nm and λem= 304nm). Specific activities are presented as mean ± SEM obtained from three independent experiments.

I)

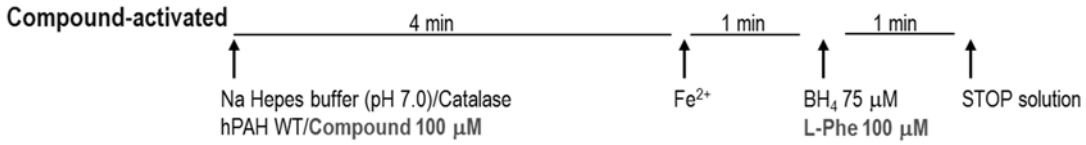

II)

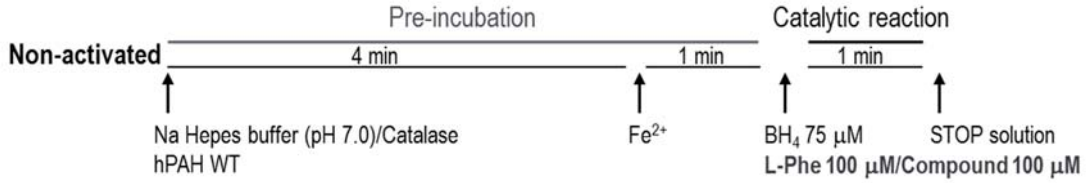

II)

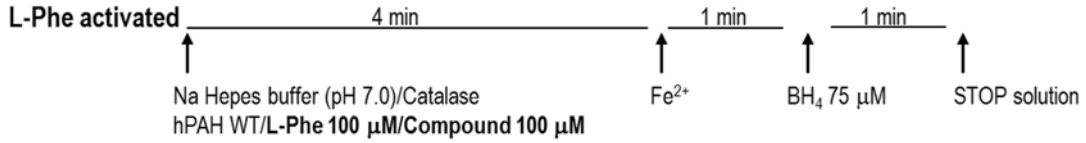

Figure B3.1 - Depiction of the enzymatic reactions used in this study for evaluation of competition between substrate and compound (I - Substrate-activated condition), and activation by the compound (II - Non-activated *versus* III – Compound-activated condition). A blank reaction without the substrate was included and subtracted for each condition in order to rule out contribution of the compound to tyrosine formation.

B4. Differential Scanning Fluorimetry

Differential scanning fluorimetry (DSF) was performed in a C1000 Touch thermal cycler equipped with a CFX96 optical reaction module (Bio Rad). For all fluorescence measurements, samples containing purified recombinant wild-type hPAH tetramers

at 100 μg·mL-1 in 20 mM NaHepes, 200 mM NaCl, pH 7, 2.5-fold Sypro Orange (Invitrogen; 5000-fold commercial stock solution), 1% DMSO (unless otherwise stated) and 100 μM of each compound were incubated at 20 ºC for 10 minutes. The PCR plate was sealed with Optical-Quality Sealing Tape (Bio-Rad) and centrifuged at 500xg for 1min. The DSF assay was carried out by increasing the temperature from 20 to 90 °C, with a 1 s hold time every 0.2 °C and fluorescence acquisition using the FRET channel. Control experiments in the absence of DMSO and/or compounds were routinely performed in each microplate. Data were processed using CFX Manager Software V3.0 (Bio-Rad) and the GraphPad Prism 6. Temperature scan curves were fitted to a biphasic dose-response function and the Tm values were obtained from the midpoint of the first and second transitions. Tests for statistical significance were performed using 1-way ANOVA by comparing the compound data to the DMSO control assay (for DSF studies) or the L-Phe activated condition III to the compound activated condition II (for the catalytic activity assays). Data was considered statistical different when $P < 0.01$

C. NMR chemical shift assignment

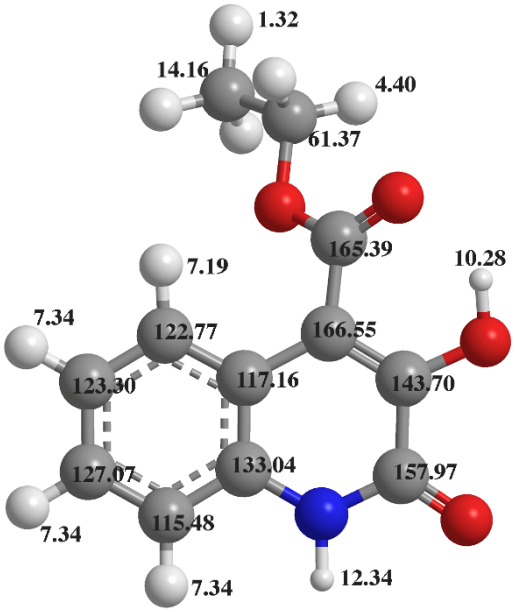

Figure C1 – Assignment of ^{1}H and ^{13}C NMR spectra of **69**.

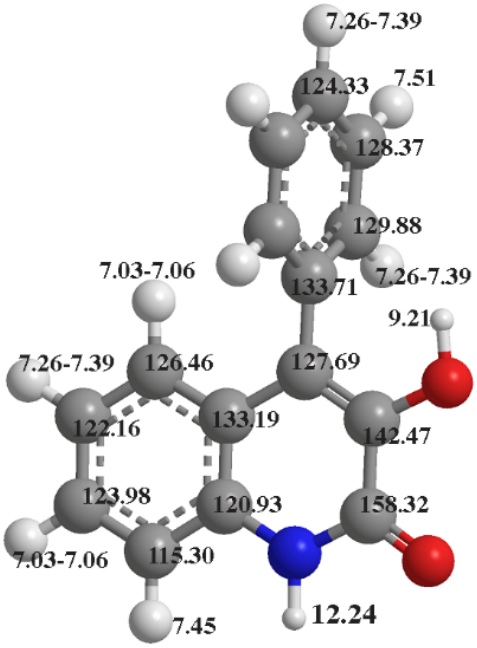

Figure C2 – Assigment of ^{1}H and ^{13}C NMR spectra of **31**.

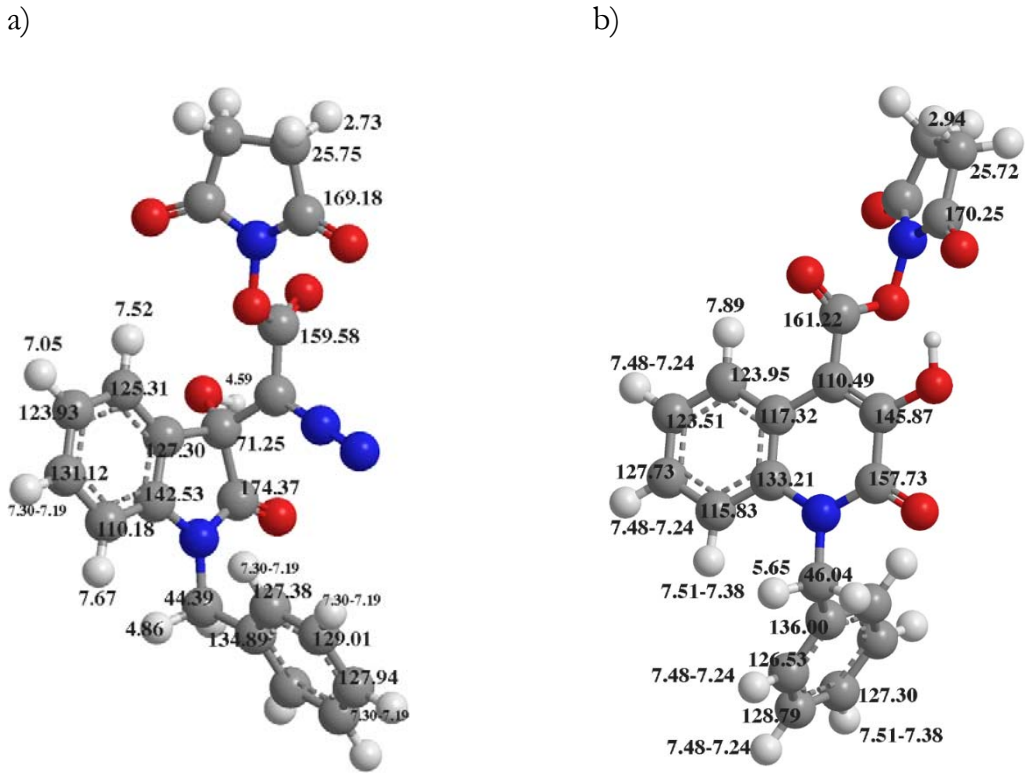

Figure C3 – Assignment of the ^{1}H and ^{13}C NMR spectra of a) **125** and b) **126**.

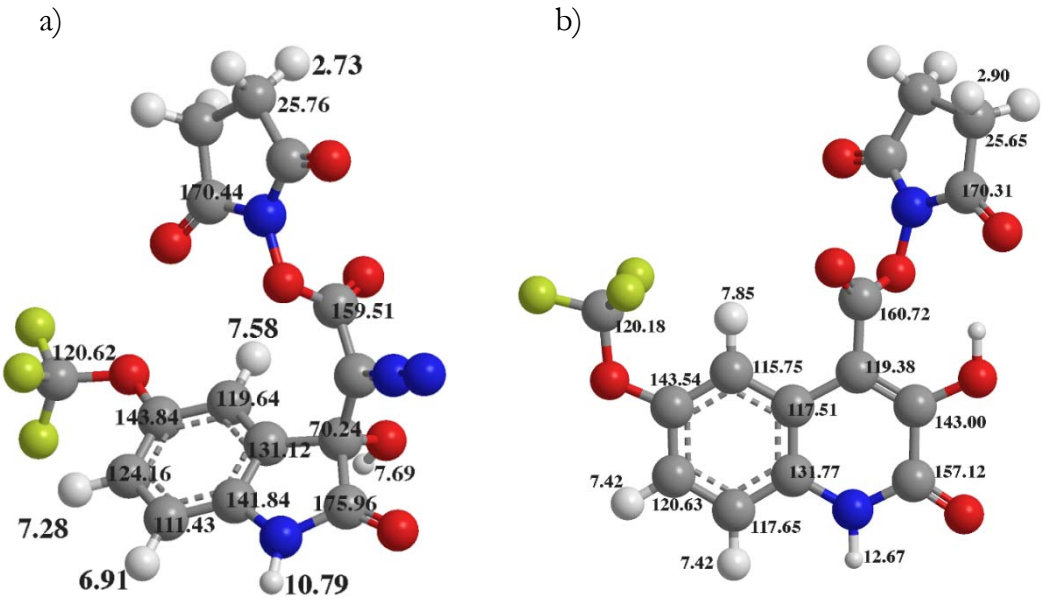

Figure C4 – Assignment of the ^{1}H and ^{13}C NMR spectra of a) **130** and b) **131**.

D. Structures tested in biological assays.

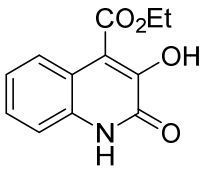

69

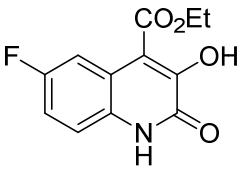

84

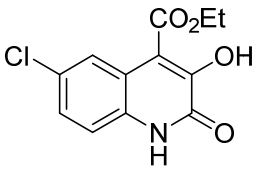

85

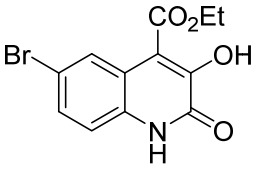

86

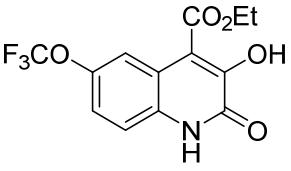

87

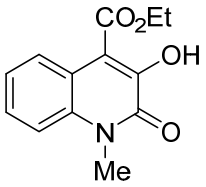

88

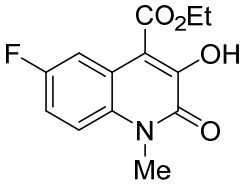

89

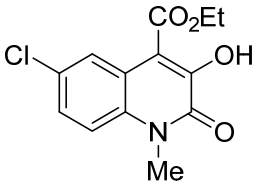

90

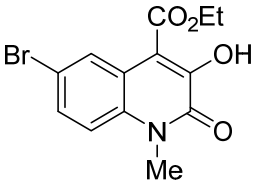

91

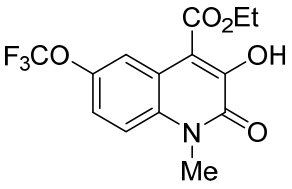

92

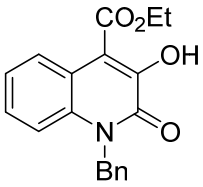

93

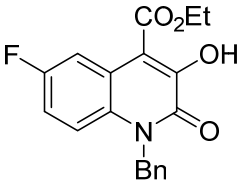

94

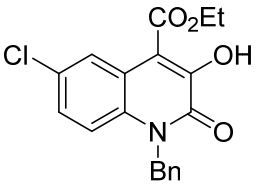

95

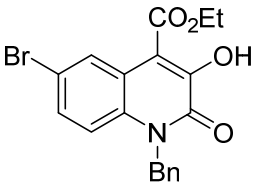

96

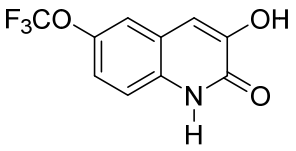

111

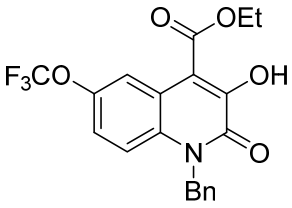

112

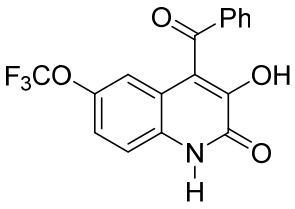

116

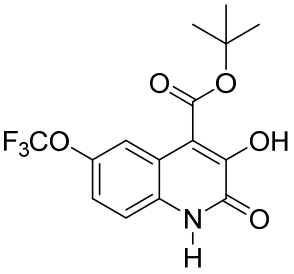

117

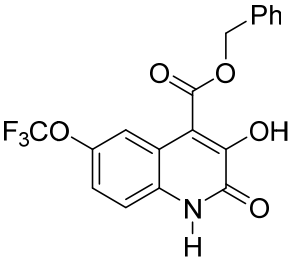

118

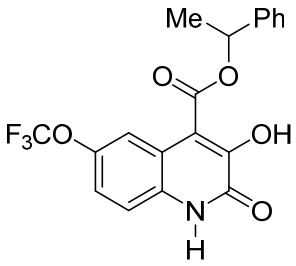

119

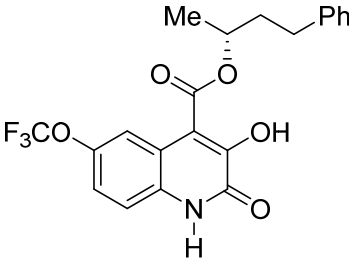

120

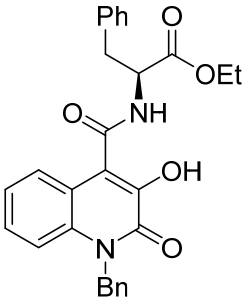

129

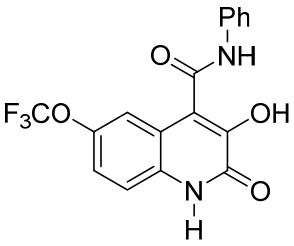

132

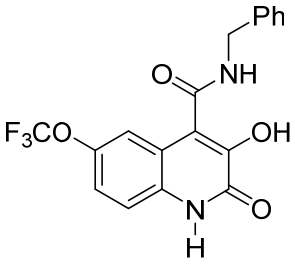

133

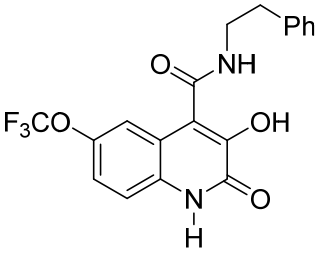

134

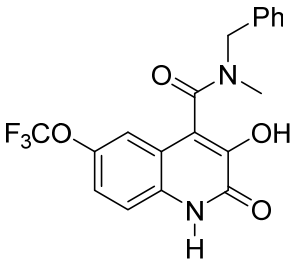

135

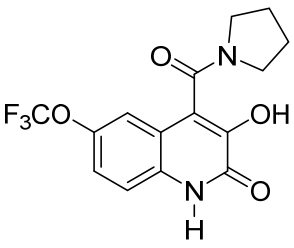

136

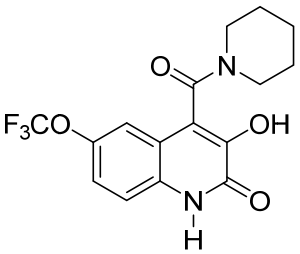

137

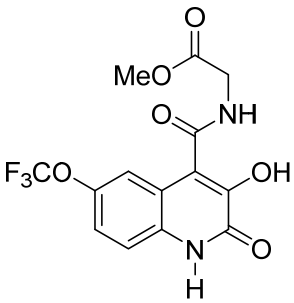

138

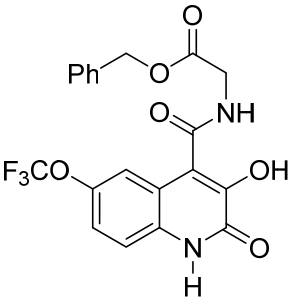

139

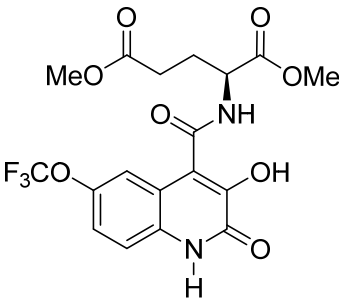

140

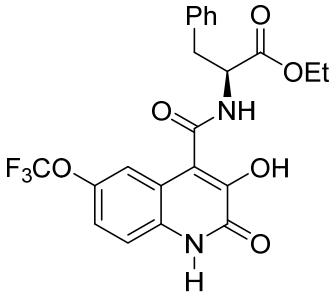

141

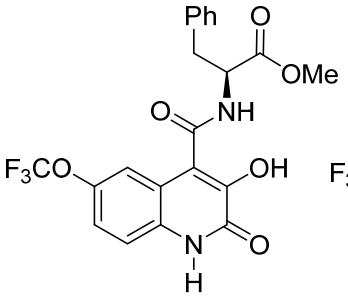

142

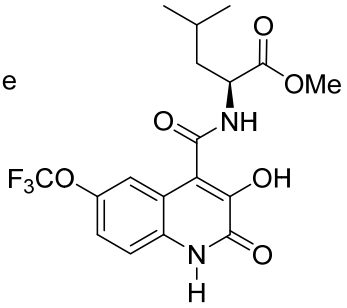

143

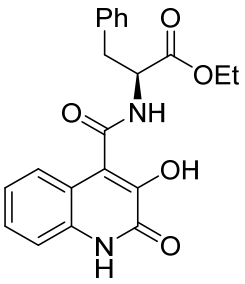

165

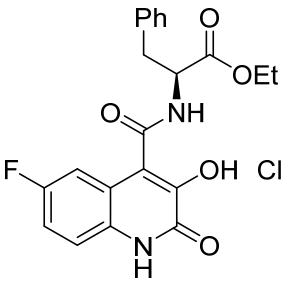

166

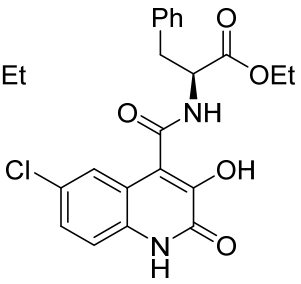

167

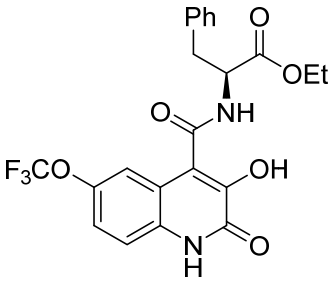

169